

# Translation Termination in Human Mitochondria: The Role of mtRF1 and mtRF1a

**Dissertation**

for the award of the degree

“Doctor rerum naturalium”

of the Georg-August-Universität Göttingen

within the doctoral program: Biomolecules: Structure – Function – Dynamics  
of the Georg-August University School of Science (GAUSS)

Submitted by

**Franziska Nadler**

from Melsungen, Germany

Göttingen, 2022



## Thesis Committee

Dr. Ricarda Richter-Dennerlein (Supervisor)	Cellular Biochemistry University Medical Center Göttingen Göttingen, Germany
Prof. Dr. Holger Stark	Structural Dynamics Max Planck Institute for Multidisciplinary Sciences Göttingen, Germany
Dr. Sarah Adio	Molecular Structural Biology Institute for Microbiology and Genetics Göttingen, Germany

## Members of the Examination Board

Dr. Ricarda Richter-Dennerlein (1 <sup>st</sup> Referee)	Cellular Biochemistry University Medical Center Göttingen Göttingen, Germany
Prof Dr. Markus Bohnsack (2 <sup>nd</sup> Referee)	Molecular Biology University Medical Center Göttingen Göttingen, Germany

## Further members of the Examination Board

Prof. Dr. Holger Stark	Structural Dynamics Max Planck Institute for Multidisciplinary Sciences Göttingen, Germany
Dr. Sarah Adio	Molecular Structural Biology Institute for Microbiology and Genetics Göttingen, Germany
Prof Dr. Ralph Kehlenbach	Molecular Biology University Medical Center Göttingen Göttingen, Germany
Dr. Alexis C. Faesen	Biochemistry of Signal Dynamics Max Planck Institute for Multidisciplinary Sciences Göttingen, Germany

**Date of oral examination:** 22<sup>nd</sup> of November, 2022



### **Affidavit**

I hereby declare that the presented dissertation with the title “Translation Termination in Human Mitochondria: The Role of mtRF1 and mtRF1a” has been written independently and with no other aids or sources than quoted.

Göttingen, October 2022

Franziska Nadler



## Abstract

Translation termination is the last step of ribosomal protein synthesis. Dedicated translation factors are imported into mitochondria to convert the information stored in the retained mitochondrial DNA (mtDNA) and to facilitate protein synthesis on mitochondrial ribosomes (mitoribosomes), which. An aberrant expression of mtDNA and a defective mitochondrial translation cause OXPHOS deficiencies associated with severe human diseases.

The genetic code used by mitochondria differs from the universal one: only two conventional stop codons, namely UAG and UAA, are present. Additionally, two mRNAs, encoding for COX1 and ND6, are terminated by AGA and AGG, respectively, which have been re-assigned as non-standard stop codons. It remains to be addressed whether a dedicated release factor or ribosomal frameshifting, resulting in standard stop codons, is responsible for translation termination of these two stop codons. Despite sharing a common ancestor, the bacterial and mitochondrial translation machinery reveal significant differences. This is not only true regarding the structure and composition of the ribosome, but also for the involved translation factors such as termination factors. While in bacteria RF1 and RF2 are required to terminate translation, mtRF1a seems to be the main release factor in human mitochondria by terminating all mitochondrial open reading frames with UAG or UAA stop codons. Interestingly, human mitochondria harbor another release factor, mtRF1, whose function still remains elusive. Although *in vitro* measurements and high-resolution structural analysis provided mechanistic insights into mtRF1a-mediated peptide release, the consequences of loss of translation termination in human mitochondria remains to be addressed.

In this doctoral thesis, the role of mtRF1 and mtRF1a are analyzed biochemically in respective human knockout cell lines. The results demonstrate that both release factors are required for proper mitochondrial function and confirmed *in vivo* that mtRF1a is the major mitochondrial release factor responsible for terminating all mtDNA-encoded transcripts, except COX1. Also, *MT-ND6*, which also harbors a non-standard stop codon, is terminated by mtRF1a. In contrast, loss of mtRF1 leads to an isolated complex IV deficiency as it specifically terminates synthesis of its core component COX1. Furthermore, this work shows that cells developed several mechanisms to rescue this isolated COX deficiency. On the one hand, mitoribosome-associated quality control (mtRQC) pathway is activated, which rescues mitoribosomes stalled upon absence of mtRF1 to maintain certain levels of COX1. This pathway triggers the degradation of respective mRNAs to not overload the system. On the other hand, this thesis shows that remaining COX1 and thus complex IV is immediately incorporated into macromolecular respiratory supercomplexes to stabilize it and protect it from turnover.

Taken together, this thesis unravels the mystery regarding the function of mtRF1, verifies the role of mtRF1a *in vivo* and therefore advance our understanding regarding translation termination in human mitochondria.

# Table of Contents

ABSTRACT .....	V
LIST OF FIGURES.....	VIII
LIST OF TABLES.....	IX
ABBREVIATIONS .....	X
<b>1 INTRODUCTION .....</b>	<b>1</b>
1.1 MITOCHONDRIA – STRUCTURE AND FUNCTION .....	1
1.2 MITOCHONDRIAL OXIDATIVE PHOSPHORYLATION SYSTEM .....	4
1.2.1 Complexes of the Electron Transport Chain .....	5
1.2.2 F <sub>1</sub> F <sub>0</sub> -type ATP synthase .....	6
1.2.3 Supramolecular Organization of OXPHOS Complexes .....	6
1.2.3.1 Composition of OXPHOS Supercomplexes.....	7
1.2.3.2 Functional Relevance of OXPHOS Supercomplexes .....	7
1.2.4 Generation of Reactive Oxygen Species .....	8
1.3 BIOGENESIS OF OXPHOS COMPLEXES .....	9
1.3.1 Assembly of Cytochrome c Oxidase .....	9
1.3.2 Integration of Complex IV into Supercomplexes.....	11
1.4 ORGANIZATION AND MAINTENANCE OF MITOCHONDRIAL DNA.....	12
1.4.1 Mitochondrial Replication and Transcription .....	13
1.4.2 Maturation of Mitochondrial Transcripts .....	14
1.5 MAMMALIAN MITOCHONDRIAL RIBOSOMES .....	15
1.6 MITOCHONDRIAL TRANSLATION .....	18
1.6.1 Initiation .....	19
1.6.2 Elongation .....	20
1.6.3 Termination.....	21
1.6.3.1 Translation Termination in Bacteria .....	21
1.6.3.2 Translation Termination in Human Mitochondria.....	25
1.6.3.3 Mitochondrial Release Factors .....	25
1.6.4 Ribosome Recycling.....	28
1.7 RIBOSOME RESCUE MECHANISMS .....	30
1.7.1 Bacterial Rescue Mechanisms .....	30
1.7.1.1 <i>Trans</i> -Translation.....	30
1.7.1.2 Alternative Rescue Pathways.....	31
1.7.1.3 Ribosome -associated Quality Control.....	32
1.7.2 Mitochondrial Rescue Mechanisms .....	32
1.7.2.1 Mitochondrial Non-Stop Rescue Pathway .....	33
1.7.2.2 Mitoribosome-associated Quality Control.....	34
1.7.2.3 Alternative Mitoribosomal Recycling Pathway.....	35
1.8 AIMS AND OBJECTIVE .....	36
<b>2 RESULTS.....</b>	<b>38</b>
PUBLICATION .....	38
AUTHOR CONTRIBUTIONS .....	38
RESEARCH ARTICLE .....	40
SUPPLEMENT.....	50
<b>3 DISCUSSION .....</b>	<b>61</b>
3.1 DEFINING THE FUNCTIONAL RELEVANCE OF MTRF1 AND MTRF1A .....	61
3.2 COX1 – THE NUCLEATION CENTER FOR COMPLEX IV ASSEMBLY.....	65
3.3 SUPERCOMPLEXES AS SAFEGUARD FOR UNSTABLE OXPHOS SUBUNITS .....	67
3.3.1 Supercomplexes Confer Stability for Complex IV when mtRF1 is Lost .....	68



3.3.2 Compensatory Mechanisms in Isolated Complex IV Deficiency.....	69
3.3.3 Supercomplexes and the Role of Reactive Oxygen Species.....	70
3.4 THE NEED FOR MITOCHONDRIAL QUALITY CONTROL SYSTEMS.....	72
3.5 SUMMARY AND FUTURE PERSPECTIVES.....	76
<b>4 MATERIALS AND METHODS.....</b>	<b>78</b>
4.1 MATERIALS.....	78
4.1.1 Chemicals.....	78
4.1.2 Buffers and Media.....	81
4.1.3 Disposables and Kits.....	83
4.1.4 Equipment, Instruments and Software.....	84
4.1.5 Antibodies.....	86
4.1.6 Oligonucleotides and Plasmids.....	87
4.1.7 Human Cell Lines and <i>E. coli</i> Strains.....	88
4.2 MOLECULAR BIOLOGICAL METHODS.....	89
4.2.1 Polymerase Chain Reaction.....	89
4.2.1 Agarose Gel Electrophoresis.....	89
4.2.3 Isolation of DNA from PCR Products and Agarose Gels.....	89
4.2.4 Molecular Cloning.....	89
4.2.5 Transformation of Competent <i>E. coli</i> Cells.....	90
4.2.6 Isolation and Purification of Plasmid DNA from <i>E. coli</i> .....	90
4.2.7 Preparation of Competent <i>E. coli</i> Cells.....	90
4.2.8 TOPO-TA™ Cloning.....	90
4.2.9 Site-directed Mutagenesis.....	91
4.2.10 Preparation of Genomic DNA from HEK293 Cells.....	91
4.2.11 Isolation of RNA from Cultured Cells.....	91
4.2.12 Northern Blotting.....	92
4.2.13 NanoString Analysis.....	92
4.3 CELL CULTURE METHODS.....	93
4.3.1 Cell Culture Conditions.....	93
4.3.2 CRISPR/Cas9-mediated Knockout Cell Lines.....	93
4.3.3 Generation of Stable Inducible Expression Cell Lines.....	94
4.3.4 Transient siRNA-mediated Knockdowns.....	94
4.3.5 Preparation of Whole Cell Extracts from HEK293 Cells.....	94
4.3.6 Isolation of Mitochondria and Mitoplasts.....	94
4.3.8 <i>In vivo</i> [ <sup>35</sup> S] Methionine Labeling.....	95
4.3.9 Measurements of Mitochondrial Radicals.....	96
4.3.10 Respirometry.....	96
4.4 PROTEINBIOCHEMICAL METHODS.....	97
4.4.1 Determination of Protein Concentration.....	97
4.4.2 Polyacrylamide-Gel Electrophoresis.....	97
4.4.3 Western Blotting.....	97
4.4.4 Immunodetection.....	98
4.4.5 Blue Native PAGE.....	98
4.4.6 <i>In-Gel</i> Activity Assay.....	99
4.4.7 Complex I Activity Measurement.....	99
4.4.8 Sucrose Density Gradients.....	99
4.5. QUANTIFICATION AND STATISTICAL ANALYSIS.....	100
<b>5 REFERENCES.....</b>	<b>101</b>
<b>APPENDIX.....</b>	<b>121</b>
<b>ACKNOWLEDGEMENT.....</b>	<b>124</b>
<b>CURRICULUM VITAE.....</b>	<b>126</b>

## List of Figures

Figure I: Mitochondria: Structure and Function. ....	2
Figure II: Assembly of Cytochrome c Oxidase. ....	10
Figure III: Mitochondrial DNA. ....	12
Figure IV: Human 55S Mitoribosome. ....	16
Figure V: Mitochondrial Translation Cycle. ....	18
Figure VI: Bacterial Termination Complex. ....	22
Figure VII: Interactions of the RF1 termination complex within the decoding center (DC) and the peptidyl transferase center (PTC). ....	23
Figure VIII: Mitochondrial Release Factors. ....	26
Figure IX: Structure of mtRF1a bound to 55S Mitoribosome. ....	28
Figure X: Mitochondrial Rescue Pathways. ....	33
Figure 1: Consequences of loss of mitochondrial translation termination factors. ....	41
Figure 2: Ablation of mitochondrial release factors affects OXPHOS. ....	43
Figure 3: Mitochondrial translation requires mtRF1 and mtRF1a. ....	44
Figure 4: Mitochondrial transcripts are altered upon ablation of mtRF1 or mtRF1a. ....	45
Figure 5: Loss of mtRF1 activates C12ORF65. ....	46
Figure 6: The role of mtRF1 and mtRF1a during translation termination in human mitochondria. ....	47
Supplementary Figure 1: Sequence alignment of mitochondrial and bacterial release factors. ....	50
Supplementary Figure 2: Genomic sequences of <i>mtRF1<sup>-/-</sup></i> and <i>mtRF1a<sup>-/-</sup></i> . ....	51
Supplementary Figure 3: Stability of newly synthesized COX1. ....	52
Supplementary Figure 4: Comparison of COX1 and ND6 termination codons in different species. ....	53
Supplementary Figure 5: CLUSTAL multiple sequence alignment of mtRF1 and mtRF1a. ....	54
Supplementary Figure 6: Antibody validation. ....	55
Figure XI: Comparison mtRF1 vs RF1. ....	62
Figure XII: COX1 as Nucleation Center for Supercomplex Assembly. ....	68
Figure XIII: Cellular ROS production. ....	71
Appendix Figure XIV: Stability of newly synthesized COX1 and ND1. ....	121
Appendix Figure XV: Steady state levels of mitochondrial release factors in <i>mtRF1a<sup>-/-</sup></i> . ....	121
Appendix Figure XVI: Steady state levels of factors in involved in RNA processing. ....	121
Appendix Figure XVII: Titration of tetracycline-inducible FLAG cell lines. ....	122

## List of Tables

Supplementary Table 1: Key reagents. ....	56
Supplementary Table 2: nCounter tube sequences for NanoString analysis (provided by IDT). .....	58
Table 1: List of chemicals and their supplier.....	78
Table 2: List of buffers, solutions and media and their formulation.....	81
Table 3: List of disposables and Kits.....	83
Table 4: List of instruments and equipment.....	84
Table 5: List of software.....	85
Table 6: List of primary antibodies.....	86
Table 7: List of oligonucleotides. ....	87
Table 8: List of plasmids.....	88
Table 9: List of human cell lines.....	88
Table 10: List of <i>E. coli</i> strains.....	89

## Abbreviations

Å	Ångström
A-site	Aminoacyl site
aa-tRNA	Aminoacylated tRNA
acetyl-CoA	Acetyl coenzyme A
ADP	Adenosine diphosphate
ATP	Adenosine triphosphate
BN PAGE	Blue native polyacrylamide gel electrophoresis
C I	Complex I, NADH:ubiquinone oxidoreductase, NADH dehydrogenase
C II	Complex II, succinate:ubiquinone oxidoreductase, Succinate dehydrogenase
C III	Complex III, ubiquinol:cytochrome <i>c</i> oxidoreductase, Cytochrome <i>bc</i> <sub>1</sub> Complex
C IV	Complex IV, cytochrome <i>c</i> oxidase
C V	Complex V, F <sub>1</sub> F <sub>0</sub> -ATP synthase
C-terminus	Carboxy terminus
CAM	Chloramphenicol
CO <sub>2</sub>	Carbon dioxide
COX	Cytochrome <i>c</i> oxidase
CP	Central protuberance
CRISPR	Clustered regularly interspaced short palindromic repeats
Cu <sub>A/B</sub>	Copper center
Cyt B	Cytochrome <i>b</i>
D-foci	Degradation foci
DC	Decoding center
DNA	Desoxyribonucleic acid
E-site	Exit site
<i>E. coli</i>	<i>Escherichia coli</i>
ETC	Electron transport chain
EF	Elongation factor
FAD(H <sub>2</sub> )	Flavin adenine dinucleotide (reduced)
Fe-S	Iron-sulfur
FMN	Flavin mononucleotide
GDP	Guanosine diphosphate
GTP	Guanosine triphosphate
H <sub>2</sub> O	Water
H-bond	Hydrogen bond
H-strand	Heavy strand
HEK	Human embryonic kidney
HSP	Heavy strand promotor
IC	Initiation complex

X

IF	Initiation factor
IMM	Inner mitochondrial membrane
IMS	Inter membrane space
INDEL	Insertion or deletion of bases in the genome
$K_{cat}$	catalytic rate constant
$K_D$	Dissociation constant
L-strand	Light strand
LSP	Light strand promotor
LSU	Large subunit
Mitoribosome	Mitochondrial ribosome
MITRAC	Mitochondrial translation regulation assembly intermediate of cytochrome <i>c</i> oxidase
MRG	Mitochondrial RNA granule
mRNA	Messenger RNA
MRP	Mitoribosomal protein
mt	Mitochondrial
mtDNA	Mitochondrial DNA
N-terminal	Amino terminus
NAD(H)	Nicotinamide adenine dinucleotide (reduced)
NADP(H)	Nicotinamide adenine dinucleotide phosphate (reduced)
NC	Nitrocellulose
nDNA	Nuclear DNA
O <sub>2</sub>	Molecular oxygen
O <sub>2</sub> <sup>•-</sup>	Superoxide anion
OMM	Outer mitochondrial membrane
ORF	Open reading frame
OXPPOS	Oxidative phosphorylation
P <sub>i</sub>	Inorganic phosphate
P-site	Peptidyl site
PBS	Phosphate buffered saline
PCR	Polymerase chain reaction
PET	Polypeptide exit tunnel
Poly(A)	Polyadenylation
PoTC	Post termination complex
PTC	Peptidyl transferase center
PTH	Peptidyl tRNA hydrolase
PVDF	Polyvinylidene fluoride
Q	Ubiquinone
RBP	RNA-binding protein
RET	Reverse electron transfer
RF	Release factor
RNA	Ribonucleic acid

ROS	Reactive oxygen species
rpm	Rotations per minute
RQC	Ribosome-associated quality control
RRF	Ribosome recycling factor
rRNA	Ribosomal RNA
RT	Room temperature
S	Svedberg unit
SC	Supercomplex
siRNA	Small interfering RNA
SSU	Small subunit
TCA cycle	Tricarboxylic acid cycle
TIM	Translocase of the inner mitochondrial membrane
TOM	Translocase of the outer mitochondrial membrane
tRNA	Transfer RNA
UTR	Untranslated region
WT	Wild type
$\Delta\Psi$	Membrane potential

Other abbreviations used in this thesis are either referring to the International system of units (SI) comprising SI base units, SI-derived units or non-SI units used with metric prefixes; or amino acids and nucleotides which are abbreviated according to the one-letter or three-letter IUPAC (International Union of Pure and Applied Chemistry) code. For Abbreviations of chemicals, buffers and media, please refer to table 1 and table 2.







# 1 Introduction

## 1.1 Mitochondria – Structure and Function

Mitochondria are organelles of essential importance and are considered to be the ‘power house’ of eukaryotic cells due to their role as the main provider of energy in form ATP. However, besides aerobic respiration, mitochondria also fulfill central functions in a plethora of cellular and metabolic processes (Figure 1a) like the citric acid (tricarboxylic acid (TCA)) cycle to catabolize carbohydrates, but also  $\beta$ -oxidation of fatty acids and catabolism of amino acids to convert them into intermediates of the TCA cycle to ultimately generate NADH. Moreover, they are involved in anabolic processes like the biosynthesis of heme or certain phospholipids as well as calcium homeostasis, apoptosis and the highly essential biogenesis of iron sulfur (Fe-S) clusters (Lill, 2009; Spinelli & Haigis, 2018). Not surprisingly, mutations in respective genes cause a variety of mitochondrial disorders which display a heterogenous, often tissue-specific group of diseases ranging from mitochondrial myopathies, Leigh syndrome, Leber’s hereditary optic neuropathy (LHON) or Mitochondrial encephalomyopathy with lactic acidosis and stroke-like episodes (MELAS). Mitochondria also have implications in common diseases for example neurological disorders like Parkinson’s or Alzheimer’s disease, cardiomyopathy, diabetes or cancer as a secondary effect. Additionally, it is well known that mitochondria play a role in aging and developmental processes (Gorman et al., 2016; Nunnari & Suomalainen, 2012; Schapira, 2012).

Although mitochondria can vary in their size and overall shape, they show a characteristic structure (Figure 1a). They are double-membraned organelles comprising a porin-rich outer mitochondrial membrane (OMM) and a highly impermeable inner mitochondrial membrane (IMM) which form two separated aqueous compartments: the intermembrane space (IMS) resembling the cytosol and the mitochondrial matrix which provides a reaction compartment for many metabolic processes. The IMM can be further divided into two functional regions. Being in parallel to the OMM, the inner boundary membrane (IBM) is divided by invaginations termed cristae which are formed from of the IMM by cristae junctions. Cristae junctions mainly consist of components of the mitochondrial contact site and cristae organizing system (MICOS) and OPA1 (optic atrophy 1, mitochondrial dynamin-related GTPase) which are responsible for the well-known architecture of the IMM. By highly enlarging the surface of the IMM, cristae provide an ideal bioenergetic reaction environment for ATP synthesis by increasing capacities for sufficient energy production since complexes required for oxidative phosphorylation (OXPHOS) are organized in this compartment (Cogliati et al., 2016b; Harner et al., 2011). Depending on the cellular context, mitochondria can not only adapt their ultrastructural morphology but also their overall shape in correspondence to cellular signaling and energy demands: they either fuse to large networks in phases of high energy demand or divide into small, individual mitochondrial fragments. Those fusion and fission events, also known as mitochondrial dynamics, must be well balanced to maintain proper mitochondrial function and are therefore highly regulated (Giacomello et al., 2020; Westermann, 2010).

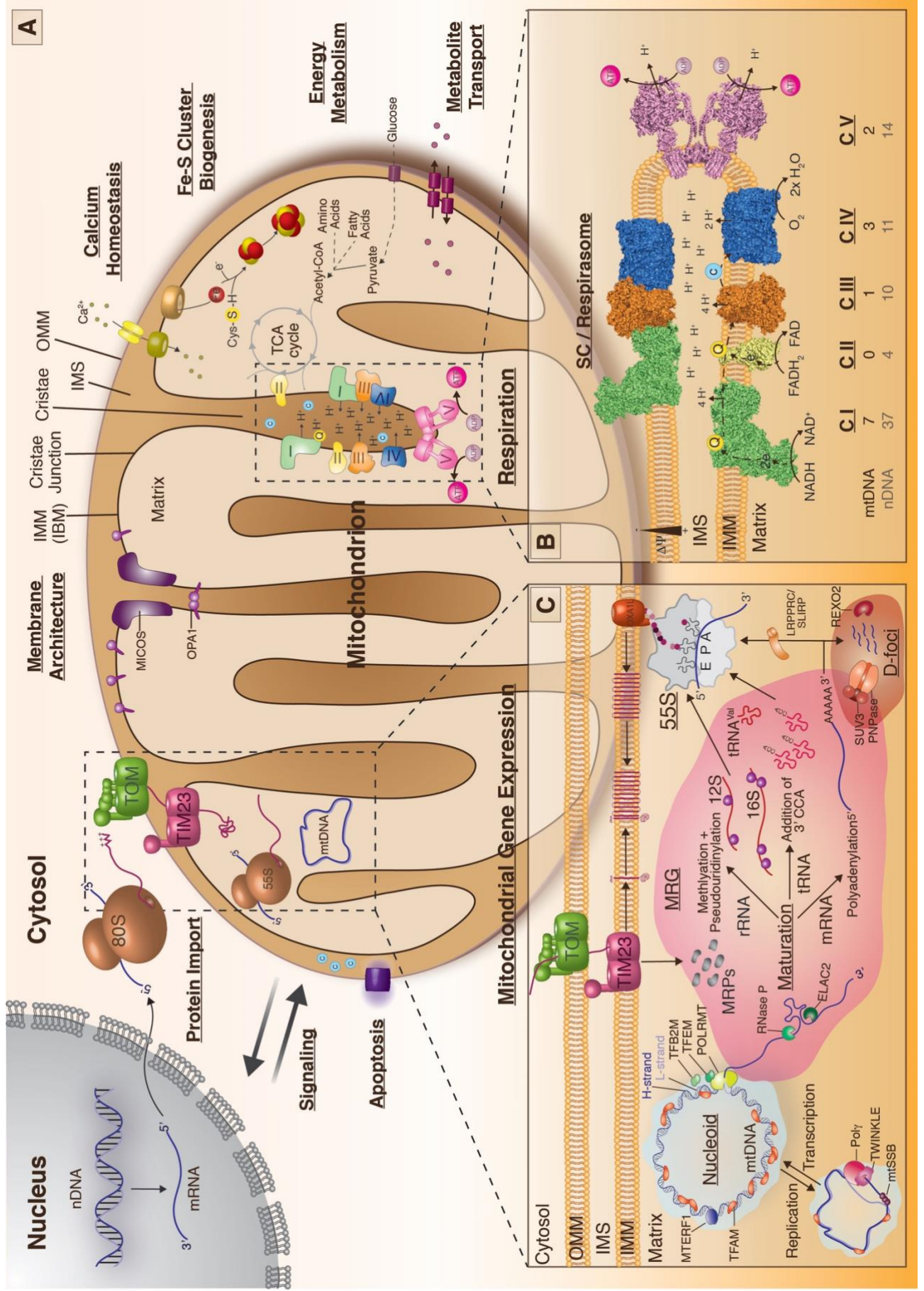


**Figure 1: Mitochondria: Structure and Function. (A) Overview.** Mitochondria are composed of four subcompartments: the outer mitochondrial membrane (OMM), the intermembrane space (IMS), the inner mitochondrial membrane (IMM) and the mitochondrial matrix. The organelle is a central hub for many essential cellular functions depicted in the figure (selected functions, without claiming completeness and not drawn to scale). Energy metabolism of nutrients like glucose, fatty acids and amino acids accumulate in the citric acid (TCA) cycle. Produced redox equivalents are used to generate energy (ATP) via oxidative phosphorylation (OXPHOS) by complexes I – V of the electron transport chain (ETC). Mitochondrial DNA (mtDNA) is translated by mitochondrial ribosomes (mitoribosomes) and nascent polypeptides are assembled together with nuclear-encoded (nDNA) subunits. Import of these subunits is carried out by the translocases of the OMM (TOM) and the IMM (TIM). Further essential functions are the biogenesis of iron-sulfur (Fe-S) clusters, apoptosis, calcium homeostasis and signaling processes. **(B) Mitochondrial gene expression.** mtDNA is compacted in nucleoids and its main component TFAM which determines whether replication or transcription is taking place. The long, polycistronic transcripts need further maturation, which occurs in RNA granules (MRG), before rRNAs, tRNA<sup>Val</sup> and imported mitoribosomal proteins (MRPs) can be assembled to mitoribosomes. Mitochondrial mRNA is then translated or degraded by the degradosome in degradation foci (D-foci). **(C) Respiration.** Shown are the complexes of the ETC that oxidize the electron carriers NADH and FADH<sub>2</sub> and couple transfer of electrons onto O<sub>2</sub> with proton pumping. This proton gradient establishes the membrane potential ( $\Delta\Psi$ ) required for proton import by the F<sub>1</sub>F<sub>0</sub> ATP synthase to generate ATP from ADP and inorganic phosphate. The complexes of dual genetic origin are organized in macromolecular supercomplexes (SC). SCs with a stoichiometry of I+III<sub>2</sub>+IV<sub>1-4</sub> are able to independently respire and are termed respirasome. Models of OXPHOS complexes I – V were generated from following PDBs: 5LDW, 1ZOY, 1BGY, 5B1A and 5ARE.

Evolving from an endosymbiotic event of an  $\alpha$ -proteobacteria-related ancestor and an eukaryotic host of archaeal origin (Martijn et al., 2018; Roger et al., 2017; Sagan, 1967), mitochondria have lost most of their genetic information as it was transferred to the nucleus during evolution (Petrov et al., 2018). Even though, mitochondria remained with a small, double-stranded and circular genome where the mitochondrial DNA (mtDNA) encodes for core components of the OXPHOS machinery (Gustafsson et al., 2016), the remaining 99 % of the approximately 1500 required mitochondrial proteins are encoded by the nuclear DNA (nDNA) and thus must be imported. These proteins are synthesized in the cytosol as unfolded precursors, marked with a variety of specific targeting sequences and sorted in their respective mitochondrial compartments via five main mitochondrial import machineries, which are essential housekeeping systems for mitochondria (Neupert, 2015; Neupert & Herrmann, 2007; Pfanner et al., 2019).

The vast majority of mitochondrial proteins are imported into the mitochondrial matrix or IMM via the presequence pathway. Precursor proteins containing an N-terminal targeting sequence composed of amino acid residues, which form an amphipathic  $\alpha$ -helix with a hydrophobic and a positively charged surface, are recognized and bound by receptors of the translocase of the outer mitochondrial membrane (TOM). Being the central mitochondrial entry gate, the TOM complex consists of three receptor proteins, small accessory subunits and multiple copies of a  $\beta$ -barrel protein, which forms a transmembrane channel with up to three pores (Mokranjac & Neupert, 2015). Precursor proteins are directed from the TOM complex to the translocase of the inner mitochondrial membrane, the TIM23 complex, which transports proteins either into the mitochondrial matrix or the IMM in a membrane potential ( $\Delta\Psi$ )-dependent manner. The TIM23 complex is similarly composed of a presequence receptor, regulatory factors and a channel-forming, lockable structural component (Callegari et al., 2020; Chacinska et al., 2005; Chacinska et al., 2010; Meinecke et al., 2006). The import of soluble matrix proteins is driven

by a second energy consuming force: the presequence translocase-associated motor (PAM). Presequences are then cleaved by the mitochondrial processing peptidase (MPP) and the mature protein is released (Wiedemann & Pfanner, 2017). Proteins designated for the IMM contain another hydrophobic stop-transfer sorting sequence adjacent to the presequence leading to arrest of the translocation in the IMM and its lateral insertion into the lipid bilayer (Ieva et al., 2014). However, a few IMM proteins can first be imported into the matrix via the TIM23-PAM import pathway and then inserted into the IMM by the oxidase assembly (OXA1L) translocase (Stiller et al., 2016). Most proteins of the IMS are translocated from the cytosol as precursors and are imported via the mitochondrial intermembrane space import and assembly (MIA) pathway. To trap and stabilize the proteins in the IMS, a oxidoreductase with disulfide isomerase activity transfers disulfide bonds to characteristic cysteine motifs of the protein and is then regenerated by a sulfhydryl oxidase (Herrmann & Köhl, 2007; Mesecke et al., 2005). Sorting of OMM proteins depends on their secondary structure. Import of  $\beta$ -barrel proteins of the OMM is carried out by translocation via TOM into the IMS, where small TIM chaperones aid to insert the proteins via the sorting and assembly (SAM) complex into the OMM, while  $\alpha$ -helical OMM proteins are sorted via the mitochondrial import (MIM) channel (Wiedemann et al., 2003; Wiedemann & Pfanner, 2017).

## 1.2 Mitochondrial Oxidative Phosphorylation System

Generation of the universal intracellular energy currency ATP via OXPHOS is the key event in mitochondria and the main energy source of eukaryotic cells. Oxidation of high-energy electron carriers NAD(P)H and FADH<sub>2</sub>, produced during catabolic processes of carbohydrates, fatty acids or amino acids, coupled to pumping protons across the IMM creates an electrochemical gradient which is required for ATP synthesis (Figure 1b). The OXPHOS system is comprised of five multimeric protein complexes of a dual genetic origin embedded in the cristae of the IMM. The described mechanism of chemi-osmotic coupling was already proposed by (Mitchell, 1961). Whereas complex I – IV are part of the electron transport chain (ETC), complex V is the F<sub>1</sub>F<sub>0</sub>-ATP synthase which utilizes the protonmotive force to synthesize ATP. Catabolism of carbohydrates and of fatty acids via glycolysis or  $\beta$ -oxidation generates the intermediate compound acetyl-CoA. In multiple reactions, acetyl-CoA enters the TCA cycle in the mitochondrial matrix and becomes stepwise oxidized to CO<sub>2</sub>, while its electrons are transferred to NAD<sup>+</sup> or FAD. Although aerobic oxidation of glucose via glycolysis and the TCA cycle already produces two ATP and two equivalent GTP molecules, the main energy is stored in the reduced electron carriers NADH and FADH<sub>2</sub>. In this form electrons are stepwise transferred via prosthetic groups within the complexes of the respiratory chain to an oxygen molecule (O<sub>2</sub>) as the final electron acceptor, which is then reduced to water (H<sub>2</sub>O). Simultaneously to the reduction of those coenzymes, the complexes of ETC pump protons from the matrix into the IMS thus building an electrochemical gradient. In this way the large redox potential is conserved in the protonmotive force, which is used for phosphorylation of ADP to ATP (Saraste, 1999).

### 1.2.1 Complexes of the Electron Transport Chain

In detail, mammalian complex I (C I) or according to its function the NADH:ubiquinone oxidoreductase or NADH dehydrogenase consists of 45 subunits, 14 of which are highly conserved from bacteria to human and more than 30 accessory subunits (Zhu et al., 2016). The huge 1 MDa complex shows an asymmetrical L-shape, formed by a highly hydrophobic membrane arm embedded in the IMM and a hydrophilic peripheral arm extending into the matrix (Vinothkumar et al., 2014). Three functional modules, comprised of the conserved core subunits, can be distinguished: first seven of the nuclear-encoded subunits are organized in the N module required for oxidation of NADH and thus the import of electrons. Second, the Q module which transfers the electrons to the lipid-soluble ubiquinone (Q). NADH is bound at the tip of the peripheral arm and oxidized by the prosthetic group FMN (flavin mononucleotide) which serves as the primary electron acceptor. Two electrons are stepwise transferred through a series of eight Fe-S clusters to their final acceptor ubiquinone which is reduced to ubiquinol. Coupled to the electron transfer, four protons are pumped from the matrix into the IMS by the membrane-embedded P module formed by the seven mtDNA-encoded subunits ND1 – ND6 and ND4L by a still unknown mechanism, likely involving conformational changes. The supernumerary subunits wrap around the core complex and have a structural and protective role (Galemou Yoga et al., 2020; Hirst, 2013; Stroud et al., 2016).

A second way to take up electrons is via complex II (C II) of the respiratory chain. C II is a rather unusual case as the succinate:ubiquinone oxidoreductase or succinate dehydrogenase is implicated in another metabolic pathway, the TCA cycle. The oxidation of succinate to fumarate liberates two electrons which reduce the cofactor FAD and are transferred via three Fe-S cluster to finally ubiquinone. Being the smallest of the ETC complexes, it only consists of four subunits which are only nuclear-encoded. Unlike the other complexes, C II does not pump protons into the IMS (Rutter et al., 2010; Yankovskaya et al., 2003).

Ubiquinol, reduced by C I or II, shuttles the electrons to complex III (C III), the ubiquinol:cytochrome *c* oxidoreductase (or cytochrome *bc*<sub>1</sub> complex). This dimeric complex consists of eleven subunits with three being highly conserved: cytochrome *b* is still encoded by mtDNA while cytochrome *c*<sub>1</sub> and the Rieske iron sulfur protein (RISP) are nuclear encoded like the remaining additional subunits of yet unknown function (Crofts, 2004; Iwata et al., 1998). Transfer of electrons is described in the Q cycle, where in a concerted process two electrons are shuttled via Fe-S clusters and heme groups from ubiquinol to another mobile electron carrier: cytochrome *c*. Simultaneously, four protons are pumped into the IMS (Trumpower, 1990).

Complex IV (C IV) or cytochrome *c* oxidase is the terminal complex of the electron transport chain. It receives a total of four electrons each from one cytochrome *c* at its IMS site and transfers them via redox active metal centers together with four protons to an O<sub>2</sub> which is then reduced to two water molecules (H<sub>2</sub>O). Per reaction cycle, four protons are pumped from the matrix into the IMS, thus contributing to the generation of the electrochemical proton gradient.

The 200 kDa-large 13-subunit holocomplex builds a homodimer under physiological conditions. Notably, the three mitochondrial-encoded core components – COX1, COX2 and COX3 – are the highly conserved, catalytically active part of this protein complex. All accessory subunits are of nuclear origin and need to be imported (Michel et al., 1998; Tsukihara et al., 1996).

The catalytic activity of C IV is well described by (Wikström et al., 2018) and can be summarized as follows: the dimetallic  $Cu_A$  center bound to the COX2 core subunit accepts the electron from reduced cytochrome *c* which binds to the IMS-facing side of C IV and is then transferred to heme *a* and further to the binuclear center (BNC) consisting of  $Cu_B$  and heme  $a_3$ , all buried in the COX1 subunit. The BNC represents the oxygen reduction center which binds the  $O_2$  as ultimate electron acceptor and reduces it to two  $H_2O$ . COX3 does not harbor a metal prosthetic group and thus has no function in redox-coupled proton pumping but rather in stabilization of the enzymatically active subunits of C IV. Simultaneously to the transfer of electrons, protons are translocated via dedicated proton channels within the enzyme from the matrix into the IMS (D-channel) or to the BNC (K-channel).

### 1.2.2 $F_1F_0$ -type ATP synthase

In this manner the energy conserved in electron carriers drives the generation of the electrochemical proton gradient across the IMM by coupling electron transfer to pumping of protons. This protonmotive force is then harnessed by the last complex of the OXPHOS machinery to generate ATP. Complex V (C V) or the  $F_1F_0$ -ATP synthase is a large multimeric protein complex consisting of two subcomplexes: the membrane-embedded  $F_0$  part represents the electrochemical motor, accessible for the back flux of protons along their concentration gradient from the IMS back into the mitochondrial matrix, whereas the soluble, globular  $F_1$  head sticks out into the matrix where it is responsible to synthesize ATP from ADP and inorganic phosphate. Both subunits are linked by the central stalk and one peripheral stalk (Abrahams et al., 1994; Zhou et al., 2015). Interestingly, ATP synthases dimerize and associate in rows which induce a curvature in the IMM leading to the formation of cristae. In this way, not only the membrane surface is enlarged to accommodate more protein complexes, but also a microcompartment is created where protons are trapped leading to an ideal reaction environment to generate ATP (Junge & Nelson, 2015; Kühlbrandt, 2019).

### 1.2.3 Supramolecular Organization of OXPHOS Complexes

Organization of the OXPHOS complexes in the IMM was under debate for decades and led to two contrary models. Whereas the '*solid-state*' model, initially proposed by Chance and Williams in 1955, claims that the complexes of the ETC are packed together to a macromolecular complex which allows efficient electron channeling, Hackenbrock et al. suggested the '*fluid-state*' or '*random-collision*' model in 1986. Kinetic studies supported the idea of a random distribution and free diffusion of the ETC complex within the membrane and their respective connection via ubiquinol and cytochrome *c*. However, the emergence of Blue Native Polyacrylamide Gel Electrophoresis (BN-PAGE) and subsequent usage of milder detergents like digitonin revealed that interactions between individual ETC complexes lead to the formation of larger supercomplexes (SC, Figure 1b, (Schägger & Pfeiffer, 2000). Experiments

with even milder detergents and sucrose density gradient ultracentrifugation showed that the existence of SCs is not an artefact but results from true interactions. The co-existence of both models led to the nowadays established '*plasticity*' model, which comprises elements from both beforementioned models (Acín-Pérez et al., 2008).

#### 1.2.3.1 Composition of OXPHOS Supercomplexes

Although the stoichiometry of supercomplexes can vary depending on the species, cell type and physiological conditions, the most commonly found SC is the so-called *respirasome*, consisting of I+III<sub>2</sub>+IV<sub>1</sub> – or with additional C IV monomers as I+III<sub>2</sub>+IV<sub>2-4</sub> (Letts et al., 2016; Schäfer et al., 2006; Wu et al., 2016). This complex alone is able to reduce NADH and ultimately transfer electrons to O<sub>2</sub>, hence to respire. Various studies suggested, that SCs can be found in complexes with even higher molecular weight, termed megacomplexes, or as binary or ternary fractions of the original respirasome in various sub-modules and stoichiometries (Guo et al., 2017). Interestingly, phospholipids were found to contribute to proper SC formation. Especially cardiolipin, a phospholipid unique to the IMM, is required for stabilizing supercomplexes yet conferring the membrane-embedded parts with flexibility for sufficient conformational changes during electron transfer and proton pumping (Pfeiffer et al., 2003; Zhang et al., 2002).

#### 1.2.3.2 Functional Relevance of OXPHOS Supercomplexes

Along with the debate which proposed model of the ETC organization might be the most correct one, also the physiological significance of SC and potential advantages still remain enigmatic. To summarize the ongoing discussion, three main functions of SCs have been postulated (Cogliati et al., 2021; Hirst, 2018; Lobo-Jarne & Ugalde, 2018; Milenkovic et al., 2017). First, electrons are thought to be transferred more efficiently if ETC are arranged in SC by substrate channeling. In this scenario, ubiquinone and cytochrome *c* can channel in sealed protein tunnels between C I and C III or C III and C IV, respectively and thus would enhance the catalytical activity (Althoff et al., 2011; Sousa et al., 2016). This hypothesis is in discrepancy with kinetic measurements and structural analysis. Actually, it is shown that the respective binding sites of the electron carriers are open, no proteinaceous, sealed channel exists and that ubiquinone and cytochrome *c* rather show a pool behavior with free diffusion. Therefore, SC formation brings the subcomplexes into the closest possible proximity, but no proper 'channeling' is taking place (Blaza et al., 2014; Hirst, 2018; Lenaz et al., 2016; Letts et al., 2016; Milenkovic et al., 2017). The second suggested role of SCs is to serve as an assembly platform, particularly for C I. It was postulated that the assembly of C I happens in stages where the last stage – insertion of the N-module – depends on the association of a premature C I with the C III<sub>2</sub> module (Moreno-Lastres et al., 2012). Even though the dependency of the stability of C I was confirmed by disease-related, mutational studies that showed a loss of C I when C III or C IV is absent (Acín-Pérez et al., 2004; D'Aurelio et al., 2006; Protasoni et al., 2020), this effect might be secondary due to functional and/or structural properties of the SC. On the one hand, C I can be degraded upon oxidative damage caused by reverse electron transfer (RET), which depends on the ubiquinol level and its oxidation status modulated by the other ETC complexes (Guarás et al., 2016). On the other hand, a study on complexome profiling of C I suggests, that

its assembly is completed before SC formation (Guerrero-Castillo et al., 2017). Mature C I can be isolated independently of SCs and this finding indicates that these interactions are not mandatory under normal conditions. Additionally, free respiratory complexes are thought to serve as some kind of 'functional reserve' (D'Aurelio et al., 2006). Since C I and C III are the main sites for production of reactive oxygen species (ROS), it is also proposed that the organization into SCs prevents or limits ROS production. It is generally thought that SCs restrict ROS production by a more efficient flow of electrons either by already mentioned substrate channeling or by minimizing the diffusion space for the electron carriers and shielding relevant redox centers which are the origin of ROS (Maranzana et al., 2013). Nonetheless, it is still unknown whether elevated ROS levels are reason or consequence of SC disassembly.

#### **1.2.4 Generation of Reactive Oxygen Species**

ROS are a by-product of the redox reactions happening within electron transfer in the respiratory chain under normal physiological conditions. To alleviate the damaging nature of ROS, these highly reactive molecules, e.g. the primary superoxide anion ( $O_2^{\bullet-}$ ), are usually first converted into hydrogen peroxide ( $H_2O_2$ ) by superoxide dismutases (SOD) and finally to  $H_2O$  by catalases (CAT), peroxiredoxins or glutathione peroxidases (Murphy, 2009). Abnormally elevated ROS level can severely damage cellular elements like DNA, proteins and lipids by reacting with those molecules via their highly reactive unpaired electron, potentially causing chain reactions and thus altering their structure and chemical properties. This oxidative stress has implications in cardiovascular, inflammatory, neurodegenerative and cancer pathologies as well as during aging. But, ROS have an ambivalent function. ROS can serve as signaling factors in cellular pathways like hypoxia, apoptosis, autophagy, stem cell differentiation and regulation of transcription factors and have protective function during immune response (Dan Dunn et al., 2015; Lennicke & Cochemé, 2021; Sies & Jones, 2020; Waypa et al., 2016).

The major source of endogenous ROS is the transport and subsequent escape of electrons during cellular respiration (Murphy, 2009). Electrons are passed by redox centers, each having a greater redox potential than the previous. Those redox centers, like Fe-S clusters, FMN or ubiquinol, which are predominantly found in C I but also in C II and C III of the ETC, are usually well shielded within the complexes to avoid premature contact with  $O_2$  and/or prevent leakage of electrons. However, in about 0.1 – 1 % of all electrons shuttled, an incomplete reduction of  $O_2$  takes place leading to generation of  $O_2^{\bullet-}$  (Dröse & Brandt, 2012; Murphy, 2009). As reviewed by (Murphy, 2009), elevated levels of  $O_2^{\bullet-}$  can occur mainly under two distinct metabolic conditions which enhance the electron leakage. A high NADH/NAD<sup>+</sup> ratio leads to a backup of electrons within the chain of Fe-S clusters, making it more likely for  $O_2$  to be prematurely reduced at the primary electron acceptor FMN of C I. Accumulation of NADH can also occur by stalling further steps of the ETC, for example by inhibiting the ubiquinone binding site of C I with rotenone. A second potential reason for elevated ROS levels is the beforementioned RET: if the ubiquinone pool is reduced, mitochondria do not generate ATP, hence the proton-motive force is high and C I functions in a 'reverse' mode leading to a backflow of electrons.



### 1.3 Biogenesis of OXPHOS Complexes

Due to the dual genetic nature of the OXPHOS components (excluding C II), their assembly must be tightly coordinated in a temporal and spatial manner. On the one hand, the mitochondrial genome encodes for highly hydrophobic, catalytic OXPHOS core components, which are translated by its own translation machinery, the mitochondrial ribosome (mitoribosome), and which are co-translationally inserted into the IMM. On the other hand, nuclear-encoded subunits are translated in the cytosol, imported into mitochondria via previously described translocases, inserted into the IMM and assembled into complexes together with mitochondria-derived subunits. This sophisticated process needs to be highly orchestrated, monitored and carefully balanced in regard of the availability of certain subunits, hence requires a so-called translational plasticity (Richter-Dennerlein et al., 2016). The intimate connection between the mitochondrial translocases, the mitoribosomes and the mitochondrial insertase OXA1L highlights the importance for a coordinated insertion into the IMM. Most mtDNA-encoded subunits are either directly positioned in the membrane by the insertase or by placing the mitoribosome into close proximity to the membrane by anchoring it to the IMM via the interaction of the large subunit constituent mL45 with OXA1L (Pfeffer et al., 2015; Thompson et al., 2018).

But the requirement for synchronization not only applies to the synthesis of the complex subunits themselves, but also the complete gene expression and assembly apparatus needs to adapt to the cellular demands. This does not only affect a plethora of assembly factors, but also transcriptional and translational regulators as well as all components involved in mitoribosome biogenesis (Richter-Dennerlein et al., 2015; Tang et al., 2020). In order to protect the cells from superfluous subunits or accumulated assembly intermediates, quality control mechanism like the activation of mitochondrial proteases also play an important role in protein turnover (Richter et al., 2015). The correct assembly of OXPHOS complexes is of high importance since a disturbed OXPHOS machinery leads to severe mitochondrial disorders. Furthermore, an abnormal mitochondrial membrane architecture caused by aberrant ETC complexes and thus a diminished membrane potential, serves as a feedback mechanism and triggers cellular signaling regarding cell proliferation (Hock et al., 2020; Richter-Dennerlein et al., 2015). Assembly of OXPHOS complexes is a rather complicated process and thus extensively studied. A great amount of evidence arose from studies in yeast and even though a lot of components are conserved, many specific factors have been identified in mammals. Unsurprisingly, all five OXPHOS complexes have their own, more or less well defined assembly machinery which ensures a stepwise assembly of subunits and respective cofactors, quite often in a modular fashion (Signes & Fernandez-Vizarra, 2018).

#### 1.3.1 Assembly of Cytochrome *c* Oxidase

One of the best studied assembly pathways is the biogenesis of the terminal electron acceptor cytochrome *c* oxidase. Whereas the three core components COX1, COX2 and COX3 are encoded by the mtDNA, all accessory subunits are nuclear-encoded. It is demonstrated, that biogenesis of C IV (Figure II) centers around COX1. The module responsible for the initial co-translational insertion and stabilization of COX1 is termed MITRAC (mitochondrial translation

regulation assembly intermediate of cytochrome *c* oxidase). MITRAC comprises a variety of different assembly factors according to the respective assembly step. (Dennerlein & Rehling, 2015; Mick et al., 2012). It can be noted that translation regulation of COX1 seems to be of particular interest since it is the only known human mitochondrial transcript so far which's synthesis is regulated by a translational activator, namely TACO1 (translational activator of cytochrome *c* oxidase). It interacts with *MT-CO1* (mRNA encoding for COX1) and thus triggers its translation (Weraarpachai et al., 2009).

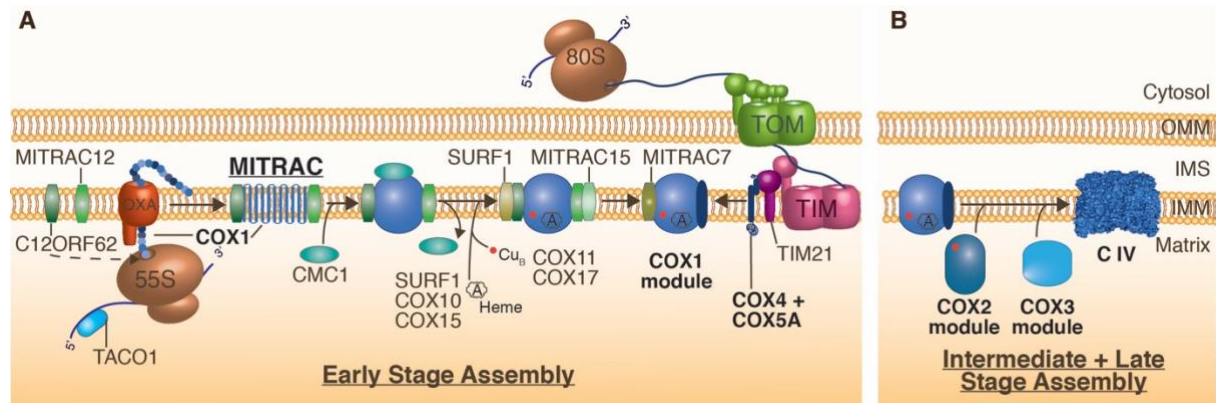


**Figure II: Assembly of Cytochrome *c* Oxidase.** Biogenesis of complex IV (C IV) occurs in a modular manner. **(A)** Mitoribosomal translation of COX1 is regulated by TACO1 (translational activator of cytochrome *c* oxidase). Early stage assembly is described in detail in the main text. Assembly is initiated by key constituents of the MITRAC (mitochondrial translation regulation assembly intermediate of cytochrome *c* oxidase) complex, C12ORF62 followed by MITRAC12, which bind nascent COX1. COX1 is further stabilized and matured by insertion of heme (A) and the copper center Cu<sub>B</sub> (red), facilitated by additional assembly factors. Biogenesis can resume when the first nuclear-encoded submodule of COX4 and COX5A are associated to the COX1 via TIM21. **(B)** During intermediate and late stage assembly, pre-assembled COX2- and COX3 modules are incorporated into matured C IV (PDB: 5B1A).

In humans, C12ORF62 (COX14) followed by MITRAC12 (COA3) bind newly synthesized COX1 and assist its membrane insertion in a first step (Figure IIa), followed by association of CMC1 (COX assembly mitochondrial protein 1) with the complex, potentially to stabilize it. Concomitantly, prosthetic groups are inserted into COX1: while COX10, COX15 – associated with PET117 – and SURF1 (Surfeit locus protein 1) are required for synthesis, delivery and incorporation of the heme *a* group, the metallochaperones COX11 (which redox status is maintained by COX19) and COX17 assemble and deliver the copper ions for the Cu<sub>B</sub> center. CMC1 is then released and MITRAC15 (COA1), which has greater importance for C I maturation, further stabilizes the assembly intermediate. MITRAC7 acts at a late stage of MITRAC-mediated assembly and its expression level represents a second assembly checkpoint by surveillance and regulation of COX1 levels in regard to the other subunits and can either induce its turnover or arrest further assembly (Dennerlein et al., 2015; Signes & Fernandez-Vizcarra, 2018; Tang et al., 2020; Wang et al., 2020). Simultaneously to this early assembly stage, a submodule of the nuclear-encoded COX4 and COX5A together with HIGD1A (homolog to yeast SC assembly factors Rcf1 and member of the *hypoxia-induced gene (domain) 1* protein family) was observed as an individual early assembly intermediate which is then to be joint with the COX1 (Vidoni et al., 2017). Interestingly, progression of assembly only takes place if COX4 is present. If this is not the case, mitochondrial translation and subsequently biogenesis of C IV is stalled, leading to a decrease of COX1 to cope with the supply of nuclear subunits, highlighting the significance

of translational plasticity (Richter-Dennerlein et al., 2016). Consistently, the interaction of MITRAC12 with TIM21, a constituent of the TIM23 import machinery, and OXA1L demonstrates the importance of precise coordination of nDNA-encoded subunits import and their assembly with mtDNA-encoded subunits (Mick et al., 2012).

During the intermediate assembly stage (Figure IIb) of C IV, the COX2 assembly module is joining the complex. Beforehand, nascent COX2 is inserted into the IMM towards the IMS via OXA1L and COX18 – stabilized by COX20 (FAM36A) and TMEM177 (Lorenzi et al., 2018) – where its metalation with the Cu<sub>A</sub> center takes place in a sequential manner. For this step, first COX17 delivers copper ions to SCO1/2 (synthesis of cytochrome *c* oxidase 1/2), which are in turn maintained by COA6 (Stroud et al., 2015). COX16, which also interacts with nascent COX2, is then implicated in insertion of Cu<sub>A</sub> and finally guides the COX2 module to the COX1 module after further nuclear encoded subunits (COX5B, COX6C, COX7C, COX8A and COX7B) have joined (Aich et al., 2018). At this stage, interaction of the recently identified assembly factor MR-S1 (myofibrillary-related protein 1 short isoform) associated with PET100 and PET117 is implicated as a prerequisite before preceding of the assembly (Vidoni et al., 2017). The late assembly stages (Figure IIb) are still ill-defined. However, joining of the COX3 module (including nuclear encoded COX6A1, COX6B1 and COX7A2) completes the biogenesis of the holo-cytochrome *c* oxidase (Dennerlein & Rehling, 2015; Tang et al., 2020). Whether NDUFA4, which was initially thought to be part of C I, is also part of the active C IV is still under debate (Balsa et al., 2012; Kadenbach, 2021; Zong et al., 2018). Notably, the picture is not complete yet considering that human mitochondria lack robust orthologs of many assembly factors identified in yeast. Additionally, one has to take into account that especially C IV is comprised of some subunits with tissue-specific isoforms, hence, its assembly pathway most likely seems to include more, hitherto unknown factors.

### 1.3.2 Integration of Complex IV into Supercomplexes

The incorporation of individual OXPHOS complexes into SCs also requires a dedicated set of assembly factors. Depending on the model, two potential functional principles are possible: either complete holo-complexes are assembled first and are then merged together to SC or subcomplexes are integrated into SC before the maturation of the single complexes is completed (Signes & Fernandez-Vizarra, 2018).

In regard of C IV, more and more evidence emerged that actually both mode of actions can be true and thus may reflect certain cellular needs due to altered metabolic conditions. HIGD1 and HIGD2 were postulated to be potential candidates. However, HIGD1 was shown to be implemented in assembly of C IV (Vidoni et al., 2017), whereas HIGD2 has rather an indirect role by stabilizing C IV during SC formation (Chen et al., 2012). A controversial debate about the role of COX7A2L (renamed Super Complex Assembly Factor 1 (SCAF1)) arose after it was discovered (Lapuente-Brun et al., 2013; Mourier et al., 2014). While its long isoform was shown to be required for the interaction between C III and C IV and thus C IV integration during SC maturation in mouse fibroblasts (Lapuente-Brun et al., 2013), its importance was doubted since SC formation and activity was not impaired in the same mouse model (Mourier et al., 2014).

Moreover, SC biogenesis was shown to be independent from human SCAF1 but may be required for stabilization (Pérez-Pérez et al., 2016). Additionally, a proteomics-based approach revealed that SCAF1 is expressed tissue-specific and therefore required in heart and skeletal muscle, but not in liver (Cogliati et al., 2016a). Structural data indicates that COX7A2L can structurally replace its isoform COX7A at the interaction interface of C III and C IV and thereby promotes SC formation (Letts et al., 2016). Taken together, the different observations regarding the role of COX7A2L/SCAF1 indicate the existence of different assembly pathways and thus different SC species mediated by different COX7A isoforms which can promote SC formation and stabilization in a tissue-specific manner, probably to adapt specific metabolic conditions (Cogliati et al., 2021; Letts & Sazanov, 2017; Lobo-Jarne et al., 2020).

### 1.4 Organization and Maintenance of Mitochondrial DNA

Mitochondrial DNA is a circular, double-stranded DNA molecule of 16.6 kilo base (kb) size (Figure III). The mitochondrial genome is highly condensed and encodes only for a set of 13 critical constituents of the OXPHOS machinery as well as for two rRNAs and 22 tRNAs (Gustafsson et al., 2016). All other factors required for proper mitochondrial function are encoded in the nuclear genome, translated by cytoplasmic ribosomes and imported into mitochondria. Accurate maintenance and expression of mtDNA (Figure 1c) are of high importance for the cell as defects in associated processes cause mitochondrial diseases which can either be tissue-specific or presented as a multi-system disorder. Hence, it is not surprising that around one fifth of the mitochondrial proteome is implicated in mtDNA maintenance and expression (Morgenstern et al., 2021). Because every cell contains multiple copies of mtDNA, mutations can be present in all mtDNA molecules and thus are homoplasmic, or just a fraction of the mtDNA is mutated leading to a phenomenon called heteroplasmy. Consequently, the level of heteroplasmy determines the grade of disease severity. Interestingly, mtDNA inheritance is exclusively maternally-mediated (Hock et al., 2020; Miranda et al., 2022).

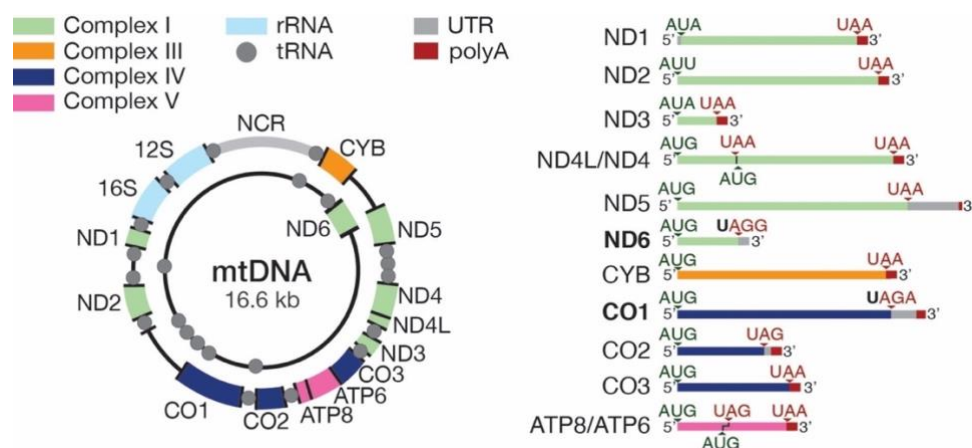


**Figure III: Mitochondrial DNA.** Left: Mitochondrial DNA (mtDNA) is shown as a circular, double-stranded DNA molecule of 16.6 kb size, encoding 37 mitochondrial genes with a small non-coding region (NCR, light grey). Protein coding sequences are shown in green (complex I), orange (complex III), blue (complex IV) and pink (complex IV). mRNAs and rRNAs (light blue) are interspersed with tRNAs (dark grey). Right: start (green) and stop (red) codons of processed indicating beginning and end of the respective open reading frame (ORF). Untranslated regions (UTRs) are depicted in grey and poly(A) tails (red) at the 3' end are required to complete the UAA stop codon. Two transcripts (*MT-CO1* and *MT-ND6*, in bold) are terminated by the non-standard stop codons AGA or AGG.

Compared to the nuclear genome, the organization of the circular mtDNA differs tremendously: the absence of introns or splicing events leads to transcription of two long, polycistronic transcripts. Whereas most of the genetic information including both rRNAs, ten mRNAs and 14 tRNAs is located on the heavy (H) strand, the light (L) strand contains only information for a single mRNA and eight additional tRNAs. There is only one non-coding region (NCR), which serves as a control region. It harbors regulatory elements required for the replication of mtDNA and dedicated promoters for transcription from the H- and L-strand, namely HSP, LSP and LSP2, as well as the 7S DNA containing triple-stranded D-loop region (Gustafsson et al., 2016; Tan et al., 2022). The mitochondrial genome is localized in discrete mtDNA foci also termed mitochondrial nucleoids, which are closely associated with the IMM. In these protein-DNA complexes the mtDNA gets compacted by its core constituent TFAM (Transcription Factor A mitochondrial), which can interact, unwind and bend mtDNA and thus also regulates levels of replication and transcription. Nucleoids mainly contain essential factors for mtDNA replication and transcription (Bogenhagen, 2012; Falkenberg & Gustafsson, 2020; Farge & Falkenberg, 2019).

#### **1.4.1 Mitochondrial Replication and Transcription**

The replication machinery comprises the core components such as the DNA polymerase gamma (Poly $\gamma$ ); the mitochondrial helicase TWINKLE, which unwinds the replication fork, and the mitochondrial single-strand binding protein (mtSSB) that stabilizes the resulting DNA single strands and protects them from nucleases. Following the strand displacement model, replication initiates at the H-strand from the origin of replication ( $O_H$ ) and after Poly $\gamma$  has synthesized approximately two-thirds from the H-strand, it passes the origin of replication of the L-strand ( $O_L$ ) and enables primer synthesis by the mitochondrial RNA polymerase (POLRMT). Only then the simultaneous synthesis of both strands can occur, leading to the complete replication of mtDNA (Farge & Falkenberg, 2019; Gustafsson et al., 2016).

Besides to its role during mtDNA replication, the highly conserved, single-subunit POLRMT is also a main factor during mtDNA transcription but requires additional factors to bind DNA and initiate transcription. First, TFAM binds upstream of the HSP, introduces a U-turn in the mtDNA and thereby recruits POLRMT, forming the pre-initiation complex. Further recruitment of mitochondrial transcription factor B2 (TFB2M) completes the initiation complex by melting the promoter region and thus allowing RNA synthesis. After dissociation of TFB2M, mitochondrial transcription elongation factor (TFEM) binds to POLRMT, enhances its processivity and starts elongation to generate two nearly full-length polycistronic transcripts of the mtDNA. Transcription termination is controversially discussed and apparently, both strands are terminated differently. To date, only one mitochondrial transcription termination factor (MTERF1) is known, which is required for termination of LSP-derived transcripts. Termination from HSP transcripts still remains poorly understood (Hillen et al., 2018; Miranda et al., 2022; Rackham & Filipovska, 2022).

### 1.4.2 Maturation of Mitochondrial Transcripts

The emerging primary transcripts are sequestered into mitochondrial RNA granules (MRG), which serve as centers for RNA processing (Figure 1c). Mitochondrial RNA-binding proteins (RBP), important for co- and posttranscriptional RNA modifications and maturation as well as mitoribosome biogenesis, are highly concentrated in these discrete foci thus allowing an efficient regulation of these processes (Antonicka & Shoubbridge, 2015; Jourdain et al., 2013). Maturation of these long polycistronic transcripts follows the '*tRNA punctuation model*' (Ojala et al., 1981): the separating tRNA sequences (Figure III) are endonucleolytically excised from the other coding sequences first at their 5' end and then at 3' termini by the ribonuclease enzymes RNase P complex and RNase Z (encoded by *ELAC2*), respectively, and thereby individual mRNAs and rRNAs are liberated. Surprisingly, mitochondrial RNase P is, unlike most other members of the RNase P family, devoid of a catalytical *trans*-acting RNA and is therefore not considered as a ribozyme. Instead, the proteinaceous complex consists of the tRNA methyltransferase MRPP1 (TRMT10), a tetramer of the dehydrogenase MRPP2 (SDR5C1) and MRPP3 (PRORP) which is the active endonuclease (Bhatta et al., 2021; Holzmann et al., 2008; Rackham et al., 2016). *ELAC2* is a highly conserved endonuclease found in all kingdoms of life and cleaves mRNAs already processed by RNase P (Brzezniak et al., 2011; Sanchez et al., 2011). However, since not all mRNAs are flanked by tRNA sequences, an alternative maturation mechanism is required to further process pre-mRNAs. This is for example the case between the bicistronic precursor transcripts of *MT-ATP8/6* and *MT-CO3*, at the junction of *MT-ND5* and *MT-CYB* and at the 5' end of pre-*MT-CO1* mRNA. Mitochondrial targeted members of the FASTK (Fas-activated serine/threonine kinases) protein family, especially FASTKD4 and FASTKD5, are involved in this non-canonical cleavage of non-punctuated precursors, although the exact mechanism is not well understood as they often exhibit opposing functions (Jourdain et al., 2017; Ohkubo et al., 2021).

Further maturation of mt-tRNAs involves a plethora of posttranscriptional modifications and the addition of a CCA trinucleotide at the 3' end by the tRNA nucleotidyltransferase TRNT1. Nucleotide modifications like methylation or pseudouridylation are important for stabilization and translational fidelity. For example, chemical modifications in the anticodon region of the tRNA enable an expanded codon recognition ability via 'wobble base pairing' since mitochondria only have 22 tRNAs which decode 60 amino acid codons. To ensure correct folding of 12S and 16S rRNA and to confer stability during mitoribosome biogenesis, a set of rRNA modifications like methylations or pseudouridylations are required. Importantly, maturation of the peptidyl transferase center (PTC) within the large mitoribosomal subunit (mtLSU) and the decoding center (DC) within the small mitoribosomal subunit (mtSSU) are relevant steps for proper mitoribosome functionality (Bohnsack & Sloan, 2018).

Mitochondrial mRNAs (Figure III) show crucial differences compared their cytosolic and bacterial counterparts: mt-mRNAs are devoid of 5' cap structures and introns and have only little or mostly no 5' and 3' untranslated regions (UTRs) like the bacterial Shine Dalgarno sequence, leading to a leaderless translation initiation. A poly(A) tail is added to all mt-mRNAs

except of *MT-ND6*. For seven mt-mRNAs the posttranscriptional polyadenylation at the 3' end by the mitochondrial poly(A) polymerase (mtPAP) is required to complete the stop codon UAA. Unlike in bacteria, where a poly(A) tail marks transcripts for degradation, polyadenylation of mitochondrial mRNAs is mostly implicated in their stabilization, although there are some cases where it leads to a transcript-specific destabilization (Chang & Tong, 2012; Temperley et al., 2010b). Another important element required for the stability of H-strand transcribed mt-mRNA is the presence of the LRPPRC/SLIRP complex. LRPPRC (member of the leucine-rich pentatricopeptide repeat (PPR) motif protein family) is an RBP which, when stabilized and protected from degradation by SLIRP (SRA stem-loop-interacting RNA-binding protein), can bind to single-stranded RNA, in this way relaxing its secondary structure and making it available for other RBPs. Thus, the LRPPRC/SLIRP complex accomplishes the task of an mtRNA chaperone (Sasarman et al., 2010; Siira et al., 2017). In this manner, it not only ensures a coordinated translation by making mRNAs available to engage with the mitoribosome, but also enables an extended access of mtPAP to further enhance polyadenylation of a subset of mt-mRNAs. Thereby it increases their stability by simultaneously preventing their degradation by the mitochondrial degradosome (Chujo et al., 2012). RNA decay is a fundamental process in mitochondria to maintain gene expression by controlling the levels of relevant RNAs. Moreover, it is important for RNA surveillance by degrading potentially toxic RNAs or anti-sense or non-coding by-products from previous mtRNA processing steps. The mitochondrial degradosome is essential for this mtRNA turnover and formed in discrete foci (D-foci) of the processive 3'-5' polynucleotide phosphorylase (PNPase) and the ATP-dependent helicase SUV3 (Borowski et al., 2013; Wang et al., 2014; Wang et al., 2009). Together as a heteropentameric complex, dimeric SUV3 mediates continuous binding initially at a 3' overhang and preferentially unwinds structured dsRNA while making it accessible for PNPase, which cleaves its substrate in 5' direction until the fragment is only six nucleotides long (Jain et al., 2022). Remaining fragments are finally degraded by additional 3'-5' exonucleases like REXO2 (Nicholls et al., 2019).

### 1.5 Mammalian Mitochondrial Ribosomes

Once all factors required for translation have been matured, they can engage with the mitoribosome and translate the transcribed information into polypeptides. The 55S mammalian mitoribosome is assembled from nuclear-encoded mitoribosomal proteins (MRPs) and mitochondrial-encoded structural rRNAs, a structural tRNA and, like all ribosomes, consist of two individual subunits: the 39S mtLSU, comprised of 16S rRNA, tRNA<sup>Phe</sup> and 52 MRPs (Brown et al., 2014; Greber et al., 2014) and the 28S mtSSU, assembled of 12S rRNA and 30 MRPs (Kaushal et al., 2014), build a ribonucleoprotein complex of 2.7 MDa in total molecular mass (Figure IV). Interestingly, high-resolution structural studies revealed that mammalian mitoribosomes differ significantly from their bacterial ancestor regarding their protein and RNA composition as well as their structure. In fact, the protein:RNA ratio is reversed in the mammalian mitoribosome (2:1) when compared to its bacterial 70S counterpart (1:2), raising the question of the functional relevance of this phenomenon. While mammalian mitoribosomes have approximately 50 % less rRNA, they acquired 36 mitochondrion-specific proteins and additionally, many proteins conserved from bacteria have mitochondrion-specific

extensions or insertions (Amunts et al., 2015; Greber et al., 2015; Sharma et al., 2003). Contrary to the common hypothesis that mitochondrion-specific ribosomal proteins have been acquired to compensate reduced rRNA components, it is now accepted that there is no correlation and instead, these proteins partially adopt new structural functions in the periphery of mitoribosomes. The more porous, structurally conserved catalytical core is surrounded by a shell of mitochondrion-specific proteins which do not interfere with catalytically conserved regions and may serve to shield the rRNA from oxidative damage by ROS (Greber et al., 2014).

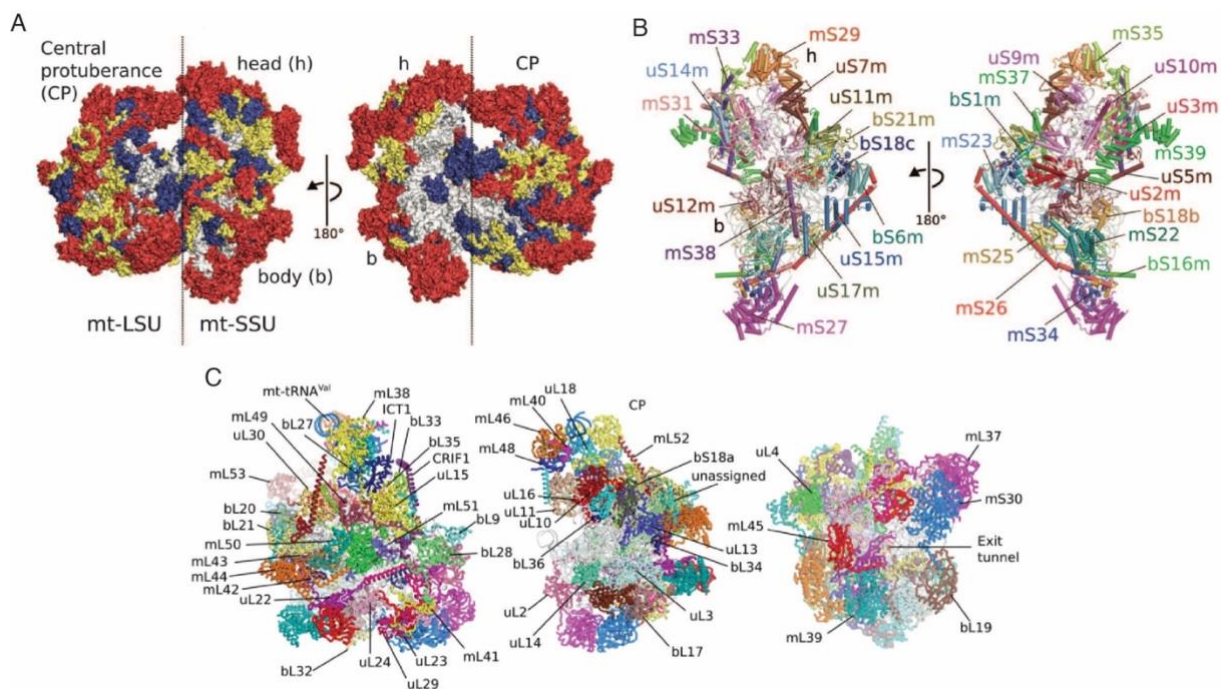


**Figure IV: Human 55S Mitoribosome.** (A) Complete Structure of the mitochondrial 55S ribosome. Depicted is the rRNA core (grey), proteins conserved from bacteria (blue), extensions of homologous proteins (yellow) and mitochondria-specific proteins (red). (B) Overview of mitoribosomal proteins (MRPs) from the mtSSU and (C) the mtLSU, shown from (left to right) the solvent-facing, side and exit tunnel view. Figures taken from (Amunts et al., 2015; Brown et al., 2014). Reprinted with permission from AAAS.

Evolutionary, remodeling from the ancestral prokaryotic ribosome to the mammalian mitoribosome can be divided into two subsequent phases. In a first constructive phase, mitochondrion-specific proteins have been acquired and only then, the gradual reduction of rRNA occurred, both due to reaction to marginally deleterious mutations or deletions in the mtDNA, respectively. Interestingly, all partially mtDNA-encoded OXPHOS complexes similarly evolved in parallel to the mitoribosomal evolution (van der Sluis et al., 2015).

Functionally, the specific roles of the two subunits and respective regions involved in translation are conserved among mammalian mitoribosomes and bacteria as well as cytoplasmic ribosomes. Whereas the mtSSU (Figure IVb) serves as a platform for engaging, binding and decoding mRNAs in the DC, the mtLSU (Figure IVc) comprises the PTC and the polypeptide exit tunnel (PET). Especially the tRNA-binding sites and the decoding mechanism is well conserved and mitoribosomes possess an aminoacyl (A), a peptidyl (P) and an exit (E) site. However, another difference to bacterial ribosomes is the absence of the structural 5S rRNA in



the central protuberance (CP) of the mtLSU, a key structural feature for intersubunit interactions and tRNA binding. A tRNA (tRNA<sup>Phe</sup> in human, tRNA<sup>Val</sup> in porcine) has replaced the 5S rRNA and serves as structural scaffold in mammalian mitoribosomes building extensive contacts to its neighboring MRPs (Brown et al., 2014; Greber et al., 2014). In mammalian mitochondria, the number and composition of the intersubunit bridges, important for the integrity of the ribosome, has changed compared to the bacterial ribosome. They are comprised mainly of protein-protein or protein-RNA interactions and are less abundant than in bacteria (Sharma et al., 2003). Since mitoribosomes only synthesize highly hydrophobic membrane proteins of the OXPHOS complexes, the PET is comprised of hydrophobic residues, resembling the hydrophobic membrane environment and thus prevents premature folding of the proteins before their engagement with specific maturation factors. Interactions of the integral MRP mL45, which serves as a PET-plug when mitoribosomes are not actively translating, with the insertase OXA1L anchors the mitoribosomes at the IMM and creates a great proximity for efficient delivery of the OXPHOS components to their destined position in the IMM (Englmeier et al., 2017; Itoh et al., 2021). Further characteristic features implicated in key translational steps will be discussed in section 1.6.

Mitoribosomes can be inhibited by antibiotics and other drugs to varying extends due to the conservation of key functional regions. Substrates often bind at the DC, the PET or inhibit involved factors and thereby directly or indirectly prevent translation initiation, elongation or peptide release. A well-studied example is the usage of chloramphenicol (CAM) which binds at the mitoribosomal A-site and thus inhibits elongation, stalls translation and prevents mitoribosomal rescue as this requires a vacant A-site (Bulkley et al., 2010; Richter et al., 2013). Therefore, antibiotics need to be designed in a way that autotoxicity is prevented. On the other hand, inhibiting the mitoribosomes using specific drugs can be used during cancer therapy as this leads to the arrest of cell proliferation (Greber & Ban, 2016).

The biogenesis of the mitoribosome starts co-transcriptionally in MRGs and is a highly complex, hierarchical process. It involves many assembly factors of a broad spectrum of mainly GTPases but also RNA helicases and other RBPs as well as aforementioned rRNA modifying enzymes, required to assemble the MRPs together with the matured rRNAs. It is accepted that assembly occurs in an energy-consuming, modular fashion and requires quality checkpoints in order to presume to the next step (Bogenhagen et al., 2018). Several maturation factors act as anti-association factors to prevent premature subunit joining. For the assembly of the mtLSU the GTPases GTPBP5, GTPBP6, GTPBP7 and GTPBP10 are among the best studied ones, whereas MTG3 and ERAL1 are involved in mtSSU biogenesis (Chandrasekaran et al., 2021; Dennerlein et al., 2010; Hillen et al., 2021; Kolanczyk et al., 2011; Lavdovskaia et al., 2020; Lavdovskaia et al., 2018; Maiti et al., 2020; Maiti et al., 2021). However, the exact scheme of maturation is controversially discussed and needs further investigations.

## 1.6 Mitochondrial Translation

In the final step of protein biosynthesis, the information stored in mRNA gets translated into functional proteins following the basic steps of translation: the mitoribosome binds to the start codon of the mt-mRNA and initiates translation, decodes the RNA sequence by codon – anti-codon matching and elongates the polypeptide. If a stop codon is reached, translation is terminated, the peptide released and the mitoribosomal subunits are recycled in order to be available for another translation cycle (Figure V). All steps are aided by a dedicated set of nuclear-encoded translation factors. Nascent polypeptide chains are then co-translationally inserted into the IMM where they are assembled into respective OXPHOS complexes. However, even though mitoribosomes evolved from a bacterial ancestor, certain features of translation differ from the prokaryotic mechanisms (Kummer & Ban, 2021; Nadler et al., 2022).

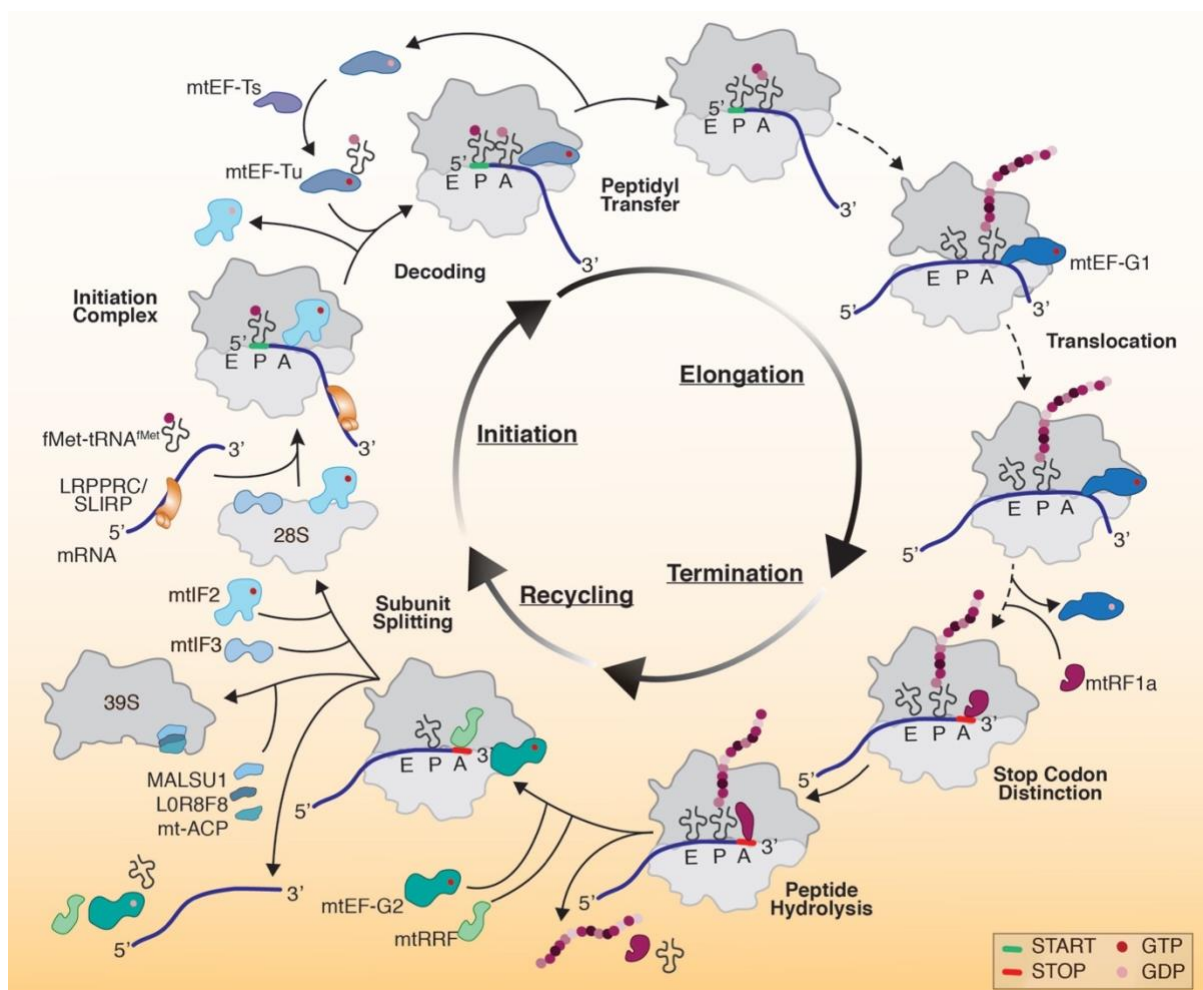


**Figure V: Mitochondrial Translation Cycle.** Synthesis of mitochondrial proteins follows in four, mechanistically conserved phases at the mitoribosome aided by specialized mitochondrial translation factors. Initiation is started by binding of mtIF3 and subsequently mtIF2 bind to the mtSSU to form pre-initiation complexes in order to prevent pre-mature subunit joining. mtIF3 dissociates from the complex and then the mtLSU and mRNA are assembled and the initiator fMet-tRNA<sup>Met</sup> is bound to start codon at the P-site to form the initiation complex. Elongation can be divided into three repetitive steps: first, the next codon is decoded by delivery of the matching aminoacylated tRNA by mtEF-Tu to the A-site of the decoding center (DC) of the mtSSU. Formation of the peptide bond is facilitated by conserved residues of the peptidyl transferase center (PTC) at the mtLSU. Then, the mRNA-tRNA module is translocated to the next codon through binding of mtEF-G1, which stabilizes tRNAs in their hybrid states and induces large-scale conformational changes and rotation of the mtSSU. This process is terminated by recognition of the stop codon by the codon-specific release factor mtRF1a, which elongates upon correct binding

and thus triggers peptide release. The mitoribosome is recycled for another round of translation by mtRRF together with mtEF-G2 to eject the remaining mRNA and tRNAs. To prevent pre-mature subunit association, mtIF3 binds to the mtSSU again and the MALSU1-LOR8F8-mtACP module binds to the mtLSU.

### 1.6.1 Initiation

Compared to prokaryotes, translation initiation is tremendously different in mammalian mitochondria in regard of initiation factors, which aid stepwise assembly of the initiation complex (IC) and also of the binding of the leaderless mRNA. Briefly, in prokaryotes, the initiation factors IF1, IF2 and IF3 form a pre-initiation complex together with the initiator tRNA. Then, the mature IC is formed by engagement of the Shine-Dalgarno (SD) sequence of the mRNA with the complementary anti-SD sequence of the SSU rRNA, start codon recognition and release of the initiation factors, which enables the joining of the LSU (Rodnina, 2018).

In mammalian mitochondria, the role of mtIF3 appears to be diverged in respect to its bacterial counterpart IF3 (Bhargava & Spremulli, 2005; Christian & Spremulli, 2009). Although it is accepted that mtIF3 has a regulatory function in regard of coordination and surveillance of the events of IC formation, its exact mode of action is not fully solved yet. On the basis of recent structural studies (Khawaja et al., 2020), the following mechanism has been suggested: first, mtIF3 may actively disassembles the 55S monosome and binds to the mtSSU in order to form the pre-initiation complex I (mtPIC1), which precludes subunit joining as well as sterically prevents binding of the initiator tRNA fMet-tRNA<sup>Met</sup>. The formed interactions induce conformational changes and allow binding of mtIF2, thus building the pre-initiation complex 2 (mtPIC2). Like in bacteria, mtIF2 recruits fMet-tRNA<sup>Met</sup> and facilitates its binding to the P-site. Simultaneously, mtIF2 can substitute for the loss of the universally conserved initiation factor IF1 which is another fundamental alteration in mammalian mitochondria. An insertion in mtIF2 blocks the mitoribosomal A-site instead, preventing premature binding of an elongator tRNA (Gaur et al., 2008; Yassin et al., 2011).

A characteristic structural feature of the mtSSU is the extensively remodeled mRNA channel. In bacteria the entry of the mRNA channel is a ring-like structure composed of uS3-5, which unwinds structured mRNA with their helicase activity ensuring that only single-stranded, unstructured mRNA molecules can enter the ribosome. In mammals uS4 and the C-terminal domain of uS3 are missing but are partially compensated by extensions of uS5m and four mitochondrion-specific MRPs (Kaushal et al., 2014). Due to the leaderless nature of mt-mRNAs, engagement and binding of them also differs in mammalian mitochondria. Particularly, the LRPPRC/SLIRP complex is implicated in the delivery of structurally relaxed mRNAs as it closely associates with mS39. This mitochondrion-specific MRP gates the channel entry and may take over the leaderless mRNA. A positively charged, mitochondrion-specific extension of uS5m then guides the mRNA towards the ribosomal P-site where the start codon can pair with the anticodon of the initiator tRNA, aligning the mitoribosome in the proper reading frame (Aibara et al., 2020; Kummer et al., 2018). *In vitro* reconstructions and ribosome profiling of knockout mice have shown that mtIF3 fulfills a proofreading function as known for prokaryotic IF3. Here, mtIF3 is required for mRNA accommodation at the mtSSU followed by subsequent pairing of fMet-tRNA<sup>Met</sup> prior to joining of the mtLSU to form the mature IC or alternatively, to prevent

an inefficient IC formation by rejecting a fMet-tRNA<sup>Met</sup> in absence of mRNA (Koripella et al., 2019a; Rudler et al., 2019). However, since the beforementioned structural study (Khawaja et al., 2020) excluded concurrent binding of mtIF3 and fMet-tRNA<sup>Met</sup>, the exact order of mRNA, fMet-tRNA<sup>Met</sup> and mtLSU recruitment for the formation of matured IC, which can then presume with elongation, still remains elusive (Khawaja et al., 2020; Lee et al., 2021).

### 1.6.2 Elongation

During peptide elongation, the genetic information saved in mRNA is translated into the functional polypeptide sequence. The mechanistic basis of this energy-consuming elongation cycle is highly conserved throughout bacteria and eukaryotes and comprises three distinct, repetitive steps surveilled by translational GTPases which mediate the high fidelity of this process in order to avoid frameshifting. First, decoding occurs by delivery and pairing an aminoacylated (aa-) tRNA with its cognate mRNA codon, then the peptide bond of the newly delivered amino acids with the nascent polypeptide chain can be formed before the mitoribosome can translocate the mRNA-tRNA complex (Kummer & Ban, 2021).

Like its bacterial counterpart, GTP-bound mtEF-Tu (mitochondrial elongation factor thermo unstable) forms a ternary complex with an aa-tRNA, thus being able to deliver the next amino acid to the vacant A-site at the DC of the mtSSU (Cai et al., 2000; Worjax et al., 1997). The codon-anticodon basepairing is proofread by two conserved decoding residues in helix 44 (h44) of the 12S rRNA and similar to prokaryotes, correct binding induces conformational changes in the switch domain of the factor, placing it in proximity to the sarcin-ricin loop (SRL) of the 16S rRNA which can then trigger the intrinsic GTPase activity of mtEF-Tu and thus GTP is hydrolyzed (Desai et al., 2020; Rodnina et al., 2017; Voorhees et al., 2010). After GTP hydrolysis, the aa-tRNA is bound to the ribosomal A-site and interactions with GDP-bound mtEF-Tu are weakened so that it is released from the mitoribosome. Regeneration of mtEF-Tu is carried out by its guanine exchange factor mtEF-Ts (mitochondrial elongation factor thermo stable). In this way, mtEF-Tu returns to its GTP-bound form (Schwartzbach & Spremulli, 1989).

Once the aa-tRNA is bound to the A-site, the nascent polypeptide chain attached to the P-site tRNA is transferred onto the aa-tRNA within the mitoribosomal active site, the PTC. The great conservation of the PTC explains the highly similar mechanism of the peptidyl transferase reaction: conserved nucleotides of the 16S rRNA coordinate the 3' CCA ends of the A- and P-site tRNAs in order to expose the P-site tRNA in a way that allows a nucleophilic attack from the  $\alpha$ -amine of the A-site tRNA. Like this, one amino acid is added to the nascent polypeptide chain, now attached at the A-site tRNA, leaving the P-site tRNA deacylated (Greber et al., 2014; Rodnina, 2018; Voorhees et al., 2009).

Simultaneously, the ribosome has to move the mRNA-tRNA module to the next codon with great accuracy in order to avoid a frameshift on the messenger. This high-fidelity translocation is aided by elongation factor G (EF-G, (Frank & Agrawal, 2000; Peng et al., 2019). Interestingly, bacterial EF-G, which has a dual function by being involved in elongational translocation and ribosome recycling, has two paralogs in mammalian mitochondria. Whereas mtEF-G1 catalyzes

mRNA-tRNA movement during elongation, mtEF-G2 is implemented in mitoribosome recycling (Tsuboi et al., 2009). However, the basic principle underlying mRNA-tRNA translocation is preserved from bacteria (Rodnina et al., 2019). Binding of mtEF-G1 stabilizes the otherwise oscillating tRNAs preferentially in the hybrid P/E or A/P state, where their 3' CCA end adopts a shifted occupation on the mtLSU but their anticodon region is still bound at the P- or A-site, within the DC (Adio et al., 2015; Desai et al., 2020). Simultaneously, a ratchet-like intersubunit rotation is enhanced upon mtEF-G1 binding, where the complete mtSSU rotates in respect to the mtLSU. In addition to this large-scale motion, also the head of the mtSSU swivels further, so that through a yet unknown mechanism, the tip of mtEF-G1 domain IV can trigger unlocking of the mRNA-tRNA module. Upon GTP hydrolysis, back-rotation of the mtSSU body and head can be observed, which positions the deacylated tRNA into the classical E-site and the aa-tRNA into the P-site (Koripella et al., 2020; Kummer & Ban, 2020). Consequently, GDP-bound mtEF-G1 leaves the ribosome and thus allows binding of the next tRNA.

### **1.6.3 Termination**

Protein synthesis is terminated when a codon triplet on the mRNA, which is not assigned to a cognate tRNA, is present in the ribosomal A-site. These stop codons are specifically recognized by dedicated release factors, which are able to trigger cleavage of the ester bond between the polypeptide chain and the peptidyl tRNA, thereby releasing it from the ribosome. Those two functions are distributed over the different protein domains (Figure VI). While domain 2 and 4 enable the protein to distinguish between sense and stop codons and consequently binding the latter (Korostelev, 2021), domain 3 harbors the essential GGQ motif critical for the peptidyl tRNA hydrolase (PTH) activity and consequently promotes the release of the newly synthesized polypeptide. This motif is highly conserved in all three kingdoms of life and thus can be found in all known release factors (Frolova et al., 1999; Mora et al., 2003). Even though the first mitochondrial release factor was already discovered in the late 90's (Lee et al., 1987; Zhang & Spremulli, 1998), comparably little is known regarding mitochondrial peptide release to date. Considering the  $\alpha$ -proteobacterial heritage of mitochondria, a lot can be learned from the bacterial counterparts.

#### **1.6.3.1 Translation Termination in Bacteria**

Decades ago a decoding mechanism in prokaryotes was described, which is required for recognizing the termination codon and for cleaving the polypeptide chain from the peptidyl-tRNA on the translating 70S ribosomes. Specific, enzymatically active release factors are responsible for the recognition of the translation termination codons UAA, UAG and UGA in a codon-anticodon-dependent manner (Capecchi, 1967). The discrimination of these codons is achieved by two different release factors: RF1 and RF2. Whereas both can recognize UAA as a stop codon, RF1 is further responsible for the recognition of UAG and RF2 can further decode UGA as stop signal (Caskey et al., 1968; Scolnick et al., 1968).

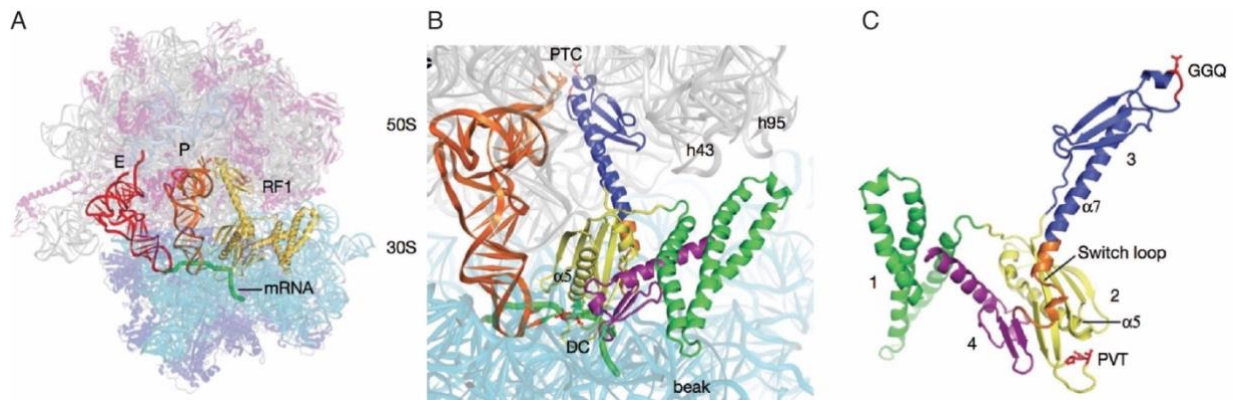


**Figure VI: Bacterial Termination Complex.** (A) *Thermus thermophilus* RF1 (yellow) binds in the A-site of the 70S ribosome next to the P-site tRNA (orange) and E-site tRNA (red) and forms the termination complex. (B) Orientation of RF1 with decoding domain 2 (yellow) and 4 (purple) bound at the decoding (center) of the 30S SSU and the PTH activity conferring domain 3 (blue) reaching the peptidyl transferase center (PTC) of the 50S LSU by opening of the switch loop (orange). (C) Domain structure of RF1, showing the essential domains (as in B) and motifs: PVT motif and  $\alpha 5$  helix of domain 2 and the GGQ motif of domain 3. Images taken from (Laurberg et al., 2008). Reprinted with permission from Springer Nature (license number 5400200768026).

### 1.6.3.1.1 Bacterial Codon Recognition

A key feature of canonical release factors is to distinguish between sense and antisense codons in the ribosomal A-site. This essential property is mediated by a tripeptide codon recognition motif of the release factor itself, which is reminiscent of a tRNA anticodon. Unlike the pairing of a codon to its cognate tRNA, no additional interactions with the ribosome or proofreading mechanisms are required for highly accurate discrimination of stop codons (Freistroffer et al., 2000; Sund et al., 2010). For bacterial RF1 and RF2 the decoding motif consists of either proline-x-threonine (PxT), or serine-proline-phenylalanine (SPF) that mediates the codon specificity for UAG and UAA or UGA and UAA, respectively. This step is an essential prerequisite to ensure that only mature polypeptides are hydrolyzed and subsequently released from the peptidyl-tRNA (Ito et al., 2000).

On a molecular basis, the precise decoding mechanism (Figure VIIa, b) has been solved with emerging high-resolution structures of the respective bacterial release factors in complex with 70S ribosomes (Korostelev et al., 2008; Laurberg et al., 2008; Petry et al., 2005; Weixlbaumer et al., 2008). It appeared that not only the aforementioned recognition motif plays an important role, but also interactions of the tip of the  $\alpha 5$  helix are necessary to recognize and bind to the stop codon. Together, both structural elements form ‘molecular tweezers’: in RF1, Gly116 and Glu119 (*Thermus thermophilus* numbering) at the tip of the  $\alpha 5$  helix and Thr186 in the PxT motif are orientated in a way that only hydrogen bonds with a uridine as the first nucleotide can be tolerated and these multiple interactions explain the strong discrimination at that first stop codon position. Thr186 is also involved in recognition of the adenine in the second position (Laurberg et al., 2008; Petry et al., 2005). Recognition of the third stop codon position seems to be somewhat independent of the one of the first two bases. This nucleotide is stacked against G530 of the 16S rRNA and, in the case of RF1, detected by Gln181 and Thr194 which allows the recognition of both, adenine and guanosine as the third nucleotide. Together, G530, A1492 and A1493 are universally conserved residues of h44 (rRNA helices of the SSU are

denoted as lower-case letters; helices of the LSU as capital letters) of the DC and are critical for stop codon discrimination. They have to adopt a different conformation, compared to a decoding event of a sense codon, to allow accommodation of a stop codon to be sandwiched between the release factor and the DC. The active termination complex is further stabilized by interactions of nucleotide A1913 of H69 of the LSU (Laurberg et al., 2008).

In comparison, in RF2 the first position uridine is solely recognized by the tip of the  $\alpha 5$  helix, whereas the respective Ser206 is only positioned against the second base and can form an H-bond either with adenine or guanosine. However, Gln181 is not present in RF2. Instead, the hydrophobic side chain of Val203 at the homologous position prevents interaction with guanine and therefore the third position is restricted to an adenine (Korostelev et al., 2008; Weixlbaumer et al., 2008).

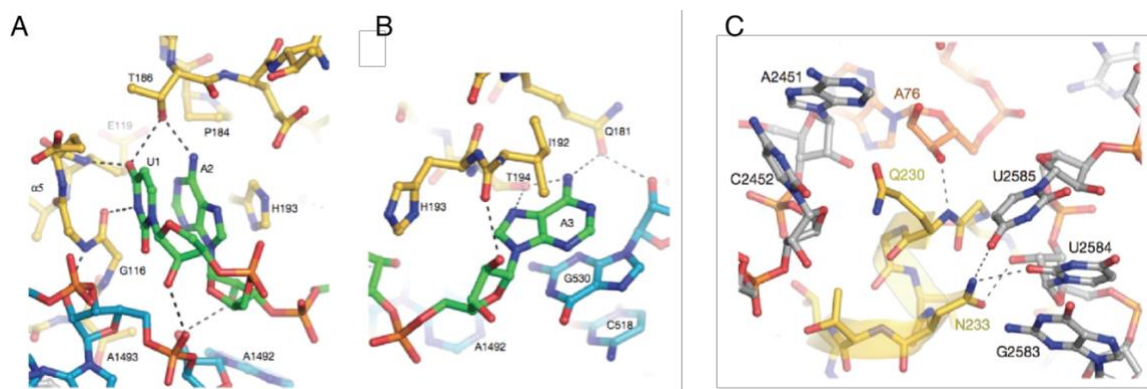


**Figure VII: Interactions of the RF1 termination complex within the decoding center (DC) and the peptidyl transferase center (PTC).** (A) + (B) The mRNA (green) is sandwiched by the DC (cyan) and RF1 (yellow). The three stop codon bases UAA are coordinated by critical nucleotides A1492, A1493 and G530 of the 16S rRNA (cyan) as well as amino acid residues Gly116, Glu119, Gln181 and Thr194 from RF1 (yellow). (C) The GGQ motif of RF1 (yellow) coordinates the 3' CCA end of the P-site tRNA (orange) within the PTC (grey). Images taken from (Laurberg et al., 2008). Reprinted with permission from Springer Nature (license number 5400200768026).

Release factors have to constantly 'test' whether a sense or antisense codon is present at the A-site. This process must happen very fast in order not to disturb protein elongation through competing with tRNAs for binding of the A-site codon, but also with high fidelity to ensure accurate translation termination. Two kinetic constants define this multi-step mechanism: in the presence of a sense codon, the rate of dissociation ( $K_D$ ) of the release factor is highly increased and the catalytic rate constant ( $k_{cat}$ ) is reduced. The latter can only be explained by conformational changes within the release factor. Release factors enter the DC in a 'closed' state, where the codon recognition domains 2 and 4 can interact with the A-site codon, but the GGQ motif containing domain 3 is positioned far away from the PTC at the LSU. If a stop codon is then sensed with high affinity, large conformational changes are triggered so that the release factor exhibits an 'open' conformation with domain 3 being able to reach the PTC. Vice versa, a fast dissociation prevents these conformational changes. The coupling of codon recognition (and subsequent binding) with conformational changes, leading to peptide release, represents a sophisticated control mechanism for efficient yet accurate translation termination without energy consumption as it is the case for proofreading steps during translation elongation (Freistroffer et al., 2000; Hetrick et al., 2009; Laurberg et al., 2008; Rawat et al., 2003).

### 1.6.3.1.2 Bacterial Peptide Release

To span the distance of approximately 75 Å from the DC of the 30S SSU to the PTC at the 50S LSU, the release factor has to elongate its compact structure, in which the recognition domain and the catalytically active GGQ domain are only 23 Å apart. Upon binding to a stop codon, structural rearrangements in the DC take place which in turn trigger the opening of the release factor. Induced by the tight association of the release factor with the stop codon, the stacking of the third nucleotide against G530 of the 16S rRNA causes residue A1492 from h44 of the 16S rRNA to flip out from its position, similar as in the decoding of sense codons, so that nucleotide A1913 at H69 of the 23S rRNA can be packed onto A1493, which now remains stacked at its original position within h44. Only then, the flexible linker between the catalytic domain 3 and the decoding domain 4, termed switch loop, can undergo structural rearrangements. Usually, in its closed conformation, domain 3 is tethered at domain 2 by hydrophobic interactions, but the structural rearrangements in the DC lead to packing of the switch loop at the rearranged h44, which before would have resulted in a steric clash. In turn, this liberates domain 3 from its compact conformation and enables the GGQ-motif containing  $\alpha 7$  helix to elongate and reach the PTC, where new interactions within the PTC are established and the GGQ motif binds in proximity to the 3' CCA end of the peptidyl-tRNA (Figure VIIc). For peptide release, access for a single water molecule must be provided to hydrolyze the ester bond between the deacetylated P-site tRNA and the nascent polypeptide chain. This kind of access channel is only possible with two glycine residues as they lack any side chain and thus provide enough space. By forming an H-bond and thereby coordinating the leaving OH-group of the terminal ribose A76 of the P-site tRNA, the highly conserved glutamine aids in hydrolyzing the ester bond of the nascent polypeptide chain and the tRNA: only through this interaction a nucleophilic attack of a water molecule and thus hydrolysis is possible and the peptide can be released (Korostelev et al., 2008; Laurberg et al., 2008; Svidritskiy & Korostelev, 2018; Weixlbaumer et al., 2008).

### 1.6.3.1.3 Recycling of Release Factors

Release Factors can be categorized into two classes: class I release factors comprise factors that bind to the ribosome upon the presence of a stop codon in the A-site which then consequently leads to the hydrolysis of the peptide bound from P-site tRNA. All class I release factors such as bacterial RF1 and RF2 harbor the universally conserved GGQ motif. After hydrolysis RF1 and RF2 remain tightly associated with the ribosome. Class II release factors are accessory factors which do not directly facilitate codon recognition and peptide release, but act after the peptide is released by accelerating the dissociation of RF1 or RF2 and thereby priming the ribosome for recycling (Youngman et al., 2008). Release Factor 3 (RF3) is a translational GTPase and the prokaryotic class II release factor implicated in the recycling of class I release factors (Freistroffer et al., 1997). Interestingly, RF3 is not an universally essential protein: even though *E. coli* strains lacking RF3 show growth defects under compromised growth conditions, there are certain bacterial lineages lacking RF3 at all (Shi & Joseph, 2016). Compared to a scenario without RF3, this mechanism accelerates the dissociation of RF1/2 from the ribosome by 40-fold (Freistroffer et al., 1997). The exact order of events is debated controversially (Adio et al., 2018; Peske et al., 2014; Rodnina, 2018; Shi & Joseph, 2016; Zavialov et al., 2001). RF3 binds to



the posttermination complex, which harbors a class I release factor bound at the A-site and a deacetylated P-site tRNA. It is a matter of debate whether RF3 associates in its GDP- or GTP-bound form. Even though RF3 has a higher affinity to GDP, under physiological conditions, where GTP is available in excess, GTP-bound RF3 is more likely. However, RF3 binding ultimately induces large-scale conformational changes within the factor, leading to its stabilized binding, and in the ribosome, which leads to a rotation of the ribosome. In this ratcheted state the interaction of RF1/2 becomes destabilized and consequently the respective factor is released from the ribosome. Upon GTP hydrolysis RF3 can finally dissociate as well. RF3 is essential for recycling of RF1 since its association with the ribosome is quite profound compared to binding of RF2 which can dissociate spontaneously, independent of RF3 (Adio et al., 2018; Peske et al., 2014). Notably, there is no RF3 homolog in mitochondria.

### 1.6.3.2 Translation Termination in Human Mitochondria

In mammalian mitochondria the genetic code differs from the highly conserved universal one. Whereas in bacteria and the eukaryotic cytosol the three codon triplets UGA, UAG and UAA serve as standard stop codons, the base triplet UGA codes for tryptophan in human mitochondria (Barrell et al., 1979). Moreover, two human mitochondrial transcripts – *MT-CO1* and *MT-ND6*, encoding for COX1 or ND6, respectively – are terminated by non-canonical stop codons (Figure III), as there is no complementary tRNA for the codons AGA and AGG in human mitochondria. It is suggested that those two base triplets are stop codons and not encoding arginine like in bacteria or the cytosol (Anderson et al., 1981). Whether the two proposed alternative stop signals function as alternative stop codons in mitochondria, recognized by dedicated release factors, is controversially debated. However, a mechanism where the ribosome shifts one position upstream in the open reading frame (ORF) has been proposed for *MT-CO1* and *MT-ND6*. As the preceding nucleotide is a uridine in both cases, this -1 frameshift would result in conventional termination on a UAG stop codon. Both transcripts have a short 3' UTR, which forms right after AGA or AGG a secondary structure and can force the ribosome to shift one position upstream. This would enable one release factor to initiate termination on UAG and would make an additional release factor dispensable (Temperley et al., 2010a).

### 1.6.3.3 Mitochondrial Release Factors

On the basis of the similarity to bacterial release factors, four mitochondrial factors – mtRF1, mtRF1a, ICT1/mL62 and C12ORF65 – have been assigned as putative mitochondrial release factors (Figure VIIIa). All four factors have a PTH domain containing the conserved GGQ motif. A codon recognition domain can only be found in mtRF1 and mtRF1a. ICT1 and C12ORF65 do not contain such a domain but have acquired positively charged C-terminal extensions. Analogous C-terminal extensions are also present in bacterial rescue factors and therefore the two factors are implemented in two distinct mitoribosomal rescue pathways (Akabane et al., 2014; Antonicka et al., 2010; Desai et al., 2020; Feaga et al., 2016; Handa et al., 2010; Kogure et al., 2012; Kummer et al., 2021; Richter et al., 2010).

Whether mtRF1 or mtRF1a would be the main mitochondrial termination factor was an open question for quite a long time. Decades ago mtRF1 was identified as the first mammalian

mitochondrial release factor (Lee et al., 1987; Zhang & Spremulli, 1998). More and more evidence supported the hypothesis of the later identified mtRF1a being the canonical release factor in mitochondria (Kummer et al., 2021; Lind et al., 2013; Nozaki et al., 2008; Soleimanpour-Lichaei et al., 2007; Temperley et al., 2010a; Young et al., 2010). A prominent difference between mtRF1 and mtRF1a is located in their codon recognition domain (Figure VIIIb). Whereas mtRF1a is highly similar to the *E. coli* RF1 in regard of the classical tripeptide motif (PKT) and the tip of the  $\alpha 5$  helix, two insertions are present in the respective domains of mtRF1: two amino acids (RT) are incorporated just before the tip of the  $\alpha 5$  helix and the codon recognition motif is extended to a hexapeptide (PEVGLS) in mtRF1. It remains elusive whether those extensions are co-evolutionary evolved features and serve mtRF1 to adapt changes within mt-rRNA and the overall mitoribosomal structure (Greber & Ban, 2016; Lind et al., 2013; Young et al., 2010).

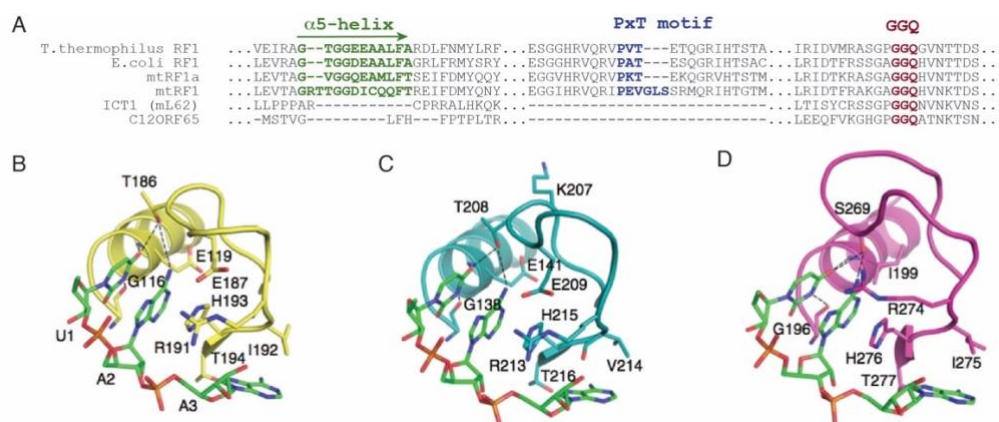


**Figure VIII: Mitochondrial Release Factors.** (A) Sequence alignment of bacterial (*Thermus thermophilus* and *E. coli*) and mitochondrial release Factors (mtRF1a, mtRF1, ICT1 and C12ORF65). Shown are the sequences of the codon recognition domain comprising the conserved PxT motif and the tip of the  $\alpha 5$  helix as well as the PTH activity conferring GGQ motif. Molecular dynamics simulations of the codon recognition domains of (B) *Thermus thermophilus* RF1 (yellow), (C) mtRF1a (cyan) and (D) mtRF1 (magenta) with key indicated key residues interacting with UAA stop codon (green). Thr206 of mtRF1a and Ser269 of mtRF1 interacts similarly with nucleotides U1 and A2 as Thr186 of RF1. H-bonds are shown as dashed line. Image of structural comparison taken from (Lind et al., 2013). Reprinted with permission from Springer Nature (license number 5400941310507).

Even though the sequence of the mitochondrial protein mtRF1 is highly similar to prokaryotic class I release factors, the role of mtRF1 remains unidentified. There is no release factor activity detectable for mtRF1 in a 70S ribosome-based heterologous *in vitro* translation system. Neither of the tested stop codons – standard stop codons UAG, UAA and UGA nor non-standard stop codons AGA and AGG – led to release of the small, radiolabeled peptides in two independent studies (Nozaki et al., 2008; Soleimanpour-Lichaei et al., 2007). Further supporting biochemical *in vivo* data or a homologous *in vitro* termination assay with mitochondrial ribosomes, which could shed light on the function of mtRF1, is not available yet. There is great controversy regarding the true function of mtRF1. Exchanging the critical domains for codon recognition of bacterial RF1 with the corresponding domains of mtRF1 in hybrid activity assays as well as homology modeling suggest that mtRF1 might be a potential candidate for decoding non-standard stop codons AGA and AGG. First, it is argued that the extended decoding motifs could accommodate a large adenine purine base. Second, the initial appearance of mtRF1 in the

vertebrate lineage overlaps with the emergence of those unconventional stop codons (Young et al., 2010). However, this option is ruled out by two research groups. Huynen and colleagues (2012) proposed a possible involvement of mtRF1 in ribosome rescue. As they suggested that a mitoribosomal-bound mtRF1 would sterically clash with a stop codon at the ribosomal A-site, they claimed that mtRF1 could only bind to ribosomes with an empty A-site. On the basis of homology modeling, molecular dynamics and free-energy calculations it was shown that mtRF1 has the same codon reading qualities like bacterial RF1 and mtRF1a by Lind and co-workers (2013). Hence conventional UAG and UAA as stop codons could be detected by mtRF1. Then again, a recent structural study could not find mtRF1 being bound to the mitoribosome in any of the aforementioned scenarios, questioning its role in translation termination once more (Kummer et al., 2021).

In contrast, there is great agreement regarding the function of mtRF1a. mtRF1a shows the same codon reading qualities on canonical UAG and UAA stop codons which is consistent with its homology to bacterial RF1. Thus, PTH activity can be detected when biochemically measured in *in vitro* translation termination assays (Nozaki et al., 2008; Soleimanpour-Lichaei et al., 2007). Considering a potential -1 frameshift, mtRF1a would be able to terminate all 13 mitochondrial ORFs. Next to the eleven canonical ORFs directly terminated by UAG or UAA, also *MT-CO1* and *MT-ND6*, which are supposed to be terminated by AGA or AGG, would be terminated by an UAG stop codon in this case (Temperley et al., 2010a). However, despite an *in vivo* study demonstrated a defective growth phenotype, resembling the one of a deficient oxidative phosphorylation, upon three days of siRNA-mediated depletion of mtRF1a, no effects on mitochondrial *de novo* translation, steady state protein levels nor the assembly of OXPHOS complexes have been detected (Soleimanpour-Lichaei et al., 2007). Nevertheless, those effects might be explained by the fact that protein levels of OXPHOS subunits are relatively stable even after four days of down-regulated mitochondrial translation (Takeuchi & Ueda, 2003). Here, knockout experiments are required to prove the role of mtRF1a being the major mitochondrial release factor.

Recently, structural studies with reconstituted termination complexes comprised of mtRF1a and mRNAs either containing UAG- or UAA (Figure IXa) further established the role of mtRF1a being the major mitochondrial release factor required to terminate translation at standard stop codons (Kummer et al., 2021). In detail, interactions observed of RF1 with the ribosome and the mRNA are greatly conserved in mtRF1a (Laurberg et al., 2008). Codon recognition follows the same structural arrangements as in bacteria: residues of the DC and the codon recognition domain of mtRF1a surround the mRNA codon. Similarly, the first position uridine is coordinated by Thr208 (bacterial Thr186) of the PKT motif and the tip of the  $\alpha 5$  helix (Figure IXb). Thr208 also directly contacts the second position adenine as well as other adjacent residues. Analogous to bacterial RF1, the third position guanosine or adenine is stacked against G256 (Figure IXb, bacterial G530) of the mitoribosomal 12S rRNA and simultaneously contacted by two residues of mtRF1a (Thr216 and Glu203). This sterical arrangement thus permits either of the two nucleotides at the last stop codon position. Binding of the stop codon induces large-scale

conformational changes in the switch-loop of mtRF1a. Opening of the factor causes the insertion of the GGQ motif containing PTH domain into the PTC. This conformation is then stabilized by similar stacking interactions as already seen in the bacterial counterpart and thus, peptide hydrolysis and release is triggered (Kummer et al., 2021). In summary, mtRF1a is the only reported release factor, which recognizes canonical stop codons and thereby terminates translation of mitochondrial-encoded transcripts whereas the role of mtRF1 still remained elusive over the past 25 years after its identification. This doctoral thesis sheds light on the physiological role of both class I human mitochondrial release factors mtRF1 and mtRF1a.

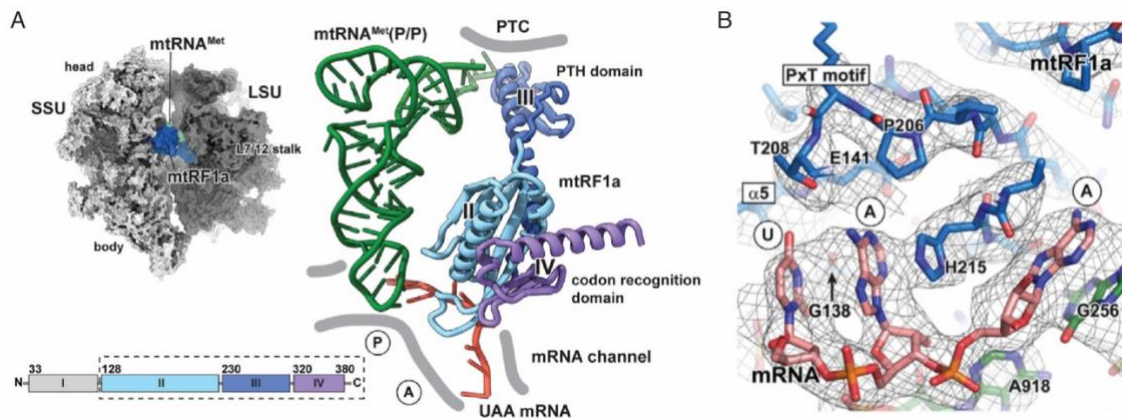


**Figure IX: Structure of mtRF1a bound to 55S Mitochondrion.** (A) Overview and close-up of the structure of mtRF1a bound in the human mitochondrial termination complex. The close-up shows interactions of mtRF1a with the mRNA stop codon (red) in the decoding center (DC) and the P-site tRNA (green) in the peptidyl transferase center (PTC). Colorization of distinct domains of mtRF1a corresponds to those depicted in the schematic domain organization. (B) Conserved interactions of the PxT motif and the  $\alpha 5$  helix of mtRF1a with the UAA stop codon in the DC. Images taken from (Kummer et al., 2021). Reprinted with permission from Elsevier (license number 5400940230132).

#### 1.6.4 Ribosome Recycling

After peptide release, the mitochondrion is present as a posttermination complex (PoTC) with a vacant A-site but still harboring mRNA and deacylated tRNAs in the P- and E-site. Consequently, the final step of the translation cycle is the recycling of this mitochondrion complex. Disassembly of the PoTC releases both subunits as well as the mRNA and tRNAs in order to initiate another translation cycle. In bacteria the ribosome recycling factor (RRF) together with EF-G (elongation factor G) preferentially binds to ribosomes in its fully rotated state with a deacylated P-site tRNA in its hybrid P/E state, ensuring that only PoTCs are recycled. Binding of RRF to the A-site stabilizes this complex and induces conformational changes since binding occurs in regions where the important intersubunit bridges B2a and B3 are formed. Subsequent binding of EF-G and GTP hydrolysis results in rotation of the flexible head domain of RRF, which causes disruption of these key intersubunit bridges and finally dissociation of the ribosome into its subunits. While RRF and EF-G stay attached to the LSU, the SSU still carries the mRNA and tRNA. The mRNA is released and ejection of the tRNA is promoted by binding of IF3 to the SSU, which then acts as an anti-association factor to prevent reassociation (Gao et al., 2005; Peske et al., 2005; Rodnina, 2018).

Except for some minor differences, the general recycling features are preserved in mammalian mitochondria: similar to bacteria, mtRRF is critical for cell viability as it indirectly ensures proper

OXPHOS function by providing sufficient free mitoribosomal subunits (Janosi et al., 1994; Rorbach et al., 2008). The second EF-G paralogue mtEF-G2, which differs in respect to its C-terminal domain from the translocation-active mtEF-G1, is indispensable for the recycling process. But in contrast to bacteria, only GTP-binding and not hydrolysis is essential for efficient subunit splitting (Tsuboi et al., 2009). Whether mtIF3 is required as an active anti-association factor in mammalian mitochondria (Christian & Spremulli, 2009) or not is still not clear since a tissue-specific knockout model showed no alterations in subunit distribution upon mtIF3 loss (Rudler et al., 2019). Mechanistically, mtRRF binds to the rotated mitoribosome first and interacts with several critical sites: (i) at the PTC, to prevent further binding of tRNAs and to secure the deacylated tRNA in its hybrid P/E position, and (ii) with h44 of 12S rRNA and H69 and H71 of 16S rRNA, both involved in B2a intersubunit bridge formation, thereby already weakening the mitoribosomal integrity. The particular relevance of the mitochondrial specific N-terminal extension (NTE) of mtRRF is still controversially debated (Koripella et al., 2021; Koripella et al., 2019b; Kummer et al., 2021). Prior binding of mtRRF is a prerequisite for association of GTP-bound mtEF-G2, which then drives the complete mitoribosome dissociation. Domain IV of mtEF-G2 pushes the flexible domain II of mtRRF and alters the position of mtRRF in a way that this ultimately leads to the intersubunit bridge disruption. GTP hydrolysis causes the dissociation of mtRRF and mtEF-G2 from the mtLSU. The properties of mtEF-G2 are sterically and electrostatically specialized to interact with mtRRF during mitoribosome recycling and this also explains why mtEF-G1 cannot act during this process. While the contact sites of mtRRF and mtEF-G2 match, mtEF-G1 would be repulsed. Additionally, the mtEF-G1-specific C-terminal extension (CTE) permits binding to mtRRF as it would sterically clash. Finally, mtEF-G2 can only poorly bind to the mitoribosome alone and depends on prior mtRRF binding, thus ensuring it only binds to PoTC and avoiding the interference with mtEF-G1 function during elongation. In this way, mitochondria developed a sophisticated mechanism to distinguish between actively elongating and splitting-competent mitoribosomes (Koripella et al., 2021; Kummer et al., 2021).

Next to canonical ribosome recycling, the translational GTPase GTPBP6 mediates an alternative recycling pathway additional to its function in mitoribosome biogenesis. This pathway is reminiscent of the bacterial GTPase HflX, which is activated under stress conditions such as heat shock and will be explained in detail in chapter 1.7.2.3 (Hillen et al., 2021; Lavdovskaia et al., 2020; Zhang et al., 2015). Furthermore, a module composed of MALSU1 (mitochondrial assembly of ribosomal large subunit 1), LOR8F8 and mtACP (mitochondrial acyl carrier protein) binds to mtLSUs and does not only function during mitoribosome assembly by serving as a steric block to prevent premature subunit joining (Brown et al., 2017; Rorbach et al., 2012), but furthermore ensures that a nascent polypeptide and/or tRNA can be removed from recycled or post-rescued mtLSUs before further re-association with a mtSSU, respectively. Thus it plays a part in the mitoribosome-associated quality control (mtRQC) process (Desai et al., 2020).

## 1.7 Ribosome Rescue Mechanisms

Protein synthesis is a high-fidelity process and its regulation on several levels is fundamental for cellular viability and fitness. Hence, it is not surprising that more than half of the energy consumption in bacteria is dedicated to maintain accurate translation (Russell & Cook, 1995). Varying environmental circumstances require translational control, which regulates expression levels of involved factors, ribosome availability and alleviates arrest. But also the general translational efficiency needs to be regulated throughout all steps of protein synthesis (Samatova et al., 2020). Ribosomes can face a plethora of challenges that lead to translational stalling. In minor cases, those challenges are reversible, ribosomal pausing can be overcome and translation can resume. Events that cause such pausing are for example series of rare codons, a more complicated incorporation of amino acids like proline(s), aa-tRNA starvation or secondary mRNA structures like pseudoknots (Buskirk & Green, 2017). However, in other circumstances, like the occurrence of aberrant mRNAs, severe aa-tRNA shortage as well as defective translation factors or defective ribosomes themselves, ribosomes are stalled and have to be rescued. Aberrant mRNAs can either result from 'no-go decay' when truncated, for example by nucleolytic degradation or false processing, or being highly structured, or 'no-stop decay' when the end of an ORF lacks or has a premature stop codon (Buskirk & Green, 2017; Müller et al., 2021; Nürenberg-Goloub & Tampé, 2019; Shoemaker & Green, 2012). In this situation, stalled ribosomes trigger specific rescue mechanisms, which are of high physiological relevance. The recycling of ribosomal subunits as well as immediate degradation of non-functional, potentially toxic polypeptides and prevention of diminished protein expression capacities are crucial, as this directly influences the cellular fitness.

### 1.7.1 Bacterial Rescue Mechanisms

Prokaryotes developed several different quality control systems, namely the *trans*-translation system, the alternative rescue pathways via ArfA or ArfB as well as the ribosome-associated quality control (RQC) pathway (Feaga et al., 2014; Keiler, 2015; Lytvynenko et al., 2019).

#### 1.7.1.1 *Trans*-Translation

The *trans*-translation system is the main bacterial rescue system and is involved in rescuing translation when ribosomes are stalled in 'non-stop' complexes. Due to a lack of a mRNA codon in the ribosomal A-site, neither elongation nor release factors or recycling factors can resume translation but the ribosome complex is still tightly formed. The central components of this rescue pathway, expressed in almost all bacteria, are the bifunctional transfer-messenger RNA (tmRNA, encoded by *ssrA*) and the RNA binding protein SmpB (Karzai et al., 1999; Keiler et al., 1996). The hybrid tmRNA has a tRNA-like domain (TLD), which resembles the acceptor arm of a classical tRNA. It can be charged with alanine by the canonical alanyl-tRNA synthetase (AlaRS) but does not have an anticodon region. Instead, it carries an internal ORF which serves as a mRNA-like template. Upon binding of SmpB, which resembles an anticodon stem-loop, the complex mimics a classical tRNA and can be bound by the canonical elongation factor EF-Tu, which delivers it to the A-site of a stalled ribosome. Subsequently, the acceptor arm is presented in the PTC, the premature polypeptide is transferred onto tmRNA and binding of EF-

G confers translocation of the tmRNA-SmpB complex into the P-site. A confusion with elongating ribosomes is prevented by the C-terminal tail of SmpB, which can sense whether the mRNA channel is empty or not as it adopts an  $\alpha$ -helical conformation when bound to the ribosome. Translocation leads to the placement of the internal ORF of SmpB in the A-site, elongation continues until the stop codon is reached and the polypeptide is released by canonical release factors. The internal ORF encodes for a short protein tag and marks the truncated polypeptide for degradation. Simultaneously, RNase R is recruited to degrade the aberrant mRNA (Keiler et al., 1996; Neubauer et al., 2012; Ramrath et al., 2012; Yamamoto et al., 2003). This confers another layer of quality control to the trans-translation system as it does not only provide recycled ribosomal subunits available for re-initiation, but also ensures that they do not re-engage on dysfunctional mRNAs and prevent toxic protein aggregation.

### 1.7.1.2 Alternative Rescue Pathways

Besides the canonical *trans*-translation system, alternative ribosome rescue pathways represent a second possibility how prokaryotes liberate stalled ribosomes and thus serve as a backup mechanism for cases when *trans*-translation is impaired. Alternative rescue factor A (ArfA, formerly *E. coli* YhdL) was identified as a factor conferring cell viability when *trans*-translation is absent. Simultaneous loss of both rescue mechanisms is lethal in *E. coli* (Chadani et al., 2010). ArfA similarly binds at the vacant A-site, where it serves as an adapter for canonical RF2, whose catalytical PTH domain is required to release the nascent polypeptide, since ArfA itself does not possess any PTH activity. In contrast to *trans*-translation, no degradation tag is added to the liberated polypeptide (Chadani et al., 2012; Shimizu, 2012). Like tmRNA, ArfA probes the vacancy of the mRNA channel. Electrostatic binding of its highly conserved, positively charged C-terminus into the mRNA channel lined with the negatively charged 16S rRNA is only possible if no mRNA occupies the channel (Huter et al., 2017b; Zeng et al., 2017). Interestingly, bacteria developed a sophisticated mechanism to regulate the expression of ArfA via *trans*-translation in order to avoid competition of the two systems. The *arfA* mRNA contains a hairpin structure which is recognized and cleaved by RNase III. This cleavage creates a truncated mRNA without stop codon and consequently, a 'non-stop' complex is formed, triggering activity of *trans*-translation factors and marking the aberrant ArfA for proteolysis. In situations when *trans*-translation is limited or overwhelmed, an active form of ArfA is generated (Chadani et al., 2011a; Garza-Sánchez et al., 2011).

A second alternative ribosome rescue pathway is mediated by ArfB (formerly *E. coli* YaeJ). ArfB can also release ribosomes stalled as non-stop complexes, but contrary to ArfA, in a RF-independent manner (Feaga et al., 2014). As ArfB possesses a RF-like GGQ motif with PTH activity, but no codon recognition domain, it can probe and eventually bind to the ribosome with a C-terminal domain similar to ArfA and SmpB (Chadani et al., 2011b; Handa et al., 2011). Structural studies and kinetic measurements demonstrated that the C-terminal domain of ArfB forms an  $\alpha$ -helical element being able to distinguish between actively translating and stalled ribosomes. It is only able to bind when short truncated mRNAs, which do not exceed from the P-site into the DC, are present. Comparable to the canonical release factors, a conformational

change within the factor is induced upon binding, which allows hydrolysis of the nascent polypeptide (Carbone et al., 2020; Chan et al., 2020; Gagnon et al., 2012). Homologs of ArfB show a high conservation in critical residues not only in the PTH domain, but also in the C-terminal tail and the flexible linker region (Kogure et al., 2014). However, the chromosomally encoded ArfB alone cannot rescue the lethal phenotype of the  $\Delta ssR\Delta arfA$  double mutant in *E. coli* and instead overexpression and/or specific growth or stress conditions are required (Chadani et al., 2011b). This leads to the assumption that ArfB is not another backup mechanism in absence of *trans*-translation and ArfA, but instead is required under certain conditions yet to be elucidated. One possible scenario is that ArfB acts in concert with the stress-induced ribosome recycling factor HflX where ArfB would release the truncated polypeptide from the stalled ribosome and subsequent binding of HflX would split the ribosomal subunits by intersubunit bridge disruption (Zhang et al., 2015)

### 1.7.1.3 Ribosome -associated Quality Control

Quite recently, this well conserved RQC pathway in eukaryotes was also detected in *Bacillus subtilis* and potentially serves as a partially redundant system to *trans*-translation to degrade cytotoxic polypeptides and mRNAs (Lytvynenko et al., 2019). Bacterial RqcH (homolog of eukaryotic NEMF/Rqc2) similarly senses LSUs obstructed with a polypeptide-tRNA complex in the P-site and triggers the recruitment of alanine-loaded tRNA in order to add an alanine tail to the trapped polypeptide chain. These alanine tails serve as a proteolytic degradation tag to be recognized by the ClpXP protease. What triggers the initial ribosome splitting and which factors might be involved in this process still remains elusive (Lytvynenko et al., 2019). Structural studies revealed that an additional protein is required to facilitate alanine tailing. RqcP (RQC P-site tRNA stabilizing factor, formerly YabO) acts in concert with RqcH to mimic canonical elongation steps and thereby driving poly-Ala synthesis in a ratchet-like manner. The suggested mechanism implies an alternating binding-dissociation modus where RqcP binds and stabilizes the P-site tRNA, RqcH recruits the Ala-tRNA<sup>Ala</sup> to the A-site (copying EF-Tu in the elongational decoding step) and a large-scale conformational change (similar to the translocation step) pushes the A-site tRNA in a hybrid A/P-state and thus transfers the nascent polypeptide chain. To complete one Ala-tailing cycle, RqcP temporarily dissociates, allowing the P-site tRNA to enter the E-site. A yet undiscovered factor has to terminate this process (Crowe-McAuliffe et al., 2021; Filbeck et al., 2021). This is mechanistically reminiscent to the well-studied RQC pathway in eukaryotes. Here, NEMF (yeast Rqc2) senses the obstructed complexes and ultimately enhances the proteasomal degradation by adding C-terminal alanine and threonine (CAT) tails to the polypeptide to further expose lysine residues outside the PET in order to be marked by ubiquitylation (Joazeiro, 2019; Nürenberg-Goloub & Tampé, 2019).

### 1.7.2 Mitochondrial Rescue Mechanisms

As mammalian mitochondria face similar challenges in regard of engaging with co-transcriptionally processed mRNAs, which apparently do not undergo any quality control, mitochondria also have rescue systems to dissolve potentially cytotoxic situations where ribosomes are stalled at truncated, aberrant mRNAs. Although factors involved in *trans*-



translation or ArfA are absent in mitochondria, two mitochondrial rescue pathways (Figure X) have been discovered, which are partially reminiscent to the bacterial ones (Ayyub et al., 2020; Nadler, Lavdovskaia, & Richter-Dennerlein, 2022). However, comparably little is known about these rescue systems and thus represents an emerging research topic.

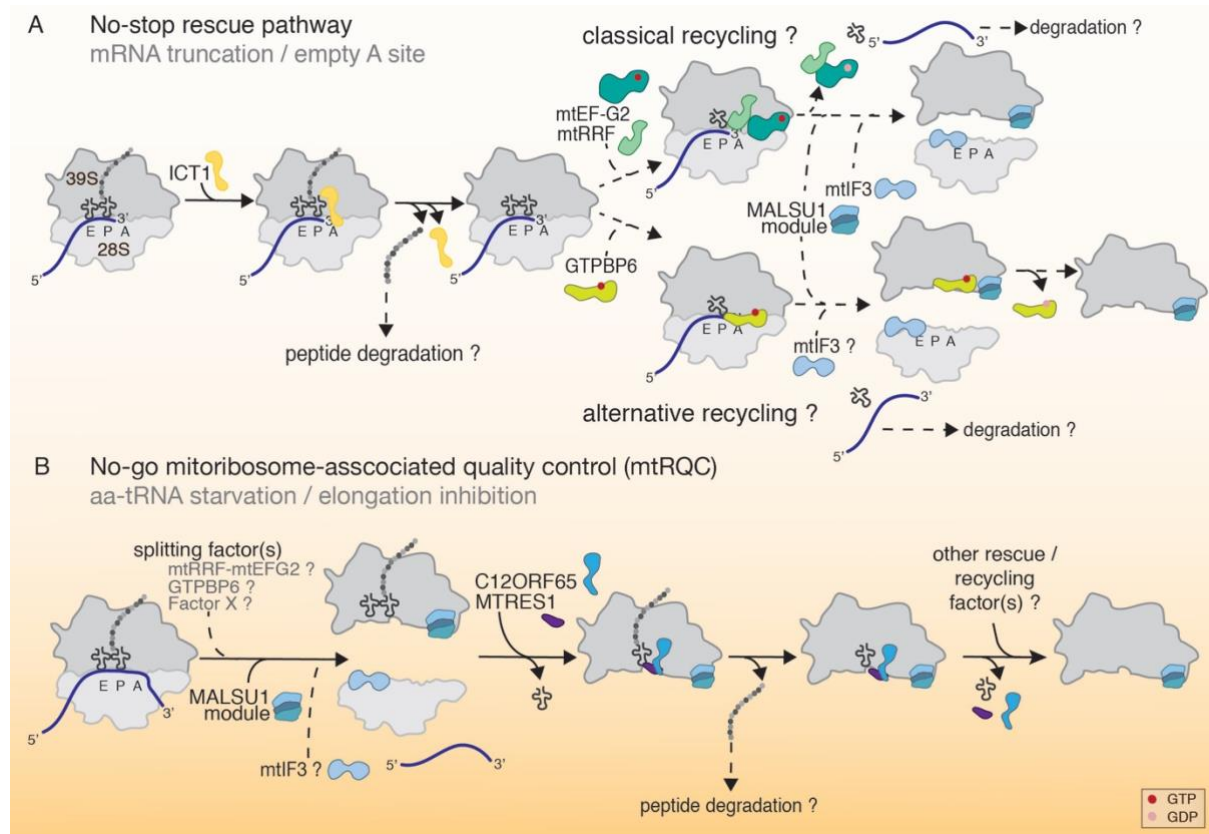


**Figure X: Mitochondrial Rescue Pathways.** (A) Depicted is a no-stop scenario with an empty A-site (e.g. due to truncated mRNAs). In this case, ICT1 (yellow) acts as a rescue factor by sensing the empty mRNA channel and releasing the polypeptide from the stalled mitoribosome. At least two different following recycling scenarios are possible: either classical recycling via mtRRF and mtEF-G2 (medium and dark green) or GTPBP6-based (light green) alternative recycling. (B) In no-go scenarios (e.g. due to lack of aminoacylated tRNAs or inhibition of elongation), C12ORF65 (mtRRF-R, orange) and MTRES1 (dark red) trigger mitoribosome-associated quality control (mtRQC). This pathway must be precluded by a preceding recycling event facilitated by yet unknown recycling factors. All other translation factors are depicted as in figure V. Figure based on (Nadler et al., 2022b).

### 1.7.2.1 Mitochondrial Non-Stop Rescue Pathway

ICT1 (immature colon carcinoma transcript-1) is a homolog of the bacterial ArfB present throughout the eukaryotic phyla (Duarte et al., 2012) and a member of the mitochondrial release factor subfamily, characterized by the presence of the PTH activity-mediating GGQ motif. But unlike codon-dependent class I release factors, ICT1 is much shorter as it does not harbor codon recognition domains. Instead, it has a conserved positively-charged C-terminal extension like ArfB. With those properties, ICT1 can bind to an empty mitoribosomal A-site and facilitate hydrolysis of the nascent polypeptides from the P-site tRNA, thus acting as a mitoribosomal rescue factor (Feaga et al., 2016; Handa et al., 2010; Kogure et al., 2014; Richter et al., 2010). Because of the codon-independent manner of polypeptide release, it was postulated that ICT1 might also be involved in termination of non-canonical stop codons by rescuing ribosomes stalled at AGA or AGG at the end of the ORF of *MT-CO1* or *MT-ND6*,

respectively (Akabane et al., 2014). In contrast, a recent structural study confirmed the role of ICT1 as a rescue factor for mitoribosomes stalled in a non-stop scenario homologous to ArfB (Kummer et al., 2021): in case of an empty mRNA channel due to a truncated mRNA, the C-terminal extension is able to sense and bind to the vacant A-site. This in turn places the GGQ motif in proximity to the 3' CCA end of the P-site tRNA in the PTC to trigger peptide hydrolysis. Notably, ICT1 is additionally known as mL62 as it is also an integral constituent of the mtLSU where it binds near the base of the CP and forms a connection to the mtLSU main body (Brown et al., 2014; Greber et al., 2014; Richter et al., 2010). Bound to this location, ICT1/mL62 is approximately 70 Å away from the PTC and thus cannot exert its PTH activity as the GGQ domain is nowhere close to the peptidyl tRNA and hence cannot function as a rescue factor. Therefore, an extraribosomal copy is required to perform this function (Akabane et al., 2014). The exact differentiation between the two ICT1/mL62 purposes still needs to be elucidated. A potential hypothesis is that under physiological conditions, ICT1/mL62 is usually integrated into the mitoribosome and special stress-conditions are required to upregulate its expression to serve as a mitoribosomal rescue factor (Huter et al., 2017a).

As its name already suggests, ICT1 was first identified as an oncogene in colorectal cancer (van Belzen et al., 1995), but its upregulation is correlated with a poor prognosis also in certain other types of cancer like breast, prostate, lung and leukemia and thus serves as a potential therapeutic target to conquer malignancy (Kummer et al., 2021). For example, ICT1 overexpression in aggressive hepatocellular carcinoma leads to unfavorable regulation of factors involved in cell cycle checkpoints and apoptosis like CDK1, cyclin B1, Bcl-1 and Bax. Abnormally high amounts of these proteins promote cell proliferation, cell cycle progression and concurrently inhibit apoptosis. Subsequently, these hallmarks of cancer are associated with larger tumor size and more advanced malignant tumors. The expression level of ICT1 can therefore be seen as a helpful diagnostic marker (Chang et al., 2017).

#### **1.7.2.2 Mitoribosome-associated Quality Control**

Another mitochondrial release factor implicated in mitoribosomal rescue is C12ORF65, (renamed mtRF-R for mitochondrial release factor in rescue). Similar as ICT1, C12ORF65 also has a catalytically active GGQ motif and lacks a codon recognition domain. However, the function of C12ORF65 remained elusive since *in vitro* translation termination assays using purified C12ORF65 and 70S *E. coli* or 55S mitochondrial ribosomes programmed as either conventional termination complexes with canonical or alternative stop-codons or as a 'non-stop' scenario could not detect any release factor activity (Antonicka et al., 2010; Kummer et al., 2021). However, its proper function seems to be critical for synthesis of mitochondrial proteins and their subsequent assembly into OXPHOS complexes (Antonicka et al., 2010). Moreover, mutations in *C12orf65* cause severe mitochondrial diseases with a growing number of patients presented with Leigh syndrome as well as optic atrophy, ophthalmoplegia, encephalomyopathy, peripheral neuropathy and spastic paraplegia and thus emphasize the importance of C12ORF65 for mitochondrial function (Antonicka et al., 2010; Heidary et al., 2014; Perrone et al., 2020; Shimazaki et al., 2012; Spiegel et al., 2014; Wesolowska et al., 2015).

Quite recently, it was shown that upon aa-tRNA starvation, C12ORF65 acts together with MTRES1 (mitochondrial RNA-binding protein, C6ORF203) on mtLSU particles, which still contain a peptidyl tRNA in the P-site, resembling the cytoplasmic/eukaryotic or bacterial RQC (Desai et al., 2020). MTRES1 has a S4-like RNA binding domain, which preferentially binds highly structured or double-stranded RNA, allowing the protein to associate with the mtLSU by interactions with the 16S rRNA or certain tRNAs. Its loss is also associated with a perturbed mitochondrial translation and OXPHOS function (Gopalakrishna et al., 2019). Mechanistically, C12ORF65 binds in the A-site of the mtLSU via its C-terminal domain in close proximity to the peptidyl tRNA, whereas the S4-like domain of MTRES1 directly binds around the anticodon stem-loop of this peptidyl tRNA. Binding of this heterodimer induces conformational changes, leading to the release of the E-site tRNA so that C12ORF65 can hydrolyze the nascent polypeptide by placing the GGQ domain into the PTC. Ejection of the remaining tRNA is aided by MTRES1. Additionally, the aforementioned anti-association module consisting of MALSU1-mtACP-LOR8F8 was found to be associated to the mtLSU throughout the rescue process to prevent re-association with the mtSSU (Desai et al., 2020). Despite structural similarities, ICT1 and C12ORF65 – the two release factors implicated in mitoribosomal rescue – appear to have different substrates and thus operate under different conditions. The initial trigger, which leads to the prerequisite dissociation of the 55S monosome and activation of this rescue mechanism is still unknown and needs further analysis.

### 1.7.2.3 Alternative Mitoribosomal Recycling Pathway

Another element of mitoribosomal rescue is the GTPBP6-mediated recycling. GTPBP6 is a GTPase with a dual function: while its canonical role is implicated in late stage mitoribosome maturation, it can also dissociate 55S monosomes alternatively to the canonical mtRRF-based recycling pathway (Hillen et al., 2021; Lavdovskaia et al., 2020). Kinetic assays show that GTPBP6 preferably splits vacant ribosomes or PoTCs *in vitro* (Lavdovskaia et al., 2020). Structural studies suggest that binding of GTPBP6 to the mitoribosome with a deacylated tRNA in the P-site disrupts essential intersubunit bridges critical for mitoribosome integrity (Hillen et al., 2021). Together, the structural study and kinetic measurements suggest that elevated levels of GTPBP6 might be responsible of rescuing stalled ribosomes like its bacterial homolog HflX. HflX acts as a ribosome-splitting factor implicated in dissociating either vacant ribosomes or stalled ribosomes containing deacylated tRNA. To avoid re-association, HflX stays bound to the LSU until the compromising situation is eliminated. It was suggested that HflX has to work in concert with another factor with PTH activity in order to operate on ribosomes with uncharged tRNAs. This factor might be ArfB. Similarly, ICT1 was suggested to act prior to GTPBP6 to release the nascent polypeptide and generate a suitable substrate for GTPBP6. It is possible that GTPBP6 splits stalled mitoribosomes in advance to mtRQC to create an mtLSU still bound to a peptidyl tRNA. However, this scenario is rather unlikely since GTPBP6 requires a deacylated tRNA in the P-site to function as an active GTPase. Consequently, the (patho-) physiological conditions under which GTPBP6 becomes relevant for ribosome rescue remain elusive (Hillen et al., 2021; Lavdovskaia et al., 2020; Nadler et al., 2022b; Zhang et al., 2015).

## 1.8 Aims and Objective

Translation termination in human mitochondria is not well defined and many open questions regarding the four putative mitochondrial release factors remained unsolved. The later identified release factor mtRF1a resembles the bacterial RF1 the most and was consequently assigned as major mitochondrial release factor which is proposed to terminate translation of all 13 mitochondrial-encoded proteins. All mitochondrial-encoded proteins are components of the OXPHOS complexes, whose assembly has to be tightly coordinated with the import of the nuclear-encoded subunits. Therefore, it is essential to understand the molecular basis of the translation cycle and particularly of termination by defining the function of required release factors.

It has been hypothesized that the two human mitochondrial transcripts, namely *MT-CO1* and *MT-ND6*, which are terminated in a non-canonical stop codon (AGA and AGG, respectively) are target of the second mitochondrial release factor mtRF1. Like mtRF1a, mtRF1 has a PTH- and a codon recognition domain and in accordance to bioinformatic predictions the same codon reading specificities. However, reconstitutions used for structural analysis and earlier knockdown approaches rejected the possibility of mtRF1 being an active release factor. Moreover, it is still an open question why the cell kept a second, possibly redundant release factor like mtRF1. Despite recent structural insights, *in vivo* evidence regarding the function of both release factors is still lacking.

To unravel the function of mtRF1 in comparison to mtRF1a, knockout models in human embryonic kidney cells were generated and subsequently used to dissect the physiological role of the two factors on a molecular level and to define the consequences of translation termination deficiency in human mitochondria. Additional knockdown approaches were used to test the possibility of potential compensating or rescue mechanisms.

The aim of this doctoral thesis is to address the following questions:

- i. Define the function of mtRF1 in human mitochondria.
- ii. Verify the role of mtRF1a as the main mitochondrial release factor *in vivo*.
- iii. What are the direct effects of the loss of either of the release factor?
  - a. How is translation of the individual mitochondrial transcripts altered?
  - b. How does this affect the biogenesis of the OXPHOS complexes of dual genetic origin?
- iv. What are the downstream consequences within mitochondria upon loss of the release factors?
  - a. Is there a factor which can compensate the deficiency?
  - b. Is there a mechanism which can release the stalled termination complexes?
  - c. Does the cell adapt to the diminished translation termination?



## 2 Results

### Publication

**Nadler, F.,** Lavdovskaia, E., Krempler, A., Cruz-Zaragoza, L. D., Dennerlein, S., & Richter-Dennerlein, R. (2022). Human mtRF1 terminates COX1 translation and its ablation induces mitochondrial ribosome-associated quality control. *Nat Commun*, 13(1), 6406. <https://doi.org/10.1038/s41467-022-34088-w>

Copyright license: This research article is published under the open access CC BY license (Creative Commons Attribution 4.0 International License). According to the Copyright Clearance Center's RightLink® the copyright ownership of the published versions belongs to the authors.

### Author contributions

**Figure 1:** CRISPR/Cas9-mediated generation of *mtRF1*<sup>-/-</sup> and *mtRF1α*<sup>-/-</sup> HEK293 knockout cell lines and subsequent selection and analysis (E.L, F.N.); cell counts, measurement of mitochondrial radicals via flow cytometry (F.N.).

**Figure 2:** Respirometry measurements via Seahorse, *in gel* and colorimetric complex I activity measurements, 1D and 2D BN-PAGE and western blot analysis of OXPHOS complex subunits and MITRAC components (F.N); *in gel* complex IV activity (S.D.); technical assistance (A.K.).

**Figure 3:** Generation of *mtRF1*<sup>-/-</sup> + mtRF1<sup>GGQ-FLAG</sup>, *mtRF1*<sup>-/-</sup> + mtRF1<sup>AAQ-FLAG</sup>, *mtRF1α*<sup>-/-</sup> + mtRF1α<sup>GGQ-FLAG</sup> and *mtRF1α*<sup>-/-</sup> + mtRF1α<sup>AAQ-FLAG</sup> rescue and mutant cell lines and [<sup>35</sup>S]Methionine *de novo* labeling of mitochondrial translation in respective cell lines, sucrose density gradient analysis of mitochondrial ribosome complexes in knockout cell lines (F.N.).

**Figure 4:** Northern blot steady state analysis of knockout cell lines (F.N.); chloramphenicol treatment and subsequent northern blot analysis in *mtRF1*<sup>-/-</sup> and *mtRF1α*<sup>-/-</sup> (F.N., E.L.); NanoString analysis of isolated mitochondria from *mtRF1*<sup>-/-</sup> cells (E.L., L.D.C.-Z.).

**Figure 5:** Western blot analysis of release factors in *mtRF1*<sup>-/-</sup> cells, siRNA-mediated knockdown of *C12orf65* in *mtRF1*<sup>-/-</sup> cell line and subsequent [<sup>35</sup>S]Methionine *de novo* labeling of mitochondrial translation (F.N.).

**Supplementary Figure 1:** Sequence alignment of mitochondrial and selected bacterial release factors (F.N.).

**Supplementary Figure 2:** Sequence analysis *mtRF1<sup>-/-</sup>* and *mtRF1a<sup>-/-</sup>* and alignment of respective sequences in comparison to HEK293 WT cells (F.N.).

**Supplementary Figure 3:** Pulse-Chase [<sup>35</sup>S]Methionine *de novo* labeling of mitochondrial translation (F.N.).

**Supplementary Figure 4:** Sequence comparison of COX1 and ND6 termination codons (R.R.-D.).

**Supplementary Figure 5:** CLUSTAL multiple sequence alignment of mtRF1 and mtRF1a (R.R.-D.).

**Supplementary Figure 6:** Antibody validation via western blotting in HEK293 WT mitochondria and 143B and 143B *Rho<sup>0</sup>* cells (F.N.).

**Supplementary Figure 6:** Antibody validation via western blotting in HEK293 WT mitochondria and 143B and 143B *Rho<sup>0</sup>* cells (F.N.).


**Non-experimental analysis:** data analysis and visualization (F.N., E.L., R.R.-D.); conceptualization and supervision of the study (R.R.-D.); manuscript writing (R.R.-D. with the contributions of all co-authors).

# Human mtRF1 terminates COX1 translation and its ablation induces mitochondrial ribosome-associated quality control

Received: 25 May 2022

Accepted: 11 October 2022

Published online: 27 October 2022

 Check for updates

Franziska Nadler<sup>1</sup>, Elena Lavdovskaia<sup>1,2</sup>, Angelique Krempler<sup>1</sup>,  
Luis Daniel Cruz-Zaragoza<sup>1</sup>, Sven Dennerlein<sup>1</sup> &  
Ricarda Richter-Dennerlein<sup>1,2,3</sup> ✉

Translation termination requires release factors that read a STOP codon in the decoding center and subsequently facilitate the hydrolysis of the nascent peptide chain from the peptidyl tRNA within the ribosome. In human mitochondria eleven open reading frames terminate in the standard UAA or UAG STOP codon, which can be recognized by mtRF1a, the proposed major mitochondrial release factor. However, two transcripts encoding for COX1 and ND6 terminate in the non-conventional AGA or AGG codon, respectively. How translation termination is achieved in these two cases is not known. We address this long-standing open question by showing that the non-canonical release factor mtRF1 is a specialized release factor that triggers COX1 translation termination, while mtRF1a terminates the majority of other mitochondrial translation events including the non-canonical ND6. Loss of mtRF1 leads to isolated COX deficiency and activates the mitochondrial ribosome-associated quality control accompanied by the degradation of COX1 mRNA to prevent an overload of the ribosome rescue system. Taken together, these results establish the role of mtRF1 in mitochondrial translation, which had been a mystery for decades, and lead to a comprehensive picture of translation termination in human mitochondria.

Translation is a multistep high-fidelity process comprising initiation, elongation, termination and ribosome recycling. While tRNA adapter molecules undergo codon-anticodon interaction during initiation and elongation, specific proteinaceous factors, called release factors (RFs), recognize the STOP codon during translation termination in a sequence-dependent manner. RFs mimic tRNA-like structures that allow the interaction with the ribosomal A-site reaching the decoding center and the peptidyl transferase center (PTC). This results in a conformational change within the ribosome that mediates the hydrolysis of the ester bond between the nascent peptide chain and the peptidyl tRNA within the PTC. In bacteria there are two RFs: RF1 and

RF2. While RF1 reads UAA and UAG codons, RF2 recognizes UAA and UGA. The codon specificity is defined by the codon-recognition motifs within domain 2, the PxT or SPF motif, respectively, and the tip of the  $\alpha 5$  helix<sup>1–4</sup>. Both factors share the highly conserved GGQ motif within domain 3 that reaches into the PTC during termination and is essential for facilitating peptide hydrolysis. As mitochondria evolved from an  $\alpha$ -proteobacterial ancestor, the human mitochondrial translation machinery reveals similarities to its bacterial counterpart, but also significant differences<sup>5</sup>. Human mitochondria use a slightly different genetic code, e.g. UGA encodes for tryptophan instead of being a STOP signal and AGA and AGG are not recognized by a tRNA<sup>Arg</sup>, but terminate

<sup>1</sup>Department of Cellular Biochemistry, University Medical Center Goettingen, D-37073 Goettingen, Germany. <sup>2</sup>Cluster of Excellence “Multiscale Bioimaging: from Molecular Machines to Networks of Excitable Cells” (MBExC), University of Goettingen, D-37075 Goettingen, Germany. <sup>3</sup>Goettingen Center for Molecular Biosciences, University of Goettingen, D-37077 Goettingen, Germany. ✉ e-mail: [ricarda.richter@med.uni-goettingen.de](mailto:ricarda.richter@med.uni-goettingen.de)



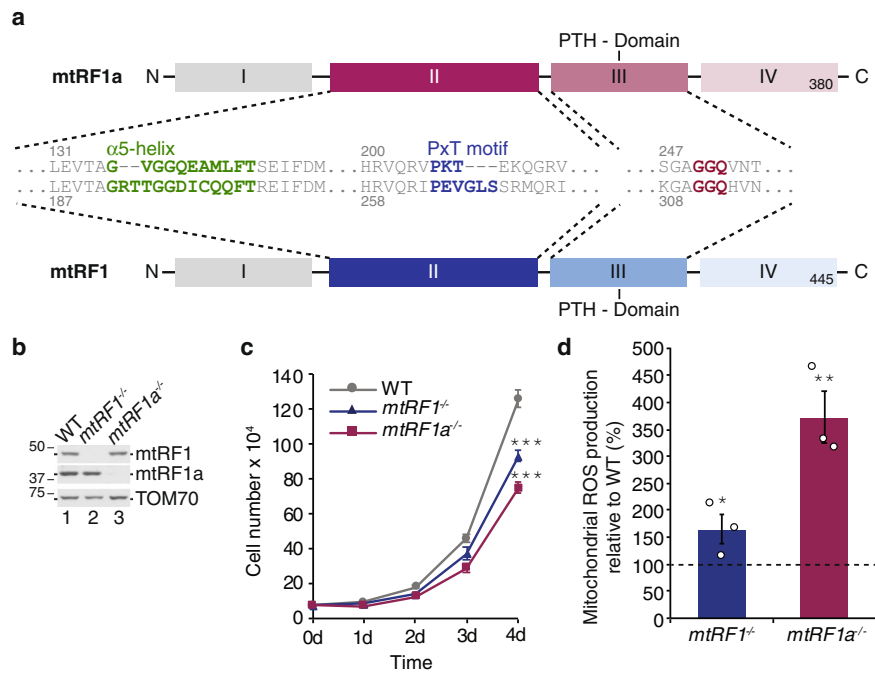


**Fig. 1 | Consequences of loss of mitochondrial translation termination factors.** **a** Comparison of mtRF1a (top, red colors) and mtRF1 (bottom, blue colors). The domains I–IV of the mitochondrial release factors are shown in boxes. Corresponding sequences of the decoding motifs in domain II (α5 helix: green; PxT motif: blue) and the GGQ motif in the peptidyl tRNA hydrolase (PTH) domain III are indicated. **b** CRISPR/Cas9-mediated knockout of mtRF1 and mtRF1a. Mitochondrial lysates (10 μg for mtRF1a and 75 μg for mtRF1) were separated by SDS-PAGE followed by western blotting and immunodetection using the indicated antibodies. **c** Ablation of mitochondrial release factors affects cellular growth. Cells ( $7.5 \times 10^4$ ) were seeded on day 0. Cell growth was monitored by cell counts for the indicated

time points in HEK293 wild-type cells (WT; gray) and in mtRF1- (*mtRF1*<sup>-/-</sup>, blue) and mtRF1a-deficient cells (*mtRF1a*<sup>-/-</sup>; red). ( $n > 6$  biological replicates; mean  $\pm$  SEM; significance for day 4 was calculated by two-sample one-tailed Student's *t*-test and defined as  $***p \leq 0.001$ ). **d** Elevated reactive oxygen species (ROS) production upon loss of mtRF1 and mtRF1a. ROS production was monitored by FACS using MitoSox Red. Relative ROS production in WT is indicated as dashed line (100%) and individual data points are shown as circles. Statistical analysis was carried out as two-sample one-tailed Student's *t*-test with  $n = 3$  biologically independent samples and shown as mean  $\pm$  SEM. Significance was defined as  $*p \leq 0.05$ ;  $**p \leq 0.01$ . Source data are provided as a Source Data file.

the translation of *MTCO1* and *MTND6* transcripts (mRNA encoding COX1 and ND6)<sup>6,7</sup>. A proposed  $-1$  ribosomal frameshift in both cases would allow the termination at a conventional UAG STOP codon<sup>8</sup>. Consequently, all thirteen mitochondrial DNA(mtDNA)-encoded proteins would terminate either in UAA or UAG. Four members of the release factor family have been identified in human mitochondria: mtRF1a, mtRF1, ICT1 (mL62) and C12ORF65 (mtRF-R)<sup>9–12</sup>. mL62 and C12ORF65 lack domains for codon specificity and are part of the ribosome rescue system in human mitochondria. While mL62 is a homolog of bacterial ArfB (alternative rescue factor B) recognizing stalled mitochondrial ribosomes with an empty A site<sup>13</sup>, C12ORF65 is involved in the mitochondrial ribosome-associated quality control (mtRQC) acting on peptidyl tRNA moieties within split large mitochondrial ribosomal subunits (mtLSU)<sup>14</sup>. The overall domain architecture of human mtRF1a and mtRF1 is highly conserved and resembles the one of bacterial RF1<sup>15</sup>. However, mtRF1a reveals the highest sequence and structural similarity to bacterial RF1 (Supplementary Fig. 1) and indeed, terminates translation when recognizing UAA or UAG within the ribosomal A site<sup>9,13</sup>. The function of the fourth member mtRF1 remains a mystery since it was discovered in 1998<sup>9,10</sup>. It is an open question why do human mitochondria retain mtRF1, if mtRF1a is able to terminate all thirteen mtDNA-encoded peptides<sup>5,8</sup>. Compared to canonical RF1 and mtRF1a, mtRF1 shows insertions in the codon-recognition motifs: a PEVGLS hexapeptide instead of the PxT tripeptide motif and an insertion of two amino acids (RT) in the α5 helix (Fig. 1a). No release activity has been measured in vitro so far and also no particles of reconstituted 55S mitochondrial ribosomes could be solved with bound mtRF1<sup>9,13</sup>.

In this work, we determine the function of mtRF1 in human cells by generating a specific knockout cell line and subsequent investigation

of the consequences of loss of function in comparison to mtRF1a-ablated cells. Our results show that mtRF1 is required for mitochondrial function by ensuring proper COX1 translation termination. Although ablation of mtRF1 results in isolated COX deficiency, the activation of mtRQC prevents respiratory incompetence by partially rescuing stalled COX1-translating ribosome complexes.

## Results

### Human mtRF1 and mtRF1a are required for mitochondrial function

Although in vitro measurements and high-resolution structures reveal mechanistic insights into the function of mtRF1a, our knowledge regarding the cellular consequences of perturbed translation termination in human mitochondria is limited and only based on short-term siRNA-mediated depletion of mtRF1a<sup>9</sup>. To study the impact of loss of function of translation termination in human mitochondria, we have generated specific knockout cell lines using CRISPR/Cas9 technology. We used guide RNAs targeting exon 1 of mtRF1a and exon 2 of mtRF1, respectively; and isolated clones were confirmed by western blotting and genomic DNA sequencing (Fig. 1b, Supplementary Fig. 2a, b). In both cases premature STOP codons were identified leading to undetectable protein levels. Loss of both mitochondrial RFs affects cellular growth in high-glucose-containing media as the cell number over time is significantly reduced in comparison to the wild-type control, however, mtRF1a ablation is more severe than mtRF1 loss (Fig. 1c). Such growth defect has also been observed in other studies when interfering with mitochondrial translation<sup>9,11,16–18</sup>. In the absence of mtRF1a, cells tend to produce more reactive oxygen species (ROS), which is in agreement with previous observations and suggest mitochondrial dysfunction<sup>9</sup>. ROS production is less pronounced in *mtRF1*<sup>-/-</sup>, but still

significantly elevated compared to wildtype. Thus, both release factors are critical for mitochondrial function and cellular growth.

### Loss of human mtRF1 leads to isolated complex IV deficiency

In contrast to previous observations, mtRF1a-deficient cells are not able to respire as monitored by real time respirometry in intact cells (Fig. 2a). Therefore, these cells can only survive in the high-glucose containing media, in which they obtain their energy via glycolysis. *mtRF1a*<sup>-/-</sup> cells acidify the media relatively fast, indicating the conversion of excess pyruvate into lactate, a typical characteristic of oxidative phosphorylation (OXPHOS)-deficient cells. The oxygen consumption rate is also reduced in mtRF1-ablated cells in comparison to wildtype control, but does not reveal such a profound defect as *mtRF1a*<sup>-/-</sup> cells, which is in agreement with the relative growth rates. Nevertheless, these results show that both RFs are required for optimal OXPHOS capacity. To dissect how the loss of mtRF1a or mtRF1, respectively, affects the function of the different respiratory chain complexes, we monitored the amounts and the activity of complex I and IV by *in gel* activity measurements and in a colorimetric assay (Fig. 2b–d). While mtRF1a ablation results in an almost complete loss of complex I and IV activity, mtRF1 loss does not affect complex I, but reveals a significant reduction in complex IV activity. We further analyzed the individual complexes by Blue-Native PAGE and western blotting, confirming the combined OXPHOS deficiency in *mtRF1a*<sup>-/-</sup> with complex II, which is entirely nuclear (nDNA)-encoded, being unaffected (Fig. 2e). No respiratory supercomplexes are formed in the absence of mtRF1a and only the nuclear-encoded F<sub>1</sub> part of the ATP synthase is detectable providing the explanation for the drastic respiratory incompetence. In contrast, respiratory supercomplex formation is comparable between wildtype and *mtRF1*<sup>-/-</sup> cells. However, the dimeric complex IV at ~400 kDa is strongly reduced in mtRF1-deficient cells as visualized by COX1 antibody on BN PAGE (Fig. 2e, lane 11) and *in gel* activity indicating an isolated cytochrome c oxidase (COX) deficiency in *mtRF1*<sup>-/-</sup>. Next, we investigated the protein steady-state levels of the mtDNA- and nDNA-encoded components of the OXPHOS complexes by western blotting (Fig. 2f, g). In agreement with reduced OXPHOS complexes, the tested mtDNA-encoded proteins are significantly reduced in *mtRF1a*<sup>-/-</sup> cells except COX1. In contrast, COX1 is strongly affected in *mtRF1*<sup>-/-</sup> while the other tested mtDNA-encoded proteins are unaltered. Similarly, nDNA-encoded structural OXPHOS components are significantly reduced in *mtRF1a*<sup>-/-</sup> while only marginally affected in *mtRF1*<sup>-/-</sup>. We also investigated the steady-state levels of MITRAC (mitochondrial translation regulation assembly intermediate of cytochrome c oxidase) components, which form an assembly platform that coordinates COX1 synthesis with its subsequent assembly into complex IV. C12ORF62 and MITRAC12 interact with nascent COX1 ribosome complexes and represent essential assembly factors mediating the first steps during COX biogenesis<sup>19–21</sup>. Mutations in C12ORF62 or MITRAC12 lead to reduced COX1 synthesis and subsequently to isolated complex IV deficiency associated with severe neurological disorders in human patients<sup>22,23</sup>. While MITRAC12 is not drastically affected in either of the knockouts, C12ORF62 is altered. Whereas mtRF1 loss leads to reduced C12ORF62 levels, mtRF1a deficiency results in elevated amounts (Fig. 2h, i). We further elaborated these findings by 2D PAGE and reveal an accumulation of COX1-containing MITRAC complex at ~200 kDa in *mtRF1a*<sup>-/-</sup> while MITRAC is strongly reduced in *mtRF1*<sup>-/-</sup> (Fig. 2j). Thus, COX1 is trapped in MITRAC in mtRF1a-deficient cells, as further assembly steps are blocked due to reduced levels of other complex IV constituents such as COX2. In *mtRF1*<sup>-/-</sup> cells MITRAC is strongly reduced as indicated by decreased levels in COX1 and C12ORF62 suggesting defects in COX1 synthesis.

### mtRF1 is specifically required for COX1 translation

We measured the synthesis of mtDNA-encoded proteins by [<sup>35</sup>S] Methionine de novo labeling and reveal that mtRF1a loss affects the

translation of most mtDNA-encoded transcripts including the non-canonically terminated transcript of ND6, but not of COX1 (Fig. 3a). Contrary, the synthesis of COX1 is exclusively affected in *mtRF1*<sup>-/-</sup> while others are produced comparable to wild-type control (Fig. 3b). Nevertheless, COX1 is still produced in *mtRF1*<sup>-/-</sup> and is detectable in respiratory supercomplexes comparable to wild-type control (Fig. 2e) indicating a higher stability of the reduced newly synthesized COX1 in mtRF1-deficient cells. To prove this hypothesis we monitored the stability of COX1 by [<sup>35</sup>S]Methionine pulse-chase experiment for 24 h. Indeed, COX1 reveals a higher stability in mtRF1-ablated cells compared to wild-type control (Supplementary Fig. 3a, b). These results suggest that the limiting amounts of COX1 are sequestered by respiratory supercomplexes to enhance its stability and to ensure respiratory competence in *mtRF1*<sup>-/-</sup>. These findings are reminiscent to previous observations, where it has been reported that reduced levels of complex IV are preferentially assembled into respiratory supercomplexes also to ensure the assembly and stability of complex I<sup>24–26</sup>.

Thus, both release factors are required for mitochondrial translation and the opposed effects indicate that the factors cannot compensate each other. To ensure that 55 S mitochondrial ribosomes are properly formed, we monitored ribosome particles by sucrose density ultracentrifugation (Fig. 3c). As 28 S small and 39 S large mitochondrial subunits as well as 55 S ribosomes are detectable, defects in mitochondrial ribosome biogenesis are unlikely. To confirm that the translation defects are specific due to the loss of mtRF1a or mtRF1, respectively, and not caused by an off-target effect due to the CRISPR/Cas9 approach, we ectopically expressed the respective FLAG-tagged open reading frames in the knockout cell lines (Fig. 3d–g). In both cases the translation defect is rescued indicating that the knockouts are specific and the FLAG-tagged variants are functional.

Both mitochondrial RFs carry the highly conserved GGQ motif in domain 3 (Fig. 1a), which is essential to facilitate peptide hydrolysis within the ribosome in all kingdoms of life. Mutations within the GGQ motif in bacterial or eukaryotic release factors as well as in human mL62 disable RFs to terminate translation while the proteins are stably expressed and the interaction with the ribosome is maintained<sup>11,27–30</sup>. We expressed mitochondrial RF variants in which we mutated the two glycine residues of the GGQ motif into alanine residues (Fig. 3d–g). Mutant variants were expressed to comparable levels as the FLAG-tagged wild-type RFs. However, mitochondrial translation could not be restored indicating that the catalytic activity of both release factors is required for their function and for mtDNA-encoded protein synthesis. Thus, our data indicate that mitochondrial RFs are indeed required for mitochondrial translation termination *in vivo* and mtRF1 is specifically assigned for COX1 synthesis, while mtRF1a terminates other mitochondrial translation events including ND6.

### Ablation of mitochondrial release factors affect mt-mRNA stability

Defects in mitochondrial translation often lead to an upregulation of mitochondrial transcripts potentially as a compensatory effect as indicated in previous studies<sup>31,32</sup>. We also investigated the steady-state levels of mitochondrial mRNAs as well as rRNAs by northern blotting in *mtRF1*<sup>-/-</sup> and *mtRF1a*<sup>-/-</sup> (Fig. 4a, b). The 12 S (*MTRNR1*) and 16 S rRNA (*MTRNR2*) remain stable in both knockouts, which is in agreement with the proper formation of mitochondrial ribosomes (Fig. 3c). However, mt-mRNAs are contrarily affected upon loss of mitochondrial RFs. While COX1-encoding mRNA (*MTCO1*) is significantly reduced in mtRF1-ablated cells, it remains stable in *mtRF1a*<sup>-/-</sup>. In contrast, transcripts encoding for COX2 or CYTB are strongly decreased in *mtRF1a*<sup>-/-</sup>, but are unaffected upon mtRF1 loss. Mitochondrial transcripts derive from two polycistronic transcripts. With the exception of *MTND6* (mRNA encoding for ND6), all of the mt-mRNAs arise from the polycistronic transcript synthesized from the heavy strand. If the loss of mitochondrial RFs would affect mitochondrial transcription, one

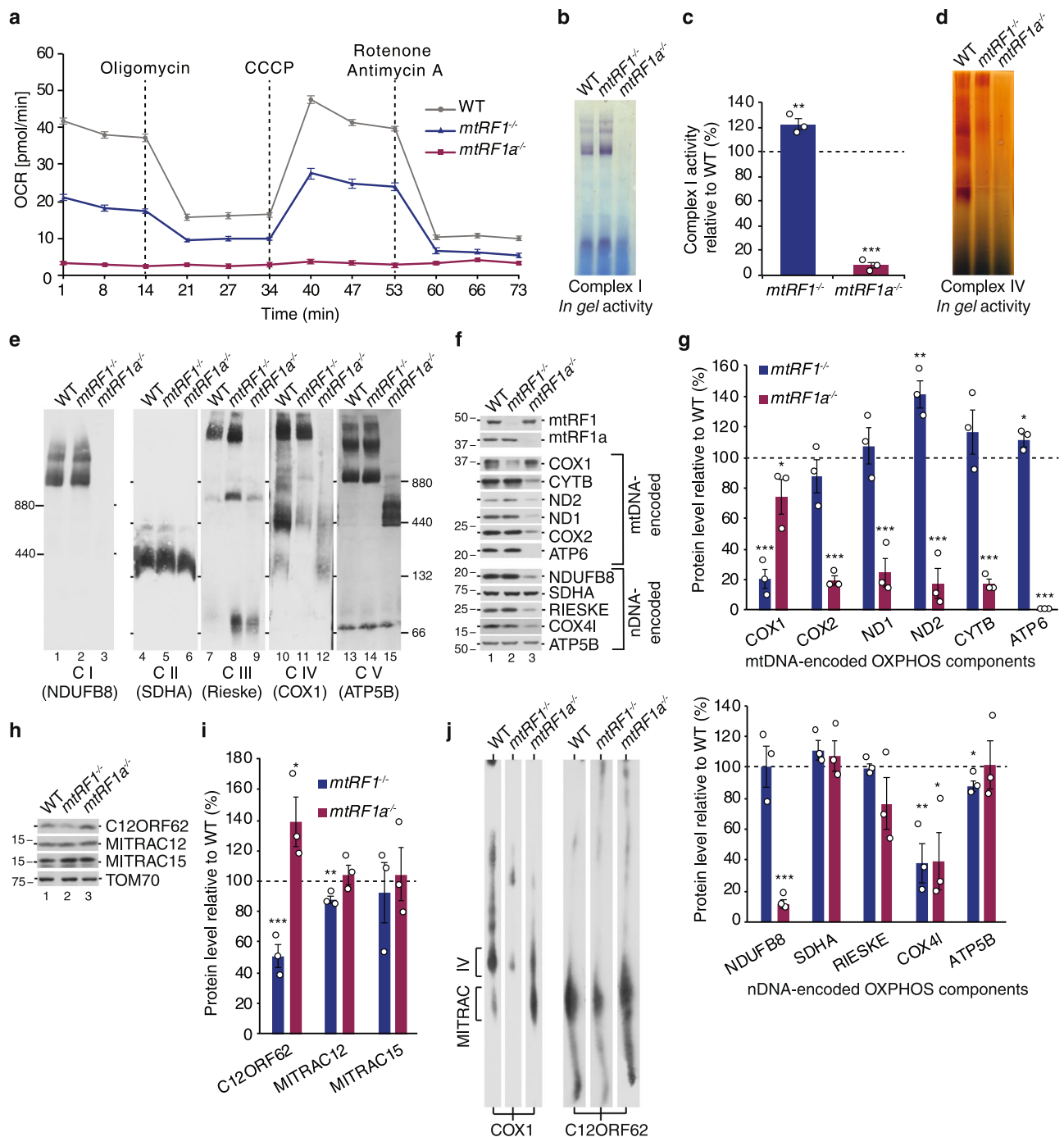


**Fig. 2 | Ablation of mitochondrial release factors affects OXPHOS.** **a** Oxygen consumption rate (OCR) is altered in *mtRF1*<sup>-/-</sup> and *mtRF1a*<sup>-/-</sup>. OCR was measured for the indicated time in wild-type cells (WT, gray), *mtRF1*<sup>-/-</sup> (blue) and *mtRF1a*<sup>-/-</sup> (red). Complex V was blocked using oligomycin, the membrane potential was uncoupled using CCCP and the activity of complex I and III was diminished by the addition of rotenone and antimycin A, respectively. **b–d** The activity of complex I and IV was measured by *in-gel* activity (**b**, **d**) or in a colorimetric assay (**c**). **c** Complex I activity of WT is indicated as dashed line and individual data points are shown. Statistical analysis was performed as two-sample one-tailed Student's *t*-test with  $n = 3$  biologically independent samples shown as mean  $\pm$  SEM. Significance was defined as  $**p \leq 0.01$ ;  $***p \leq 0.001$ . **e** The effect of *mtRF1* and *mtRF1a* loss on OXPHOS complexes. Isolated mitochondria (30  $\mu$ g) were separated by BN-PAGE (2.5–10% gradient gel: C I–14% gradient gel: C II–CV) followed by western blotting and

immunodetection using the indicated antibodies in brackets for complex I–V. **f–i** Loss of release factors affects mtDNA-encoded OXPHOS components. Mitochondria were analyzed by western blotting using the indicated antibodies for mtDNA- and nDNA-encoded OXPHOS components (**f**, **g**) as well as for MITRAC constituents (**h**, **i**). The relative protein steady-state levels were measured from three independent experiments and are presented as mean  $\pm$  SEM (individual data points are shown as circles) relative to WT indicated as dashed line (100%). Statistical analysis was performed as two-sample one-tailed Student's *t*-test and significance was defined as  $*p \leq 0.05$ ;  $**p \leq 0.01$ ;  $***p \leq 0.001$ . **j** MITRAC is contrarily affected in *mtRF1*- and *mtRF1a*-ablated cells. Isolated mitochondria (150  $\mu$ g) were subjected to BN-PAGE in the first dimension followed by SDS-PAGE in the second dimension prior to immunoblotting. Source data are provided as a Source Data file.

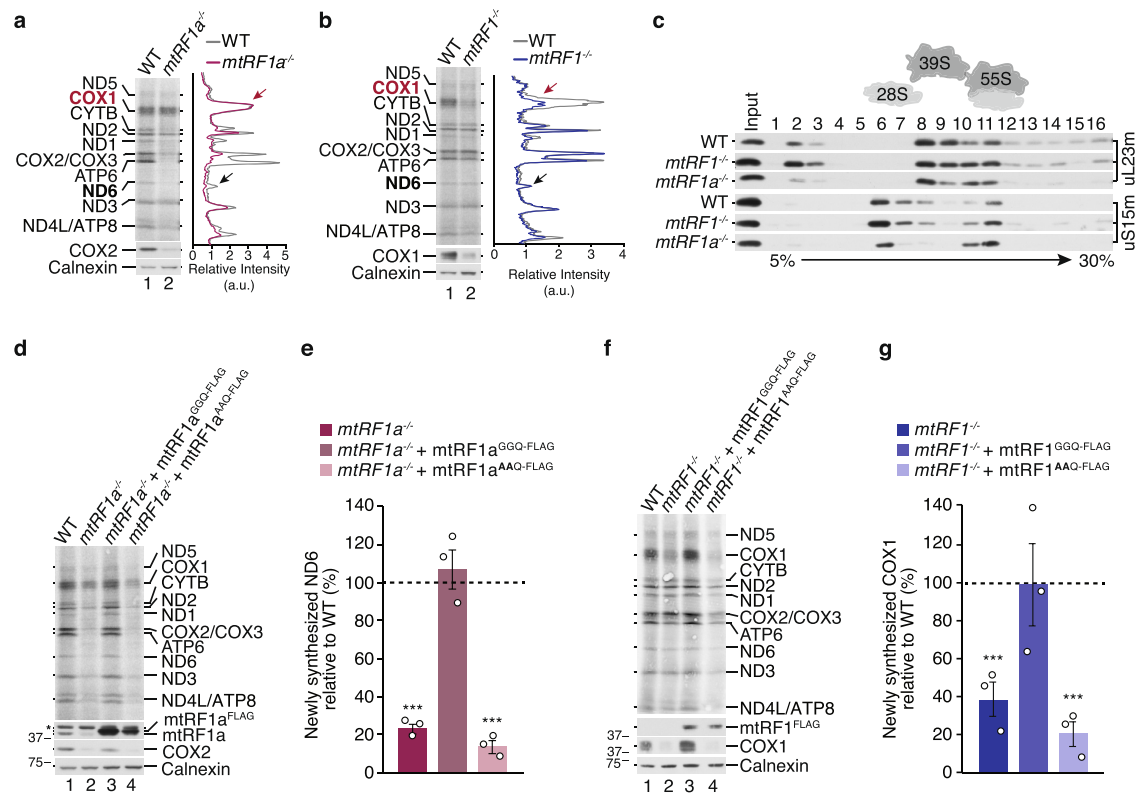


**Fig. 3 | Mitochondrial translation requires mtRF1 and mtRF1a.** **a, b** The synthesis of mtDNA-encoded proteins was analyzed by [<sup>35</sup>S]Methionine de novo incorporation in wild-type (WT), *mtRF1a*<sup>-/-</sup> (**a**) and *mtRF1*<sup>-/-</sup> cells (**b**). Samples were analyzed by autoradiography and western blotting, respectively, and relative intensity was measured using ImageJ software. Similar results were obtained in  $n \geq 3$  biologically independent experiments. **c** Loss of mitochondrial release factors does not affect mitochondrial ribosome biogenesis. Purified mitoplasts (500  $\mu$ g) from indicated cell lines were separated by sucrose density ultracentrifugation. Collected fractions (1–16) were analyzed by western blotting using uL23m as a marker of the large mitoribosomal subunit (mtLSU) and uS15m to indicate the small mitoribosomal

subunit (mtSSU). Input = 10% of total. Similar results were obtained in  $n \geq 3$  biologically independent experiments. **d–g** The GGQ motif is required for mtRF1 and mtRF1a function. C-terminal FLAG-tagged variants of mtRF1a and mtRF1 were ectopically expressed in the respective knockout cell line. Mitochondrial translation was monitored as in **a**. Newly synthesized ND6 (**e**) and COX1 (**g**) were measured in the indicated cell lines (individual data points are shown as circles) and calculated relative to WT (dashed line, 100%). Statistical analysis was performed as two-sample one-tailed Student's *t*-test with  $n = 3$  biologically independent samples and shown as mean  $\pm$  SEM. Significance was defined as \*\*\* $p \leq 0.001$ . Asterisk in (**d**) indicates unspecific signals. Source data are provided as a Source Data file.

would expect an overall decrease in all mitochondrial transcripts. However, as we observe a selective decrease in specific transcripts in the individual knockouts, we conclude that it is more likely an issue of RNA stability rather than synthesis. To support this hypothesis, we blocked mitochondrial translation using chloramphenicol and show that *MTCO1* levels can be restored in *mtRF1*<sup>-/-</sup> (Fig. 4c, d) indicating that the degradation of *MTCO1* transcripts is dependent on translation. To ensure that *MTCO1* is the only affected transcript in *mtRF1*<sup>-/-</sup>, we measured the steady-state level of all mt-mRNAs by NanoString analysis (Fig. 4e). In agreement with our northern blot results, *MTCO1* was the only reduced transcript in mtRF1-ablated cells whereas all the other transcripts were comparable to wildtype. Thus, mtRF1 loss induces the degradation of *MTCO1*, which might be part of a quality control system. Nevertheless, COX1 is not completely diminished and still detectable in mitochondrial supercomplexes in the absence of mtRF1, which ensures respiratory competence in *mtRF1*<sup>-/-</sup>. Consequently, an alternative factor must fulfill the task of COX1 translation termination and thus compensate for the loss of mtRF1.

#### Loss of mtRF1 induces mitochondrial ribosome-associated quality control

A potential alternative factor responsible for the release of newly synthesized COX1 if mtRF1 is missing might be another member of the mitochondrial release factor family. We measured the steady-state level of mtRF1a, mL62 and C12ORF65 in *mtRF1*<sup>-/-</sup> and reveal significant elevated levels of C12ORF65 in mtRF1-ablated cells suggesting that the

mitochondrial ribosome-associated quality control machinery is responsible for the rescue of stalled COX1-translating ribosomes (Fig. 5a, b). Levels of mL62, which represents another system to rescue ribosomes stalled on truncated mRNAs, are comparable to wildtype. As mL62 requires an empty A site, it seems to be less likely that mL62 would rescue COX1-translating ribosomes in *mtRF1*<sup>-/-</sup>. mtRF1a also appears unaltered in *mtRF1*<sup>-/-</sup> and our results actually suggest that mtRF1a and mtRF1 cannot compensate each other. Therefore, C12ORF65, which together with MTRES1 represents the mtRQC, is a promising candidate to facilitate the release of COX1 from the ribosome if mtRF1 is missing. We tested this hypothesis by depleting C12ORF65 in *mtRF1*<sup>-/-</sup> and monitored the level of newly synthesized COX1 upon [<sup>35</sup>S]Methionine metabolic labeling (Fig. 5c, d). C12ORF65 is efficiently downregulated and also leads to a decrease in MTRES1 indicating an interdependence of these factors. In line with our assumption, COX1 synthesis is significantly more decreased upon C12ORF65 depletion in *mtRF1*<sup>-/-</sup> than in non-targeting siRNA-treated knockout cells. Thus, loss of mtRF1 induces mtRQC to compensate for deficient termination events during COX1 translation in *mtRF1*<sup>-/-</sup>.

#### Discussion

The role of mtRF1 during translation termination in human mitochondria was a long standing open question since it was discovered in 1998<sup>10</sup>. Here, we show that mtRF1 is required for COX1 translation termination and thus for cytochrome c oxidase function (Fig. 6). MITRAC is the first assembly platform for newly synthesized COX1, where nascent COX1

interacts with the early MITRAC constituents C12ORF62 and MITRAC12<sup>19,20</sup>. Both factors are associated with severe mitochondrial diseases with isolated COX deficiency<sup>22,23</sup>. While patients with mutation

in C12ORF62 display fatal neonatal lactic acidosis, mutations in MITRAC12 are associated with neuropathy and exercise intolerance. As the loss of mtRF1 leads specifically to a reduction in COX1 and subsequently to decreased levels of C12ORF62, mtRF1 is a potential candidate when screening patients with isolated COX deficiency.

Our data also show the physiological importance of mtRQC during mitochondrial translation termination. It has been recently demonstrated that C12ORF65 is part of the mtRQC and required as a rescue factor for stalled ribosome complexes under conditions of aminoacyl tRNA starvation<sup>14</sup>. This population of stalled ribosomes with intact mRNA are not a preferred substrate for mL62, which requires an empty A site to protrude its C-terminal tail into the mRNA channel, similarly to its bacterial counterpart ArfB<sup>13,33</sup>. This makes it unlikely that mL62 rescues COX1-translating ribosomes in *mtRF1*<sup>-/-</sup> as the A-site would be still occupied with mRNA. The mtRQC would first allow the dissociation of these stalled complexes into the large (mtLSU) and the small mitochondrial ribosomal subunit (mtSSU) followed by the binding of C12ORF65 and MTRES1 to the split mtLSU with the peptidyl tRNA in the P-site (Fig. 6). Finally, C12ORF65 would facilitate the hydrolysis of nascent COX1 from the tRNA. Thus, the activation of mtRQC in *mtRF1*<sup>-/-</sup> partially compensate for the abolished COX1 translation termination by mtRF1. This enables mitochondria to produce a certain fraction of COX1, which assembles as part of complex IV into the stable supercomplexes capable of respiration, although to a reduced level compared to wildtype. In agreement with previous studies is that the reduced COX1 tends to be assembled within the supercomplexes and not within the free complex IV, which likely enhances the stability of the reduced newly synthesized COX1 in mtRF1-deficient cells<sup>24–26</sup>. The reduction of mtRQC by siRNA-mediated depletion of C12ORF65 in *mtRF1*<sup>-/-</sup> shows further reduction in COX1 translation indicating the importance of mtRQC for mitochondrial function. This central importance of mtRQC is also demonstrated by a growing group of patients with mutations in *C12orf65* developing Leigh syndrome<sup>12,34</sup>. It is currently unknown which factor acts upstream of C12ORF65-MTRES1, allowing the dissociation of the ribosome into the subunits. Besides the canonical recycling system composed of mtRRF and mtEFG2, the alternative recycling factor GTPBP6 is a potential candidate to be part of the mitochondrial ribosome rescue system<sup>5,17,35</sup>. However, both recycling pathways do not prefer ribosomes with a peptidyl tRNA in the P-site. Thus, a so far unidentified factor might be part of the mtRQC, facilitating the dissociation of the ribosome prior to binding of C12ORF65 to the mtLSU.

The decrease in *MTCO1* suggests a feedback mechanism that allows the specific degradation of this transcript in *mtRF1*<sup>-/-</sup>, potentially to prevent an overload of the mtRQC (Fig. 6), which already responds with a higher expression of C12ORF65 to cope with these stalling events. Consequently, mtRQC seems to involve not only the rescue of stalled ribosomes but also the degradation of the respective mRNA to avoid mtRQC stress and to minimize proteotoxic burden. A similar scenario would apply if mtRF1a is missing and e.g. *MTCO2* is degraded to avoid too many stalling events of COX2-translating ribosomes. Contrarily to *mtRF1*<sup>-/-</sup>, COX1 remains stable in *mtRF1a*<sup>-/-</sup>, but becomes stalled in the MITRAC complex as COX2 and COX3 translation are diminished (Fig. 6). Thus, both mitochondrial RFs exhibit substrate specificity and cannot compensate each other.

COX1 is a rather unusual case as it terminates in AGA (Supplementary Fig. 4)<sup>6</sup>. However, a -1 ribosomal frameshift would allow the termination in the conventional STOP codon UAG<sup>8</sup>. It is still under debate whether a -1 ribosomal frameshift is really occurring during COX1 and also during ND6 translation termination or whether a specialized factor might be responsible in reading AGA and AGG codons. In the past it has been suggested that mtRF1 might be able to recognize these unconventional STOP signals<sup>9</sup>, although experimental evidence is completely missing. Nevertheless, bioinformatic studies using homology modeling and molecular dynamics simulation suggest that

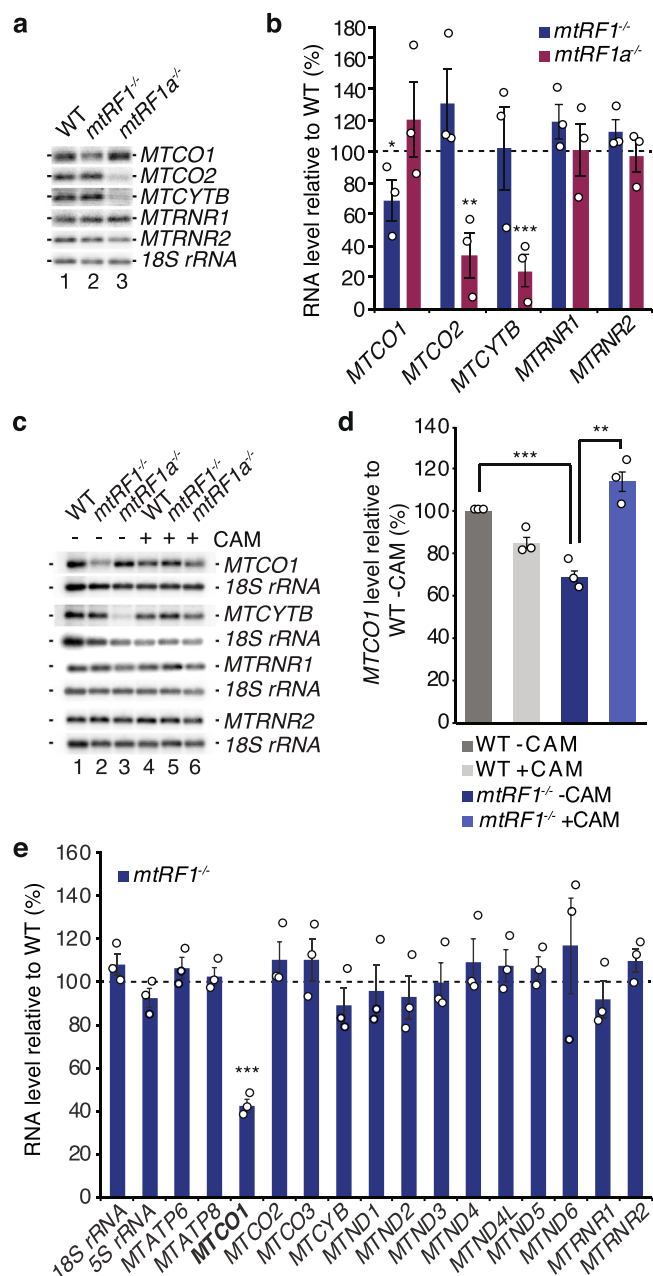


**Fig. 4 | Mitochondrial transcripts are altered upon ablation of mtRF1 or mtRF1a.** **a, b** RNA was isolated from wild-type (WT) cells, *mtRF1*<sup>-/-</sup> and *mtRF1a*<sup>-/-</sup> and subjected to northern blot analysis. Mitochondrial mRNAs encoding for COX1 (*MTCO1*), COX2 (*MTCO2*) and CYTB (*MTCYTB*) as well as the mt-rRNAs 12 S rRNA (*MTRNR1*) and 16 S rRNA (*MTRNR2*) were detected using specific probes. 18 S rRNA was used as loading control. RNA levels are calculated relative to WT (dashed line) and individual data points are indicated as circles. Statistical analysis was performed as two-sample one-tailed Student's *t*-test with *n* = 3 biologically independent samples and shown as mean ± SEM. Significance was defined as \**p* ≤ 0.05; \*\**p* ≤ 0.01; \*\*\**p* ≤ 0.001. **c, d** RNA was isolated from WT, *mtRF1*<sup>-/-</sup> and *mtRF1a*<sup>-/-</sup> treated with chloramphenicol (CAM, 50 µg/ml) for 24 h as indicated. Northern blot and statistical analysis were performed as in **a, b**. **e** Isolated RNA from WT and *mtRF1*<sup>-/-</sup> mitochondria was subjected to NanoString analysis. 18 S and 5 S rRNA were used as controls. The relative RNA levels of WT are indicated as dashed line. Statistical analysis was performed as two-sample one-tailed Student's *t*-test with *n* = 3 biologically independent samples and shown as mean ± SEM. Significance was defined as \*\*\**p* ≤ 0.001. Source data are provided as a Source Data file.

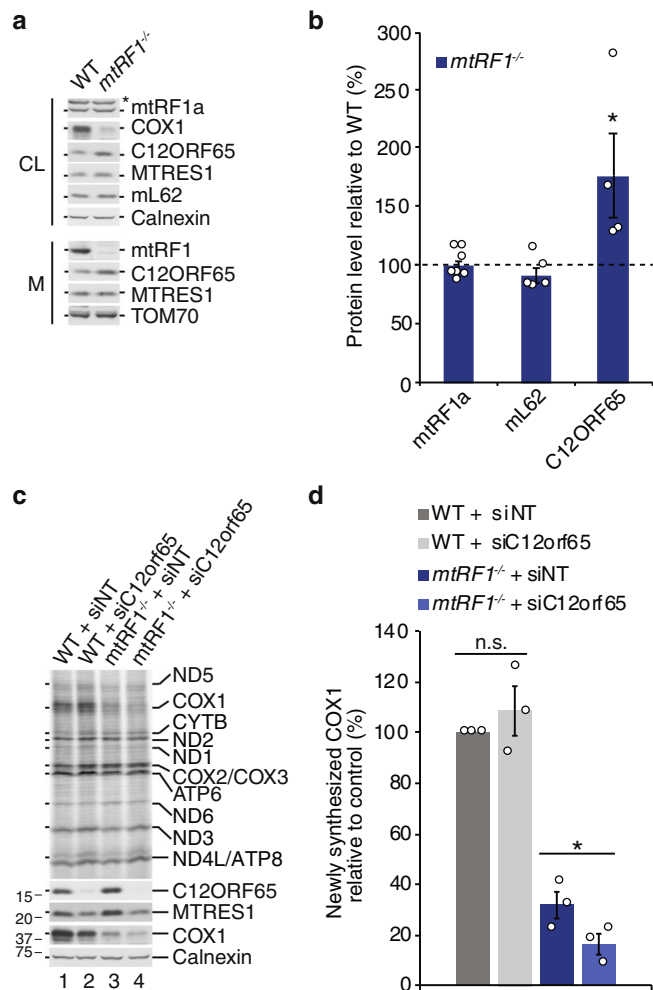


**Fig. 5 | Loss of mtRF1 activates C12ORF65.** **a, b** C12ORF65 protein levels are elevated in mtRF1-deficient cells. Whole cell lysates (CL, 25  $\mu$ g or 50  $\mu$ g) or isolated mitochondria (M, 75  $\mu$ g) were analyzed by western blotting using the indicated antibodies. Protein levels were quantified and calculated relative to the wild-type control (WT; dashed line; 100%) and individual data points are shown as circles. Statistical analysis was performed as two-sample one-tailed Student's *t*-test with  $n \geq 4$  biologically independent samples shown as mean  $\pm$  SEM. Significance was defined as  $*p \leq 0.05$ . Asterisk in **a** indicates unspecific signals. **c, d** Depletion of C12ORF65 in *mtRF1<sup>-/-</sup>* further reduces COX1 levels. WT and *mtRF1<sup>-/-</sup>* cells were transfected with siNT or siC12orf65. After 3 days mitochondrial protein synthesis was monitored as described in Fig. 3 and efficiency of siRNA-mediated depletion was controlled by western blotting. Newly synthesized COX1 was quantified from three independent experiments shown as mean  $\pm$  SEM with individual data points indicated as circles. Statistical analysis was performed as two-sample one-tailed Student's *t*-test and significance was defined as  $*p \leq 0.05$  and  $p > 0.05$  as not significant (n.s.). Source data are provided as a Source Data file.

the non-canonical mtRF1 with its insertion in the  $\alpha 5$  helix and the PEVGLS motif co-evolutionary adapted to the changes within the mitoribosome and that it has a preference for UAA and UAG codons and neither for AGA or AGG or an empty A site<sup>15</sup>. This actually supports the  $-1$  ribosomal frameshift hypothesis. Additionally, COX1 terminates in UAA and not in AGA in other species including mice, rat or bovine, although they also possess mtRF1 and mtRF1a (Supplementary Fig. 4, 5). Thus, if mtRF1 is a specialized release factor for COX1 termination in other species as well and if one considers the bioinformatic preference for UAA and UAG STOP codon by mtRF1, then this would be in favor with the  $-1$  ribosomal frameshift theory in human mitochondria that allows termination in UAG. Along this line, we observed a decrease in ND6 in *mtRF1a<sup>-/-</sup>*, but no in *mtRF1<sup>-/-</sup>* suggesting that mtRF1a is

responsible for ND6 termination (Fig. 3a, b). However, mtRF1a reads specifically UAA and UAG codons, but does not exhibit release activity on AGG codon<sup>9,11</sup>, which also supports the hypothesis that a  $-1$  ribosomal frameshift allows the conventional termination of ND6 in UAG recognized by mtRF1a.

Taken together, we have solved the mystery of the function of mtRF1 in human mitochondria and show that mtRF1 is specifically responsible for the termination of COX1 translation, which likely requires a  $-1$  ribosomal frameshift by the human mitochondrial ribosome.

## Methods

### Key reagents

An extended table of plasmids, oligonucleotides, antibodies and other materials used is provided in Supplementary Table 1 and 2.

### Cell culture

HEK293 (Human Embryonic Kidney 293-Flp-In T-Rex, Thermo Fisher Scientific) cells were cultured in DMEM (Dulbecco's modified Eagle's medium) supplemented with 10% [v/v] FCS (Fetal Calf Serum), 2 mM L-glutamine, 1 mM sodium pyruvate and 50  $\mu$ g/ml uridine at 37  $^{\circ}$ C under 5% CO<sub>2</sub> humidified atmosphere. Cells were regularly monitored for the absence of Mycoplasma by GATC Biotech.

HEK293 mtRF1 and mtRF1a knockout cell lines were generated using Alt-R CRISPR/Cas9 technology (Integrated DNA Technologies, IDT) according to the manufacturer's instructions. In brief, cells were co-transfected with crRNA-tracrRNA duplex and Cas9 nuclease. The crRNA was designed to target the first or second exon of either the mtRF1a or mtRF1 gene, respectively. Clones were screened by immunoblotting and verified by TOPO cloning and subsequent sequencing. Usage of the TOPO<sup>TM</sup>-TA Cloning<sup>TM</sup> Kit (Thermo Fisher Scientific) allows simple analysis of gDNA from respective clones. TOPO cloning is based on ligation of the amplified PCR product of the gDNA sequence targeted by the CRISPR guide RNA into a pCR4-TOPO TA vector. After transformation into OneShot<sup>TM</sup> competent *E.coli* cells, clones were selected on ampicillin LB-Agar plates. Picking a statistical relevant number of clones ( $\geq 20$ ), their plasmid DNA were sequenced using M13 forward and reverse primers, allowing analysis of occurring INDELS in the genome caused by CRISPR/Cas9 technology.

Stable inducible cell lines expressing C-terminal FLAG-tagged versions of mtRF1 or mtRF1a were generated following established protocols<sup>19,20</sup>. Briefly, HEK293 cell lines were transfected with pOG44 and pcDNAs/FRT/TO plasmids harboring respective FLAG constructs using Lipofectamine3000 (Invitrogen) as transfection reagent according to the manufacturer's instructions. Cells were selected using 100  $\mu$ g/ml hygromycin B.

Transient siRNA-mediated knockdown was performed by transfecting HEK293 cells with 33 nM siRNA oligonucleotides (Eurogentec) targeting the transcript of interest (see Supplementary Table 1) or non-targeting siRNA as control by using Lipofectamine RNAiMax (Invitrogen) as transfection reagent. Cells were incubated for 72 h at 37  $^{\circ}$ C under 5% CO<sub>2</sub> humidified atmosphere prior to further investigation.

### Measurements of mitochondrial radicals

Cells ( $10^6$ ) were stained with 5  $\mu$ M MitoSox Red (Invitrogen) according to the manufacturer's instructions to detect ROS. For flow cytometry analysis, 10,000 gated events were recorded on a BD FACS Canto II (Becton Dickinson) and analyzed using FACS-Diva software.

### Respirometry

Oxygen consumption rates (OCR) were measured using a XF96 Extracellular Flux Analyzer (Seahorse Bioscience). Cells ( $4 \times 10^4$  per well) were directly seeded in assay buffer into a 96-well sample plate, spun down and incubated for 1 h in a non-CO<sub>2</sub> incubator at 37  $^{\circ}$ C

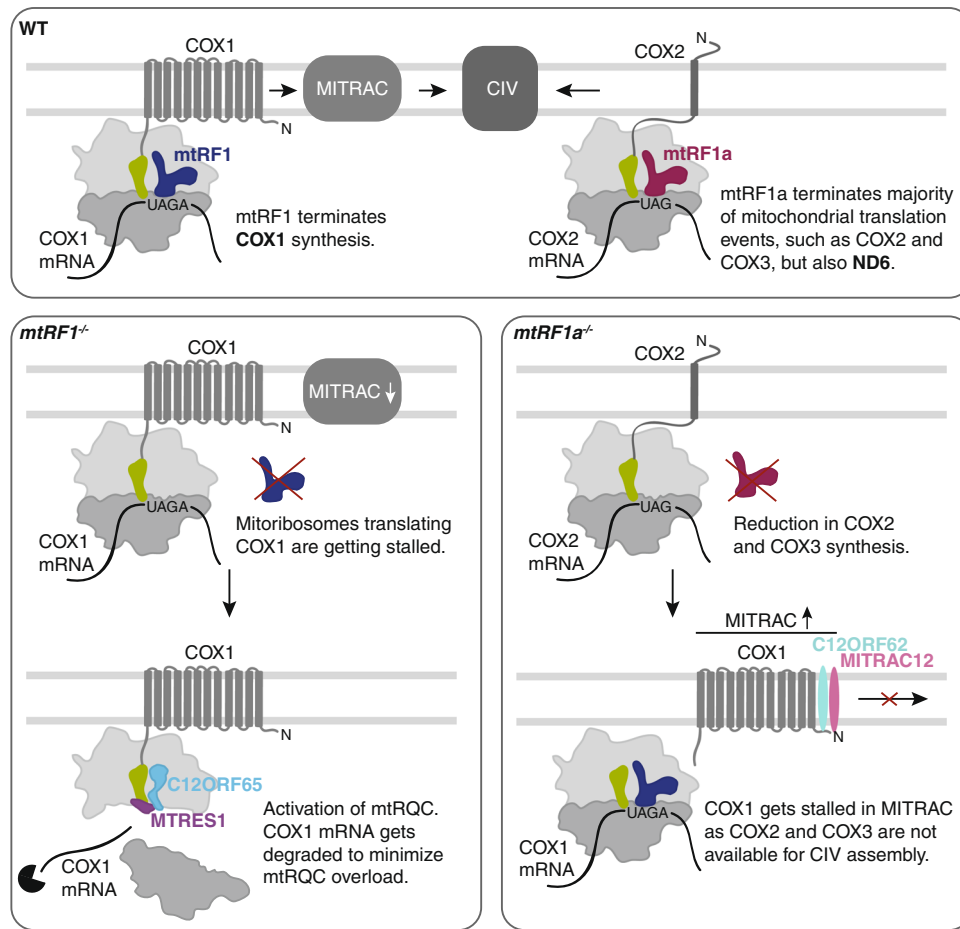


**Fig. 6 | The role of mtRF1 and mtRF1a during translation termination in human mitochondria.** mtRF1 (blue) specifically terminates COX1, whose synthesis and subsequent assembly is coordinated by MITRAC. In contrast mtRF1a (red) facilitates the release of COX2 and other mtDNA-encoded proteins including ND6. In the absence of mtRF1, termination of COX1 translation is affected and ribosomes are getting stalled. The decrease of newly synthesized COX1 leads to a reduction of MITRAC in *mtRF1*<sup>-/-</sup>. Stalled COX1-translating ribosomes are rescued by the

mitochondrial ribosome-associated quality control (mtRQC) composed of C12ORF65 (light blue) and MTRES1 (purple). COX1 mRNA gets degraded in *mtRF1*<sup>-/-</sup> to reduce stalling events and therefore to prevent a mtRQC overload. Loss of mtRF1a does not affect COX1 translation termination, but causes severe reduction in COX2 and COX3. Thus, synthesized COX1 gets stalled in MITRAC as COX2 and COX3 are not available for further complex IV assembly in *mtRF1a*<sup>-/-</sup>.

before basal respiration was measured. Subsequent automated addition of 3  $\mu$ M oligomycin, 1.5  $\mu$ M CCCP and 1  $\mu$ M antimycin A plus 1  $\mu$ M rotenone was used to monitor maximal respiration.

#### Preparation of whole cell lysates, isolation of mitochondria from cultured cells and immunodetection via western blotting

Lysis of whole cells was carried out in nonionic lysis buffer (50 mM Tris-HCl pH 7.4, 130 mM NaCl, 2 mM MgCl<sub>2</sub>, 1% NP-40, 1 mM PMSF and 1x Protease Inhibitor (PI) Cocktail (Roche)). For isolation of mitochondria, cultured cells were harvested and resuspended in homogenization buffer (300 mM trehalose, 10 mM KCl, 10 mM HEPES-KOH pH 7.4) with 1 mM PMSF and 0.2% BSA and homogenized using a Homogenplus Homogenizer Size S (Schuett-Biotec). The crude cell homogenate was separated using differential centrifugation steps: 400  $\times$  g, 10 min, 4  $^{\circ}$ C to remove cell debris, 11,000  $\times$  g for 10 min, 4  $^{\circ}$ C to pellet mitochondria. Mitochondria were resuspended in homogenization buffer and were used immediately or stored at -80  $^{\circ}$ C.

Cell lysates or mitochondria samples were separated on 10–18% Tris-Tricine gels and transferred onto Amersham<sup>TM</sup> Protran<sup>TM</sup> 0.2  $\mu$ M nitrocellulose membranes (NC, GE Healthcare). For immunodetection, primary antibodies were incubated overnight (4  $^{\circ}$ C) as indicated (see Supplementary Table 1), secondary antibodies were incubated for 2 h at room temperature and visualized on X-ray films using enhanced chemiluminescence detection kit (GE Healthcare).

#### Sucrose gradient centrifugation

Mitoplasts were purified by incubating fresh isolated mitochondria in 0.1% digitonin for 30 min on ice and 0.5  $\mu$ g Proteinase K per 100  $\mu$ g mitochondria for 15 min on ice. Proteinase K was blocked by addition of 2 mM PMSF followed by four washing steps. Mitoplasts (500  $\mu$ g) were lysed (3% sucrose, 100 mM NH<sub>4</sub>Cl, 15 mM MgCl<sub>2</sub>, 20 mM Tris-HCl pH 7.5, 1% Digitonin, 1x PI-Mix, 0.08 U/ $\mu$ l RiboLock RNase Inhibitor) and separated by sucrose density gradient centrifugation (5–30% sucrose [w/v] in 100 mM NH<sub>4</sub>Cl, 15 mM MgCl<sub>2</sub>, 20 mM Tris-HCl pH 7.5, 1x PI-Mix) at 79,000  $\times$  g for 15 h, 4  $^{\circ}$ C using a SW41Ti rotor (Beckman Coulter). A BioComp fractionator was used to collect fractions 1–16, which were then ethanol precipitated and analyzed via western blotting.

#### Blue-Native (BN) PAGE and *in gel* activity measurements

To investigate native protein complexes, mitochondria were solubilized (1% digitonin, 10 mM Tris-HCl pH 7.4, 0.1 mM EDTA, 50 mM NaCl, 10% Glycerol [v/v], 1 mM PMSF) at a concentration of 1  $\mu$ g/ $\mu$ l for 20 min, 4  $^{\circ}$ C. Lysates were cleared from insoluble materials by centrifugation for 15 min at 21,000  $\times$  g, 4  $^{\circ}$ C prior to addition of BN Loading Dye (5% Coomassie Brilliant Blue G250 (w/v), 500 mM 6-aminocaproic acid, 100 mM Bis-Tris-HCl pH 7.0). Samples were separated by electrophoresis using 4–14% or 2.5–10% polyacrylamide gradient gels. Proteins were either blotted on PVDF membranes for 1 dimensional

analysis via western blotting or further separated into the 2nd dimension via 10–18% Tris-Tricine gels.

To monitor *in gel* activities, the gel was incubated either in complex I (1 mg/ml nitrotetrazoliumbluechlorid and 1 mg/ml NADH in 5 mM Tris-HCl pH 7.4) or complex IV (0.5 mg/ml diaminobenzidine, 20 µg/ml catalase, 1 µg/ml cytochrome *c* and 75 mg/ml sucrose in 50 mM KP<sub>i</sub> pH 7.4) solution<sup>36</sup>.

### Activity measurement complex I

To determine complex I activity, the activity assay kit by abcam was used according to the manufacturer's instructions. Briefly, 200 µg of cell lysate was loaded per well and oxidation of NADH by complex I was colorimetrically detected as increase in absorbance at OD = 450 nm.

### [<sup>35</sup>S]Methionine de novo mitochondrial protein synthesis

De novo labeling of newly synthesized mitochondrial proteins was performed as followed: Cultured cells were starved in FCS- and methionine-free media, cytosolic translation was inhibited by using 100 µg/ml emetine and incubated in the presence of 200 µCi/ml [<sup>35</sup>S]Methionine for 1 h in fully supplemented but methionine-free DMEM media<sup>16</sup>. For pulse-chase labeling, cytosolic translation was inhibited using 100 µg/ml anisomycin instead of emetine and after 1 h pulse-labeling, media was changed to normal growth media and cells were harvested at indicated chase-time points. Cell lysates were subjected to SDS-PAGE followed by western blotting. Radioactive labeled mitochondrial translation products were detected using Phosphor screens and Amersham Typhoon imaging system (GE Healthcare).

### RNA isolation and northern blotting

Total RNA from cultured cells was isolated using TRIzol Reagent (Invitrogen) according to the manufacturer's instructions. RNA (2 µg) was separated on a denaturing formaldehyde/formamide 1.2% agarose gel and transferred and UV-crosslinked onto Amersham Hybond<sup>TM</sup>-N membrane (GE Healthcare). RNA was visualized using [<sup>32</sup>P]-radiolabeled probes targeting mitochondrial RNAs as indicated (see Supplementary Table 1).

### NanoString analysis

The experiment was performed following established protocols<sup>20,37</sup>. Briefly, equal amounts of mitochondria (100 µg) were isolated from the respective cell lines and solubilized into lysis buffer (50 mM Tris-HCl pH 7.4, 150 mM NaCl, 10% Glycerol, 10 mM MgCl<sub>2</sub>, 1% Digitonin, 1 mM PMSF, 1x PI-Mix (Roche) and 0.08 U/µl RiboLock RNase inhibitor (Thermo Scientific)). RNA isolation from the lysates was performed according to the Ambion/Life Technologies protocol using TRIzol reagent and RNA Clean and Concentrator kit (Zymo Research). Isolated RNA pool was hybridized with TagSet master mix (nCounter Elements<sup>TM</sup> XT Reagents, nanoString) and probes targeting individual mitochondrial transcripts or cytosolic 18 S rRNA/5 S rRNA (Supplementary Table 2). Subsequently, the samples were analyzed in a nCounter MAX system (nanoString) following the nanoString Technologies instructions. Collected data were evaluated with nSolver software (nanoString). To assess the abundance of the transcripts of interest, the raw data were normalized to the abundance of cytosolic transcripts (18 S rRNA and 5 S rRNA).

### Quantification and statistical analysis

All experiments were carried out at least in biological triplicate and data is presented as means with standard error of the mean (SEM). Protein or RNA signals from western and northern blots were quantified using ImageJ (<https://imagej.nih.gov/ij>) or ImageQuant TL (GE Healthcare) and data was statistically analyzed by two-sample (equal variances) one-tailed Student's *t*-test. Statistical significance was

defined by \* for  $p \leq 0.05$ , \*\* for  $p \leq 0.01$  and \*\*\* for  $p \leq 0.001$ . Exact *p*-values are provided with the source data.

### Reporting summary

Further information on research design is available in the Nature Research Reporting Summary linked to this article.

### Data availability

Material will be available upon reasonable request and source data are provided with this paper. The original data generated in this study are provided in the supplementary information and the source data file, and are available through <https://figshare.com/> with the digital object identifier <https://doi.org/10.6084/m9.figshare.21276411>. Source data are provided with this paper.

### References

- Ito, K., Uno, M. & Nakamura, Y. A tripeptide 'anticodon' deciphers stop codons in messenger RNA. *Nature* **403**, 680–684 (2000).
- Laurberg, M. et al. Structural basis for translation termination on the 70S ribosome. *Nature* **454**, 852–857 (2008).
- Petry, S. et al. Crystal structures of the ribosome in complex with release factors RF1 and RF2 bound to a cognate stop codon. *Cell* **123**, 1255–1266 (2005).
- Weixlbaumer, A. et al. Insights into translational termination from the structure of RF2 bound to the ribosome. *Science* **322**, 953–956 (2008).
- Nadler, F., Lavdovskaia, E. & Richter-Dennerlein, R. Maintaining mitochondrial ribosome function: the role of ribosome rescue and recycling factors. *RNA Biol.* **19**, 117–131 (2022).
- Anderson, S. et al. Sequence and organization of the human mitochondrial genome. *Nature* **290**, 457–465 (1981).
- Barrell, B. G., Bankier, A. T. & Drouin, J. A different genetic code in human mitochondria. *Nature* **282**, 189–194 (1979).
- Temperley, R., Richter, R., Dennerlein, S., Lightowlers, R. N. & Chrzanowska-Lightowlers, Z. M. Hungry codons promote frame-shifting in human mitochondrial ribosomes. *Science* **327**, 301 (2010).
- Soleimanpour-Lichaei, H. R. et al. mtRF1a is a human mitochondrial translation release factor decoding the major termination codons UAA and UAG. *Mol. Cell* **27**, 745–757 (2007).
- Zhang, Y. & Spremulli, L. L. Identification and cloning of human mitochondrial translational release factor 1 and the ribosome recycling factor. *Biochim. Biophys. Acta* **1443**, 245–250 (1998).
- Richter, R. et al. A functional peptidyl-tRNA hydrolase, ICT1, has been recruited into the human mitochondrial ribosome. *EMBO J.* **29**, 1116–1125 (2010).
- Antonicka, H. et al. Mutations in C12orf65 in patients with encephalomyopathy and a mitochondrial translation defect. *Am. J. Hum. Genet.* **87**, 115–122 (2010).
- Kummer, E., Schubert, K. N., Schoenhut, T., Scaiola, A. & Ban, N. Structural basis of translation termination, rescue, and recycling in mammalian mitochondria. *Mol. Cell* **81**, 2566–2582.e6 (2021).
- Desai, N. et al. Elongational stalling activates mitoribosome-associated quality control. *Science* **370**, 1105–1110 (2020).
- Lind, C., Sund, J. & Aqvist, J. Codon-reading specificities of mitochondrial release factors and translation termination at non-standard stop codons. *Nat. Commun.* **4**, 2940 (2013).
- Lavdovskaia, E. et al. The human Obg protein GTPBP10 is involved in mitoribosomal biogenesis. *Nucleic Acids Res.* **46**, 8471–8482 (2018).
- Lavdovskaia, E. et al. Dual function of GTPBP6 in biogenesis and recycling of human mitochondrial ribosomes. *Nucleic Acids Res.* **48**, 12929–12942 (2020).



18. Rorbach, J. et al. The human mitochondrial ribosome recycling factor is essential for cell viability. *Nucleic Acids Res.* **36**, 5787–5799 (2008).
19. Mick, D. U. et al. MITRAC links mitochondrial protein translocation to respiratory-chain assembly and translational regulation. *Cell* **151**, 1528–1541 (2012).
20. Richter-Dennerlein, R. et al. Mitochondrial protein synthesis adapts to influx of nuclear-encoded protein. *Cell* **167**, 471–483.e10 (2016).
21. Richter-Dennerlein, R., Dennerlein, S. & Rehling, P. Integrating mitochondrial translation into the cellular context. *Nat. Rev. Mol. Cell Biol.* **16**, 586–592 (2015).
22. Ostergaard, E. et al. Mutations in COA3 cause isolated complex IV deficiency associated with neuropathy, exercise intolerance, obesity, and short stature. *J. Med. Genet.* **52**, 203–207 (2015).
23. Weraarpachai, W. et al. Mutations in C12orf62, a factor that couples COX I synthesis with cytochrome c oxidase assembly, cause fatal neonatal lactic acidosis. *Am. J. Hum. Genet.* **90**, 142–151 (2012).
24. D'Aurelio, M., Gajewski, C. D., Lenaz, G. & Manfredi, G. Respiratory chain supercomplexes set the threshold for respiration defects in human mtDNA mutant cybrids. *Hum. Mol. Genet.* **15**, 2157–2169 (2006).
25. Lazarou, M., Smith, S. M., Thorburn, D. R., Ryan, M. T. & McKenzie, M. Assembly of nuclear DNA-encoded subunits into mitochondrial complex IV, and their preferential integration into supercomplex forms in patient mitochondria. *FEBS J.* **276**, 6701–6713 (2009).
26. Milenkovic, D., Blaza, J. N., Larsson, N.-G. & Hirst, J. The enigma of the respiratory chain supercomplex. *Cell Metab.* **25**, 765–776 (2017).
27. Frolova, L. Y. et al. Mutations in the highly conserved GGQ motif of class 1 polypeptide release factors abolish ability of human eRF1 to trigger peptidyl-tRNA hydrolysis. *RNA* **5**, 1014–1020 (1999).
28. Mora, L. et al. The essential role of the invariant GGQ motif in the function and stability in vivo of bacterial release factors RF1 and RF2. *Mol. Microbiol.* **47**, 267–275 (2003).
29. Shaw, J. J. & Green, R. Two distinct components of release factor function uncovered by nucleophile partitioning analysis. *Mol. Cell* **28**, 458–467 (2007).
30. Brown, A., Shao, S., Murray, J., Hegde, R. S. & Ramakrishnan, V. Structural basis for stop codon recognition in eukaryotes. *Nature* **524**, 493–496 (2015).
31. Cámara, Y. et al. MTERF4 regulates translation by targeting the methyltransferase NSUN4 to the mammalian mitochondrial ribosome. *Cell Metab.* **13**, 527–539 (2011).
32. Metodiev, M. D. et al. NSUN4 is a dual function mitochondrial protein required for both methylation of 12S rRNA and coordination of mitoribosomal assembly. *PLoS Genet* **10**, e1004110 (2014).
33. Chan, K.-H. et al. Mechanism of ribosome rescue by alternative ribosome-rescue factor B. *Nat. Commun.* **11**, 4106–4111 (2020).
34. Perrone, E. et al. Leigh syndrome in a patient with a novel C12orf65 pathogenic variant: case report and literature review. *Genet Mol. Biol.* **43**, e20180271 (2020).
35. Hillen, H. S. et al. Structural basis of GTPase-mediated mitochondrial ribosome biogenesis and recycling. *Nat. Commun.* **12**, 3672 (2021).
36. Korwitz, A. et al. Loss of OMA1 delays neurodegeneration by preventing stress-induced OPA1 processing in mitochondria. *J. Cell Biol.* **212**, 157–166 (2016).
37. Cruz-Zaragoza, L. D. et al. An in vitro system to silence mitochondrial gene expression. *Cell* **184**, 5824–5837.e15 (2021).

## Acknowledgements

We thank Peter Rehling for providing antibodies, Angela Boshnakovska for technical advice regarding oxygen consumption measurements and Sabine Poerschke regarding Blue-Native PAGE. This work was funded by the Deutsche Forschungsgemeinschaft: the Emmy-Noether grant [RI 2715/1-1 to R.R.-D.], the Cluster of Excellence [EXC 2067/1-390729940 to R.R.-D.] and the Collaborative Research Center 860 [SFB860/A14 to R.R.-D.]. We acknowledge support by the Open Access Publication Funds of the Goettingen University.

## Author contributions

F.N., E.L., A.K., L.D.C.-Z. and S.D. performed experiments. F.N. and R.R.-D. prepared figures. R.R.-D. designed the study and provided supervision. R.R.-D. wrote the manuscript. F.N., E.L. and R.R.-D. reviewed and edited the text.

## Funding

Open Access funding enabled and organized by Projekt DEAL.

## Competing interests

The authors declare no competing interests.

## Additional information

**Supplementary information** The online version contains supplementary material available at <https://doi.org/10.1038/s41467-022-34088-w>.

**Correspondence** and requests for materials should be addressed to Ricarda Richter-Dennerlein.

**Peer review information** *Nature Communications* thanks Yaser Hashem and the other, anonymous, reviewer(s) for their contribution to the peer review of this work. Peer reviewer reports are available.

**Reprints and permissions information** is available at <http://www.nature.com/reprints>

**Publisher's note** Springer Nature remains neutral with regard to jurisdictional claims in published maps and institutional affiliations.

**Open Access** This article is licensed under a Creative Commons Attribution 4.0 International License, which permits use, sharing, adaptation, distribution and reproduction in any medium or format, as long as you give appropriate credit to the original author(s) and the source, provide a link to the Creative Commons license, and indicate if changes were made. The images or other third party material in this article are included in the article's Creative Commons license, unless indicated otherwise in a credit line to the material. If material is not included in the article's Creative Commons license and your intended use is not permitted by statutory regulation or exceeds the permitted use, you will need to obtain permission directly from the copyright holder. To view a copy of this license, visit <http://creativecommons.org/licenses/by/4.0/>.

© The Author(s) 2022

## Human mtRF1 terminates COX1 translation and its ablation induces mitochondrial ribosome-associated quality control

Franziska Nadler<sup>1</sup>, Elena Lavdovskaia<sup>1,2</sup>, Angelique Krempfer<sup>1</sup>, Luis Daniel Cruz-Zaragoza<sup>1</sup>, Sven Dennerlein<sup>1</sup> and Ricarda Richter-Dennerlein<sup>1,2,3\*</sup>

<sup>1</sup>Department of Cellular Biochemistry, University Medical Center Goettingen, D-37073 Goettingen, Germany. <sup>2</sup>Cluster of Excellence “Multiscale Bioimaging: from Molecular Machines to Networks of Excitable Cells” (MBExC), University of Goettingen, D-37075 Goettingen, Germany. <sup>3</sup>Goettingen Center for Molecular Biosciences, University of Goettingen, D-37077 Goettingen, Germany.

\* correspondence: ricarda.richter@med.uni-goettingen.de

### Supplementary information

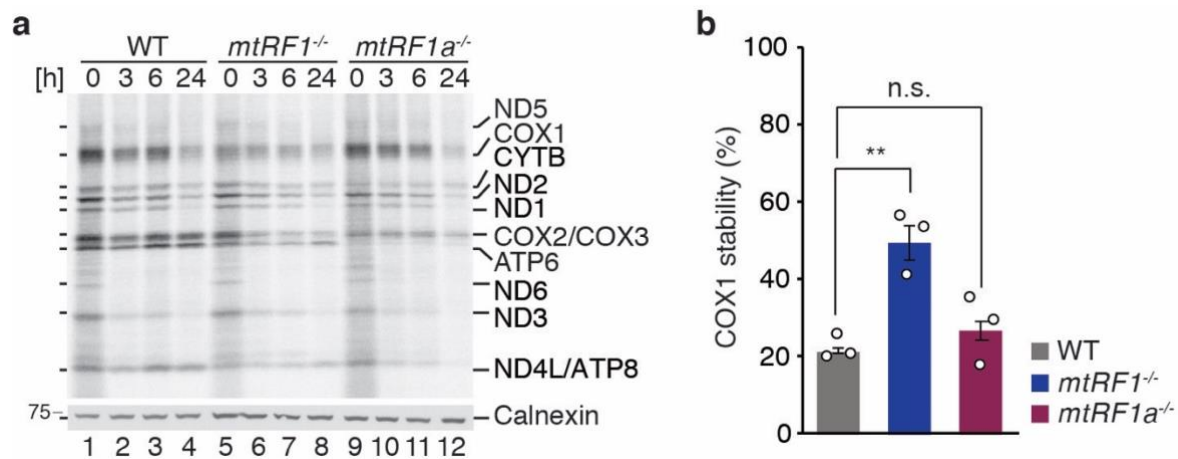
#### Supplementary Figures

	<b>α5-helix</b>	<b>PxT</b>	<b>GGQ</b>
T.thermophilus RF1	..VEIRAG-- <b>TGEEAALF</b> ARDLFNMYLRF...ESGGHRVQRV <b>PVT</b> ---ETQGRHTSTA...IRIDVMRASGF <b>GGQ</b> GVNTTDS...		
E.coli RF1	..LEVRAG-- <b>TGGDEAALF</b> AGRLFRMYSRY...ESGGHRVQRV <b>PAT</b> ---ESQGRHTSAC...LRIDTFRSSGA <b>GGQ</b> HVNTTDS...		
mtRF1a	..LEVTA <b>G</b> -- <b>VGGQEAML</b> FTSEIFDMYQOY...EGGVHRVQRV <b>PKT</b> ---EKQGRVHTSTM...LRIDTKRASGA <b>GGQ</b> HVNTTDS...		
mtRF1	..LEVTA <b>GRTTGGD</b> ICQ <b>Q</b> FTREIFDMYQOY...EGGIHRVQRI <b>PEVGLS</b> SRMQRIHTGTM...LRIDTFRAKGA <b>GGQ</b> HVNTTDS...		
ICT1 (mL62)	..LLPPPAR-----CPRRALHKQK...-----LTI SYCRSSGF <b>GGQ</b> VNKNVNS...		
C12ORF65	..-MSTVG-----LFH---FPTPLTR...-----LLEEQVKGHG <b>GGQ</b> ATNKTSN...		

**Supplementary Fig. 1. Sequence alignment of mitochondrial and bacterial release factors.** Extended alignment as shown in Fig. 1a is provided with the decoding motifs labeled in green and blue and the GGQ motif in red.



**Supplementary Fig. 2. Genomic sequences of *mtRF1*<sup>-/-</sup> and *mtRF1a*<sup>-/-</sup>.** Genomic DNA was isolated from the respective knockout cell lines, respective target region was PCR amplified and products were analyzed using TOPO cloning and subsequent sequencing. Chromatograms and respective DNA sequences of allele 1 and 2 with corresponding amino acid sequences are provided. Source data are provided as a Source Data file.



**Supplementary Fig. 3. Stability of newly synthesized COX1.** a) Mitochondrial translation products were labelled by [<sup>35</sup>S]Methionine incorporation for 1h in anisomycin treated cells. Radioactive media was replaced for the indicated time points and samples were analysed by western blotting and autoradiography. b) COX1 protein levels were quantified after 24h chase and are presented as percentage of the starting point (t = 0h) in the respective cell lines. Individual data points are shown as circles. Statistical analysis was carried out as two-sample (equal variances) one-tailed Student's t-test with n = 3 biologically independent samples and shown as mean ± SEM. Significance was defined as p ≤ 0.01 \*\* and p > 0.05 as not significant (n.s.). Source data are provided as a Source Data file.

## a COX1 termination codons

Homo sapiens

5`...CCACCCUACCACACAUUCGAAGAACCCGUAUACAUAAAAUC**UAGA**CAAAAAAGGAAGGAAUCGAA...3`  
... P P Y H T F E E P V Y M K S \*

Pan troglodytes

5`...CCACCCUACCACACAUUCGAAGAACCCGUAUACAUAAAAUC**UAGA**CAAAAAAGGAAGGAAUCGAA...3`  
... P P Y H T F E E P V Y M K S \*

Mus musculus

5`...CCAUAUCACACAUUCGAGGAACCAACCUAUGUAAAAAGUAAAA**UAA**GAAAGGAAGGAAUCGAACCC...3`  
... P Y H T F E E P T Y V K V K \*

Rattus norvegicus

5`...CCCUACCACACAUUCGAAGAACCUUCCUAUGUAAAAAGUAAAA**UAA**GAAAGGAAGGAUUCGAACCC...3`  
... P Y H T F E E P S Y V K V K \*

Bos taurus

5`...CCAUAUCACACAUUGAAGAACCCACCUAUGUUAACCUAAAA**UAA**GAAAGGAAGGAAUCGAACCC...3`  
... P Y H T F E E P T Y V N L K \*

Sus scrofa

5`...CCCUAUCACACAUUGAAGAACCAACAUAUAUCAACCUAAAA**UAA**GCAUAAGAAAGGAAGGAAUC...3`  
... P Y H T F E E P T Y I N L K \*

## b ND6 termination codons

Homo sapiens

5`...UUUGUUGGUGUAUAUAUUGUAAUUGAGAUUGCUCGGGGGAA**UAGG**UUAUGUGAUUAGGAGUAGGG...3`  
... F V G V Y I V I E I A R G N \*

Pan troglodytes

5`...UUUGUUGGUGUAUAUAUUGUAAUUGAGAUUGCUCGGGGGAA**UAGG**UUAUGUGAUUAGGAGUAAGG...3`  
... F V G V Y I V I E I A R G N \*

Mus musculus

5`...UUGUUUGCGGGUAUUUUUAUUUAUUCGAGAUUCUCGAGAU**UAA**UUGAGUAUAAGAUAAUAAUU...3`  
... L F A G I F I I I E I T R D \*

Rattus norvegicus

5`...UUGUUUGCGGGGAUUUUUAUUUAUUGAAAUCACUCGGGAU**UAA**GUGUGUGUAAGAUAAAAAU...3`  
... L F A G I F I I I E I T R D \*

Bos taurus

5`...UUAUUGGUGUUGUGGUUAUAUAGAAAUCUCGUGGAAA**UAA**AUAAGAUUAUGCUGAUUAGG...3`  
... L I G V V V I M E I T R G N \*

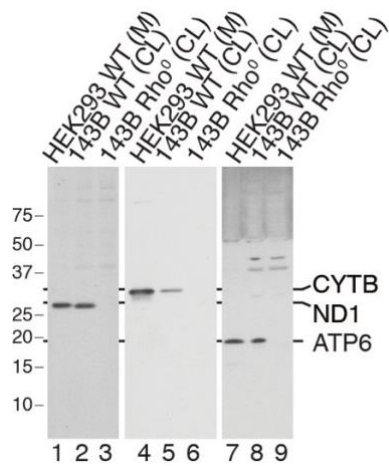
Sus scrofa

5`...CUUAUUGGAGUUGUUGUUAUAUAGAGAUUCUCGUGGUA**UAA**AUAGUGUUAUGCUGAUUAUA...3`  
... L I G V V V I M E I T R G N \*

**Supplementary Fig. 4. Comparison of COX1 (a) and ND6 (b) termination codons in different species.** Only the 3' end for COX1 and ND6 mRNA including the UTRs are presented with the corresponding amino acid sequence. Termination codons are marked in bold.

mtRF1	M.musculus	-MSHHL CIWLF RNP-FLRACFPQRHVFLSCQQFRQISLDRPW NFRQKKT HVLVLYQLLNKSW	58
mtRF1	R.norvegicus	-MSFHL CVWLF RNLSSLSACSQRHVFLYGGQQFRQINLDPRLWNFRQNKTHVLVRLLNKSW	59
mtRF1	H.sapiens	-MNRHLCVWLF RHP SL-NGYLQCH IQLHSHQFRQIHLDTRLQVFRQNRNCILH-LLSKNW	57
mtRF1	B.taurus	MNRHHLFAWLF RHL SL-NGHLQCHVHRHSHQLTQ IPLDTRLVWVFRNRNHTVHRLLNKNC	59
mtRF1a	M.musculus	-----M	1
mtRF1a	R.norvegicus	-----M	1
mtRF1a	H.sapiens	-----M	1
mtRF1a	B.taurus	-----M	1
mtRF1	M.musculus	SRGCCHQGTRKRLWKHKALQKYMEDLNKEYQTLDQCLQGISSENEGDRR-----A	106
mtRF1	R.norvegicus	SRGYC-QGTRKRLWKHKALQKYMEDLNDEYQSLDQCLQDISSEDEGDRR-----A	106
mtRF1	H.sapiens	SRRYCHQDTRKMLWKHKALQKYMENLSKEYQTLQCLQHI PVNEENRR-----A	105
mtRF1	B.taurus	SRRYCHQDTRKMLWKHKALQKYMEDLNKEYQTLDHCLHHISASEGDRR-----S	107
mtRF1a	M.musculus	RSGFLS-GARRLWARR-----AFSRTPPPEEEL-----ARGGPLRAFLERRVGSAGG	49
mtRF1a	R.norvegicus	RSGFLR-SARRLWARR-----AISRMPPEEEL-----ARGGPLRAFLERRVGSAGG	49
mtRF1a	H.sapiens	RSRVLWGAAARWLWPRRAVGPARRPLSSGSPPELEEL-----TRGGPLRTFLERQAGSEAH	56
mtRF1a	B.taurus	RPRLVNVVFRGFWRARRGVPACRHLSCSNLPLEEEL-----ARGGALRTFLERQVGAEAQ-	56
		: * : : : : : : : : : : * :	
mtRF1	M.musculus	LHRRHAQLAPLA VYQEI QEA EAQAI EELS LCKSLNKQDEKQLQELVSEERQIIDQKIHR	166
mtRF1	R.norvegicus	SHRRHAELAPLAVYQEI QEA EAQAI EELS MCKSLNKQDEKQLQELVSEERQIIDQKIHR	166
mtRF1	H.sapiens	LNRRAHAELAPLAAYQEIQETEQAIEELS MCKSLNKQDEKQLQELALAEERQTIDQKIM	165
mtRF1	B.taurus	LTRRAHAELAPLAVIYKEIQEA EAQAI EELS MCKSLNKQDEKQLQELALEERQTIAQKIM	167
mtRF1a	M.musculus	LDAGYPQ---LAAAARLLSEKERE LRDTESLLH---DENEDLKKALESEIALCQKQITE	102
mtRF1a	R.norvegicus	LDAGSPQ---LAAAARLLNEKERE LRDTESLLH---DENEDLKKALESEIALCQKEIAE	102
mtRF1a	H.sapiens	LKVRPE---LLAVIKLLNEKERE LRQTEHLLH---DENEDLRKLAENEITLCQKEITQ	109
mtRF1a	B.taurus	FQVRPE---LVAVAKLLSDKEQLQELQHLLH---DENEDLRKLAENEITSCKEIAQ	109
		: * . : : : * : : : : : : : : : : : : : : : * . * : : *	
mtRF1	M.musculus	LYSELLERLVPKEKYDWSVILEVTSGRITGGD ICQQFTREIFDMYQNYSSYKHWKFELL	226
mtRF1	R.norvegicus	LYSELLEHLPKCKDRSNVILEVTSGRITGGD ICQQFTREIFDMYQNYSSYKHWKFELL	226
mtRF1	H.sapiens	LYNELFQSLVPKKEYDKNDVILEVTAGRITGGD ICQQFTREIFDMYQNYSSYKHWKFELL	225
mtRF1	B.taurus	LYSELFQSLLPKKEYDKNDVILEVTSGRITGGD ICQQFTREIFDMYQNYSSYKHWKFELL	227
mtRF1a	M.musculus	LKHQIISLLVPSEEMDGLDILEVLAG--VGGQ EAM LFTSEMFDYQYAAAFKRWHFETL	160
mtRF1a	R.norvegicus	LKHRIISLLVPSMDGLDILEVLAG--VGGQ EAM LFTSEMFDYQYAAAFKRWHFETL	160
mtRF1a	H.sapiens	LKHQIISLLVPSEETDNDLILEVLAG--VGGQ EAM LFTSEIFDMYQYAAAFKRWHFETL	167
mtRF1a	B.taurus	LKHQIISLLVPSEETDKNDLILEVLAG--VGGQ EAM LFTSEIFDMYQYAAAFKRWHFETL	167
		* : : * : * * . : * . : * : * : * : * : * : * : * : * : * : * : * : * : * : *	
mtRF1	M.musculus	NYTPADYGG LHHAAARI S GDSVYKHLKYEGGIHRVQRIPEVGLSSRMQRIHTGTMSVIVL	286
mtRF1	R.norvegicus	NYTPADYGG LHHAAARI S GDSVYKHLKYEGGIHRVQRIPEVGLSSRMQRIHTGTMSVIVL	286
mtRF1	H.sapiens	NYTPADYGG LHHAAARI S GDSVYKHLKYEGGIHRVQRIPEVGLSSRMQRIHTGTMSVIVL	285
mtRF1	B.taurus	NYTPADYGG LHHAAARI S GDNVYKHLKYEGGIHRVQRIPEVGLSSRMQRIHTGTMSVIVL	287
mtRF1a	M.musculus	EYFPSELGGLRHASASVGGPEAYRHMKFEGGVHRVQRPKTE---KQRIHTSTMTVAIL	217
mtRF1a	R.norvegicus	EYFPSELGGLRHASASIGGPEAYRHMKFEGGVHRVQRPKTE---RQGRHTSTMTVAIL	217
mtRF1a	H.sapiens	EYFPSELGGLRHASASIGGSEAYRHMKFEGGVHRVQRPKTE---KQGRVHTSTMTVAIL	224
mtRF1a	B.taurus	EYFPSEIGGLRHASASIGGSEAYRHMKFEGGVHRVQRPKTE---KQGRHTSTMTVAIL	224
		: * * : : * : * : * : * . : * . : * : * : * : * : * : * : * : * : * : * :	
mtRF1	M.musculus	PQPDEVDVKVDPKDLRVDTFRAGAGGQHVN T TDSAVRLVHIPTGLVVECQ QERSQLKKN	346
mtRF1	R.norvegicus	PQPDEVDVKVDPRDLRVDTFRAGAGGQHVN T TDSAVRLVHIPTGLVVECQ QERSQLKKN	346
mtRF1	H.sapiens	PQPDEVDVKLDPKDLRIDTFRAGAGGQHVNKTDSAVRLVHIPTGLVVECQ QERSQIKKN	345
mtRF1	B.taurus	PHPDEVDVKVDPKDLRIDTFRAGAGGQHVN T TDSAVRLVHIPTGLVVECQ QERSQIKKN	347
mtRF1a	M.musculus	PQPTEIKLVINPKDLRIDTKRASGAGGQHVN T TDSAVRIVHLPTGISECQ QERSQLKKN	277
mtRF1a	R.norvegicus	PQPTEIKLVINPKDLRIDTKRASGAGGQHVN T TDSAVRIVHLPTGISECQ QERSQLKKN	277
mtRF1a	H.sapiens	PQPTEINLVINPKDLRIDTKRASGAGGQHVN T TDSAVRIVHLPTGIVSECQ QERSQLKKN	284
mtRF1a	B.taurus	PQPTEINLVINPKDLRIDTKRASGAGGQHVN T TDSAVRIVHLPTGIVSECQ QERSQLKKN	284
		* : * * : : : : * : * : * : * . * : * : * : * : * : * : * : * : * : * : *	
mtRF1	M.musculus	EIALRVLRLRLYQQIEKDKCQQQ NARKLQVGTQRAQSERIRTYNFTQDRVTDHRIAYEVR	406
mtRF1	R.norvegicus	EIALRVLRLRLYQQIEKDKCQQQ NARKLQVGTQRAQSERIRTYNFTQDRVTDHRIAYEVR	406
mtRF1	H.sapiens	EIAFRVLRRLYQQIEKDKRQQSARKLQVGTQRAQSERIRTYNFTQDRVSDHRIAYEVR	405
mtRF1	B.taurus	EIALRVLRLRLYQQIEKDKCQQSARKLQVGTQRAQSERIRTYNFTQDRVTDHRIAYEVR	407
mtRF1a	M.musculus	ELAMKRLRLRLYSMHL EEETAKRYNARKIQVGTGRSEKIRTYNFPQNRVTDHRINKSLH	337
mtRF1a	R.norvegicus	ELAMKRLRLRLYSMHL EEETAKRYNARKIQVGTGRSEKIRTYNFPQNRVTDHRINKSLH	337
mtRF1a	H.sapiens	ELAMTKLRAKLYSMHL EEENKRNQARKIQIGSKGRSEKIRTYNFPQNRVTDHRINKSLH	344
mtRF1a	B.taurus	EMAMKRLRAKLYSLQE EETS KRYNARKIQIGTKGRSEKIRTYNFPQNRVTDHRINKSLH	344
		* : * : * : * : * : * . : * : * : * : * : * : * : * : * : * : * : * : * :	
mtRF1	M.musculus	DIKEFLRGEKCLDQLIERLLQSADEEAI SEFLDESLSQSVK	446
mtRF1	R.norvegicus	DIKEFLRGEKCLDQLIERLLQSADEEAI SEFLDESLSQSVK	446
mtRF1	H.sapiens	DIKEFLCGGKGLDQLIQRLLQSADEEAI AIELLDEHLKSAK	445
mtRF1	B.taurus	NIKEFLCGEKCLDQLIQRLLQSADEEAI TEFLDENLKS VK	447
mtRF1a	M.musculus	DLESFMQGDCLLDQSLKDCSDYEALVEMISR RD----	373
mtRF1a	R.norvegicus	DLESFMQGDCLLDLQSLKDYSDYESLVEIISQKV----	373
mtRF1a	H.sapiens	DLETFMQGDYLLDELVQSLKEYADYESLVEIISQKV----	380
mtRF1a	B.taurus	DLETFMQGEYLLDELVQSLKDYANYESLVEIAKEV----	380
		: : : * : * * : : * : * : * : * : * : * : * :	

Supplementary Fig. 5. CLUSTAL multiple sequence alignment of mtRF1 and mtRF1a.



**Supplementary Fig. 6. Antibody validation.** Isolated mitochondria (M) from HEK293 cells, and cell lysates (CL) from 143B wildtype (WT) and Rho<sup>0</sup> cells were subjected to SDS-PAGE followed by western blotting. Antibodies against ND1 (lane 1-3), CYTB (4-6) and ATP6 (7-9) were applied as indicated. Antibodies were tested once using Rho<sup>0</sup> cells and further confirmed by using *mtRF1 $\alpha$* <sup>-/-</sup> cells. Source data are provided as a Source Data file.

**Supplementary Table 1. Key reagents**

REAGENT or RESOURCE	SOURCE	IDENTIFIER
<b>Antibodies</b>		
Rabbit polyclonal anti-uS15m (dilution: 1:5000)	ProteinTech	Cat# 17006-1-AP
Rabbit polyclonal anti-uL23m (dilution: 1:10 000)	<sup>1</sup>	PRAB1716
Mouse monoclonal anti-FLAG (dilution: 1:1000)	Sigma Prestige	Cat# F1804; Clone# M2
Rabbit polyclonal anti-TIM23 (dilution: 1:1000)	<sup>1</sup>	PRAB1527
Rabbit polyclonal anti-TOM70 (dilution: 1:1000)	<sup>2</sup>	PRAB3280
Mouse monoclonal anti-Calnexin (dilution: 1:500 000)	ProteinTech	Cat# 66903-1-Ig; Clone# 2A2C6
Rabbit polyclonal anti-ND1 (dilution: 1:100 000)	This study*	PRAB5021
Rabbit polyclonal anti-ND2 (dilution: 1:200)	ProteinTech	Cat# 19704-1-AP
Rabbit polyclonal anti-NDUFB8 (dilution: 1:5 000)	<sup>3</sup>	PRA3765
Mouse monoclonal anti-SDHA (dilution: 1:20 000)	Invitrogen	Cat#459200; Clone# 2E3GC12FB2AE2
Rabbit polyclonal anti-CYTB (dilution: 1:1000)	This study*	PRAB5131
Rabbit polyclonal anti-RIESKE (dilution: 1:10 000)	<sup>1</sup>	PRAB1512
Rabbit polyclonal anti-COX1 (dilution: 1:2000)	<sup>1</sup>	PRAB5121
Mouse monoclonal anti-COX2 (dilution: 1:1000)	Abcam	Cat# ab110258; Clone# 12C4F12
Rabbit polyclonal anti-COX4I (dilution: 1:10 000)	<sup>1</sup>	PRAB1522
Rabbit polyclonal anti-ATP5B (dilution: 1:20 000)	<sup>1</sup>	PRAB4826
Rabbit polyclonal anti-ATP6 (dilution: 1:5000)	This study*	PRAB5159
Rabbit polyclonal anti-C12orf62 (dilution: 1:1000)	<sup>1</sup>	PRAB 4845
Rabbit polyclonal anti-MITRAC12 (dilution: 1:1000)	<sup>1</sup>	PRAB3761
Rabbit polyclonal anti-MITRAC15 (dilution: 1:2000)	<sup>2</sup>	PRAB4814
Rabbit polyclonal anti-mtRF1 (dilution: 1:500)	This study	RRDAB5461
Rabbit polyclonal anti-mtRF1a (dilution: 1:1000)	ProteinTech	Cat# 16694-1-AP
Rabbit polyclonal anti-mL62/ICT1 (dilution: 1:1000)	ProteinTech	Cat# 10403-1-AP
Rabbit polyclonal anti-C12ORF65 (dilution: 1:500)	ProteinTech	Cat# 24646-1-AP
Rabbit polyclonal anti-MTRES1 (dilution: 1:1000)	Sigma	Cat# HPA049535
Goat IgG anti-rabbit IgG (H+L)-HRPO (dilution: 1:5000)	dianova	Cat# 111-035-144
Goat IgG anti-mouse IgG (H+L)-HRPO (dilution: 1:5000)	dianova	Cat# 115-035-146
* antibodies were verified as shown in Supplementary Fig. S6		
<b>Chemicals</b>		
L-[ <sup>35</sup> S]methionine	Hartmann Analytic	Cat# SCM-01
Adenosine 5'-triphosphate, [ $\gamma$ - <sup>32</sup> P]	Hartmann-Analytic	Cat# SRP-501
Emetine dihydrochloride hydrate	Sigma-Aldrich	Cat# 219282
Anisomycin	Sigma-Aldrich	Cat# A5862
Lipofectamine 3000	Invitrogen	Cat# L3000-015
GeneJuice	Novagen	Cat# 70967-3
Alt-R® CRISPR-Cas9 tracrRNA, ATTO™ 550	Integrated DNA technologies	Cat# 1075927
Alt-R® S.p. Cas9 Nuclease V3	Integrated DNA technologies	Cat# 1081058
TRIzol® Reagent	Ambion	Cat# 15596018
<b>Critical Commercial Assays</b>		
Rapid DNA Ligation Kit	ThermoFisher Scientific	Cat# K1423



T4 Polynucleotide Kinase (T4 PNK)	ThermoFisher Scientific	Cat# EK0031
KOD Hot Start DNA Polymerase	Merck	Cat# 71086-3
Wizard® Plus SV Minipreps DNA Purification System	Promega	Cat# A1460
Wizard® SV Gel and PCR Clean-Up System	Promega	Cat# A9282
QuikChange Lightning Site-Directed Mutagenesis Kit	Agilent Technologies	Cat# 210519-5
TOPO TA Cloning® Kit	ThermoFisher Scientific	Cat# 45-0030
OneShot®TOP10 Chemically Competent Cells	ThermoFisher Scientific	Cat# C404004
Complex I Enzyme Activity Assay Kit (Colorimetric)	abcam	Cat# ab109721
Seahorse FluxPaks	Agilent Technologies	Cat# 102416-100
MitoSOX™ Red Mitochondrial Superoxide Indicator	ThermoFisher Scientific	Cat# M36008
<b>Experimental Models: Cell Lines</b>		
HEK293-Flp-In T-Rex	ThermoFisher Scientific	R78007
HEK293-Flp-In T-Rex- <i>mtRF1</i> <sup>-/-</sup>	This study	N/A
HEK293-Flp-In T-Rex- <i>mtRF1<math>\alpha</math></i> <sup>-/-</sup>	This study	N/A
HEK293-Flp-In T-Rex- <i>mtRF1</i> <sup>FLAG-GGQ</sup>	This study	N/A
HEK293-Flp-In T-Rex- <i>mtRF1</i> <sup>FLAG-AAQ</sup>	This study	N/A
HEK293-Flp-In T-Rex- <i>mtRF1<math>\alpha</math></i> <sup>FLAG-GGQ</sup>	This study	N/A
HEK293-Flp-In T-Rex- <i>mtRF1<math>\alpha</math></i> <sup>FLAG-AAQ</sup>	This study	N/A
<b>Oligonucleotides</b>		
Guide RNA: targeting the Exon 2 of <i>mtRF1</i> : 5'-TGTTAAGTAAGAATTGGTCC-3'	This study; IDT	N/A
Guide RNA: targeting the Exon 1 of <i>mtRF1<math>\alpha</math></i> : 5'-CTCCGGTAGCCCGCCGCTGG-3'	This study; IDT	N/A
siRNA C12orf65 Oligo: GCAAAGGAAACCCUGGAAA	This study; Eurogentec	N/A
Primer: Generation of the FLAG-tagged version of <i>mtRF1</i> Forward: 5'- CTCTCCAAGCTTCCACCATGAATCGTCACCTGTGTGTTGG C-3'	This study; Microsynth	N/A
Primer: Generation of the FLAG-tagged version of <i>mtRF1</i> Reverse: 5'- CTTTCTCTCGAGCTACTTATCGTCGTCATCCTTGTAATCTTT TGCTGATTTAAGGTGTTTCATCC-3'	This study; Microsynth	N/A
Primer: Generation of the FLAG-tagged mutant (GGQ→AAQ) version of <i>mtRF1</i> : Forward: 5'- GATACATTTTCGAGCCAAAGGAGCAGCAGCGCAGCATGTTA ATAAAAC-3'	This study; Microsynth	N/A
Primer: Generation of the FLAG-tagged mutant (GGQ→AAQ) version of <i>mtRF1</i> Reverse: 5'- CACTATCAGTTTTATTAACATGCTGCGCTGCTGCTCCTTTGG CTC-3'	This study; Microsynth	N/A

Primer: Generation of the FLAG-tagged version of mtRF1a Forward: 5'-CTCTCCAAGCTTCCACCATGCGGTCCCGGTTCTGTGGG-3'	This study; Microsynth	N/A
Primer: Generation of the FLAG-tagged version of mtRF1a Reverse: 5'-CTTTCTGATATCCTACTTATCGTCGTCATCCTTGTAATCAAC TTTTGGGAAATAATTTCTACTAAAGATTC-3'	This study; Microsynth	N/A
Primer: Generation of the FLAG-tagged mutant (GGQ→AAQ) version of mtRF1a Forward: 5'-GACACTAAGCGAGCCAGTGGAGCTGCGGCGCAGCATGTAA ATAC-3'	This study; Microsynth	N/A
Primer: Generation of the FLAG-tagged mutant (GGQ→AAQ) version of mtRF1a Reverse: 5'-CACTGTCCGTGGTATTACATGCTGCGCCGAGCTCCACTG GCTC-3'	This study; Microsynth	N/A
Probe: targeting MTRNR1 (12S rRNA) 5'-TCGATTACAGAACAGGCTCCTCTAG-3'	4	N/A
Probe for northern blot: targeting MTRNR2 (16S rRNA) 5'-GTTTGGCTAAGGTTGTCTGGTAGTA-3'	4	N/A
Probe for northern blot: targeting MTCO1 5'-GTCAGTTGCCAAAGCCTCCGATTATG-3'	4	N/A
Probe for northern blot: targeting MTCO2 5'-GACGTCCGGGAATTGCATCTGTTTT-3'	4	N/A
Probe for northern blot: targeting MTCYTB 5'-CGTGTGAGGGTGGGACTGTCTACTG-3'	This study; Microsynth	N/A
Probe for northern blot: targeting 18S-rRNA 5'-TTTACTTCCTCTAGATAGTCAAGTTCGACC-3'	5	N/A
<b>Recombinant DNA</b>		
pOG44 Flp-Recombinase Expression Vector	ThermoFisher Scientific	Cat# V600520
pcDNA5/FRT/TO	ThermoFisher Scientific	Cat# V6520-20
<b>Software and Algorithms</b>		
ImageJ	6	<a href="https://imagej.nih.gov/ij/">https://imagej.nih.gov/ij/</a> ; v.2.1.0
ImageQuant TL	GE Healthcare	v.8.1
Seahorse Wave Desktop	Agilent Technologies	v.2.6.1.53
FACS-Diva software	BD Biosciences	v.9.0.1
nSolver software	NanoString	v.4.0.70

**Supplementary Table 2. nCounter tube sequences for NanoString analyses (provided by IDT)**

Mito_JCM__008.1 :591_T001	CTTCATCAGGGTTTGCTGAAGATGGCGGTATATAGGCTGAGCAAGAGGTGC CTCAAGACCTAAGCGACAGCGTGACCTTGTTTCA
Mito_JCM__009.1 :481_T002	CTTTCTTAATTGGTGGCTGCTTTTAGGCCTACTATGGGTGTAAATTTTTCAT CCTCTTCTTTCTTGGTGTGAGAAGATGCTC
HSMT_ND1.1:46 1_T003	GTTCTTGTTGTGATAAGGGTGGAGAGGTTAAAGGAGCCACTTATTAGTC ACAATTCTGCGGGTTAGCAGGAAGTTAGGGAAC
HSMT_ND2.1:44 4_T004	CCTGCTATGATGGATAAGATTGAGAGAGTGAGGAGAAGGCTTACGTTTACG TGTTGAGATTATTGAGCTTCATCATGACCAGAAG
HSMT_COX1.1:8 73_T005	GCGGAGGTGAAATATGCTCGTGTGTCTACGTCTATTCTACTGTAAATATCA AAGACGCCTATCTCCAGTTTGATCGGGAAACT

HSMT_COX2.1:2 16_T006	TCGTCTGTTATGTAAAGGATGCGTAGGGATGGGAGGGCGATGAGGACTAGC GAACCTAACTCCTCGCTACATTCTATTGTTTC
HSMT_ATP8.1:82 T007	TATTTTTATGGGCTTTGGTGAGGGAGGTAGGTGGTAGTTTGTGTTAATACC AATTTGGTTTTACTCCCCTCGATTATGCGGAGT
HSMT_ATP6.1:33 1_T008	GTGGGCTAGGGCATTTTTAATCTTAGAGCGAAAGCCTATAATCACTGTGCCT TTCGGGTTATATCTATCATTTACTTGACACCT
HSMT_COX3.1:5 39_T009	ATGTTGAGCCGTAGATGCCGTGCGAAATGGTGAAGGGAGACTCGAAGTACC AACAGCCACTTTTTTCCAAATTTGCAAGAGCC
HSMT_ND3.1:13 5_T010	AAGGTAATAGCTACTAAGAAGAATTTATGGAGAAAGGGACGCGGGCGGG CACCGTGTGGACGGCAACTCAGAGATAACGCATAT
HSMT_ND4L.1:5 8_T011	TATTCCTTCTAGGCATAGTAGGGAGGATATGAGGTGTGAGCGATATACTAC CTGGAGTTTATGTATTGCCAACGAGTTTGTCTTT
HSMT_ND4.1:96 7_T012	ACTGTGAGTGCGTTCGTAGTTTGAGTTTGCTAGGCAGAATAGTAATGAGGC AGATAAGGTTGTTATTGTGGAGGATGTTACTACA
HSMT_ND5.1:11 47_T013	TGCGGTTTCGATGATGTGGTCTTTGGAGTAGAAACCTGTGAGGAAAGGTAC TTCCTTCTGTGTTCCAGCTACAACTTAGAAAAC
HSMT_ND6.1:19 1_T014	CCTCAGGATACTCCTCAATAGCCATCGCTGTAGTATATCCAAAGACAACCC ATAAAATTGGTTTTGCCTTTCAGCAATTCAACTT
HSMT_CYTB.1:9 46_T015	GAGGTCTGCGGCTAGGAGTCAATAAAGTGATTGGCTTAGTGGGCGAAATAC TGGTCAAGACTTGCATGAGGACCCGCAAATTCCT
NR_003286.2:164 0_T016	AGGGCAGGGACTTAATCAACGCAAGCTTATGACCCGCACTTACTGGGAATC TTTCGTTGGGACGCTGAAGCGCAAGTAGAAAAC
NR_023379.1:8_T 017	TGCTTAGCTTCCGAGATCAGACGAGATCGGGCGCGTTCAGGGCCAGCAGAC CTGCAATATCAAAGTTATAAGCGCGT
Mito_JCM_008.1 :591_ProbeB	CGAAAGCCATGACCTCCGATCACTCTACACCTTGACCTAACGTCTTTACGTG GGTACTTGCCTTACTTTGTAGC
Mito_JCM_009.1 :481_ProbeB	CGAAAGCCATGACCTCCGATCACTCTTCAGTTATATGTTTGGGATTTTTAG GTAGTGGGTGTTGAGCTTGAACG
HSMT_ND1.1:46 1_ProbeB	CGAAAGCCATGACCTCCGATCACTCGATAAATCATATTATGGCCAAGGGTC ATGATGGCAGGAGTAATCAGAGGT
HSMT_ND2.1:44 4_ProbeB	CGAAAGCCATGACCTCCGATCACTCAGTATGCTAAGATTTTGCCTAGCTGG GTTTGGTTAATCCACCTCAACTG
HSMT_COX1.1:8 73_ProbeB	CGAAAGCCATGACCTCCGATCACTCCGAGTCAGCTAAATACTTTGACGCCG GTGGGGATAGCGATGATTATGGTA
HSMT_COX2.1:2 16_ProbeB	CGAAAGCCATGACCTCCGATCACTCAGTACCATTGGTGGCCAATTGATTTGA TGTTAAGGGAGGGATCGTTGACC
HSMT_ATP8.1:82 ProbeB	CGAAAGCCATGACCTCCGATCACTCAGCGAACAGATTTTCGTTTCATTTTGGT TCTCAGGGTTTGTATAATTTTT
HSMT_ATP6.1:33 1_ProbeB	CGAAAGCCATGACCTCCGATCACTCATAATAACTAGTATGGGGATAAGGGG TGTAGGTGTGCCTTGTGGTAAGAA
HSMT_COX3.1:5 39_ProbeB	CGAAAGCCATGACCTCCGATCACTCAGTTGAGCCAATAATGACGTGAAGTC CGTGGAAGCCTGTGGCTACAAAAA
HSMT_ND3.1:13 5_ProbeB	CGAAAGCCATGACCTCCGATCACTCGGGCTCATGGTAGGGGTAAAAGGAGG GCAATTTCTAGATCAAATAATAAG
HSMT_ND4L.1:5 8_ProbeB	CGAAAGCCATGACCTCCGATCACTCGAGTGGGTGTTGAGGGTTATGAGAGT AGCTATAATGAACAGCGATAGTAT
HSMT_ND4.1:96 7_ProbeB	CGAAAGCCATGACCTCCGATCACTCGCTATTAGTGGGAGTAGAGTTTGAAG TCCTTGAGAGAGGATTATGATGCG
HSMT_ND5.1:11 47_ProbeB	CGAAAGCCATGACCTCCGATCACTCGTAGCGATGAGAGTAATAGATAGGGC TCAGGCGTTTGTGTATGATATGTT
HSMT_ND6.1:19 1_ProbeB	CGAAAGCCATGACCTCCGATCACTCCGCTAACCCCACTAAAACACTCACCA AGACCTCAACCCCTGACCCCATG
HSMT_CYTB.1:9 46_ProbeB	CGAAAGCCATGACCTCCGATCACTCATGGTAAAAGGGTAGCTTACTGGTTG TCCTCCGATTCAGGTTAGAATGAG
NR_003286.2:164 0_ProbeB	CGAAAGCCATGACCTCCGATCACTCGCCTCACTAAACCATCCAATCGGTAG TAGCGACGGGCGGTGTGTACAA
NR_023379.1:8_P robeB	CGAAAGCCATGACCTCCGATCACTCCGGTCTCCCATCCAAGTACTAACCAG GCCCGACCC

## References

1. Richter-Dennerlein, R. *et al.* Mitochondrial Protein Synthesis Adapts to Influx of Nuclear-Encoded Protein. *Cell* **167**, 471–483.e10 (2016).
2. Dennerlein, S. *et al.* MITRAC7 Acts as a COX1-Specific Chaperone and Reveals a Checkpoint during Cytochrome c Oxidase Assembly. *Cell Reports* **12**, 1644–1655 (2015).
3. Dennerlein, S. *et al.* Defining the interactome of the human mitochondrial ribosome identifies SMIM4 and TMEM223 as respiratory chain assembly factors. *Elife* **10**, (2021).
4. Lavdovskaia, E. *et al.* Dual function of GTPBP6 in biogenesis and recycling of human mitochondrial ribosomes. *Nucleic Acids Research* **48**, 12929–12942 (2020).
5. Larburu, N. *et al.* Structure of a human pre-40S particle points to a role for RACK1 in the final steps of 18S rRNA processing. *Nucleic Acids Research* **44**, 8465–8478 (2016).
6. Schneider, C. A., Rasband, W. S. & Eliceiri, K. W. NIH Image to ImageJ: 25 years of image analysis. *Nat Methods* **9**, 671–675 (2012).

### 3 Discussion

Mitochondrial protein synthesis is fundamental to ensure proper respiratory function and thus to provide energy in form of ATP for a myriad of essential cellular processes. Albeit mitochondria share many similarities with their bacterial ancestors, specific factors have evolved in mammalian mitochondria to adapt to the evolutionary changes of the mitoribosome. Decades ago, the first human mitochondrial class I release factor, mtRF1, was identified (Zhang & Spremulli, 1998). However, its role in mitochondrial translation remained mysterious. Moreover, the characterization of another mitochondrial class I release factor made the situation even more complex (Soleimanpour-Lichaei et al., 2007): mtRF1a has a greater sequence similarity to its bacterial counterpart RF1 and is commonly accepted to be the main mitochondrial release factor as it was also shown to bind to reconstituted, canonical termination complexes in a manner very similar to bacterial RF1 (Kummer et al., 2021). Nevertheless, *in vivo* data verifying this notion is still lacking. Moreover, the question arises why would the cell keep two, otherwise redundant release factors?

The emergence of CRISPR/Cas9 technology allowed us to generate knockout models to analyze the physiological role of mtRF1 and mtRF1a *in vivo*. Human cell lines lacking either of the factors were used to subsequently test their function in mitochondrial *de novo* protein synthesis of OXPHOS complex subunits, their assembly into macromolecular (super-) complexes as well as mechanisms that are activated to prevent potential damage interfering with proper cellular function.

#### 3.1 Defining the Functional Relevance of mtRF1 and mtRF1a

During the last decades, much work was done to unravel the distinct steps of mitochondrial translation. A plethora of dedicated translational factors is required to ensure proper mitochondrial protein synthesis and even though many were shown to mechanistically operate in the same manner as their bacterial counterparts, certain differences highlight the divergence of mitochondria from the prokaryotic ancestors. An enigma regarding translation termination remained unsolved over the past 25 years. The second identified human mitochondrial release factor mtRF1a was suggested as mitochondrial release factor to be able to terminate translation on standard stop codons in an *in vitro* heterologous termination assay (Soleimanpour-Lichaei et al., 2007). As a recent structural study showed that mtRF1a binds to homologous termination complexes (Kummer et al., 2021), it was proposed as the main mitochondrial release factor. Additionally, mtRF1a also has greater sequence identity to its bacterial homolog RF1 when compared to mtRF1 (Lind et al., 2013). However, *in vivo* evidence verifying this consumption was missing.

Here, we show for the first time that mtRF1a indeed is the main mitochondrial release factor as it is able to terminate the translation of all mitochondrial transcribed transcripts, except *MT-CO1*, and is therefore highly critical for proper mitochondrial function (Figure 2 and 3; Nadler et al., 2022a). Loss of mtRF1a is comparable to *rho*<sup>0</sup> cells, which lack mtDNA. As a consequence

of this extensive drawback, *mtRF1a*<sup>-/-</sup> cells do not possess functional OXPHOS complexes and therefore cannot oxidatively respire (Figure 2a). Instead, they are forced to produce ATP via glycolysis, which is a less productive, but the only possible way to generate minimal amounts of energy sufficient for survival. This also explains the reduced growth rate when compared to control cells (Figure 1c). It is therefore essential to culture *mtRF1a*<sup>-/-</sup> cells in high-glucose media as a shift to non-fermentable galactose-containing media, which is used to force cells to generate energy solely via OXPHOS, could not be tolerated and consequently, cells would not survive.

The role of mtRF1 as release factor was rejected several times. Nevertheless, the question remained why the cell would keep two otherwise redundant release factors. Compared to mtRF1a and bacterial RF1, the most striking difference of mtRF1 are insertions in the codon recognition domain (Figure 1a, Figure XIa): the classical PxT tripeptide is extended into a hexapeptide and two additional amino acids are inserted at the tip of the  $\alpha$ 5 helix. These changes were proposed to serve as co-evolutionary adaptations upon the evolutionary changes of the mitoribosome (Lind et al., 2013). In fact, these alterations were described to be necessary to establish suitable interactions with the mitoribosome by computational homology modelling (Figure XIb). The bacterial residue A1913 of H69, critical for stabilization of RF1 at the decoding center, is substituted by a cytosine in the mammalian mitoribosome. Together with the  $\alpha$ 5 insertion, these alterations would subsequently allow the accommodation of these rRNA changes and still can form H-bonds necessary for effective interaction (Lind et al., 2013). As described in 1.6, many factors required for translation slightly differ from their bacterial ancestors and both structural and mechanistic alterations were shown to be beneficial. Quite often they add another layer of quality control to the system. Whether this is also the case for mtRF1 remains the subject for further studies.

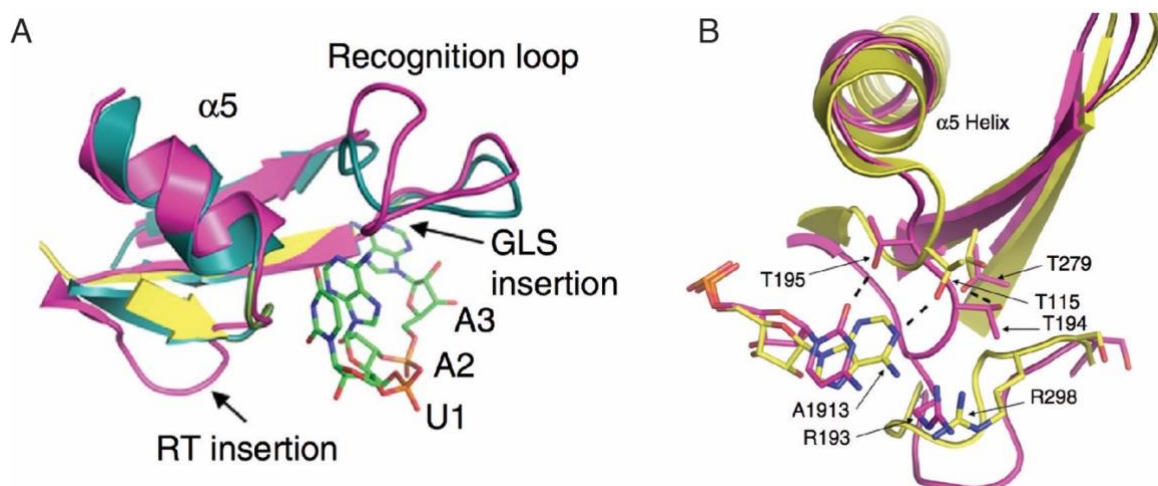


**Figure XI: Comparison mtRF1 vs RF1.** (A) Superimposition homology model of mtRF1 (magenta) and mtRF1a (cyan) on the crystal structure of bacterial RF1 (yellow) demonstrate the alterations in the structure of mtRF1 caused by the insertions (PEVGLS and RT) within the decoding domain. (B) Structural comparison of bacterial RF1 (yellow) and mtRF1 shows that mtRF1 may co-evolved to accommodate and interact more favorable with the key nucleotides of the 12 rRNA, which are positioned slightly different in respect to bacterial rRNA. Image of structural comparison taken from (Lind et al., 2013). Reprinted with permission from Springer Nature (license number 5400941310507).

The work of this thesis shows for the first time that mtRF1 has a special role during translation termination as it was shown to be a dedicated release factor for COX1 (Figure 2 and 3) (Nadler et al., 2022a). COX1 is among the most hydrophobic mitochondrial-encoded OXPHOS subunits. It was shown to be not only highly important for the progression of C IV maturation, but also consequently is a rate-limiting factor for cellular respiration. At this point it can only be speculated that the importance of COX1 is the reason why mtRF1 was kept during evolution. However, it remains unknown what the specificity-conferring property might be.

For quite a long time it was thought that mtRF1 is the release factor required for terminating the two mitochondrial transcripts harboring a non-canonical stop codon, which is either AGA in the case of *MT-CO1* or AGG for *MT-ND6* (Young et al., 2010). However, in human and some other species, these codons are preceded by an uridine and a proposed -1 frameshift would lead to termination in a standard stop codon (Temperley et al., 2010a). Nevertheless, two consecutive studies from Huynen and co-workers initially ruled out this theory. Molecular modeling of mtRF1 predicted that apparently, mtRF1 cannot recognize any stop codon at all. The alterations within the codon recognition domain are proposed to be too hydrophobic to react with mRNA. From this they concluded that mtRF1 may act as a rescue factor to resolve scenarios where mitoribosomes are trapped with an empty A-site (Huynen et al., 2012). An additional phylogenetic analysis supported this assumption as they analyzed all vertebrate genomes and figured out that not all unconventional stop codons are preceded in a way that neither a -1 nor a -2 frameshift would lead to termination in a standard stop codon (Duarte et al., 2012). However, unlike previous work by (Huynen et al., 2012), a following study also using homology modeling (Lind et al., 2013) included mitochondrial rRNA and mRNA into their modelling. They show that accommodation of mtRF1 within the translating human mitoribosome is indeed possible (Figure X1b). Furthermore, free energy calculations demonstrate that mtRF1 has in theory the same codon reading qualities for the standard UAA and UAG stop codons and not for non-standard AGA/AGG stop codons, comparable to mtRF1a and bacterial RF1 (Lind et al., 2013). More recently a structural screening approach based on *in vitro* reconstitutions did not obtain mtRF1 bound to 'no-stop' mitoribosomes with an empty A-site (Kummer et al., 2021). Hence, there is no evidence for mtRF1 being a rescue factor.

In line with the results from (Lind et al., 2013), we demonstrate for the first time *in vivo* that mtRF1 is indeed an active release factor, specified for the termination of COX1 (Nadler et al., 2022a). Moreover, we can rule out that mtRF1 is responsible for termination of non-standard stop codons AGA and AGG by two lines of evidence. First, in other vertebrate species termination of *MT-CO1* and *MT-ND6* is not restricted to non-standard stop codons but instead, there are certain species, like mice, rat or bovine, which do express mtRF1 and *MT-CO1* and *MT-ND6* are terminated by classical stop codons (Supplementary Figure 4). Second, in HEK293 cells, mtRF1 is not responsible for termination of *MT-ND6*, which harbors AGG as a non-standard stop codon at the end of the reading frame. By *in vivo* labeling of mitochondrial *de novo* synthesis in knockout and respective rescue cell lines, we can clearly show that not mtRF1

but the main mitochondrial release factor mtRF1a is responsible for the release of ND6. Instead, mtRF1 is dedicated for the termination of COX1 (Figure 3). However, as mtRF1a is not able to bind to an AGG stop codon and can only trigger peptide hydrolysis upon recognizing standard UAA or UAG stop codons, our findings conclusively support a ribosomal frameshift. In this manner mtRF1a could facilitate translation termination of *MT-ND6* (Nadler et al., 2022a).

In summary, the results obtained in this thesis together with the previous bioinformatic characterization of mtRF1 (Lind et al., 2013) support the -1 frameshift hypothesis (Temperley et al., 2010a). Translational frameshifting can either happen accidentally, for example during elongation on so-called 'slippery' mRNA sequences where the same tRNA can read the codon up- or downstream from the in-frame codon as well. It can also happen intentionally as a response to internal signals as either a regulatory mechanism, by sensing the availability of interacting factors, or lastly, to correct 'problems' like INDELS (Atkins et al., 2016; Peng et al., 2019). It is generally known that secondary structures within the mRNA, like stem loops or pseudoknots, can cause ribosomal frameshifting. As both *MT-CO1* and *MT-ND6* have short 3'UTR region at the end of their ORF, it is tempting to speculate that these sequences also may form a pseudoknot structure and thus force the mitoribosome to shift in the -1 direction in order to terminate on a standard stop codon. Additionally, this assumption might explain why mtRF1 was not found to be bound to the canonical termination complex in the recent structural study by (Kummer et al., 2021). In this *in vitro* approach, termination complexes were reconstituted on the basis of 55S mitoribosomes, respective release factors and *MT-CO3* mRNA, where the start codon is directly followed by conventional or non-standard stop codons. Since *MT-CO3* is lacking any 3' UTR, it is reasonable to assume that due to the alterations in the specific *MT-CO1* termination complex mtRF1 was not able to bind and catalyze peptide release in this situation. Potentially, capture of transiently associated mtRF1 is highly difficult as kinetic studies of release factor binding of bacterial RF1 indicate that the  $K_D$  is increased in the presence of a sense codon and absence of a stop codon, thus resulting in a decrease in  $K_{cat}$  (Hetrick et al., 2009). Furthermore, it cannot be excluded that additional, yet unknown factor(s) play a role in mtRF1-based translation termination. As already mentioned by the authors, the recent structural study reconstitutes termination or rescue complexes *in vitro* and is therefore limited in regard of potential unknown factors, which are consequently missing in the samples (Kummer et al., 2021).

It remains elusive what the specificity-conferring mechanism might be, which enables mtRF1 to dedicatedly and solely terminate *MT-CO1* translation. A potential reason could be the presence of a specific secondary structure at the 3' region of *MT-CO1*. This might only allow the slightly altered, extended decoding motif of mtRF1 – and not the canonical mtRF1a – to recognize and specifically bind to *MT-CO1*. Alternatively, the involvement of additional factors is also possible. It is highly suspicious that translation of *MT-CO1* apparently requires certain dedicated factors to facilitate its translation. Not only seems mtRF1 to be a release factor specialized for releasing COX1, but *MT-CO1* is the only known mitochondrial mRNA which has a dedicated translational activator, namely TACO1 (Weraarpachai et al., 2009). Unlike in yeast



or plants, where several translational regulators are known, these factors do not have homologs in animal mitochondria. Additionally, mammalian mRNAs lack sequence elements like 5'UTRs required for interactions with translational activators or suppressors. It is therefore an open question how these regulatory processes are facilitated. TACO1 binds specifically to *MT-CO1*, preferentially at the 5' end of the transcript, and this interaction leads to engagement with the mitoribosome, thus initiates translation of *MT-CO1* by a yet unknown mechanism. Loss of TACO1 in knockout mice is not lethal but leads to decreased translation of COX1, consequently isolated C IV deficiency and ultimately to a rather subtle version of Leigh syndrome (Richman et al., 2016). Whether or not TACO1 acts in concert with other factors to facilitate and/or enhance COX1 translation remains elusive.

### 3.2 COX1 – the Nucleation Center for Complex IV Assembly

Assembly of OXPHOS subunits into functional respiratory chain complexes is a highly regulated, orchestrated process, as protein synthesis from two different genetic origins has to be coordinated (Richter et al., 2015). Synthesis of COX1 and its subsequent co-translational assembly into C IV facilitated by MITRAC is a well-established example of how mitochondrial-nuclear communication can set the scene for progression of the assembly. Since COX1 is the first subunit to be assembled, absence of mtRF1 leads to depletion of COX1 and consequently to the abortion of C IV assembly (Figure 2d-e and 2j). This is further demonstrated by the diminished levels of the early MITRAC constituents C12ORF62 and MITRAC12 (Figure 2h-j), which are the two factors first engaging with nascent COX1 (Mick et al., 2012; Richter-Dennerlein et al., 2016). Both factors have been shown to be implicated in mitochondrial diseases when mutated, causing isolated C IV deficiencies (Ostergaard et al., 2015; Weraarpachai et al., 2012). Especially mutations in *C12orf62* cause fatal neurological and respiratory symptoms, accompanied from dysmorphic characteristics and lactic acidosis, leading to an early death of the patients. However, it was demonstrated that residual COX1 levels in this patient-derived fibroblasts were relatively stable (Weraarpachai et al., 2012) and this phenomenon is also appearing in the case of mtRF1 loss and will be discussed in more detail in 3.3.1. Thus, it can be assumed that the association of COX1 with the MITRAC complex displays a crossroad for maturation of the holoenzyme and highlights the role of COX1 as rate-limiting nucleation center for maturation of C IV: if nascent COX1 cannot be released from the ribosomes, as it is the case in cells lacking mtRF1, C IV assembly is aborted. If COX1 is translated properly like in mtRF1a deficient cells, assembly of the COX holoenzyme is initiated by COX1, but then gets stalled due to the absence of further constituents like COX2 (Figure 2j and 6).

The results of the analysis of the respective knockout cell lines suggest that either a diminished stability of synthesized proteins due to OXPHOS deficiency or a feedback mechanism from mitochondria to the nucleus is occurring. The steady state level of one of the nuclear-encoded subunits of C IV, COX4I, is decreased in both knockout cell lines in response to diminished COX1 or COX2 and COX3 levels in cells lacking mtRF1 or mtRF1a, respectively. Consequently, loss of mtRF1a also leads to reduced levels of nuclear-encoded subunits of other affected OXPHOS complexes, especially C I but also C III and C V (Figure 2e-g). Abundance of OXPHOS subunits is

co-regulated on several levels. First, bidirectional mitonuclear communication allows the cell to control transcription of both nuclear and mitochondrial gene expression (Quirós et al., 2016). Anterograde signaling from the nucleus to mitochondria occurs to adjust mitochondrial function to changing cellular energy demands and availability of substrates. For example, mitochondria pause translation to adapt to the influx from the cytosol (Dennerlein et al., 2015; Richter-Dennerlein et al., 2016). In the case of anterograde signaling, expression of several transcription factors like NRF1 (nucleus respiratory factor 1), as well as co-activators like PGC-1 $\alpha$  and PGC-1 $\beta$  (PPAP $\gamma$  (peroxisome proliferator-activated receptor) co-activator) and co-repressors, is induced upon changes of basal metabolic conditions. This can for example be an increase of AMP/ATP ratio or calcium concentration (Isaac et al., 2018; Quirós et al., 2016). Vice versa, retrograde signals from mitochondria back to the nucleus can be caused by an abolished OXPHOS function and a consequent loss of membrane potential, as well as alterations in calcium homeostasis and elevated levels of ROS (Isaac et al., 2018; Quirós et al., 2016).

However, regulation of mitochondrial respiration can also occur post-transcriptionally through the degradation of OXPHOS subunits by compartment-specific mechanisms. In the cytosol and the nucleus, degradation of non-assembled components is primarily facilitated by the ubiquitin-proteasome pathway. Dedicated mitochondrial proteases (mitoproteases) execute this function in mitochondria. Protease-mediated quality control is important to process newly imported polypeptides and degrade damaged (e.g. by ROS) or misfolded, cytotoxic proteins. Furthermore, mitoproteases also remove non-stoichiometric subunits resulting from an imbalanced mitonuclear gene expression. (Ahola et al., 2019). This proteolytic function is mainly carried out by LONP (Lon protease homolog), CLPP (ATP-dependent Clp protease proteolytic subunit) and AAA proteases (ATPases associated with diverse cellular activities). The latter can be further divided into the heterooligomeric matrix-facing (*m*-AAA, consisting of an AFG3L2 (AFG3-like protein 2) and SPG7 (paraplegin) subunits) and the IMS-facing (*i*-AAA, composed of YME1L subunits) AAA proteases bound to the IMM and are specifically required for degradation of membrane-associated OXPHOS subunits (Ahola et al., 2019; Quirós et al., 2015). Additionally, in yeast, the metalloprotease Oma1 is responsible for the degradation of Cox1 when maturation of C IV is stalled. Even though the primary role of human OMA1 is maintenance in membrane architecture – as its main function is processing of OPA1 – further implementations in mitochondrial quality control cannot be excluded (Bohovych et al., 2015; Khalimonchuk et al., 2012). It has been postulated that nuclear- and mitochondrial-encoded OXPHOS subunit are produced in a superstoichiometric manner to increase the possibility to establish the required protein interactions for complex formation. This process is dependent from the specific affinity of the subunit to each other and their abundance. By elevating the concentration of low-affinity binding partners, respective interactions become more likely (Isaac et al., 2018). Balancing of overproduction by a frequent turnover of excess subunits is of high importance to avoid potentially toxic accumulations which are implicated in mitochondrial diseases and ageing (Isaac et al., 2018; Quirós et al., 2015).

Within the scope of this work, it cannot be demonstrated whether diminished levels of analyzed OXPHOS subunits is due to reduced synthesis upon mitonuclear signaling or to upregulated

proteolytic activity. It is tempting to speculate that this fine-tuned system potentially requires both processes. However, this thesis shows that under physiological conditions, subunits, which are not required and their non-assembly can be potentially harmful, are consequently rapidly depleted. Pulse chase experiments (Appendix Figure I) confirm that indeed, newly synthesized levels of COX1 or ND1 are diminished by over 50 % after 6 h of chase in WT. In contrast, in situations of COX1 shortage, like it is the case when mtRF1 is absent, the turnover of this critical subunit is decelerated. This leads to residual COX1 protein levels of approximately 50 % after 24 h of chase (Supplementary Figure 3). This effect is not observed for other mitochondrial-encoded subunits, e.g. for ND1 in absence of mtRF1a. It can only be speculated what might be the reason for this observation. One possibility is that the comprehensiveness of the translational defect caused by loss of the major mitochondrial release factor cannot be compensated. Instead, the severe effects of mtRF1a ablation lead to a complete shutdown of energy production via OXPHOS (Figure 2a-d). By which mechanism the production of nuclear-encoded subunits is adjusted also remains elusive in this case. Furthermore, the specific activation of C12ORF65-mediated mtRQC rescue pathway upon decreased levels of COX1 in *mtRF1*<sup>-/-</sup> cells (Figure 5a-d) serves to keep a certain threshold of COX1 in order to maintain a sufficient amount of the terminal electron acceptor of the ETC for productive OXPHOS function. Consequently, respiration in mtRF1-ablated cells is only mildly diminished when compared to WT (Figure 2a). No upregulation of C12ORF65 can be observed in cells lacking mtRF1a (Appendix Figure II) and will be further discussed in chapter 3.4.

Taken together, it is currently not clear how exactly levels of certain mitochondrial OXPHOS subunits are regulated. As mentioned, there are no translational regulators known in human mitochondria. The only exception is TACO1 as translational activator for COX1 synthesis. So far, OXPHOS assembly factors like constituents of MITRAC can be seen as indirect translational regulators. For example, MITRAC7 is acting in a chaperone-like manner during early C IV assembly by stabilizing COX1-containing assembly intermediates to prime them for interactions with further constituents. It was shown that in this way, abundance of MITRAC7 regulates the progression of C IV biogenesis (Dennerlein et al., 2015). Thus, members of the MITRAC can sense the presence of nuclear-encoded and, as also shown in this work by the stalling of MITRAC-sequestered COX1 in mtRF1a-ablated cells (Figure 2j), mitochondrial-encoded subunits, as COX2 and COX3 are absent in these knockout cells. Thereby, MITRAC constituents serve as a gatekeeper for the assembly of OXPHOS complexes and necessarily require COX1 to trigger progression of C IV biogenesis.

### **3.3 Supercomplexes as Safeguard for Unstable OXPHOS Subunits**

As already discussed in 1.2.3.2, the functional relevance of SCs is still debated and clearly not fully understood. Their role of catalytically enhancing OXPHOS is broadly debated. However, this doctoral thesis provides insights to the assumption that SCs may also carry out a non-catalytic function by preserving and stabilizing certain subunits of ETC complexes under specific metabolic conditions to counteract potential dysfunctions.

### 3.3.1 Supercomplexes Confer Stability for Complex IV when mtRF1 is Lost

An observation within this thesis is that even though translation and steady state levels of COX1 are reduced in cells lacking mtRF1 (Figures 2f-g, 3b and 3f-g), the fraction of COX1, which is rescued by mtRQC, is associated with the macromolecular SCs. The holoenzyme is not detectable as an individual complex nor in its homodimeric form (~ 400 kDa) in the BN-PAGE with usage of mild detergent, but instead appears in the high molecular band corresponding to the respiratory SC (Figure 2e). Additionally, this doctoral thesis shows that newly synthesized COX1 is more stable compared to the WT situation (Supplementary Figure 3), indicating either a slower turn-over and/or higher stability of this subunit (Figure XII).

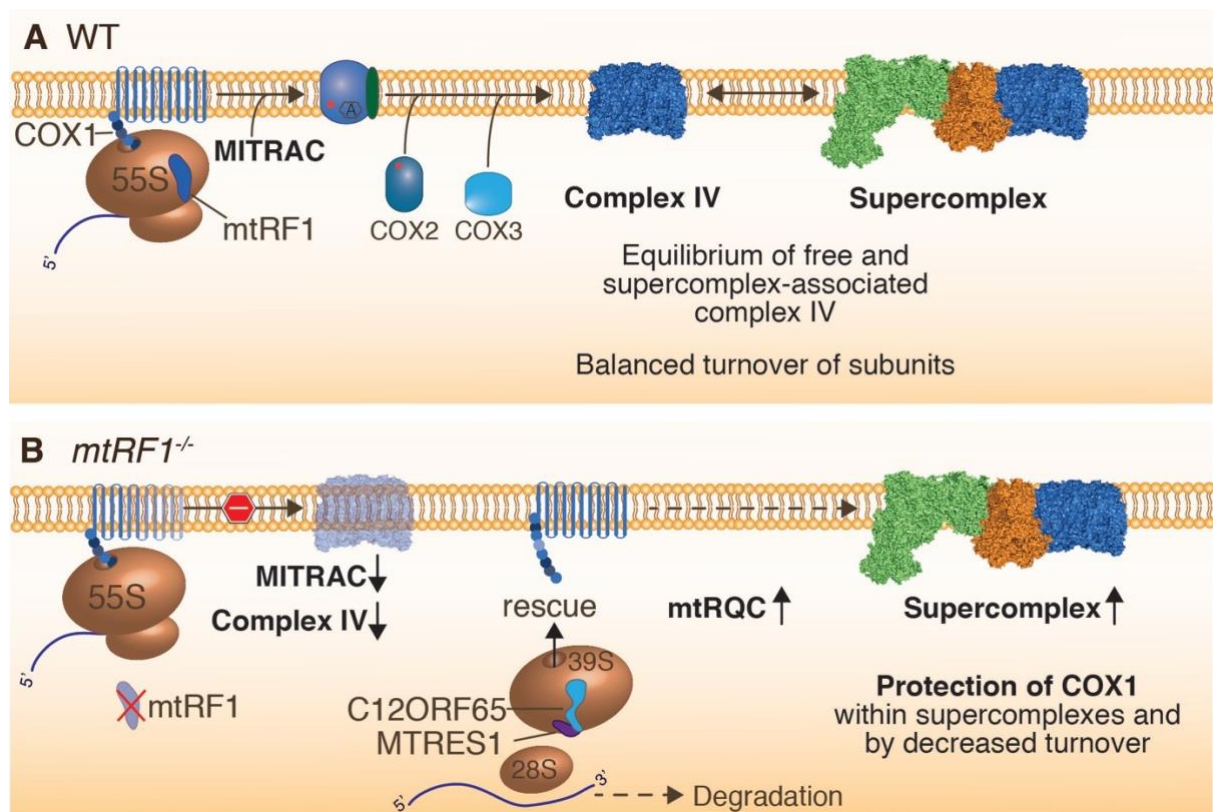


**Figure XII: COX1 as Nucleation Center for Supercomplex Assembly.** (A) Translation of COX1 is terminated by mtRF1 and co-translationally assembled into complex IV via MITRAC and further distinct modular steps. Under normal physiological conditions, there is an equilibrium between freely diffusing and into supercomplexes assembled complex IV. (B) In absence of mtRF1, MITRAC-based assembly of C IV is diminished. Residual synthesis of COX1 and subsequent OXPHOS function is preserved by several mechanisms: 1) C12ORF65-mediated mtRQC is activated to rescue stalled COX1 translation and 2) existing subunits are then assembled within stable SC. Model of matured complex IV was generated from PDB 5B1A, complex I and complex III from PDBs 5LDW and 1BGY.

As it was shown in earlier studies, assembly of C IV into SCs is a mechanism to protect its constituents in situations where individual components are limited in order to avoid the formation of rather unstable individual complexes (Kovářová et al., 2012; Lazarou et al., 2009). Under physiological conditions, an equilibrium exists with a smaller portion of SC-assembled COX in different stoichiometries (I-III<sub>2</sub>-IV<sub>1-3</sub>) and the main fraction as free holo-C IV (Kovářová et al., 2012). This finding is also demonstrated in this study where the complex is assembled into SCs, but also free monomers, dimers and assembly intermediates can be observed (Figure 2e, lane 10). Cell hybridization models demonstrated that apparently, there is a certain

'respiratory threshold' amount of COX1, which is required to promote SC formation. Here, ETC complexes and subunits not incorporated into the macromolecular SCs are suggested to serve as functional reserve to potentially compensate damaged SC constituents (D'Aurelio et al., 2006). For C IV, the critical threshold of COX1 are 40 – 50 % of the WT control (D'Aurelio et al., 2006). As this is the case in this study (Figure 3g), it can be speculated that in situations of isolated C IV deficiency, the rescued COX1 is directly incorporated into the SC. Thus, insertion of COX1 might serve as a checkpoint to ensure the proper formation and functionality of the SC. Previous studies revealed that maturation of C IV can occur in several distinct pathways: C IV can either be assembled as free holoenzyme or within simultaneous incorporation into SCs. Moreover, assembly of individual C IV does not necessarily have to be completed before incorporation into the SC (Lobo-Jarne et al., 2020). This is even more important when considering that COX1 is essential for C IV biogenesis as already elaborated in 3.2. If COX1 levels drop below the respiratory threshold, SC assembly is generally aborted. It is suggested that stabilization of C I requires proper SC formation (D'Aurelio et al., 2006). Thus, defective C IV biogenesis affects also the assembly of C I and C III and thereby severely diminishes viability of the cell in the hybridization model (D'Aurelio et al., 2006). This thesis shows that a disturbed maturation of C IV in mtRF1-ablated cells perturbs assembly of C III as well, as indicated by an accumulation of faster-migrating assembly intermediates and free C III (Figure 2e, lane 8). The fact that COX is the rate-limiting complex of the respiratory chain, explains the cellular need to activate rescue mechanisms (see 3.4) to maintain critical COX1 levels. Thus, pronounced SC formation appears to be a general mechanism of the cell to stabilize otherwise compromised ETC complexes. Moreover, integration of COX1 into SCs seems to be an important checkpoint in order to preserve proper respiration (Lobo-Jarne et al., 2020). It is suggested that this is not only due to avoid the accumulation of unshielded assembly intermediates, which are more redox-reactive and thus could cause generation of ROS. But, also the sequential integration of alternative assembly intermediates can serve as a way to repair otherwise perturbed SC structures with a reasonably good energetic expense. By adapting the turnover of certain subunits, cells can regulate the availability of ETC subunit for effective SC formation (Lobo-Jarne et al., 2020).

### **3.3.2 Compensatory Mechanisms in Isolated Complex IV Deficiency**

Assembly of COX1 into C IV is critical for the formation of SC. But, vice versa, SCs can associate with unconventional C IV assembly intermediates in order to ensure proper respiratory function (Lazarou et al., 2009; Lobo-Jarne et al., 2020; Moreno-Lastres et al., 2012). It is suggested that a certain amount of COX1 is required to be directly incorporated into SCs together with nuclear-encoded subunits. Therefore, it is proposed that next to the conventional assembly pathway of individual C IV, an alternative assembly pathway exists, which enables the incorporation of 'non-canonical' subassembly modules directly into SCs (Lobo-Jarne et al., 2020). Even though COX1 is significantly diminished in cells lacking mtRF1, the results obtained in this thesis demonstrate that respiration is still possible, albeit to a lesser extent as in WT control (Figure 2a). Additionally, elevated C I activities (Figure 2b-c) along with a slight increase in mitochondrial-encoded ND1 and a significant increase in ND2 (Figure 2f-g) can be observed

in mtRF1 ablated cells. The notion of compensatory mechanisms in cases of isolated C IV deficiencies was already made before in a case study of patients with Leigh syndrome caused by mutations in *SURF1* (Kovářová et al., 2012). In patients with a dysfunctional SC assembly factor, C IV subunit are solely assembled within SCs and not rather unstable individual complexes. The severe C IV deficiency is compensated via upregulation of the remaining mtDNA-encoded complexes of the respiratory chain: the abundance of the other proton-pumping complexes C I and C III and the ATPase is approximately 50 % or respectively 30 % higher, in order to still provide sufficient amounts of energy (Kovářová et al., 2012).

The results of this doctoral thesis highlight the plasticity of the complexes of the ETC and the ability of mitochondria to adapt to altered metabolic conditions. By enhancing synthesis of certain subunits and promoting SC formation in order to confer higher stability, arising OXPHOS deficiencies can be counteracted. Even though translation of the individual subunit COX1 is highly disturbed in absence of mtRF1, a residual cellular respiration can be observed which is achieved by two mechanisms. First, mtRQC is activated in response to stalled mitoribosomes. C12ORF65-mediated rescue can partially compensate for the loss of mtRF1 and concomitant decreased COX1 levels to attain amounts of COX1 above the respiratory threshold, which subsequently enables productive energy generation via OXPHOS. This again emphasizes the importance of COX1 and the physiological relevance of mtRF1. Second, it is tempting to speculate that the preferable incorporation of COX1 and/or unconventional COX subassembly intermediates, in situations where C IV maturation is disturbed, is a reaction of the cell to prevent its otherwise faster turnover. Free C IV not associated with supercomplexes is thought to serve as excess enzyme capacity (Kovářová et al., 2012). Under conditions of comprised COX1 level, this reserve cannot be built. Instead, available components are preserved within SCs and subunits are shielded from proteolytic cleavage.

Taken together, a preferential integration of C IV into SCs in absence of mtRF1, subsequent deceleration of COX1 turnover and elevated activity of other ETC complexes, as observed here for C I, helps to partially compensate the reduced COX1 level and to confer the cells with the ability to still respire aerobically.

### **3.3.3 Supercomplexes and the Role of Reactive Oxygen Species**

Another interesting finding within this work is the increased incidence of ROS. Under physiological conditions, ROS occur when electrons, which are shuttled via well-shielded prosthetic groups within the complexes of the ETC, get in premature contact with O<sub>2</sub> molecules (Figure XIII). Then an incomplete reduction leads to generation of damaging ROS, like O<sub>2</sub><sup>•-</sup>. As described in 1.2.4, C I with its many prosthetic groups is the major source of ROS followed by C III. C II and C IV only play a minor part. Additionally, one proposed function of SCs is to protect components of the complexes even more to further avoid oxidative stress (Milenkovic et al., 2017). Even though C IV is not contributing much to the generation of ROS, elevated levels of ROS are also observed in mtRF1-deficient cells (Figure 1d). This notion can be explained by the fact that C IV is the rate limiting step of electron transfer within the respiratory chain. If its level is decreased due to loss of mtRF1, cytochrome *c* and subsequently ubiquinol accumulate. This

in turn triggers RET in C I and ultimately  $O_2^{\bullet-}$  formation. Furthermore, the slightly elevated levels of C I constituents and increased activity to counteract decreased levels of C IV also contribute to the elevated ROS levels. This finding adds another layer of relevance to SC assembled COX1 and subsequently C IV. SCs form a protective environment and sequester C IV intermediates prone to cause oxidative stress (Lobo-Jarne et al., 2020). Therefore, it can be speculated that in this way, even elevated ROS levels can be tolerated.

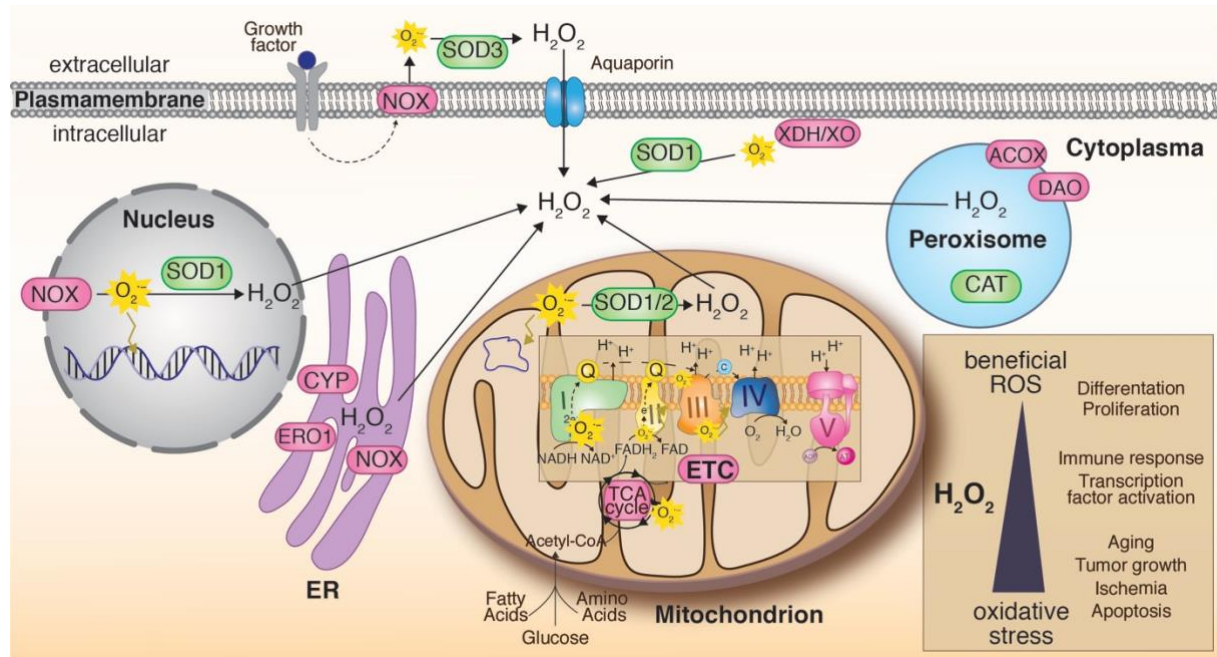


**Figure XIII: Cellular ROS production.** Overview of subcellular sources of ROS. Generation of  $H_2O_2$  via  $O_2^{\bullet-}$  (yellow) can occur at the plasmamembrane, in the nucleus, in peroxisomes, in the endoplasmic reticulum (ER) and mainly in mitochondria.  $H_2O_2$ -producing enzymes are depicted in magenta and abbreviations are as followed: ACOX = acyl-CoA oxidase; CYP = cytochrome P450-dependent monooxygenase; DAO = D-amino acid oxidase; ERO1 = ER oxidoreduction-1; ETC = electron transport chain, comprising complex I – IV and complex V; NOX = NADPH oxidase; TCA cycle = tricarboxylic acid cycle; XDH/XO = Xanthine dehydrogenase/oxidase. ROS converting enzymes are depicted in green and are either SOD = superoxide dismutases 1-3 or CAT = catalase. Influx of extracellular  $H_2O_2$  is possible via aquaporin channels. ROS damage is indicated by dark-yellow flash. The box on the right shows the concentration-dependent cellular response to (patho-)physiological levels of ROS. Selected enzymes and functions, without claiming completeness and not drawn to scale.

In contrast, ROS levels in mtRF1a-depleted cells are highly increased. This result seems counterintuitive when considering the global respiratory deficiency in this cell line (Figure 2a). However, if one contemplates that a) some OXPHOS complexes might be assembled partially from their nuclear-encoded subunits; b) that those intermediates may indeed contribute to the generation of ROS and c) that there are additional sources of ROS within mitochondria and in the cytosol, the observed elevated ROS levels may reflect the overall poor phenotype of these cells. An imbalanced production of OXPHOS subunits due to the dual-genetic nature of OXPHOS complexes leads to an aberrant generation of ROS (Isaac et al., 2018). For example, the peripheral arm of C I, which harbors Fe-S clusters and FMN to reduce NADH, is comprised of the N- and Q-module, which solely consists of nuclear-encoded components. All mitochondrial-encoded subunits are assembled into the membrane-embedded P-module which is responsible for proton pumping (Galemou Yoga et al., 2020). As in the scope of this doctoral thesis, only

the steady state level of one nuclear-encoded subunit of each OXPHOS complex was tested, no conclusion in regard to potential assembly intermediates of C I can be drawn. Obviously, the formation of SCs is highly perturbed in this case and consequently further enhances the production of ROS in a vicious circle (Maranzana et al., 2013).

However, next to the major mitochondrial ROS generation by C I and – under physiological conditions negligible – C III (Murphy, 2009), there are several further cellular processes which also contribute to endogenous ROS levels (Figure XIII). Examples are transmembrane NADPH oxidases (NOX) at various localizations within the cell (Bedard & Krause, 2007) as well as cytochrome P450-dependent monooxygenases in the ER and peroxisomal enzymes (Sies & Jones, 2020). The influence of lipid metabolism within mitochondria is also worth mentioning as it indirectly modulates ROS levels. As the electron carriers NADH and FADH<sub>2</sub> can be generated via  $\beta$ -oxidation of fatty acids by their integration into the TCA cycle, substrates for OXPHOS are generated, which have to match with the capability of the ETC. If this is not the case, the system is prone to increase ROS levels (Cortassa et al., 2017). It is therefore tempting to speculate that the highly elevated ROS level in mtRF1a-deficient cells are generated because of the imbalance of the whole system due to the collapse of the OXPHOS system.

### 3.4 The Need for Mitochondrial Quality Control Systems

The results of this study demonstrate the importance of a mtRQC-based mitochondrial rescue system (Nadler, Lavdovskaia, Krempler, et al., 2022). Ribosome rescue in mammalian mitochondria is not well defined as no orthologous system to *trans*-translation can be found. Additionally, ‘back-up’ systems like in bacteria are lost in mitochondria. Nevertheless, the two other mitochondrial release factors – ICT1 and C12ORF65 – which have a GGQ motif but no codon recognition domain, were potential candidates for being rescue factors. Based on its homology to ArfB, ICT1 is a designated mitochondrial rescue factor to act on truncated mRNAs and indeed was shown to bind to ‘no-stop’ complexes presenting an empty A-site, thus being an active rescue factor (Feaga et al., 2016; Kummer et al., 2021; Richter et al., 2010). But even though the overall structures of ICT1 and C12ORF65 are generally similar, the role of C12ORF65 remained elusive. It was not shown to bind to 55S mitoribosomes despite being known that mutations within C12ORF65 impair cellular fitness and cause Leigh syndrome (Antonicka et al., 2010; Kummer et al., 2021). However, a recent structural study revealed C12ORF65 together with MTRES1 bound to the mtLSU as a response to elongational stalling caused by starvation of aa-tRNAs. C12ORF65, or therefore renamed mtRRF-R, binds to the mtLSU post dissociation and triggers the release of the peptide chain from the peptidyl-tRNA in the P-site (Desai et al., 2020).

Here, we observed the upregulation of C12ORF65 and MTRES1 upon loss of mtRF1 to partially rescue COX1 translation (Figure 5), demonstrating again the importance of COX1 as this subunit is crucial for C IV assembly. It is of high physiological relevance to maintain levels of COX1 above the ‘respiratory threshold’ and thus to ensure respirational competence, as it is indeed the case in mtRF1-ablated cells (Figure 2). Without mtRQC, C IV assembly and its subsequent immediate



insertion into SCs would be hampered, cells would consequently suffer more extremely. The results obtained in this study therefore highlight the significance of ribosome rescue systems like mtRQC and demonstrate a hitherto unknown scenario in which mtRQC becomes relevant. However, the preceding mechanism which initially dissociates the mitochondrial monosome remains unknown. The canonical mtRRF recycling pathway and the alternative recycling system including GTPBP6 rather seem to be not the ideal candidates. Both factors cannot bind simultaneously with a peptidyl tRNA in the mitoribosomal P-site. Hence, it is tempting to speculate that this system requires a yet unknown splitting factor which identifies and disassembles ribosomes stalled upon disability of release factors.

Mitochondrial disorders are a diverse group of inherited metabolic diseases all connected by dysfunctional mitochondria. However, the clinical manifestation is extremely diverse, ranging from isolated, organ-specific symptoms to multisystem appearances, preferably occurring in tissues with high energy demands. Moreover, also onset and phenotype of the disease can vary immensely, even for the same disease-causing pathogenic variant. This is due to the complex inheritance pattern. If the pathogenic variant is mtDNA-encoded, the level of heteroplasmy determines the expression and thus severity of the disorder. Great effort over the last decades have been made to identify mitochondrial disease genes. Although next-generation sequencing and multi-omics helped tremendously and to date over 330 disease-causing genes are discovered (Stenton & Prokisch, 2020), the offspring of many mitochondrial diseases is currently unknown. Therefore, it is essential to know the underlying cause for development of potential therapeutics. It is of great interest to understand the physiological function and pathophysiological consequences of disease-causing mitochondrial proteins.

Since loss of mtRF1 causes an isolated C IV deficiency in the cellular knockout model, it is tempting to speculate whether this COX1-specific release factor can be a potential candidate when screening for mutations in patients with isolated C IV deficiency. This situation is reminiscent of patients with mutations in *C12orf65* (Antonicka et al., 2010; Heidary et al., 2014; Perrone et al., 2020; Shimazaki et al., 2012; Wesolowska et al., 2015). To date, no clinical implementation for mtRF1 is known according to 'The Human Protein Atlas' database ([www.proteinatlas.org](http://www.proteinatlas.org), last visited: 09.10.2022).

Interestingly, the rescue system appears to be well balanced and implicated in further quality control steps as we propose that the degradation of *MT-CO1* (Figure 4) serves as a mechanism to avoid overloading of C12ORF65-based mtRQC. In case of impaired translation termination, the cell has to prevent the accumulation of stalled mitoribosomes in order to ensure sufficient amounts of free subunits to be engaged in another translational cycle as their *de novo* assembly is extremely energy-consuming. The fact that mRNAs are specifically degraded in response to incomplete peptide release – for example, solely *MT-CO1* in *mtRF1*<sup>-/-</sup> and vice versa *MT-CO2* and *MT-CYB* in mtRF1a-ablated cells – suggests that this is a general mechanism of the cell in order to be able to cope with the respective compromising situation. However, if translation elongation is blocked at all, for instance by using antibiotics like chloramphenicol (CAM), degradation of mRNA does not take place. In this case, the mitoribosomal A-site is blocked,

translation factors cannot bind and dissociation of the mitoribosome is not possible. As C12ORRF65 was shown to require disassembled 39S subunits still containing a peptidyl-tRNA in the P-site, it is likely that mtRQC is not activated without a suitable substrate. Thus, also degradation of mRNA is not triggered (Figure 4c-d).

Consequently, it is of further interest which factors might be responsible for the degradation upon mtRQC activation. A possible candidate is the PNPase-based degradosome. Together, SUV3 and PNPase facilitate the turnover of aberrant, cytotoxic mRNAs and thus contribute to RNA surveillance (Borowski et al., 2013; Jain et al., 2022; Wang et al., 2009). SUV3 is an energy-consuming helicase, which interacts with a 3' single-stranded RNA overhang and is implicated in recruiting mRNAs to the degradosome (Wang et al., 2009). This feeds the 3'-to-5' phosphate-dependent exoribonuclease PNPase, which ultimately degrades RNAs to six nucleotide-long fragments (Jain et al., 2022; Wang et al., 2009). It is demonstrated that degradation by the mitochondrial degradosome is dependent on the length of the poly(A) tail of respective transcripts (Razew et al., 2018; Wang et al., 2014). Moreover, polyadenylation is dependent on the activity of the respiratory chain, as the  $P_i$ /ATP ratio directly influences the length of the poly(A) tails (Wang et al., 2014). If the concentration of  $P_i$  in the matrix is low, i.e. when ATPase activity is high, mtPAP associates with the degradosome via SUV3 and promotes elongation of the poly(A) tails and vice versa. Additionally, further stabilization of mtPAP via the LRPPRC/SLIRP complexes inhibits degradosome activity and further enhances polyadenylation and thus stabilization of respective mRNAs (Chujo et al., 2012). Taken together, the activity of the degradosome and the opposing protective role of the LRPPRC/SLIRP complex define the turnover-rate of mRNAs.

It is therefore the matter of interest, how the fate of a mRNA is decided. Until now, we do not see any indication of upregulated degradosome activity and/or downregulated LRPPRC activity by preliminary testing the steady levels of the individual components (Appendix Figure III). Additionally, we tested the steady state level of LACTB2. LACTB2 is a mitochondrial matrix protein with endonucleolytic activity, capable of cleaving single-stranded RNA and thus another potential candidate, which might play a role in mRNA processing and/or degradation mechanisms (Levy et al., 2016). However, no altered expression level of LACTB2, neither in *mtRF1*<sup>-/-</sup> or *mtRF1a*<sup>-/-</sup> cells, can be detected (Appendix Figure III).

It can only be speculated whether in respect to degradation of the aberrant mRNA, similar mechanisms as in the cytosol or bacteria are occurring in mitochondria. In the cytosol, truncated mRNAs are degraded by the exoribonuclease Xrn1 as well as the exosome complex to prevent re-engagement with the defective mRNA (Joazeiro, 2019). In comparison, degradation of mRNA, liberated from non-stop complexes rescued by *trans*-translation, is facilitated via the recruitment of RNase R (Keiler, 2015). Nevertheless, it cannot be excluded that a yet unknown mechanism is responsible for the degradation of mRNAs as any potential downstream process of mtRQC still remain elusive.

In contrast to *mtRF1*<sup>-/-</sup>, we do not observe an upregulation of mtRQC constituents in cells lacking mtRF1a (Appendix Figure II). This might be explained by the severity of mtRF1a-loss-induced diminished translation: potentially, this quality control system cannot cope with such highly impacted translation. Whether or not another rescue mechanism is activated in this case remains speculative. Interestingly, mtRF1a ablation seems to affect mitochondrial-encoded OXPHOS constituents to a different extent. *De novo* synthesis of certain subunits appears to be less affected when compared to others. For example, residual levels of ND2 and ND3 are still detectable in the knockout cells, whereas levels of ND6 as well as COX2 and COX3 are highly diminished (Figure 3a). It can only be speculated that there might be the existence of a yet unknown rescue mechanism or release factor that can compensate for the loss of mtRF1a. If so, a possible explanation for the differential stabilization of certain subunits could be their integration into assembly submodules. ND2 and ND3 assemble at an early stage of C I maturation into the ND2-submodule, ND6 joins at an intermediate stage (Signes & Fernandez-Vizarra, 2018). Similarly, COX2 and COX3 are assembled at the intermediate and late stage of C IV biogenesis, respectively (Vidoni et al., 2017). Thus, it is tempting to believe, that later formed interactions are less stable and rapid degradation seems more likely. Dissecting this phenomenon in regard of the consequences upon loss of mtRF1a is a future perspective of further studies.

However, there has to be a similar mechanism, which is responsible for degradation of mtRF1a-dependent mRNAs and nascent polypeptide chains as effects comparable but reversed to the *mtRF1*<sup>-/-</sup> phenotype can be observed. This system appears to be rather focused on protecting the cell from further cytotoxic accumulations of unfunctional proteins rather than rescuing the stalled proteins in order to be incorporated into OXPHOS complexes. Therefore, it also might be possible that a tagging-mechanism, similar to the cytosolic CAT- or bacterial Ala-tailing, is responsible for marking the respective polypeptides for degradation.

In conclusion, this thesis demonstrates an example for C12ORF65-mediated mitoribosomal-associated quality control. Mitochondrial rescue mechanisms are a surprisingly ill-defined topic given the plethora of bacterial rescue systems. Thus, defining up- and downstream processes of mtRQC and identifying potential additional rescue mechanisms thus represents a fascinating research subject.

### 3.5 Summary and Future Perspectives

In this doctoral thesis, CRISPR/Cas9-mediated knockout cell models were generated to dissect the roles of the human mitochondrial class I release factors mtRF1 and mtRF1a during translation termination. It was a long, outstanding debate whether mtRF1 is a genuine codon-dependent release factor. Even though a recent structural study demonstrated that mtRF1a interacts with reconstituted canonical termination complexes, *in vivo* evidence for the proposed role as main mitochondrial release factor was missing. Protein biochemical and molecular biological techniques allowed the analysis of the direct consequences of loss of either of the factors in HEK293 cells and further revealed downstream effects in regard of mitochondrial quality control.

The results obtained by this work confirmed for the first time *in vivo* and thus further strengthen the hypothesis, that indeed, mtRF1a is the major mitochondrial release factor in human mitochondria. With only one exception, mtRF1a is able to terminate translation of all mitochondrial encoded transcripts. COX1, the core component of complex IV, however, is specifically terminated by mtRF1. For these reasons, we propose that indeed mtRF1 is an active release factor dedicated to the termination of COX1. Consequently, mtRF1 is not dispensable for proper mitochondrial function and furthermore, mtRF1 and mtRF1a are not just two redundant release factors compensating each other. Although broadly debated, we suggest that the mechanism by which mtRF1 terminates translation is not dependent on the presence of the alternative stop codon at the end of the ORF of *MT-CO1*. Since *MT-ND6*, the second mRNA harboring a non-canonical stop codon, is terminated by mtRF1a, this theory seems unlikely.

Even though loss of mtRF1a affects the cell more severely by diminishing the complete OXPHOS machinery, thus cellular respiration and overall cell vitality, loss of mtRF1 impairs maturation of the cytochrome *c* oxidase and thereby cell growth and respiration as well, albeit to a reduced level. Here we show that several mechanisms are activated that ensure sufficient respiratory function in the case of loss of mtRF1. First, an immediate integration into macromolecular SC confers greater stability and a reduced turnover of COX1 / C IV. Second, mtRQC is activated by a yet unknown mechanism to rescue translation of COX1. The obtained amounts of COX1 are sufficient to be incorporated and function in SC. Furthermore, we show that in the knockout cells, respective mRNAs are degraded by a yet unknown mechanism, potentially in order to minimize the burden of the rescue system.

With respect to the remarkable specificity by which translation of COX1 is apparently achieved, it is of further interest what the specificity-conferring property might be. A possible theory is that a secondary structure in the short 3' UTR of *MT-CO1* leads to a -1 frameshift and thus termination at a standard stop codon. To test this hypothesis, a homologous *in vitro* termination assay could be utilized to clarify this open question, if reconstituted with a *MT-CO1*-like mRNA. Additionally, structural information is required to determine whether the extensions in the codon recognition domain of mtRF1 are required to specifically recognize elements in *MT-CO1* and/or to adopt changes within the mammalian mitoribosome. For both

approaches, 55S mitoribosomes have to be purified in large scale which is currently the bottle neck for these kinds of experiments. To overcome this, large-scale isolation of mitochondria and preparation of mitoribosomes have to be optimized.

Since *MT-CO1* and *MT-ND6* are not terminated by unconventional stop codons in all mammalian species, it is therefore intriguing to know, whether mtRF1 carries out the same function in these species, for example in mice. Comparable knockouts of both release factors and subsequent analysis are required to further explore whether the mechanism by which mtRF1 terminates translation is conserved in vertebrates.

In regard of the quality control mechanisms, which rescue translation of COX1 in absence of mtRF1, further work is needed to identify factors required for mRNA degradation and turnover of aberrant translation events. Transcriptome analysis or mass spectrometry-based approaches may indicate altered expression levels of certain factors, which are up- or downregulated in response to loss of either of the release factors. Moreover, it might be interesting to test whether manipulation of mtRQC, for example by overexpressing C12orf65, can a) further rescue COX1 levels in mtRF1-ablated cells and b) might be able to also rescue mitoribosomes stalled upon loss of mtRF1a after all. Taken together, investigating mitochondrial quality control represents a highly fascinating, ongoing research topic.

## 4 Materials and Methods

### 4.1 Materials

#### 4.1.1 Chemicals

A list of all chemicals and reagents and respective suppliers used in this study is listed below in table 1.

**Table 1:** List of chemicals and their supplier.

CHEMICAL	SUPPLIER
[ <sup>35</sup> S]-L-Methionine	Hartmann Analytics
[ $\gamma$ - <sup>32</sup> P] Adenosine 5'-triphosphate (ATP)	Hartmann-Analytic
$\epsilon$ -Amino-Caproic Acid	Sigma-Aldrich
2-Propanol	Roth
Acetic Acid	Roth
Acetone	Roth
Acrylamide (2x crystallized)	Roth
Acrylamide/Bisacrylamide (37.5:1) Solution	Roth
Agarose NEEO ultra-quality	Roth
Ammonium Acetate (NH <sub>4</sub> CH <sub>3</sub> CO <sub>2</sub> )	Roth
Ammonium Chloride (NH <sub>4</sub> Cl)	Merck Millipore
Ammonium Hydroxide Solution	Sigma-Aldrich
Ammonium Persulfide (APS)	Roth
Ampicilin (Amp)	AppliChem
Anisomycin, 10 mg/ml in DMSO	Sigma-Aldrich
Antimycin A	Sigma-Aldrich
Apo-ferritin	Sigma-Aldrich
Bacto™ Agar	BD
Bacto™ Peptone	BD
Bacto™ Tryptone	BD
Bacto™ Yeast Extract	BD
BIS-TRIS	Roth
Blasticidin S HCl	Thermo Fisher Scientific
Bovine Serum Albumin (BSA)	Sigma-Aldrich
Bromphenol Blue (BPB)	Merck Millipore
Calcium Chloride (CaCl <sub>2</sub> * 2xH <sub>2</sub> O)	Roth
Carbonyl cyanide <i>m</i> -chlorophenylhydrazone (CCCP)	Sigma-Aldrich
Catalase	Sigma-Aldrich
Chloramphenicol (CAM)	Sigma-Aldrich
Chloroform	Roth
cOmplete™ Protease Inhibitor (PI) Cocktail Tablets	Roche
Coomassie Brilliant Blue (CBB) R-250	Serva
Coomassie Brilliant Blue (CBB) G-250	Serva

Cytochrome c	Merck Millipore
D(+)-Sucrose	Roth
Di-Potassium Hydrogen Phosphate (KH <sub>2</sub> PO <sub>4</sub> )	Roth
Di-Sodium Hydrogen Phosphate (Na <sub>2</sub> HPO <sub>4</sub> * 2xH <sub>2</sub> O)	AppliChem
Diaminobenzidine (DAB)	Sigma-Aldrich
Developing Solution Developer G153	Agfa
Digitonin	Calbiochem
DMSO (Dimethylsulphoxide)	Merck Millipore
dNTP Mix	Thermo Fisher Scientific
Dithiothreitol (DTT)	Roth
EDTA (Ethylenediaminetetraacetate)	Roth
Emetine dihydrochloride hydrate	Sigma-Aldrich
Ethanol	Roth
Ethidium Bromide (0.025 %)	Roth
Fetal Calf Serum (FCS)	Capricorn Scientific
Fixing Solution Rapid Fixer G354	Agfa
Formaldehyde	Sigma-Aldrich
GeneRuler DNA Ladder Mix	Thermo Fisher Scientific
L-Glutamine 200 mM (100x)	Gibco
Glycerol	Sigma-Aldrich
Glycine	Roth
HEPES (4-(2-Hydroxyethyl)-1-Piperazineethanesulfonic Acid)	Roth
Hydrochloric acid, 37 % (w/v)	Roth
Hydrogen peroxide (H <sub>2</sub> O <sub>2</sub> )	Sigma-Aldrich
Hygromycin B	Thermo Fisher Scientific
Magnesium Chloride (MgCl <sub>2</sub> * 7x H <sub>2</sub> O)	Merck Millipore
Magnesium Sulfate (MgSO <sub>4</sub> )	AppliChem
Manganese (II) Chloride (MnCl <sub>2</sub> * 4x H <sub>2</sub> O)	Roth
Methanol	Roth
Milk powder	Frema Reform
MOPS (Morpholinopropanesulfonic Acid)	Roth
n-dodecyl-β-D-maltoside (DDM)	Sigma-Aldrich
N,N'-Methylen-bisacrylamide (2x crystalized)	Serva
Nicotinamide Adenine Dinucleotide (NADH)	Roche
Nitrotetrazoliumblausulfid (NBT)	Sigma-Aldrich
NP-40 (Nonident P40, 4-Nonylphenyl-Polyethylene Glycol)	Sigma-Aldrich
Oligomycin	Sigma-Aldrich
Opti-MEM™	Gibco
Penicillin Streptomycin	Gibco
Phenol	Roth
Plasmocin™	Invitrogen
PMSF (Phenylmethylsulphonylfluoride)	Roth

Ponceau S	Roth
Potassium Chloride (KCl)	Roth
Potassium Dihydrogen Phosphate (K <sub>2</sub> HPO <sub>4</sub> )	Roth
Potassium Hydroxide (KOH)	Roth
Precision Plus Protein™ All Blue Standard (10 – 250 kDa)	BioRad
Protein-A Sepharose	GE Healthcare
Proteinase K	Roth
RiboLock RNase Inhibitor (40 U/μl)	Thermo Fisher Scientific
Rotenone	Sigma-Aldrich
ROTI®Quant Reagent	Roth
Rubidium Chloride (RbCl)	Roth
Sodium Acetate (NaOAc, NaCH <sub>3</sub> CO <sub>2</sub> )	Roth
Sodium Azide (NaN <sub>3</sub> )	Sigma-Aldrich
Sodium Carbonate (Na <sub>2</sub> CO <sub>3</sub> )	Merck Millipore
Sodium Chloride (NaCl)	Roth
Sodium Deoxycholate	Roth
Sodium Dodecyl Sulfate (SDS)	Roth
Sodium Dihydrogen Phosphate (NaH <sub>2</sub> PO <sub>4</sub> )	Roth
Sodium Hydrogen Carbonate (NaHCO <sub>3</sub> )	Merck Millipore
Sodium Hydroxid (NaOH)	AppliChem
Sodium Pyruvate Solution	Sigma-Aldrich
Sodium Tetraborate (Borax)	Sigma-Aldrich
Sodium Thiosulfate	Sigma-Aldrich
Trichloroacetic Acid (TCA)	Roth
TEMED (Tetramethylethylenediamine)	Roth
Trehalose	Roth
Tricine	Roth
TRIS (Tris(Hydroxymethyl)aminomethane)	Roth
Tri-sodium Citrate	Roth
Triton X-100	Roth
TRIzol™ Reagent	Ambion
Tween20	Roth
UltraPure™ Agarose	Thermo Fisher Scientific
Uridine	Sigma-Aldrich



#### 4.1.2 Buffers and Media

All buffers, solutions and media used in this were prepared with bd H<sub>2</sub>O as listed in table 2. If not otherwise stated, every solution was autoclaved.

**Table 2:** List of buffers, solutions and media and their formulation.

BUFFER / SOLUTION	COMPOSITION
ACRYLAMIDE MIX	45 % (w/v) Acrylamide, 1.5 % (w/v) Bis-Acrylamide (32:1), sterile filtered
BLOCKING SOLUTION	5 % (w/v) Milk powder in TBS-T
BN ANODE BUFFER, 40X	500 mM Bis-TRIS, pH 7.0
BN CATHODE BUFFER, 10X	150 mM Bis-TRIS, 1 M Tricine, 0.2 % Coomassie Blue G-250
BN GEL BUFFER, 3X	200 mM ε–Amino-Caproic Acid, 150 mM Bis-TRIS, pH 7.0
BN LOADING DYE	100 mM Bis-TRIS pH 7.0, 500 mM ε–Amino-Caproic Acid, 5 % Coomassie Brilliant Blue G-250
BN-PAGE MARKER	50-150 mg/ml Ferritin, 25 mg/ml BSA, 50 mg/ml Catalase, 2x S-Buffer, 1 % CBB G-250
CELL LYSIS BUFFER	50 mM TRIS/HCl pH 7.4, 130 mM NaCl, 2 mM MgCl <sub>2</sub> , 1 % NP-40, 1 mM PMSF, 1x PI Mix
COMPLEX I BUFFER	1 mg/ml NBT, 1 mg/ml NADH, 5 mM TRIS/HCl pH 7.4
COMPLEX IV BUFFER	0.5 mg/ml DAB, 10 mg/ml Catalase, 1 µg/ml Cytochrome c and 75 mg/ml Sucrose, 50 mM KP <sub>i</sub> pH 7.4
COOMASSIE STAINING SOLUTION	0.25 % (w/v) Coomassie Brilliant Blue R-250, 10 % (v/v) Acetic Acid, 40 % (v/v) Ethanol
DESTAINER	40 % (v/v) Ethanol, 10 % (v/v) Acetic Acid
DMEM (DULBECCO'S MODIFIED EAGLE'S MEDIA)	10 % (v/v) FCS, 1 mM L-Glutamine, 1 mM Sodium Pyruvate, 50 µg/ml Uridine (additional Antibiotics; sterile filtered)
FREEZING MEDIA	18 % (v/v) FCS, 9 % (v/v) DMSO in DMEM Media, sterile filtered
HOMOGENIZATION BUFFER	300 mM Trehalose, 10 mM KCl, 10 mM HEPES-KOH pH 7.4, 1 mM PMSF, 0.2 % BSA
KP <sub>i</sub>	1 M K <sub>2</sub> HPO <sub>4</sub> : 1 M KH <sub>2</sub> PO <sub>4</sub> (pH 7.4 = 80.2 % : 19.8 %)
LB (LYSOGENY BROTH) MEDIA	1 % (w/v) Tryptone, 0.5 % (w/v) NaCl, 1 % (w/v) Yeast extract (+ 2 % Agar for solid growth media)
MOPS BUFFER, 10X	0.4 M MOPS, 0.1 M NaOAc, 10 mM EDTA, pH 7.2

MP LYSIS BUFFER	3 % (w/v) Sucrose, 100 mM NH <sub>4</sub> Cl, 15 mM MgCl <sub>2</sub> , 20 mM TRIS/HCl pH 7.5, 1 % Digitonin, 1x PI Mix, 0.08 U/μl RiboLock RNase Inhibitor
MP DILUTION BUFFER	3 % (w/v) Sucrose, 100 mM NH <sub>4</sub> Cl, 15 mM MgCl <sub>2</sub> , 20 mM TRIS/HCl pH 7.5, 1x PI Mix, 0.08 U/μl RiboLock RNase Inhibitor
NANOSTRING LYSIS BUFFER	
PBS (PHOSPHATE-BUFFERED SALINE)	0.14 M NaCl, 2.7 mM KCl, 0.01 M Na <sub>2</sub> HPO <sub>4</sub> , 1.8 mM KH <sub>2</sub> PO <sub>4</sub> , pH 7.4
PONCEAU RED	0.2 % Ponceau-S, 3 % (w/v) TCA
RF1 BUFFER	100 mM RbCl, 50 mM MnCl <sub>2</sub> , 30 mM NaAc, 10 mM CaCl <sub>2</sub> , 15 % Glycerol, pH 5.8
RF2 BUFFER	10 mM RbCl, 50 mM MnCl <sub>2</sub> , 10 mM MOPS, 75 mM CaCl <sub>2</sub> , 15 % Glycerol, pH 6.8
S-BUFFER	20 mM TRIS/HCl pH 7.4, 0.1 mM EDTA, 50 mM NaCl, 10 % (v/v) Glycerol, 1 mM PMSF and 1 % Digitonin or 0.2 % DDM
SDS SAMPLE BUFFER, 4X	8 % (w/v) SDS, 40 % (w/v) Glycerol, 0.04 % (w/v) Bromophenol Blue, 5 mM DTT, 250 mM TRIS/HCl, pH 6.8
SES1 BUFFER	250 mM NaP <sub>i</sub> pH 7.4 (81 % Na <sub>2</sub> HPO <sub>4</sub> + 19 % NaH <sub>2</sub> PO <sub>4</sub> ), 1 mM EDTA, 7 % (w/v) SDS
SOB MEDIA	2 % Tryptone, 0.5 % Yeast extract, 10 mM NaCl, 2.5 mM KCl, 10 mM MgCl <sub>2</sub> , 10 mM MgSO <sub>4</sub> , pH 7.0
SSPE BUFFER, 20X	3 M NaCl, 0.2 M NaH <sub>2</sub> PO <sub>4</sub> , 20 mM EDTA, pH 7.4
SSC BUFFER, 20X	3 M NaCl, 300 mM NaCitrates pH 7.0
SUCROSE GRADIENT SOLUTIONS	5 – 30 % (w/v) Sucrose, 100 mM NH <sub>4</sub> Cl, 15 mM MgCl <sub>2</sub> , 20 mM Tris/HCl pH 7.5, 1x PI mix
TAE BUFFER	40 mM TRIS/Acetate pH 8.0, 0.2 mM EDTA
TBS-T (TRIS-BUFFERED SALINE WITH TWEEN20)	20 mM TRIS/HCl, pH 7.5, 125 mM NaCl, 0.1 % (v/v) Tween20
TRANSFER BUFFER	20 mM TRIS, 0.02 % (w/v) SDS, 150 mM Glycine, 20 % (v/v) Ethanol
T/T ANODE BUFFER,	0.2 M Tris, pH 8.9
T/T CATHODE BUFFER	0.1 M TRIS, 0.1 M Tricine, 0.1 % (w/v) SDS, pH 8.25
T/T GEL BUFFER	1 M TRIS/HCl, 0.1 % (w/v) SDS, pH 8.45

### 4.1.3 Disposables and Kits

Disposables and commercial kits used in this study are listed in table 3.

**Table 3:** List of disposables and Kits.

ITEM	MANUFACTURER
Alkaline phosphatase	Roche
Alt-R® CRISPR-Cas9 tracrRNA, ATTO™ 550	IDT
Alt-R® <i>S.p.</i> Cas9 Nuclease V3	IDT
Amicon® Ultra-0.5 Centrifugal Filter Devices 100K	Merck Millipore
Amicon® Ultra-15 Centrifugal Filter Devices 100K	Merck Millipore
Amicon® Ultra-4 Centrifugal Filter Devices 100K	Merck Millipore
Bottle Top Filter 500 ml, 45 mm neck	Corning
Cell Culture Flasks, surface 25 cm <sup>2</sup> , 75 cm <sup>2</sup>	Greiner Bio-One
Cell Culture Dishes, PS, 145/20 mm	Greiner Bio-One
Cell culture Plate 6-, 12-, 24-, 96-well	Greiner Bio-One
Centrifuge Bottles Polypropylene w/ Caps (29x104 mm), 50 ml	Beckman Coulter
Centrifuge Tubes Polyallomer (25x89 mm), open top	Seton
Centrifuge Tubes Polyclear™ (14x89 mm), open top	Seton
Complex I Enzyme Activity Assay Kit (Colorimetric)	abcam
CryoPure Tube 1.6 ml	Sarstedt
Complex I Enzyme Activity Assay Kit (Colorimetric)	abcam
Counting Chambers Hycor KOVA Glasstic Slide 10 with Grids	Thermo Fisher Scientific
CyQUANT™ Cell Proliferation Assay, for cells in culture	Thermo Fisher Scientific
Disposable hypodermic needle Sterican®	B.Braun
21G x3 1/8"/∅ 0.80 x 80 mm, 14G x3 1/8"/∅ 2.10 x 80 mm	
DreamTaq Hot Start DNA Polymerase	Thermo Fisher Scientific
Falcon Centrifuge Tube, 50 ml, 15 ml	Sarstedt
FastDigest Restriction Enzymes	Thermo Fisher Scientific
Graduated Filter Tips 1000 µl, 300 µl, 20 µl, 10 µl	Greiner Bio-One
KOD Hot Start DNA Polymerase	Novagen
Lipofectamine™ RNAiMax Transfection Reagent	Invitrogen
Lipofectamine™ 3000 Transfection Reagent	Invitrogen
MitoSOX™ Red Mitochondrial Superoxide Indicator	Thermo Fisher Scientific
Nitrocellulose Membrane Amersham™ Protan™ 0.2 µm NC	GE Healthcare
Nylon Membrane Amersham Hybond™-N 0.45 µm	GE Healthcare
OneSot®TOP10 Chemically Competent Cells	Thermo Fisher Scientific
PCR Multiply®-Pro Cup 0.2 ml	Sarstedt
Pierce™ ECL Western Blotting Substrate	Life Technologies
Pipette Tips 1000 µl, 200 µl, 10 µl	Sarstedt
PVDF membrane, 0.45 µm, Immobion®-P-membrane	Merck Millipore
QuikChange Lightning Site-Directed Mutagenesis Kit	Agilent Technologies
QuickExtract™ DNA Extraction Solution	Lucigen

Rapid DNA Ligation Kit,	Thermo Fisher Scientific
Reaction Tube 1.5 ml Low Binding	Sarstedt
Reaction Tube 1.5 ml, 2.0 ml	Sarstedt
Reaction Tube 0.6 ml	Biozym
Seahorse XF96 Cell Culture Microplate V3-PS, TC-Treated	Agilent Technologies
Seahorse XF assay media	Agilent Technologies
Seahorse XF calibrant solution	Agilent Technologies
Seahorse XF FluxPaks	Agilent Technologies
Super RX-N Fuji Medical X-ray Film	Fujifilm
Syringe Omnifox® LuerLock Solo 50 ml, 10 ml	B.Braun
T4 Polynucleotide Kinase (T4 PNK), 10 U/μl	Thermo Fisher Scientific
TOPO™-TA Cloning™ Kit	Thermo Fisher Scientific
Whatman Blotting Paper	Heinemann Labortechnik
Wizard® SV Gel and PCR Clean-Up system	Promega
Wizard® Plus SV Minipreps DNA Purification System	Promega

#### 4.1.4 Equipment, Instruments and Software

Instruments and equipment used in this study are listed in table 4, Software in table 5.

**Table 4:** List of instruments and equipment.

EQUIPEMNT	MODEL	MANUFACTURER
Centrifuges	5418	Eppendorf
	5427R	Eppendorf
	5804R	Eppendorf
	Optima L-90K	Beckman Coulter
	Sorvall RC 6 Plus	Thermo Fisher Scientific
Rotors	SW-41 Ti	Beckman Coulter
	SW-32 Ti	Beckman Coulter
	SS-34	Sorvall
Electrophoresis	Power Supply EV3020, EV2650	Consort
	PerfectBlue™ SemiDry Blotter M	Peqlab
	Wide Mini-Sub® Cell GT	Bio-Rad
	PowerPac HC™ Power Supply	Bio-Rad
	SE600 Ruby™ System	GE-Healthcare
	T/T Gel Running Chamber	homemade
Miscellaneous	BD FACS Canto II	Becton Dickinson
	BD LSR Fortessa X20	Becton Dickinson
	GeneTouch Thermocycler	BIOER
	Gradient Station™	Biocomp

	Homogenisator Potter-Elvehjem with PTFE pistil 15 ml	Sartorius
	Homogenisator Potter-Elvehjem with PTFE pistil 2 ml, 5 ml	Omnilab
	Homogenisator Machine homogen <sup>plus</sup>	Schuett-biotec
	Incubator Heraeus® Hera Cell 150	Thermo Fisher Scientific
	Light microscope	Zeiss
	Magnetic Stirrer MR3001	HEIDOLPH
	NanoDrop™ One <sup>C</sup> UV/Vis Spectrophotometer	Thermo Fisher Scientific
	Non- CO <sub>2</sub> Incubator	Agilent Technologies
	nCounter MAX analysis system	nanoString Technologies
	Pipettes	Gilson, Eppendorf
	Pipetting aid Accu-Jet® pro	Brand
	Rocking Table RS-RR10	PHOENIX Instruments
	Sterile Hood Heraeus® Hera Safe	Thermo Fisher Scientific
	Storage Phosphor Screen	GE Healthcare
	Synergy H1 Microplate Reader	BioTek
	Thermomixer Comfort	Eppendorf
	UV Stratalinker 1800 Crosslinker	Stratagene
	Vortex-Genie 2	Scientific Industries
	XF96 Extracellular Flux Analyzer	Agilent Technologies
	X-ray cassette 24x30	rego X-ray GmbH
Visualization	Developing Machine Curix 60	AGFA
	Typhoon FLA 9500 Phosphoimager	GE Healthcare

**Table 5:** List of software.

<b>SOFTWARE</b>	<b>DEVELOPER</b>
Adobe® Illustrator® CS6	Adobe Systems, San Jose, CA, USA
Adobe® Photoshop® CS6	Adobe Systems, San Jose, CA, USA
BD FACSDiva™ v9.0.1	Becton Dickinson, Franklin Lakes, New Jersey, USA
EndNote Web	Clarivate Analytics, London, UK
Genious® 11.1.4	Biomatters Ltd., Auckland New Zealand
FIJI v2.1.0	ImageJ OpenSource, (Schindelin et al., 2012)
ImageQuant TL v8.1	GE Healthcare BioSciences AB, Uppsala, Sweden
Microsoft® Office v16.16.27	Microsoft Corporation, Redmond, Washington, USA
nSolver Software v4.0.70	nanoString Technologies, Seattle, Washington, USA
PyMOL v2.3.5	Schrödinger LLC, Inc., New York, NY, USA
Seahorse Wave Desktop v2.6.1.53	Agilent Technologies, Santa Clara, CA, USA

#### 4.1.5 Antibodies

Commercially available primary antibodies were purchased from ProteinTech (via Fisher Scientific GmbH, Schwerte, Germany), abcam (Cambridge, United Kingdom), Sigma Prestige (via Merck KGaA, Darmstadt, Germany) or Invitrogen (via Thermo Fisher Scientific Inc., Waltham, Massachusetts, USA). Polyclonal, homemade antibodies were produced by injection of purified proteins or synthetic peptides into rabbits and subsequent serum purification. Respective antibodies were validated in previous studies (Dennerlein et al., 2015; Richter-Dennerlein et al., 2016) or in this study (Supplementary Figure 6). Secondary goat- $\alpha$ -mouse or goat- $\alpha$ -rabbit coupled to HRP (Horse Radish Peroxidase) were purchased from Dianova GmbH (Hamburg, Germany). All primary antibodies used in this study are listed in table 6.

**Table 6:** List of primary antibodies.

PROTEIN	COMPANY	IDENTIFIER
Rabbit polyclonal anti-uS15m	ProteinTech	Cat# 17006-1-AP
Rabbit polyclonal anti-uL23m	n/a	PRAB1716
Mouse monoclonal anti-FLAG	Sigma Prestige	Cat# F1804
Rabbit polyclonal anti-TIM23	n/a	PRAB1527
Rabbit polyclonal anti-TIM70	n/a	PRAB3280
Mouse monoclonal anti-Calnexin	ProteinTech	Cat# 66903-1-Ig
Rabbit polyclonal anti-ND1	n/a	PRAB5021
Rabbit polyclonal anti-ND2	ProteinTech	Cat# 19704-1-AP
Rabbit polyclonal anti-NUDFB8	n/a	PRA3765
Mouse monoclonal anti-SDHA	Invitrogen	Cat# 459200
Rabbit polyclonal anti-CYTB	n/a	PRAB5131
Rabbit polyclonal anti-RIESKE	n/a	PRAB1512
Rabbit polyclonal anti-COX1	n/a	PRAB5121
Mouse monoclonal anti-COX2	Abcam	Cat# ab110258
Rabbit polyclonal anti-COX4l	n/a	PRAB1522
Rabbit polyclonal anti-ATP5B	n/a	PRAB4826
Rabbit polyclonal anti-ATP6	n/a	PRAB5159
Rabbit polyclonal anti-C12orf62	n/a	PRAB 4845
Rabbit polyclonal anti-MITRAC12	n/a	PRAB3761
Rabbit polyclonal anti-MITRAC15	n/a	PRAB4814
Rabbit polyclonal anti-mtRF1	n/a	PRAB5461
Rabbit polyclonal anti-mtRF1a	ProteinTech	Cat# 16694-1-AP
Rabbit polyclonal anti-mL62/ICT1	ProteinTech	Cat# 10403-1-AP
Rabbit polyclonal anti-C12ORF65	ProteinTech	Cat# 24646-1-AP
Rabbit polyclonal anti-MTRES1	Sigma	Cat# HPA049535
Rabbit polyclonal anti-LRPPRC	ProteinTech	Cat# 21175-1-AP
Rabbit polyclonal anti-SUV3L1	ProteinTech	Cat# 12826-1-AP
Rabbit polyclonal anti-PNPase	Abcam	Cat# ab96176
Rabbit monoclonal anti-LACTB2	ProteinTech	Cat# 67399-1-Ig

#### 4.1.6 Oligonucleotides and Plasmids

Oligonucleotides used for molecular cloning, CRISPR/Cas9-mediated knockouts siRNA-mediated knockdowns and northern blots were purchased from Microsynth SEQLAB (Göttingen, Germany) and listed in table 7. Table 8 shows plasmids used in this doctoral thesis which were either purchased from Fisher Scientific (Schwerte, Germany) or generated via molecular cloning and subsequently purified from competent *E. coli* (XL1-blue).

**Table 7:** List of oligonucleotides.

PURPOSE	SEQUENCE (5' → 3')	SOURCE
<b>Guide RNA for CRISPR/Cas9-mediated KO</b>		
Guide RNA targeting Exon 2 of mtRF1	TGTTAAGTAAGAATTGGTCC	This study
Guide RNA targeting Exon 1 of mtRF1a	CTCCGGTAGCCCGCCGCTGG	This study
<b>PCR primer for Molecular Cloning</b>		
Forward Primer: FLAG-tagged version of mtRF1	CTCTCCAAGCTTCCACCATGAATCGTCACC TGTGTGTTTGGC	This study
Reverse Primer: FLAG-tagged version of mtRF1	CTTTCTCTCGAGCTACTTATCGTCGTCATC CTTGTAATCTTTTGCTGATTTAAGGTGTTCC ATCC	This study
Forward Primer: FLAG-tagged mutant (GGQ→AAQ) version of mtRF1	GATACATTTTCGAGCCAAAGGAGCAGCAG CGCAGCATGTTAATAAAAAC	This study
Reverse Primer: FLAG-tagged mutant (GGQ→AAQ) version of mtRF1	CACTATCAGTTTTATTAACATGCTGCGCTG CTGCTCCTTTGGCTC	This study
Forward Primer: FLAG-tagged version of mtRF1a	CTCTCCAAGCTTCCACCATGCGGTCCCGG GTTCTGTGGG	This study
Reverse Primer: FLAG-tagged version of mtRF1a	CTTTCTGATATCCTACTTATCGTCGTCATC CTTGTAATCAACTTTTTGGGAAATAATTTCC TACTAAAGATTC	This study
Forward Primer: FLAG-tagged mutant (GGQ→AAQ) version of mtRF1a	GACACTAAGCGAGCCAGTGGAGCTGCGG CGCAGCATGTAAATAC	This study
Reverse Primer: FLAG-tagged mutant GGQ→AAQ) version of mtRF1a	CACTGTCCGTGGTATTTACATGCTGCGCC GCAGCTCCACTGGCTC	This study
<b>Northern Blot Probes</b>		
MTRNR1 (12S rRNA)	TCGATTACAGAACAGGCTCCTCTAG	This study
MTRNR2 (16S rRNA)	GTTTGGCTAAGGTTGTCTGGTAGTA	This study
MTCO1	GTCAGTTGCCAAAGCCTCCGATTATG	This study

MTCO2	GACGTCCGGGAATTGCATCTGTTTT	This study
MTCYTB	CGTGTGAGGGTGGGACTGTCTACTG	This study
18S-rRNA	TTTACTTCCTCTAGATAGTCAAGTTCGACC	(Larburu et al., 2016)
<b>Oligos for siRNA-mediated Knockdowns</b>		
Oligo siRNA C12orf65	GCAAAGGAAACCCUGGAAA	This study

**Table 8:** List of plasmids.

PLASMID	FUNCTION	SOURCE
pCR <sup>TM</sup> 4-TOPO <sup>®</sup>	Rapid TOPO <sup>®</sup> Cloning	Invitrogen
pOG44	Expression of Flp recombinase	Thermo Fisher Scientific, Cat# V600520
pcDNA5/FRT/TO	Insertion of tetracycline-inducible constructs into FRT sites in Flp-In <sup>TM</sup> host cells	Thermo Fisher Scientific, Cat# V6520-20
pcDNA5-mtRF1 <sup>FLAG</sup>	Expression of WT version of mtRF1	This study
pcDNA5-mtRF1 <sup>FLAG-AAQ</sup>	Expression of mtRF1 AAQ mutant	This study
pcDNA5-mtRF1a <sup>FLAG</sup>	Expression of WT version of mtRF1a	This study
pcDNA5-mtRF1a <sup>FLAG-AAQ</sup>	Expression of mtRF1a AAQ mutant	This study

#### 4.1.7 Human Cell Lines and *E. coli* Strains

In this doctoral thesis, Human Embryonic Kidney 293 (HEK293 Flp-In<sup>TM</sup> T-REX) cells were used as experimental models and listed in table 9. This cell line contains an integrated, stable FRT site. Co-transfection of a Flp-In<sup>TM</sup> expression vector and Flp-recombinase vector pOG44 enables stable integration of a gene of interest into the cell's genome. 143B cells, derived from human osteosarcoma cells, and 143B *Rho*<sup>0</sup> cells, depleted from mitochondrial DNA, were used to test antibodies targeting mitochondrial-encoded proteins.

In table 10, bacterial strains used in this study are listed.

**Table 9:** List of human cell lines.

CELL LINE	SOURCE
HEK293-Flp-In T-REX	Thermo Fisher Scientific, R78007
HEK293-Flp-In T-REX- <i>mtRF1</i> <sup>-/-</sup> cl. 25	This study
HEK293-Flp-In T-REX- <i>mtRF1a</i> <sup>-/-</sup> cl.16	This study
HEK293-Flp-In T-REX- <i>mtRF1</i> <sup>-/-</sup> + mtRF1 <sup>FLAG-GGQ</sup>	This study
HEK293-Flp-In T-REX- <i>mtRF1</i> <sup>-/-</sup> + mtRF1 <sup>FLAG-AAQ</sup>	This study
HEK293-Flp-In T-REX- <i>mtRF1a</i> <sup>-/-</sup> + mtRF1a <sup>FLAG-GGQ</sup>	This study
HEK293-Flp-In T-REX- <i>mtRF1a</i> <sup>-/-</sup> + mtRF1a <sup>FLAG-AAQ</sup>	This study
143B	Provided by R. Richter-Dennerlein
143B <i>Rho</i> <sup>0</sup>	Provided by R. Richter-Dennerlein



**Table 10:** List of *E. coli* strains.

STRAIN	SOURCE
<i>E. coli</i> XL1-blue Chemically Competent Cells	Stratagene
<i>E. coli</i> TOPO10 OneShot® Chemically Competent Cells	Invitrogen

## 4.2 Molecular Biological Methods

### 4.2.1 Polymerase Chain Reaction

Polymerase Chain Reaction (PCR) was performed by using KOD Hot Start DNA Polymerase (Novagen®) according to the manufacturer's instructions to amplify specific DNA fragments to be further used for molecular cloning. One PCR reaction mix contained 100 ng template DNA (plasmid DNA, gDNA or cDNA), 10 µM forward and reverse primer, 2 mM dNTP mix, 25 mM MgSO<sub>4</sub>, 1 U/µl polymerase in 50 µl of 1x reaction buffer. Using a thermocycler (GeneTouch, Bioer), the polymerase was initially activated at 95 °C for 2 min. In 35 cycles of PCR, the template DNA was first denatured at 95 °C for 20 sec, then primer annealing was allowed for 10 sec at a temperature depending of the respective melting temperature of the primer pair (usually +/- 55 – 60 °C) and subsequently DNA fragments were elongated at 70 °C for 30 sec. PCR products were further analyzed by agarose gel electrophoresis.

### 4.2.1 Agarose Gel Electrophoresis

To visualize and purify obtained PCR products or other DNA samples, agarose gel electrophoresis was used. To cast the gel, 1 % (w/v) agarose was dissolved in TAE buffer by heating the mixture until fully dissolved and after cooling down to approximately 50 °C, ethidium bromide (EtBr, Roth) or a substitute was added at a concentration of 1 µg/ml. Samples were mixed with DNA Loading Dye (e.g. 10 % Fast Digest Green Buffer, Thermo Fischer Scientific), loaded together with an appropriate molecular weight marker (GeneRuler DNA Ladder Mix) on the polymerized gel and run for 10 – 15 min at 110 V in TAE buffer. Separated DNA fragments were analyzed by exposing the EtBr-intercalated DNA fragments to UV light.

- TAE buffer: 40 mM TRIS/Acetate pH 8.0, 0.2 mM EDTA

### 4.2.3 Isolation of DNA from PCR Products and Agarose Gels

PCR products were either purified directly in case a single clean PCR product using the Wizard® SV Gel and PCR Clean-Up system (Promega) or if unspecific bands occur, the remaining reaction can be loaded onto a 1 % preparative agarose gel, the correct DNA band excised and then purified according to the manufacturer's instructions. The final DNA concentration was calculated by using NanoDrop™ UV/VIS spectrophotometer (Thermo Scientific).

### 4.2.4 Molecular Cloning

Molecular cloning was used to clone a desired DNA fragment into a certain plasmid. In brief, 2 µg PCR product (= insert) and 4 µg of plasmid DNA (=vector) were digested with suitable FastDigest restriction enzymes (Thermo Fisher) in a reaction mix containing 1x FastDigest buffer

and 2 µl of each restriction enzyme at 37 °C for 60 – 75 min. To avoid re-ligation, the cut vector was dephosphorylated by the addition of 2 µl alkaline phosphatase (Roche) in 1x phosphatase buffer for 30 min at 37 °C. Insert and vector were purified as described in 4.2.3 and subsequently ligated. Ligation of 50 – 100 ng vector was carried out by using T4 DNA ligase (Rapid DNA ligation Kit, Thermo Scientific) in 1x ligation buffer and the respective amount of insert in a 1:2 or 1:3 molar ratio for 90 min at RT. The ligation mix was transformed into competent XL1 blue *E. coli* cells as described in 4.2.5, test digestion was performed and potentially positive plasmids were sequenced (Microsynth SEQLAB, Göttingen)

#### 4.2.5 Transformation of Competent *E. coli* Cells

For transformation, 100 µl of chemically-competent *E. coli* cells were incubated with 100 ng plasmid or 20 µl ligation mix for 15 min on ice, followed by a heat-shock (90 sec, 42 °C). The cells were cooled down on ice and then incubated for 45 min to 1 h at 37 °C in 1 ml LB media. After incubation, the cells were pelleted for 3 min, resuspended in 100 µl LB media and plated on LB-agar plates containing respective antibiotics (usually ampicillin or kanamycin), as selection marker.

- LB media: 1 % (w/v) Tryptone, 0.5 % (w/v) NaCl, 1 % (w/v) Yeast extract

#### 4.2.6 Isolation and Purification of Plasmid DNA from *E. coli*

Single colonies were picked, inoculated in LB-media plus respective antibiotic (usually 100 µg/ml ampicillin) and incubated at 37 °C overnight while shaking. Plasmids were purified by using Wizard® Plus SV Minipreps DNA Purification System (Promega). DNA concentration was measured by using NanoDrop™ UV/VIS spectrophotometer (Thermo Scientific).

#### 4.2.7 Preparation of Competent *E. coli* Cells

Preparation of chemically-competent *E. coli* cells was performed as followed: a volume of 200 ml SOB media was inoculated with 2 ml overnight culture and grown at 37 °C until mid-log phase to an OD<sub>600</sub> of 0.3. Cells were cooled down on ice for 15 min and pelleted for 10 min at max. speed and 4 °C. The cell pellet was resuspended in 67 ml of ice-cold RF1 buffer and incubated on ice for 30 min. Afterwards cells were pellet and resuspended in 16 ml of RF2 buffer. After 15 min incubation, the cells were aliquoted and stored at -80 °C.

- SOB media: 2 % Tryptone, 0.5 % Yeast extract, 10 mM NaCl, 2.5 mM KCl, 10 mM MgCl<sub>2</sub>, 10 mM MgSO<sub>4</sub>, pH 7.0
- RF1 buffer: 100 mM RbCl, 50 mM MnCl<sub>2</sub>, 30 mM NaAc, 10 mM CaCl<sub>2</sub>, 15 % Glycerol, pH 5.8
- RF2 buffer: 10 mM RbCl, 50 mM MnCl<sub>2</sub>, 10 mM MOPS, 75 mM CaCl<sub>2</sub>, 15 % Glycerol, pH 6.8

#### 4.2.8 TOPO-TA™ Cloning

Usage of the TOPO™-TA Cloning™ Kit (Thermo Scientific) allows simple analysis of gDNA from respective KO clones. TOPO cloning is based on ligation of an amplified PCR product of the gDNA sequence targeted by the CRISPR guide RNA into a linearized pCR4-TOPO TA vector. This vector has 3'T overhangs and is coupled to DNA topoisomerase I, which has properties of a restriction enzyme and a ligase, thus can quickly and efficiently incorporate PCR fragments with

3'A overhangs. In brief, 4 µl PCR product obtained using the "DreamTaq Hot Start DNA Polymerase" kit (Thermo Scientific) as described in 4.2.1, were incubated with 1 µl of vector and 1 µl provided salt solution, incubated 5 min at RT and afterwards cooled on ice. After transformation of 2 µl reaction into OneShot™ competent *E. coli* cells using the provided S.O.C medium, clones are selected on ampicillin LB-agar plates. Picking a statistical relevant number of approximately 20 clones, their plasmid DNA can be sequenced using common M13 forward and reverse primers. A single colony contains just one allele variant of the heterozygous cell line. This allows analysis of potentially occurring INDELS in the genome caused by CRISPR/Cas9 technology using Genious® software.

#### **4.2.9 Site-directed Mutagenesis**

For site-directed mutagenesis, QuikChange Site-Directed Mutagenesis Kit (Agilent) was used as recommended by the manufacturer. In brief, 100 ng purified plasmid DNA was used in a PCR reaction mix containing 10 µM of each forward and reverse primers carrying the mutated sequence, 1 µl dNTPs, 1.5 µl QuikSolution and 2.5 U/µl PfuTurbo polymerase in 50 µl 1x reaction buffer. The PCR program was adjusted as following: 94 °C for 3 min followed by 7 cycles of 94 °C, 1 min denaturing, 50 °C, 1 min annealing and 68 °C, 5 min elongation followed by 13 cycles with the same conditions but with 60 °C annealing temperature and a final elongation step at 68 °C for 20 min. The obtained PCR products were digested with 1 µl DpnI at 37 °C for 60 min to remove wildtype DNA before it was transfected to competent *E. coli* XL1 blue cells and clones sent for sequencing for analysis as described before in 4.2.5 and 4.2.6).

#### **4.2.10 Preparation of Genomic DNA from HEK293 Cells**

Genomic DNA from cultured cells was isolated using QuickExtract™ DNA Extraction Solution (Lucigen) according to the manufacturer's instructions. A small cell pellet was resuspended in according volume of QuickExtract™ solution (usually 50 – 150 µl), vortexed for 15 sec and incubated at 65 °C for 6 min before vortexing again for 15 sec and incubation at 98 °C for 2 min. DNA concentration was measured by using NanoDrop™ UV/VIS spectrophotometer (Thermo Scientific) and DNA was stored at -20 °C.

#### **4.2.11 Isolation of RNA from Cultured Cells**

Total RNA from cultured cells was isolated using TRIzol™ (Invitrogen) as recommended by the manufacturer. Briefly, cells pellets harvested from a 6-well cell culture plate or 25 cm<sup>2</sup> cell culture flask were carefully resuspended in 500 µl TRIzol™ Reagent, incubated for 5 min at RT before 100 µl chloroform were added. To separate the RNA from DNA and proteins, samples were shaken for 15 sec, incubated for 3 min at RT and centrifuged for 10 min at 12 000 xg at 4 °C. Afterwards, three phases have been built and the upper aqueous phase containing the RNA was transferred into a new reaction tube. RNA precipitation was achieved by adding 250 µl isopropanol, carefully inverting the tubes and incubation for 10 min at RT. The samples were centrifuged for 10 min at 12 000 xg at 4 °C and the RNA pellet was washed twice with 75 % ethanol, dried by several short centrifugation rounds and eluted in 20 – 50 µl dd H<sub>2</sub>O containing 0.5 µl RiboLock RNase Inhibitor (Thermo Scientific) at 65 °C for 10 min. Concentration was

determined using NanoDrop™ UV/VIS spectrophotometer (Thermo Scientific). Purified RNA was stored at -80 °C.

#### 4.2.12 Northern Blotting

To analyze RNA fragments, 2 µg isolated RNA were separated on a 1.2 % formaldehyde agarose gel. Samples were denatured by adding 5.5 % (v/v) formaldehyde and 35 % (v/v) formamide in 1x MOPS buffer at 55 °C for 15 min. After cooling on ice, 3 ml RNA loading dye was added and samples were loaded onto the polymerized gel, which was run for approximately 6 – 7 h at 80 – 100 V and 80 mA in 1x MOPS buffer. RNA was transferred overnight onto a nylon membrane (Amersham Hybond™-N, GE Healthcare) using 10x SSC buffer in a blotting sandwich consisting of two sheets of soaked whatman paper, 2x bd H<sub>2</sub>O rinsed gel, the bd H<sub>2</sub>O activated membrane, two further sheets of dry whatman paper and a stack of approximately 5 cm of paper towels with weights on top. Afterwards, RNA was permanently UV-crosslinked to the membrane in an UV crosslinker (UV Stratagene 1800, Stratagene). Membranes were stained for 5 min with methylene blue and destained with H<sub>2</sub>O in to show accurate loading of the samples. Visualization of RNA was performed using [<sup>32</sup>P]-radiolabeled probes targeting particular mitochondrial RNA sequences. Probes were generated by coupling [<sup>32</sup>P]-γ-ATP to the respective oligonucleotide (listed in table 7) by incubation with 1 µl T4 Polynucleotide kinase (PNK) in 1x PNK buffer at 37 °C for 40 min before addition to 40 ml SES1 buffer. Hybridization with respective RNA sequences on SES1-prehybridized membranes was performed overnight at 37 °C on a rotating wheel. Afterwards membranes were washed for 30 min in 6x SSC buffer and 2x SSC buffer containing 0.1 % SDS each before the membrane were exposed on a storage phosphor screen (*GE healthcare*) and then visualized using a Typhoon FLA9500 Phosphoimaging system (*GE healthcare*). For further decorations, membranes were eventually stripped by addition of boiling 0.1x SSC buffer containing 0.1 % SDS and incubation at 70 °C for 60 min.

- 10x MOPS buffer: 0.4 M MOPS, 0.1 M NaOAc, 10 mM EDTA, pH 7.2
- 20x SSPE buffer: 3 M NaCl, 0.2 M NaH<sub>2</sub>PO<sub>4</sub>, 20 mM EDTA, pH 7.4
- SES1 buffer: 250 mM NaP<sub>i</sub>, pH 7.4, 1 mM EDTA, 7 % (w/v) SDS
- 20x SSC buffer: 3 M NaCl, 300 mM NaCitrate pH 7.0

#### 4.2.13 NanoString Analysis

NanoString technology was used to directly detect mitochondrial RNA and analysis was carried out by Dr. Elena Lavdovskaia, a post-doctoral researcher in our group and former GGNB PhD student of the 'Molecular Biology of the Cells' program, and Dr. Luis Daniel Cruz-Zaragoza, a post-doctoral researcher in the research group of Prof. Dr. Peter Rehling, who supervised the experiments.

The experiment was performed as described before (Cruz-Zaragoza et al., 2021; Richter-Dennerlein et al., 2016). For preparation of the sample, 100 µg mitochondria of respective cell lines were isolated, solubilized in digitonin-containing lysis buffer and RNA was isolated using TRIzol® (Ambion, Life Technologies) and RNA Clean and Concentrator Kit (Zymo Research) according to the manufacturer's instructions. To directly quantify mitochondrial RNAs, without

further steps of cDNA synthesis and amplification, the isolated RNA pool was hybridized with TagSet master mix (nCounter Elements™ XT Reagents, nanoString) and probes targeting individual mitochondrial transcripts or as a control 18S rRNA or 5S rRNA (Supplementary Table S2). Like this, individual, specific target-probe complexes are formed by binding of respective complementary capture and fluorescently-labeled reporter probes to tag the RNA of interest with a 'molecular barcode'. This allows analysis via an nCounter MAX system (nanoString) following the instructions of nanoString Technologies. In brief, the hybridized complexes get immobilized and scanned by an automated fluorescence microscope in order to directly count the individual RNA-labels and the obtained data is subsequently analyzed with nSolver software (nanoString). To calculate the abundance of the mitochondrial transcripts, raw data were normalized to the abundance of the cytosolic transcripts. The protocol was carried out as suggested by the manufacturer.

- nanoString Lysis buffer: 50 mM TRIS/HCl pH 7.4, 150 mM NaCl, 10 % (v/v) Glycerol, 10 mM MgCl<sub>2</sub>, 1 % (w/v) Digitonin, 1 mM PMSF, 1x PI-Mix (Roche) and 0.08 U/μl RiboLock RNase inhibitor (Thermo Scientific)

## 4.3 Cell Culture Methods

### 4.3.1 Cell Culture Conditions

HEK293 (Human Embryonic Kidney 293-Flp-In T-Rex, Thermo Fisher Scientific) cell lines were cultured in DMEM (Dulbecco's modified Eagle's Media, homemade or Capricorn) supplemented with 10 % [v/v] FCS (Fetal Calf Serum, Capricorn Scientific), 2 mM L-glutamine, 1 mM sodium pyruvate and 50 μg/ml uridine at 37 °C under 5 % CO<sub>2</sub> humidified atmosphere. To inhibit translation, cells were incubated with 50 μg/ml Chloramphenicol (CAM) for 24 h before further analysis. Cells were passaged by harvesting confluent flasks with PBS/1 mM EDTA, pelleted at 2000 xg for 5 min at RT. The pellet was resuspended in DMEM and respective amounts were seeded into 75 cm<sup>2</sup> cell culture flasks or 140 cm<sup>2</sup> cell culture dishes for expansion. For long-term storage, cells were resuspended in freezing media and stored in liquid nitrogen. The absence of mycoplasma was regularly monitored by GATC Biotech.

- DMEM (Dulbecco's Modified Eagle Media): 10 % (v/v) FCS, 1 mM L-Glutamine, 1 mM Sodium Pyruvate, 50 μg/ml Uridine, sterile filtered
- Freezing media: 18 % (v/v) FCS, 9 % (v/v) DMSO in DMEM, sterile filtered
- PBS: 0.14 M NaCl, 2.7 mM KCl, 0.01 M Na<sub>2</sub>HPO<sub>4</sub>, 1.8 mM KH<sub>2</sub>PO<sub>4</sub>, pH 7.4

### 4.3.2 CRISPR/Cas9-mediated Knockout Cell Lines

Genome editing to obtain desired knockout cell lines (see table 9) was carried out using Alt-R CRISPR/Cas9 technology (Integrated DNA Technology, IDT) according to the manufacturer's instructions. Briefly, 40 000 cells per 96-well were co-transfected with a ribonucleoprotein consisting of a duplex formed by crRNA-tracrRNA and the Alt-R® *Streptococcus pyogenes* HiFi Cas9 nuclease using RNAiMax (Invitrogen) transfection reaction and OptiMEM (Gibco) media. While the crRNA serves as a guide and is designed to target exons within the genes of interest downstream to a PAM (protospacer-adjacent motif) site, the tracrRNA is coupled to the

fluorophore Atto-550 required for subsequent fluorescent-activated cell sorting (FACS). The guide RNA targets Cas9 to the region of interest where it can induce a double-strand break in the target DNA. This disruption is repaired by the endogenous cell repair system either through non-homologous end joining (NHEJ), often leading to insertions or deletions (INDEL) at the breakpoint or homology-directed repair (HDR). After 1 day of incubation, Atto-550 positive cells were sorted and emerging clones were screened by immunoblotting, further verified by TOPO cloning and subsequent sequencing (see 4.2.8).

#### **4.3.3 Generation of Stable Inducible Expression Cell Lines**

Generation of cell lines expressing a stably inducible, C-terminal FLAG-tagged copy of the protein of interest (see table 9) was performed as following: a 50 % confluent 6-well with the respective background cell line, seeded one day prior, was transfected with 2.25 µg pOG44 and 0.25 µg of pcDNA5/FRT/TO plasmids harboring the respective FLAG construct by using Lipofectamine<sup>TM</sup>3000 (Invitrogen) transfection reagent in OptiMEM media (Gibco) according to the manufacturer's instructions. Selection of positive clones was started two days after transfection using 100 mg/ml Hygromycin B and 5 µg/ml Blasticidin S. After approximately four weeks of selection, single clones were isolated, further cultivated and their ability to express the respective FLAG construct upon tetracycline induction was analyzed via western blot. To adjust the expression level of FLAG-tagged proteins to their endogenous counterpart, the required amount of tetracycline was titrated. Therefore, concentrations from 0, 0.1, 1, 10, 100 and 250 ng/ml were tested in DMEM media at respective cells seeded in a 6-well cell culture dish under standard cell culture conditions for 24 h, cells were harvested and expression was analyzed via western blot (see appendix Figure IV).

#### **4.3.4 Transient siRNA-mediated Knockdowns**

To transiently deplete a protein, siRNA targeting the transcript of interest (see table 7) were transfected into respective cell lines. Knockdown was achieved by transfecting a 50 % confluent 6-well with a transfection mix of 33 nM siRNA oligonucleotide (Eurogentec), 4 µl Lipofectamine RNAiMax (Invitrogen) in OptiMEM media (Gibco). After 72 h of incubation in cell culture, cells were harvested and/or further investigated.

#### **4.3.5 Preparation of Whole Cell Extracts from HEK293 Cells**

For preparation whole cell extracts from cultured cells, cells were harvested, the cell pellet was resuspended in an appropriate amount of nonionic cell lysis buffer and vortexed for 30 sec. Cell lysates were pelleted for 2 min at 600 g and the supernatant was transferred into a new reaction tube.

- Cell lysis buffer: 50 mM TRIS/HCl pH 7.4, 130 mM NaCl, 2 mM MgCl<sub>2</sub>, 1 % NP-40, 1 mM PMSF, 1x Protease Inhibitor (PI) Mix (Roche)

#### **4.3.6 Isolation of Mitochondria and Mitoplasts**

The isolation of mitochondria from cultured cells was carried out by differential centrifugation as described by. For the preparation of mitochondria, adherently growing cells with a

confluency of 80 – 100 % were harvested with PBS/EDTA and pelleted for 5 min at 2000 g. The cell pellet was resuspended in homogenization buffer and incubated for 10 min on ice. Cells were mechanically disrupted by using a motor-driven Homogenplus homogenizer size S (Schuett-BioTech) by 20x pottering at 800 rpm and the crude cell homogenate was isolated by subsequent differential centrifugation at 400 g, 10 min, 4 °C to remove debris. The supernatant was transferred into a new reaction tube and the homogenization step was repeated twice to three times (until cell pellet appeared white-ish). Next the mitochondria were pelleted at 11 000 g for 10 min at 4 °C. Afterwards, the cell pellet was washed once with homogenization buffer without PMSF and BSA, pelleted again and resuspended in an according amount of homogenization buffer without PMSF and BSA and centrifuged for 1 min at 400 xg, 4 °C. The supernatant containing mitochondria was transferred into a new reaction tube, protein concentration was determined as described in 4.4.1 and mitochondria were immediately used for further analysis or stored at -80 °C.

For large-scale isolations in order to purify mitoribosomes, centrifugations steps were modified to the sample volume: slow spin occurred at 1 000 xg for 10 min at 4 °C and fast pelleting of mitochondria was performed at 20 000 xg for 30 min, 4 °C.

For preparation of mitoplasts, first mitochondria are isolated as described in 4.3.6, pelleted at 11 000 g for 10 min at 4 °C and resuspended in respective amount of homogenization buffer without PMSF and BSA to adjust a specific mitochondria concentration. Usually, the working concentration was 4 mg/ml. Next 0.1 % digitonin was added to the mitochondria solution and incubated for 30 min at 4 °C to permeabilize the OMM. After this, mitochondria were treated with 0.5 µg proteinase K per 100 µg mitochondria for 20 min at 4 °C to digest proteins from the OMM and IMS, followed by incubation of 2 mM PMSF to block proteinase K. Mitoplasts were first pelleted, then washed 2 times with homogenization buffer containing 2 mM PMSF and 0.2 % BSA and the washed again 2 times with homogenization buffer containing only 2 mM PMSF and no BSA. After each washing step, mitoplasts were transferred into a new reaction tube and finally resuspended in homogenization buffer without PMSF and BSA. The protein concentration was determined as described in 4.4.1.

- Homogenization buffer: 300 mM Trehalose, 10 mM KCl, 10 mM HEPES-KOH pH 7.4, 1 mM PMSF, 0.2 % BSA

#### **4.3.8 *In vivo* [<sup>35</sup>S] Methionine Labeling**

*De novo* synthesis of mitochondrial encoded proteins was analyzed by incorporating [<sup>35</sup>S] Methionine. Respective cells were seeded in 25 cm<sup>2</sup> cell culture flasks, cultured under standard cell culture conditions until > 80 % confluent and then starved with growth media without methionine, cysteine and FCS for 10 min. To inhibit cytosolic translation, cells were incubated for 10 min with growth media supplemented with 10 % FCS but without methionine and cysteine containing either 100 µg/ml emetine or 100 µg/ml anisomycin for reversible inhibition required for pulse chase labeling. For *in vivo* labelling of newly synthesized mitochondrial proteins, 200 µCi of [<sup>35</sup>S] methionine mix was incubated for 1 h at 37 °C. After labelling, cells were harvested with PBS/EDTA and the pellet was washed 3 times with PBS. Chase labeling was

performed by removing radioactive media and exchanging it to normal growth media. Whole cell lysates were prepared as described in 4.3.5, separated in Tris-Tricine polyacrylamide gels and analyzed via western blot. Radioactive labeled newly synthesized mitochondrial translation products bound onto NC membrane were exposed for 1 day or up to 5 days on a storage phosphor screen (*GE healthcare*) and then visualized using a Typhoon FLA9500 Phosphoimaging system (*GE healthcare*).

#### **4.3.9 Measurements of Mitochondrial Radicals**

To measure reactive oxygen species (ROS) like the  $O_2^-$  superoxide produced by mitochondria, the fluorescently-labeled ROS indicator MitoSOX™ Red (Invitrogen) was used according to the manufacturer's instructions and subsequently analyzed via flow cytometry. MitoSOX™ Red is a dye which gets taken up by actively respiring mitochondria and oxidized at the presence of superoxides. Briefly,  $10^6$  cells were stained with 5  $\mu$ M MitoSOX™ Red for 10 min under standard cell culture conditions and washed out afterwards with PBS. Samples were immediately prepared for flow cytometry on a BD FACS Canto II (Becton Dickinson). The dye was excited at 510 nm, emission was detected at 580 nm and 10 000 gated events were recorded. FACS-Diva software was used for analysis and gating excluded

#### **4.3.10 Respirometry**

For measurement of mitochondrial oxygen consumption rates (OCR), a XF96 Extracellular Flux Analyzer (Agilent) was used by running a Mito Stress Test protocol. One day prior to the assay, a XF FluxPaks (Agilent) cartridge was incubated for 24 h in a non-CO<sub>2</sub> incubator at 37 °C in XF Calibrant solution (Agilent) to hydrate the sensors of the cartridge. Approximately 1 h before the assay is started,  $4 \times 10^4$  cells of each cell line were seeded into the Seahorse XF96 Cell Culture Microplate V3-PS, TC-Treated (Agilent) directly into XF assay media (Agilent, supplemented with 1 mM pyruvate, 2 mM glutamine and 10 mM glucose), spun down for 5 min at RT at 400 xg with slow deceleration and incubated for 1 h in a non-CO<sub>2</sub> incubator. In the meantime, the port plate was prepared with modulating drugs used to test key parameters of mitochondrial respiration and put into the Analyzer for calibration. After the incubation time, basal respiration was measured first before the automated addition of the following drugs: 3  $\mu$ M oligomycin were used to inhibit complex V ( $F_1F_0$ -ATP synthase). This drug reveals the ATP-linked respiration since inhibiting complex V decreases the electron flow through the electron transport chain (ETC) and in this way the OCR. The remaining respiration refers to a proton leak which corresponds to respiration not coupled to the ATP production. Addition of 1.5  $\mu$ M CCCP uncouples that collapses the membrane potential and enables unhindered electron flow through the ETC which pushes the mitochondrial respiration to its maximum. By subtracting the basal respiration, the spare capacity with which cells can react to higher energy demands can be calculated. The last injection is a mixture of 1  $\mu$ M rotenone and 1  $\mu$ M antimycin, which are inhibitors of complex I and complex III, respectively. In this way, the mitochondrial respiration gets completely diminished and thus enables the calculation of non-mitochondrial respiration by otherwise processes. Data was analyzed using Seahorse Wave (Agilent) software by applying Seahorse XF Stress Test Report Generator.



## 4.4 Proteinbiochemical methods

### 4.4.1 Determination of Protein Concentration

To determine protein amounts in samples, the Bradford assay was utilized. For generating a standard curve amounts of 0, 2, 5, 10, 15 and 20  $\mu\text{g}/\mu\text{l}$  BSA were used. To determine unknown protein concentrations, 2  $\mu\text{l}$  of the solution were adjusted to a volume of 800  $\mu\text{l}$  with ddH<sub>2</sub>O and 200  $\mu\text{l}$  ROTI®Quant Bradford solution (1:5, Roth) was added. The absorption at 595 nm was measured in a microplate reader (Synergy H1, BioTek) and protein concentrations were calculated.

### 4.4.2 Polyacrylamide-Gel Electrophoresis

Separation of proteins from cell lysates or mitochondria samples was obtained via SDS polyacrylamide gel electrophoresis (PAGE) using TRIS-Tricine (T/T) gradient polyacrylamide gels containing 0.1 % SDS as they confer the best separation for mitoribosomal proteins. In Brief, proteins were focused in a 4 % stacking gel separated within a 10 – 18 % gradient separating gel. Gels were polymerized by the addition of 0.05 % APS and 0.04 % TEMED. Before loading, samples were mixed with SDS loading buffer and incubated 15 min at 37 °C. Electrophoresis occurred at 80 V 25 mA for 16 h in a homemade gel running system with according cathode and anode running buffers. As a protein size standard, Precision Plus Protein™ All Blue Prestained Standard (BioRad) was used.

- T/T Anode Buffer: 0.2 M TRIS, pH 8.9
- T/T Cathode Buffer: 0.1 M TRIS, 0.1 M Tricine, 0.1 % (w/v) SDS, pH 8.25
- T/T Gel Buffer: 1 M TRIS, 0.1 % (w/v) SDS, pH 8.45

### 4.4.3 Western Blotting

To transfer proteins from the polyacrylamide gels onto a membrane, semi-dry blotting technique was used. Facing the positively charged anode, an in transfer buffer equilibrated Amersham™ Protran™ 0.2  $\mu\text{M}$  nitrocellulose (NC) membrane (GE Healthcare) or in methanol activated Polyvinylidene Fluoride (PVDF) membrane (Merck Millipore) was placed on three, in transfer buffer soaked Whatman blotting papers. On top of the membrane the polyacrylamide gel, soaked in transfer buffer, was put together with three additional layers of soaked Whatman blotting paper. Transfer of the negatively charged protein samples occurred at 250 mA, 25 V for 2 h.

After the proteins were transferred onto nitrocellulose membranes, the membrane was stained with Ponceau red solution to visualize proteins, as ponceau S reversibly binds to the positively charged amino group of proteins. The membrane was cut in parts of the required protein size. To destain the membranes, Ponceau S stain was removed by continuous washing with water. To directly detect proteins on polyacrylamide gels or on PVDF membranes, they were stained with Coomassie staining solution. Destaining solution was used until distinct protein bands appeared.

- Transfer Buffer: 20 mM TRIS, 0.02 % (w/v) SDS, 150 mM Glycine, 20 % (v/v) Ethanol
- Ponceau Red solution: 0.2 % Ponceau S, 3.0 % TCA

- Coomassie Staining Solution: 0.25 % (w/v) Coomassie Brilliant Blue R-250, 10 % (v/v) Acetic Acid, 40 % (v/v) Ethanol
- Destainer: 40 % (v/v) Ethanol, 10 % (v/v) Acetic Acid

#### 4.4.4 Immunodetection

To detect specific proteins, respective membrane pieces were incubated in 5 % milk in TBS-T for 1 h to block unspecific binding sites before they were further incubated in respective primary antibodies over night at 4 °C in the cold room. After this, the membranes were washed 3x for 10 min with TBS-T, before they were incubated with HRP (horse radish peroxidase) coupled secondary antibody and washed again 3x with TBS-T. Visualization of proteins was achieved by using ECL (enhanced chemiluminescence) detection kit by *GE Healthcare* and X-ray films.

- TBS-T: 20 mM TRIS/HCl, pH 7.5, 125 mM NaCl, 0.1 % (v/v) Tween20

#### 4.4.5 Blue Native PAGE

To investigate large, intact mitochondrial protein complexes in non-denaturing conditions BN-PAGE was used. Mitochondria were pelleted at 16 000 xg for 10 min at 4 °C and solubilized for 15 min on ice to a final protein concentration at 1 mg/ml in S-buffer by vigorous mixing. Digitonin was used to preserve supercomplex structures, whereas with dodecyl maltoside (DDM) individual complexes can be detected. The sample was clarified from unsolubilized material by centrifugation at 21 000 xg for 15 min and supernatant was mixed and incubated for 5 min on ice with BN Loading Dye. BN gels were prepared as 4 – 14 % polyacrylamide gradient gels or as 2.5 – 10 % low pore gradient gel to particularly visualize the high molecular weight complex I, both with a 2.5 % (dis)continuous stacking gel. Samples were loaded together with homemade BN marker at 4 °C in a SE600 Ruby™ System (*GE Healthcare*) and run at 600 V, 15 mA for approximately 60 min in deep blue cathode buffer, which was then exchanged for clear cathode buffer and separation was completed overnight at 100 V, 30 mA. For separation in one dimension (1D), 30 µg mitochondria were loaded, western blotting was performed on PVDF membranes according to 4.4.3. For analysis of individual proteins that run as part of complexes, 150 µg mitochondria were solubilized, separated in the first, nondenaturing dimension and a respective gel stripe was cut out, assembled on top of a standard TRIS/Tricine SDS-PAGE (as described in 4.4.2) to dissect the sample in a second, denaturing dimension.

- S-buffer: 20 mM TRIS/HCl pH 7.4, 0.1 mM EDTA, 50 mM NaCl, 10 % (v/v) Glycerol, 1 mM PMSF and 1 % Digitonin or 0.2 % DDM
- BN Loading Dye: 5 % Coomassie Brilliant Blue G250 (w/v), 500 mM ε-aminocaproic acid, 100 mM BIS-TRIS/HCl pH 7.0
- 3x BN Gel Buffer: 200 mM ε-aminocaproic acid, 150 mM BIS-TRIS, pH 7.0
- BN Cathode Buffer: 150 mM BIS-TRIS, 1 M Tricine (+ 0.2 % Coomassie blue G250)
- BN Anode: Buffer: 500 mM BIS-TRIS, pH 7.0
- BN Marker: 50-150 mg/ml Apo-ferritin, 25 mg/ml BSA, 50 mg/ml Catalase, 2x S-buffer, 1 % Coomassie Brilliant Blue G250 (w/v)

#### 4.4.6 In-Gel Activity Assay

To determine in-gel activities of complex I and complex IV, mitochondria were first solubilized with 1 % digitonin and natively separated via BN PAGE (see 4.4.5). For complex I activity, the equilibrated gel was incubated in NADH-containing complex I buffer until bands appeared. Complex IV activity was visualized in complex IV buffer containing cytochrome *c*.

- Complex I Buffer: 1 mg/ml Nitrotetrazoliumbluechlorid (NBT), 1 mg/ml NADH, 5 mM TRIS/HCl pH 7.4
- Complex IV Buffer: 0.5 mg/ml Diaminobenzidine (DAB), 10 mg/ml Catalase, 1 µg/ml Cytochrome *c* and 75 mg/ml Sucrose, 50 mM KPi pH 7.4

#### 4.4.7 Complex I Activity Measurement

Photometric measurement of complex I activity was carried out using Complex I Enzyme Activity Microplate Assay Kit (Colorimetric, abcam) as suggested by the manufacturer. Briefly, cells from 25 cm<sup>2</sup> cell culture flasks were harvested, washed twice and protein concentration was determined. The sample concentration was adjusted to 5.5 mg/ml and proteins were extracted upon addition of 1:10 detergent for 30 min on ice. Lysed cells were spun down for 20 min at 16 000 xg at 4 °C and accordingly 200 µg of cell lysate supernatant was loaded per well in a volume of 200 µl. The microplate wells coated with a specific antibody against complex I were loaded to immobilize the enzyme in the well by incubation for 3 h at RT. After incubation time, plate was washed three times with 1x wash buffer supplied with the kit and immediately before the assay is started, 200 µl assay solution was added as fast as possible and air bubbles were eliminated instantly. The assay solution contains 2 mM NADH, which gets oxidized to NAD<sup>+</sup> by complex I activity, and 1x dye (extinction coefficient 25.9 mM/well), which is simultaneously reduced by NAD<sup>+</sup>. Reduction of the dye leads to an increase in absorbance at OD = 450 nm which is colorimetrically detected by a Synergy H1 Microplate Reader (BioTek) at RT in a kinetic program for 30 min with an interval of 30 sec with shaking between the readings. For analysis, significant sample background measured in a buffer control was subtracted from the samples and complex I activity rate was calculated as mOD/min ( $\Delta\text{mOD}/\Delta\text{min}$ ).

#### 4.4.8 Sucrose Density Gradients

For the separation of mitoribosomal compounds, sucrose density gradients were used. In brief, mitoplasts of respective HEK293 cell lines were prepared as described in 4.3.7. Before loading on the gradient, 0.55 mg mitoplasts were lysed in 275 ml lysis buffer and incubated for 30 min on ice with occasional vortexing. Mitoplasts lysates were then centrifuged for 30 min at 16 000 g, the supernatant was transferred onto a new tube and diluted with dilution buffer to 300 µl. The samples were then loaded onto a 5 – 30 % sucrose gradient, which was mixed using BioComp™ Gradient Master. Separation of the sample was achieved by sucrose gradient centrifugation at 79 000 g for 15 hours at 4 °C (Beckman Coulter Optima L-90K centrifuge, SW41Ti rotor). After centrifugation, the gradient was fractionated into 16 fractions by a BioComp™ piston gradient fractionator and fractions were ethanol precipitated using 2.5 vol. of 100 % ethanol and 1/3 vol. of 3 M NaAc pH 6.5. After 24 hours at -20 °C, samples were once

washed with ice-cold 80 % ethanol, centrifuged at top speed and the pellet was analyzed via western blot.

- MP Lysis Buffer: 3 % (w/v) Sucrose, 100 mM NH<sub>4</sub>Cl, 15 mM MgCl<sub>2</sub>, 20 mM TRIS/HCl pH 7.5, 1 % Digitonin, 1x PI Mix, 0.08 U/μl RiboLock RNase Inhibitor
- MP Dilution Buffer: 3 % (w/v) Sucrose, 100 mM NH<sub>4</sub>Cl, 15 mM MgCl<sub>2</sub>, 20 mM TRIS/HCl pH 7.5, 1x PI Mix, 0.08 U/μl RiboLock RNase Inhibitor
- Sucrose Gradient Solutions: 5 – 30 % (w/v) Sucrose, 100 mM NH<sub>4</sub>Cl, 15 mM MgCl<sub>2</sub>, 20 mM TRIS/HCl pH 7.5, 1x PI Mix

#### **4.5. Quantification and Statistical Analysis**

For Quantification of protein from western blots or RNA signals from northern blots, at least three biological triplicates were considered for quantification using FIJI (Schindelin et al., 2012) or ImageQuant TL (GE Healthcare). Calculations are presented as mean values and error bars are shown as standard error of the mean (SEM). Data was statistically analyzed for significant differences by one-sample *t*-test and statistical significance was defined as \* for  $p \leq 0.05$ , \*\* for  $p \leq 0.01$  and \*\*\* for  $p \leq 0.001$ . P values  $> 0.05$  are defined as not significant (n.s.).

## 5 References

- Abrahams, J. P., Leslie, A. G., Lutter, R., & Walker, J. E. (1994). Structure at 2.8 Å resolution of F1-ATPase from bovine heart mitochondria. *Nature*, *370*(6491), 621-628. <https://doi.org/10.1038/370621a0>
- Acín-Pérez, R., Bayona-Bafaluy, M. P., Fernández-Silva, P., Moreno-Loshuertos, R., Pérez-Martos, A., Bruno, C., . . . Enríquez, J. A. (2004). Respiratory complex III is required to maintain complex I in mammalian mitochondria. *Mol Cell*, *13*(6), 805-815. [https://doi.org/10.1016/s1097-2765\(04\)00124-8](https://doi.org/10.1016/s1097-2765(04)00124-8)
- Acín-Pérez, R., Fernández-Silva, P., Peleato, M. L., Pérez-Martos, A., & Enriquez, J. A. (2008). Respiratory active mitochondrial supercomplexes. *Mol Cell*, *32*(4), 529-539. <https://doi.org/10.1016/j.molcel.2008.10.021>
- Adio, S., Senyushkina, T., Peske, F., Fischer, N., Wintermeyer, W., & Rodnina, M. V. (2015). Fluctuations between multiple EF-G-induced chimeric tRNA states during translocation on the ribosome. *Nat Commun*, *6*, 7442. <https://doi.org/10.1038/ncomms8442>
- Adio, S., Sharma, H., Senyushkina, T., Karki, P., Maracci, C., Wohlgemuth, I., . . . Rodnina, M. V. (2018). Dynamics of ribosomes and release factors during translation termination in. *Elife*, *7*. <https://doi.org/10.7554/eLife.34252>
- Ahola, S., Langer, T., & MacVicar, T. (2019). Mitochondrial Proteolysis and Metabolic Control. *Cold Spring Harb Perspect Biol*, *11*(7). <https://doi.org/10.1101/cshperspect.a033936>
- Aibara, S., Singh, V., Modelska, A., & Amunts, A. (2020). Structural basis of mitochondrial translation. *Elife*, *9*. <https://doi.org/10.7554/eLife.58362>
- Aich, A., Wang, C., Chowdhury, A., Ronsör, C., Pacheu-Grau, D., Richter-Dennerlein, R., . . . Rehling, P. (2018). COX16 promotes COX2 metallation and assembly during respiratory complex IV biogenesis. *Elife*, *7*. <https://doi.org/10.7554/eLife.32572>
- Akabane, S., Ueda, T., Nierhaus, K. H., & Takeuchi, N. (2014). Ribosome rescue and translation termination at non-standard stop codons by ICT1 in mammalian mitochondria. *PLoS Genet*, *10*(9), e1004616. <https://doi.org/10.1371/journal.pgen.1004616>
- Althoff, T., Mills, D. J., Popot, J. L., & Kühlbrandt, W. (2011). Arrangement of electron transport chain components in bovine mitochondrial supercomplex I1III2IV1. *EMBO J*, *30*(22), 4652-4664. <https://doi.org/10.1038/emboj.2011.324>
- Amunts, A., Brown, A., Toots, J., Scheres, S. H. W., & Ramakrishnan, V. (2015). Ribosome. The structure of the human mitochondrial ribosome. *Science*, *348*(6230), 95-98. <https://doi.org/10.1126/science.aaa1193>
- Anderson, S., Bankier, A. T., Barrell, B. G., de Bruijn, M. H., Coulson, A. R., Drouin, J., . . . Young, I. G. (1981). Sequence and organization of the human mitochondrial genome. *Nature*, *290*(5806), 457-465. <https://doi.org/10.1038/290457a0>
- Antonicka, H., Ostergaard, E., Sasarman, F., Weraarpachai, W., Wibrand, F., Pedersen, A. M., . . . Shoubridge, E. A. (2010). Mutations in C12orf65 in patients with encephalomyopathy and a mitochondrial translation defect. *Am J Hum Genet*, *87*(1), 115-122. <https://doi.org/10.1016/j.ajhg.2010.06.004>
- Antonicka, H., & Shoubridge, E. A. (2015). Mitochondrial RNA Granules Are Centers for Posttranscriptional RNA Processing and Ribosome Biogenesis. *Cell Rep*, *10*(6), 920-932. <https://doi.org/10.1016/j.celrep.2015.01.030>
- Atkins, J. F., Loughran, G., Bhatt, P. R., Firth, A. E., & Baranov, P. V. (2016). Ribosomal frameshifting and transcriptional slippage: From genetic steganography and cryptography to adventitious use. *Nucleic Acids Res*, *44*(15), 7007-7078. <https://doi.org/10.1093/nar/gkw530>

- Ayyub, S. A., Gao, F., Lightowlers, R. N., & Chrzanowska-Lightowlers, Z. M. (2020). Rescuing stalled mammalian mitoribosomes - what can we learn from bacteria? *J Cell Sci*, *133*(1). <https://doi.org/10.1242/jcs.231811>
- Balsa, E., Marco, R., Perales-Clemente, E., Szklarczyk, R., Calvo, E., Landázuri, M. O., & Enríquez, J. A. (2012). NDUFA4 is a subunit of complex IV of the mammalian electron transport chain. *Cell Metab*, *16*(3), 378-386. <https://doi.org/10.1016/j.cmet.2012.07.015>
- Barrell, B. G., Bankier, A. T., & Drouin, J. (1979). A different genetic code in human mitochondria. *Nature*, *282*(5735), 189-194. <https://doi.org/10.1038/282189a0>
- Bedard, K., & Krause, K. H. (2007). The NOX family of ROS-generating NADPH oxidases: physiology and pathophysiology. *Physiol Rev*, *87*(1), 245-313. <https://doi.org/10.1152/physrev.00044.2005>
- Bhargava, K., & Spremulli, L. L. (2005). Role of the N- and C-terminal extensions on the activity of mammalian mitochondrial translational initiation factor 3. *Nucleic Acids Res*, *33*(22), 7011-7018. <https://doi.org/10.1093/nar/gki1007>
- Bhatta, A., Dienemann, C., Cramer, P., & Hillen, H. S. (2021). Structural basis of RNA processing by human mitochondrial RNase P. *Nat Struct Mol Biol*, *28*(9), 713-723. <https://doi.org/10.1038/s41594-021-00637-y>
- Blaza, J. N., Serreli, R., Jones, A. J., Mohammed, K., & Hirst, J. (2014). Kinetic evidence against partitioning of the ubiquinone pool and the catalytic relevance of respiratory-chain supercomplexes. *Proc Natl Acad Sci U S A*, *111*(44), 15735-15740. <https://doi.org/10.1073/pnas.1413855111>
- Bogenhagen, D. F. (2012). Mitochondrial DNA nucleoid structure. *Biochim Biophys Acta*, *1819*(9-10), 914-920. <https://doi.org/10.1016/j.bbagr.2011.11.005>
- Bogenhagen, D. F., Ostermeyer-Fay, A. G., Haley, J. D., & Garcia-Diaz, M. (2018). Kinetics and Mechanism of Mammalian Mitochondrial Ribosome Assembly. *Cell Rep*, *22*(7), 1935-1944. <https://doi.org/10.1016/j.celrep.2018.01.066>
- Bohnsack, M. T., & Sloan, K. E. (2018). The mitochondrial epitranscriptome: the roles of RNA modifications in mitochondrial translation and human disease. *Cell Mol Life Sci*, *75*(2), 241-260. <https://doi.org/10.1007/s00018-017-2598-6>
- Bohovych, I., Fernandez, M. R., Rahn, J. J., Stackley, K. D., Bestman, J. E., Anandhan, A., . . . Khalimonchuk, O. (2015). Metalloprotease OMA1 Fine-tunes Mitochondrial Bioenergetic Function and Respiratory Supercomplex Stability. *Sci Rep*, *5*, 13989. <https://doi.org/10.1038/srep13989>
- Borowski, L. S., Dziembowski, A., Hejnowicz, M. S., Stepień, P. P., & Szczesny, R. J. (2013). Human mitochondrial RNA decay mediated by PNPase-hSuv3 complex takes place in distinct foci. *Nucleic Acids Res*, *41*(2), 1223-1240. <https://doi.org/10.1093/nar/gks1130>
- Brown, A., Amunts, A., Bai, X. C., Sugimoto, Y., Edwards, P. C., Murshudov, G., . . . Ramakrishnan, V. (2014). Structure of the large ribosomal subunit from human mitochondria. *Science*, *346*(6210), 718-722. <https://doi.org/10.1126/science.1258026>
- Brown, A., Rathore, S., Kimanius, D., Aibara, S., Bai, X. C., Rorbach, J., . . . Ramakrishnan, V. (2017). Structures of the human mitochondrial ribosome in native states of assembly. *Nat Struct Mol Biol*, *24*(10), 866-869. <https://doi.org/10.1038/nsmb.3464>
- Brzezniak, L. K., Bijata, M., Szczesny, R. J., & Stepień, P. P. (2011). Involvement of human ELAC2 gene product in 3' end processing of mitochondrial tRNAs. *RNA Biol*, *8*(4), 616-626. <https://doi.org/10.4161/rna.8.4.15393>

- Bulkley, D., Innis, C. A., Blaha, G., & Steitz, T. A. (2010). Revisiting the structures of several antibiotics bound to the bacterial ribosome. *Proc Natl Acad Sci U S A*, *107*(40), 17158-17163. <https://doi.org/10.1073/pnas.1008685107>
- Buskirk, A. R., & Green, R. (2017). Ribosome pausing, arrest and rescue in bacteria and eukaryotes. *Philos Trans R Soc Lond B Biol Sci*, *372*(1716). <https://doi.org/10.1098/rstb.2016.0183>
- Cai, Y. C., Bullard, J. M., Thompson, N. L., & Spremulli, L. L. (2000). Interaction of mitochondrial elongation factor Tu with aminoacyl-tRNA and elongation factor Ts. *J Biol Chem*, *275*(27), 20308-20314. <https://doi.org/10.1074/jbc.M001899200>
- Callegari, S., Cruz-Zaragoza, L. D., & Rehling, P. (2020). From TOM to the TIM23 complex - handing over of a precursor. *Biol Chem*, *401*(6-7), 709-721. <https://doi.org/10.1515/hsz-2020-0101>
- Capecchi, M. R. (1967). Polypeptide chain termination in vitro: isolation of a release factor. *Proc Natl Acad Sci U S A*, *58*(3), 1144-1151. <https://doi.org/10.1073/pnas.58.3.1144>
- Carbone, C. E., Demo, G., Madireddy, R., Svidritskiy, E., & Korostelev, A. A. (2020). ArfB can displace mRNA to rescue stalled ribosomes. *Nat Commun*, *11*(1), 5552. <https://doi.org/10.1038/s41467-020-19370-z>
- Caskey, C. T., Tompkins, R., Scolnick, E., Caryk, T., & Nirenberg, M. (1968). Sequential translation of trinucleotide codons for the initiation and termination of protein synthesis. *Science*, *162*(3849), 135-138. <https://doi.org/10.1126/science.162.3849.135>
- Chacinska, A., Lind, M., Frazier, A. E., Dudek, J., Meisinger, C., Geissler, A., . . . Rehling, P. (2005). Mitochondrial presequence translocase: switching between TOM tethering and motor recruitment involves Tim21 and Tim17. *Cell*, *120*(6), 817-829. <https://doi.org/10.1016/j.cell.2005.01.011>
- Chacinska, A., van der Laan, M., Mehnert, C. S., Guiard, B., Mick, D. U., Hutu, D. P., . . . Rehling, P. (2010). Distinct forms of mitochondrial TOM-TIM supercomplexes define signal-dependent states of preprotein sorting. *Mol Cell Biol*, *30*(1), 307-318. <https://doi.org/10.1128/MCB.00749-09>
- Chadani, Y., Ito, K., Kutsukake, K., & Abo, T. (2012). ArfA recruits release factor 2 to rescue stalled ribosomes by peptidyl-tRNA hydrolysis in Escherichia coli. *Mol Microbiol*, *86*(1), 37-50. <https://doi.org/10.1111/j.1365-2958.2012.08190.x>
- Chadani, Y., Matsumoto, E., Aso, H., Wada, T., Kutsukake, K., Sutou, S., & Abo, T. (2011a). trans-translation-mediated tight regulation of the expression of the alternative ribosome-rescue factor ArfA in Escherichia coli. *Genes Genet Syst*, *86*(3), 151-163. <https://doi.org/10.1266/ggs.86.151>
- Chadani, Y., Ono, K., Kutsukake, K., & Abo, T. (2011b). Escherichia coli YaeJ protein mediates a novel ribosome-rescue pathway distinct from SsrA- and ArfA-mediated pathways. *Mol Microbiol*, *80*(3), 772-785. <https://doi.org/10.1111/j.1365-2958.2011.07607.x>
- Chadani, Y., Ono, K., Ozawa, S., Takahashi, Y., Takai, K., Nanamiya, H., . . . Abo, T. (2010). Ribosome rescue by Escherichia coli ArfA (YhdL) in the absence of trans-translation system. *Mol Microbiol*, *78*(4), 796-808. <https://doi.org/10.1111/j.1365-2958.2010.07375.x>
- Chan, K. H., Petrychenko, V., Mueller, C., Maracci, C., Holtkamp, W., Wilson, D. N., . . . Rodnina, M. V. (2020). Mechanism of ribosome rescue by alternative ribosome-rescue factor B. *Nat Commun*, *11*(1), 4106. <https://doi.org/10.1038/s41467-020-17853-7>
- Chance, B., & Williams, G. R. (1955). A method for the localization of sites for oxidative phosphorylation. *Nature*, *176*(4475), 250-254. <https://doi.org/10.1038/176250a0>

- Chandrasekaran, V., Desai, N., Burton, N. O., Yang, H., Price, J., Miska, E. A., & Ramakrishnan, V. (2021). Visualizing formation of the active site in the mitochondrial ribosome. *Elife*, *10*. <https://doi.org/10.7554/eLife.68806>
- Chang, J. H., & Tong, L. (2012). Mitochondrial poly(A) polymerase and polyadenylation. *Biochim Biophys Acta*, *1819*(9-10), 992-997. <https://doi.org/10.1016/j.bbagr.2011.10.012>
- Chang, W., Yu, Z., Tian, M., & Lin, X. (2017). Immature colon carcinoma transcript-1 promotes cell growth of hepatocellular carcinoma via facilitating cell cycle progression and apoptosis resistance. *Oncol Rep*, *38*(6), 3489-3496. <https://doi.org/10.3892/or.2017.6046>
- Chen, Y. C., Taylor, E. B., Dephore, N., Heo, J. M., Tonhato, A., Papandreou, I., . . . Rutter, J. (2012). Identification of a protein mediating respiratory supercomplex stability. *Cell Metab*, *15*(3), 348-360. <https://doi.org/10.1016/j.cmet.2012.02.006>
- Christian, B. E., & Spremulli, L. L. (2009). Evidence for an active role of IF3mt in the initiation of translation in mammalian mitochondria. *Biochemistry*, *48*(15), 3269-3278. <https://doi.org/10.1021/bi8023493>
- Chujo, T., Ohira, T., Sakaguchi, Y., Goshima, N., Nomura, N., Nagao, A., & Suzuki, T. (2012). LRPPRC/SLIRP suppresses PNPase-mediated mRNA decay and promotes polyadenylation in human mitochondria. *Nucleic Acids Res*, *40*(16), 8033-8047. <https://doi.org/10.1093/nar/gks506>
- Cogliati, S., Cabrera-Alarcón, J. L., & Enriquez, J. A. (2021). Regulation and functional role of the electron transport chain supercomplexes. *Biochem Soc Trans*, *49*(6), 2655-2668. <https://doi.org/10.1042/BST20210460>
- Cogliati, S., Calvo, E., Loureiro, M., Guaras, A. M., Nieto-Arellano, R., Garcia-Poyatos, C., . . . Enriquez, J. A. (2016a). Mechanism of super-assembly of respiratory complexes III and IV. *Nature*, *539*(7630), 579-582. <https://doi.org/10.1038/nature20157>
- Cogliati, S., Enriquez, J. A., & Scorrano, L. (2016b). Mitochondrial Cristae: Where Beauty Meets Functionality. *Trends Biochem Sci*, *41*(3), 261-273. <https://doi.org/10.1016/j.tibs.2016.01.001>
- Cortassa, S., Sollott, S. J., & Aon, M. A. (2017). Mitochondrial respiration and ROS emission during  $\beta$ -oxidation in the heart: An experimental-computational study. *PLoS Comput Biol*, *13*(6), e1005588. <https://doi.org/10.1371/journal.pcbi.1005588>
- Crofts, A. R. (2004). The cytochrome bc<sub>1</sub> complex: function in the context of structure. *Annu Rev Physiol*, *66*, 689-733. <https://doi.org/10.1146/annurev.physiol.66.032102.150251>
- Crowe-McAuliffe, C., Takada, H., Murina, V., Polte, C., Kasvandik, S., Tenson, T., . . . Haurlyuk, V. (2021). Structural Basis for Bacterial Ribosome-Associated Quality Control by RqcH and RqcP. *Mol Cell*, *81*(1), 115-126.e117. <https://doi.org/10.1016/j.molcel.2020.11.002>
- Cruz-Zaragoza, L. D., Dennerlein, S., Linden, A., Yousefi, R., Lavdovskaia, E., Aich, A., . . . Rehling, P. (2021). An in vitro system to silence mitochondrial gene expression. *Cell*, *184*(23), 5824-5837.e5815. <https://doi.org/10.1016/j.cell.2021.09.033>
- D'Aurelio, M., Gajewski, C. D., Lenaz, G., & Manfredi, G. (2006). Respiratory chain supercomplexes set the threshold for respiration defects in human mtDNA mutant cybrids. *Hum Mol Genet*, *15*(13), 2157-2169. <https://doi.org/10.1093/hmg/ddl141>
- Dan Dunn, J., Alvarez, L. A., Zhang, X., & Soldati, T. (2015). Reactive oxygen species and mitochondria: A nexus of cellular homeostasis. *Redox Biol*, *6*, 472-485. <https://doi.org/10.1016/j.redox.2015.09.005>



- Dennerlein, S., Oeljeklaus, S., Jans, D., Hellwig, C., Bareth, B., Jakobs, S., . . . Rehling, P. (2015). MITRAC7 Acts as a COX1-Specific Chaperone and Reveals a Checkpoint during Cytochrome c Oxidase Assembly. *Cell Rep*, *12*(10), 1644-1655. <https://doi.org/10.1016/j.celrep.2015.08.009>
- Dennerlein, S., & Rehling, P. (2015). Human mitochondrial COX1 assembly into cytochrome c oxidase at a glance. *J Cell Sci*, *128*(5), 833-837. <https://doi.org/10.1242/jcs.161729>
- Dennerlein, S., Rozanska, A., Wydro, M., Chrzanowska-Lightowlers, Z. M., & Lightowlers, R. N. (2010). Human ERAL1 is a mitochondrial RNA chaperone involved in the assembly of the 28S small mitochondrial ribosomal subunit. *Biochem J*, *430*(3), 551-558. <https://doi.org/10.1042/BJ20100757>
- Desai, N., Yang, H., Chandrasekaran, V., Kazi, R., Minczuk, M., & Ramakrishnan, V. (2020). Elongational stalling activates mitoribosome-associated quality control. *Science*, *370*(6520), 1105-1110. <https://doi.org/10.1126/science.abc7782>
- Dröse, S., & Brandt, U. (2012). Molecular mechanisms of superoxide production by the mitochondrial respiratory chain. *Adv Exp Med Biol*, *748*, 145-169. [https://doi.org/10.1007/978-1-4614-3573-0\\_6](https://doi.org/10.1007/978-1-4614-3573-0_6)
- Duarte, I., Nabuurs, S. B., Magno, R., & Huynen, M. (2012). Evolution and diversification of the organellar release factor family. *Mol Biol Evol*, *29*(11), 3497-3512. <https://doi.org/10.1093/molbev/mss157>
- Englmeier, R., Pfeffer, S., & Förster, F. (2017). Structure of the Human Mitochondrial Ribosome Studied In Situ by Cryoelectron Tomography. *Structure*, *25*(10), 1574-1581.e1572. <https://doi.org/10.1016/j.str.2017.07.011>
- Falkenberg, M., & Gustafsson, C. M. (2020). Mammalian mitochondrial DNA replication and mechanisms of deletion formation. *Crit Rev Biochem Mol Biol*, *55*(6), 509-524. <https://doi.org/10.1080/10409238.2020.1818684>
- Farge, G., & Falkenberg, M. (2019). Organization of DNA in Mammalian Mitochondria. *Int J Mol Sci*, *20*(11). <https://doi.org/10.3390/ijms20112770>
- Feaga, H. A., Quickel, M. D., Hankey-Giblin, P. A., & Keiler, K. C. (2016). Human Cells Require Non-stop Ribosome Rescue Activity in Mitochondria. *PLoS Genet*, *12*(3), e1005964. <https://doi.org/10.1371/journal.pgen.1005964>
- Feaga, H. A., Viollier, P. H., & Keiler, K. C. (2014). Release of nonstop ribosomes is essential. *mBio*, *5*(6), e01916. <https://doi.org/10.1128/mBio.01916-14>
- Filbeck, S., Cerullo, F., Paternoga, H., Tsaprailis, G., Joazeiro, C. A. P., & Pfeffer, S. (2021). Mimicry of Canonical Translation Elongation Underlies Alanine Tail Synthesis in RQC. *Mol Cell*, *81*(1), 104-114.e106. <https://doi.org/10.1016/j.molcel.2020.11.001>
- Frank, J., & Agrawal, R. K. (2000). A ratchet-like inter-subunit reorganization of the ribosome during translocation. *Nature*, *406*(6793), 318-322. <https://doi.org/10.1038/35018597>
- Freistroffer, D. V., Kwiatkowski, M., Buckingham, R. H., & Ehrenberg, M. (2000). The accuracy of codon recognition by polypeptide release factors. *Proc Natl Acad Sci U S A*, *97*(5), 2046-2051. <https://doi.org/10.1073/pnas.030541097>
- Freistroffer, D. V., Pavlov, M. Y., MacDougall, J., Buckingham, R. H., & Ehrenberg, M. (1997). Release factor RF3 in E.coli accelerates the dissociation of release factors RF1 and RF2 from the ribosome in a GTP-dependent manner. *EMBO J*, *16*(13), 4126-4133. <https://doi.org/10.1093/emboj/16.13.4126>
- Frolova, L. Y., Tsivkovskii, R. Y., Sivolobova, G. F., Oparina, N. Y., Serpinsky, O. I., Blinov, V. M., . . . Kisselev, L. L. (1999). Mutations in the highly conserved GGQ motif of class 1 polypeptide release factors abolish ability of human eRF1 to trigger peptidyl-tRNA hydrolysis. *RNA*, *5*(8), 1014-1020. <https://doi.org/10.1017/s135583829999043x>

- Gagnon, M. G., Seetharaman, S. V., Bulkley, D., & Steitz, T. A. (2012). Structural basis for the rescue of stalled ribosomes: structure of YaeJ bound to the ribosome. *Science*, 335(6074), 1370-1372. <https://doi.org/10.1126/science.1217443>
- Galemou Yoga, E., Angerer, H., Parey, K., & Zickermann, V. (2020). Respiratory complex I - Mechanistic insights and advances in structure determination. *Biochim Biophys Acta Bioenerg*, 1861(3), 148153. <https://doi.org/10.1016/j.bbabi.2020.148153>
- Gao, N., Zavialov, A. V., Li, W., Sengupta, J., Valle, M., Gursky, R. P., . . . Frank, J. (2005). Mechanism for the disassembly of the posttermination complex inferred from cryo-EM studies. *Mol Cell*, 18(6), 663-674. <https://doi.org/10.1016/j.molcel.2005.05.005>
- Garza-Sánchez, F., Schaub, R. E., Janssen, B. D., & Hayes, C. S. (2011). tmRNA regulates synthesis of the ArfA ribosome rescue factor. *Mol Microbiol*, 80(5), 1204-1219. <https://doi.org/10.1111/j.1365-2958.2011.07638.x>
- Gaur, R., Grasso, D., Datta, P. P., Krishna, P. D., Das, G., Spencer, A., . . . Varshney, U. (2008). A single mammalian mitochondrial translation initiation factor functionally replaces two bacterial factors. *Mol Cell*, 29(2), 180-190. <https://doi.org/10.1016/j.molcel.2007.11.021>
- Giacomello, M., Pyakurel, A., Glytsou, C., & Scorrano, L. (2020). The cell biology of mitochondrial membrane dynamics. *Nat Rev Mol Cell Biol*, 21(4), 204-224. <https://doi.org/10.1038/s41580-020-0210-7>
- Gopalakrishna, S., Pearce, S. F., Dinan, A. M., Schober, F. A., Cipullo, M., Spähr, H., . . . Rorbach, J. (2019). C6orf203 is an RNA-binding protein involved in mitochondrial protein synthesis. *Nucleic Acids Res*, 47(17), 9386-9399. <https://doi.org/10.1093/nar/gkz684>
- Gorman, G. S., Chinnery, P. F., DiMauro, S., Hirano, M., Koga, Y., McFarland, R., . . . Turnbull, D. M. (2016). Mitochondrial diseases. *Nat Rev Dis Primers*, 2, 16080. <https://doi.org/10.1038/nrdp.2016.80>
- Greber, B. J., & Ban, N. (2016). Structure and Function of the Mitochondrial Ribosome. *Annu Rev Biochem*, 85, 103-132. <https://doi.org/10.1146/annurev-biochem-060815-014343>
- Greber, B. J., Bieri, P., Leibundgut, M., Leitner, A., Aebersold, R., Boehringer, D., & Ban, N. (2015). Ribosome. The complete structure of the 55S mammalian mitochondrial ribosome. *Science*, 348(6232), 303-308. <https://doi.org/10.1126/science.aaa3872>
- Greber, B. J., Boehringer, D., Leibundgut, M., Bieri, P., Leitner, A., Schmitz, N., . . . Ban, N. (2014). The complete structure of the large subunit of the mammalian mitochondrial ribosome. *Nature*, 515(7526), 283-286. <https://doi.org/10.1038/nature13895>
- Guarás, A., Perales-Clemente, E., Calvo, E., Acín-Pérez, R., Loureiro-Lopez, M., Pujol, C., . . . Enríquez, J. A. (2016). The CoQH2/CoQ Ratio Serves as a Sensor of Respiratory Chain Efficiency. *Cell Rep*, 15(1), 197-209. <https://doi.org/10.1016/j.celrep.2016.03.009>
- Guerrero-Castillo, S., Baertling, F., Kownatzki, D., Wessels, H. J., Arnold, S., Brandt, U., & Nijtmans, L. (2017). The Assembly Pathway of Mitochondrial Respiratory Chain Complex I. *Cell Metab*, 25(1), 128-139. <https://doi.org/10.1016/j.cmet.2016.09.002>
- Guo, R., Zong, S., Wu, M., Gu, J., & Yang, M. (2017). Architecture of Human Mitochondrial Respiratory Megacomplex I. *Cell*, 170(6), 1247-1257.e1212. <https://doi.org/10.1016/j.cell.2017.07.050>
- Gustafsson, C. M., Falkenberg, M., & Larsson, N. G. (2016). Maintenance and Expression of Mammalian Mitochondrial DNA. *Annu Rev Biochem*, 85, 133-160. <https://doi.org/10.1146/annurev-biochem-060815-014402>

- Hackenbrock, C. R., Chazotte, B., & Gupte, S. S. (1986). The random collision model and a critical assessment of diffusion and collision in mitochondrial electron transport. *J Bioenerg Biomembr*, *18*(5), 331-368. <https://doi.org/10.1007/BF00743010>
- Handa, Y., Hikawa, Y., Tochio, N., Kogure, H., Inoue, M., Koshihara, S., . . . Nameki, N. (2010). Solution structure of the catalytic domain of the mitochondrial protein ICT1 that is essential for cell vitality. *J Mol Biol*, *404*(2), 260-273. <https://doi.org/10.1016/j.jmb.2010.09.033>
- Handa, Y., Inaho, N., & Nameki, N. (2011). YaeJ is a novel ribosome-associated protein in *Escherichia coli* that can hydrolyze peptidyl-tRNA on stalled ribosomes. *Nucleic Acids Res*, *39*(5), 1739-1748. <https://doi.org/10.1093/nar/gkq1097>
- Harner, M., Körner, C., Walther, D., Mokranjac, D., Kaesmacher, J., Welsch, U., . . . Neupert, W. (2011). The mitochondrial contact site complex, a determinant of mitochondrial architecture. *EMBO J*, *30*(21), 4356-4370. <https://doi.org/10.1038/emboj.2011.379>
- Heidary, G., Calderwood, L., Cox, G. F., Robson, C. D., Teot, L. A., Mullon, J., & Anselm, I. (2014). Optic atrophy and a Leigh-like syndrome due to mutations in the c12orf65 gene: report of a novel mutation and review of the literature. *J Neuroophthalmol*, *34*(1), 39-43. <https://doi.org/10.1097/WNO.0000000000000076>
- Herrmann, J. M., & Köhl, R. (2007). Catch me if you can! Oxidative protein trapping in the intermembrane space of mitochondria. *J Cell Biol*, *176*(5), 559-563. <https://doi.org/10.1083/jcb.200611060>
- Hetrick, B., Lee, K., & Joseph, S. (2009). Kinetics of stop codon recognition by release factor 1. *Biochemistry*, *48*(47), 11178-11184. <https://doi.org/10.1021/bi901577d>
- Hillen, H. S., Lavdovskaia, E., Nadler, F., Hanitsch, E., Linden, A., Bohnsack, K. E., . . . Richter-Dennerlein, R. (2021). Structural basis of GTPase-mediated mitochondrial ribosome biogenesis and recycling. *Nat Commun*, *12*(1), 3672. <https://doi.org/10.1038/s41467-021-23702-y>
- Hillen, H. S., Temiakov, D., & Cramer, P. (2018). Structural basis of mitochondrial transcription. *Nat Struct Mol Biol*, *25*(9), 754-765. <https://doi.org/10.1038/s41594-018-0122-9>
- Hirst, J. (2013). Mitochondrial complex I. *Annu Rev Biochem*, *82*, 551-575. <https://doi.org/10.1146/annurev-biochem-070511-103700>
- Hirst, J. (2018). Open questions: respiratory chain supercomplexes-why are they there and what do they do? *BMC Biol*, *16*(1), 111. <https://doi.org/10.1186/s12915-018-0577-5>
- Hock, D. H., Robinson, D. R. L., & Stroud, D. A. (2020). Blackout in the powerhouse: clinical phenotypes associated with defects in the assembly of OXPHOS complexes and the mitoribosome. *Biochem J*, *477*(21), 4085-4132. <https://doi.org/10.1042/BCJ20190767>
- Holzmann, J., Frank, P., Löffler, E., Bennett, K. L., Gerner, C., & Rossmannith, W. (2008). RNase P without RNA: identification and functional reconstitution of the human mitochondrial tRNA processing enzyme. *Cell*, *135*(3), 462-474. <https://doi.org/10.1016/j.cell.2008.09.013>
- Huter, P., Müller, C., Arenz, S., Beckert, B., & Wilson, D. N. (2017a). Structural Basis for Ribosome Rescue in Bacteria. *Trends Biochem Sci*, *42*(8), 669-680. <https://doi.org/10.1016/j.tibs.2017.05.009>
- Huter, P., Müller, C., Beckert, B., Arenz, S., Berninghausen, O., Beckmann, R., & Wilson, D. N. (2017b). Structural basis for ArfA-RF2-mediated translation termination on mRNAs lacking stop codons. *Nature*, *541*(7638), 546-549. <https://doi.org/10.1038/nature20821>

- Huynen, M. A., Duarte, I., Chrzanowska-Lightowlers, Z. M., & Nabuurs, S. B. (2012). Structure based hypothesis of a mitochondrial ribosome rescue mechanism. *Biol Direct*, *7*, 14. <https://doi.org/10.1186/1745-6150-7-14>
- Ieva, R., Schrempp, S. G., Opaliński, L., Wollweber, F., Höß, P., Heißwolf, A. K., . . . van der Laan, M. (2014). Mgr2 functions as lateral gatekeeper for preprotein sorting in the mitochondrial inner membrane. *Mol Cell*, *56*(5), 641-652. <https://doi.org/10.1016/j.molcel.2014.10.010>
- Isaac, R. S., McShane, E., & Churchman, L. S. (2018). The Multiple Levels of Mitonuclear Coregulation. *Annu Rev Genet*, *52*, 511-533. <https://doi.org/10.1146/annurev-genet-120417-031709>
- Ito, K., Uno, M., & Nakamura, Y. (2000). A tripeptide 'anticodon' deciphers stop codons in messenger RNA. *Nature*, *403*(6770), 680-684. <https://doi.org/10.1038/35001115>
- Itoh, Y., Andréll, J., Choi, A., Richter, U., Maiti, P., Best, R. B., . . . Amunts, A. (2021). Mechanism of membrane-tethered mitochondrial protein synthesis. *Science*, *371*(6531), 846-849. <https://doi.org/10.1126/science.abe0763>
- Iwata, S., Lee, J. W., Okada, K., Lee, J. K., Iwata, M., Rasmussen, B., . . . Jap, B. K. (1998). Complete structure of the 11-subunit bovine mitochondrial cytochrome bc1 complex. *Science*, *281*(5373), 64-71. <https://doi.org/10.1126/science.281.5373.64>
- Jain, M., Golzarroshan, B., Lin, C. L., Agrawal, S., Tang, W. H., Wu, C. J., & Yuan, H. S. (2022). Dimeric assembly of human Suv3 helicase promotes its RNA unwinding function in mitochondrial RNA degradosome for RNA decay. *Protein Sci*, *31*(5), e4312. <https://doi.org/10.1002/pro.4312>
- Janosi, L., Shimizu, I., & Kaji, A. (1994). Ribosome recycling factor (ribosome releasing factor) is essential for bacterial growth. *Proc Natl Acad Sci U S A*, *91*(10), 4249-4253. <https://doi.org/10.1073/pnas.91.10.4249>
- Joazeiro, C. A. P. (2019). Mechanisms and functions of ribosome-associated protein quality control. *Nat Rev Mol Cell Biol*, *20*(6), 368-383. <https://doi.org/10.1038/s41580-019-0118-2>
- Jourdain, A. A., Koppen, M., Wydro, M., Rodley, C. D., Lightowlers, R. N., Chrzanowska-Lightowlers, Z. M., & Martinou, J. C. (2013). GRSF1 regulates RNA processing in mitochondrial RNA granules. *Cell Metab*, *17*(3), 399-410. <https://doi.org/10.1016/j.cmet.2013.02.005>
- Jourdain, A. A., Popow, J., de la Fuente, M. A., Martinou, J. C., Anderson, P., & Simarro, M. (2017). The FASTK family of proteins: emerging regulators of mitochondrial RNA biology. *Nucleic Acids Res*, *45*(19), 10941-10947. <https://doi.org/10.1093/nar/gkx772>
- Junge, W., & Nelson, N. (2015). ATP synthase. *Annu Rev Biochem*, *84*, 631-657. <https://doi.org/10.1146/annurev-biochem-060614-034124>
- Kadenbach, B. (2021). Complex IV - The regulatory center of mitochondrial oxidative phosphorylation. *Mitochondrion*, *58*, 296-302. <https://doi.org/10.1016/j.mito.2020.10.004>
- Karzai, A. W., Susskind, M. M., & Sauer, R. T. (1999). SmpB, a unique RNA-binding protein essential for the peptide-tagging activity of SsrA (tmRNA). *EMBO J*, *18*(13), 3793-3799. <https://doi.org/10.1093/emboj/18.13.3793>
- Kaushal, P. S., Sharma, M. R., Booth, T. M., Haque, E. M., Tung, C. S., Sanbonmatsu, K. Y., . . . Agrawal, R. K. (2014). Cryo-EM structure of the small subunit of the mammalian mitochondrial ribosome. *Proc Natl Acad Sci U S A*, *111*(20), 7284-7289. <https://doi.org/10.1073/pnas.1401657111>

- Keiler, K. C. (2015). Mechanisms of ribosome rescue in bacteria. *Nat Rev Microbiol*, *13*(5), 285-297. <https://doi.org/10.1038/nrmicro3438>
- Keiler, K. C., Waller, P. R., & Sauer, R. T. (1996). Role of a peptide tagging system in degradation of proteins synthesized from damaged messenger RNA. *Science*, *271*(5251), 990-993. <https://doi.org/10.1126/science.271.5251.990>
- Khalimonchuk, O., Jeong, M. Y., Watts, T., Ferris, E., & Winge, D. R. (2012). Selective Oma1 protease-mediated proteolysis of Cox1 subunit of cytochrome oxidase in assembly mutants. *J Biol Chem*, *287*(10), 7289-7300. <https://doi.org/10.1074/jbc.M111.313148>
- Khawaja, A., Itoh, Y., Remes, C., Spåhr, H., Yukhnovets, O., Höfig, H., . . . Rorbach, J. (2020). Distinct pre-initiation steps in human mitochondrial translation. *Nat Commun*, *11*(1), 2932. <https://doi.org/10.1038/s41467-020-16503-2>
- Kogure, H., Handa, Y., Nagata, M., Kanai, N., Güntert, P., Kubota, K., & Nameki, N. (2014). Identification of residues required for stalled-ribosome rescue in the codon-independent release factor YaeJ. *Nucleic Acids Res*, *42*(5), 3152-3163. <https://doi.org/10.1093/nar/gkt1280>
- Kogure, H., Hikawa, Y., Hagihara, M., Tochio, N., Koshihara, S., Inoue, Y., . . . Nameki, N. (2012). Solution structure and siRNA-mediated knockdown analysis of the mitochondrial disease-related protein C12orf65. *Proteins*, *80*(11), 2629-2642. <https://doi.org/10.1002/prot.24152>
- Kolanczyk, M., Pech, M., Zemojtel, T., Yamamoto, H., Mikula, I., Calvaruso, M. A., . . . Mundlos, S. (2011). NOA1 is an essential GTPase required for mitochondrial protein synthesis. *Mol Biol Cell*, *22*(1), 1-11. <https://doi.org/10.1091/mbc.E10-07-0643>
- Koripella, R. K., Deep, A., Agrawal, E. K., Keshavan, P., Banavali, N. K., & Agrawal, R. K. (2021). Distinct mechanisms of the human mitoribosome recycling and antibiotic resistance. *Nat Commun*, *12*(1), 3607. <https://doi.org/10.1038/s41467-021-23726-4>
- Koripella, R. K., Sharma, M. R., Bhargava, K., Datta, P. P., Kaushal, P. S., Keshavan, P., . . . Agrawal, R. K. (2020). Structures of the human mitochondrial ribosome bound to EF-G1 reveal distinct features of mitochondrial translation elongation. *Nat Commun*, *11*(1), 3830. <https://doi.org/10.1038/s41467-020-17715-2>
- Koripella, R. K., Sharma, M. R., Haque, M. E., Risteff, P., Spremulli, L. L., & Agrawal, R. K. (2019a). Structure of Human Mitochondrial Translation Initiation Factor 3 Bound to the Small Ribosomal Subunit. *iScience*, *12*, 76-86. <https://doi.org/10.1016/j.isci.2018.12.030>
- Koripella, R. K., Sharma, M. R., Risteff, P., Keshavan, P., & Agrawal, R. K. (2019b). Structural insights into unique features of the human mitochondrial ribosome recycling. *Proc Natl Acad Sci U S A*, *116*(17), 8283-8288. <https://doi.org/10.1073/pnas.1815675116>
- Korostelev, A., Asahara, H., Lancaster, L., Laurberg, M., Hirschi, A., Zhu, J., . . . Noller, H. F. (2008). Crystal structure of a translation termination complex formed with release factor RF2. *Proc Natl Acad Sci U S A*, *105*(50), 19684-19689. <https://doi.org/10.1073/pnas.0810953105>
- Korostelev, A. A. (2021). Diversity and Similarity of Termination and Ribosome Rescue in Bacterial, Mitochondrial, and Cytoplasmic Translation. *Biochemistry (Mosc)*, *86*(9), 1107-1121. <https://doi.org/10.1134/S0006297921090066>
- Kovářová, N., Cížková Vrbacká, A., Pecina, P., Stránecký, V., Pronicka, E., Kmoch, S., & Houštek, J. (2012). Adaptation of respiratory chain biogenesis to cytochrome c oxidase deficiency caused by SURF1 gene mutations. *Biochim Biophys Acta*, *1822*(7), 1114-1124. <https://doi.org/10.1016/j.bbadis.2012.03.007>

- Kummer, E., & Ban, N. (2020). Structural insights into mammalian mitochondrial translation elongation catalyzed by mtEFG1. *EMBO J*, *39*(15), e104820. <https://doi.org/10.15252/embj.2020104820>
- Kummer, E., & Ban, N. (2021). Mechanisms and regulation of protein synthesis in mitochondria. *Nat Rev Mol Cell Biol*, *22*(5), 307-325. <https://doi.org/10.1038/s41580-021-00332-2>
- Kummer, E., Leibundgut, M., Rackham, O., Lee, R. G., Boehringer, D., Filipovska, A., & Ban, N. (2018). Unique features of mammalian mitochondrial translation initiation revealed by cryo-EM. *Nature*, *560*(7717), 263-267. <https://doi.org/10.1038/s41586-018-0373-y>
- Kummer, E., Schubert, K. N., Schoenhut, T., Scaiola, A., & Ban, N. (2021). Structural basis of translation termination, rescue, and recycling in mammalian mitochondria. *Mol Cell*, *81*(12), 2566-2582.e2566. <https://doi.org/10.1016/j.molcel.2021.03.042>
- Kühlbrandt, W. (2019). Structure and Mechanisms of F-Type ATP Synthases. *Annu Rev Biochem*, *88*, 515-549. <https://doi.org/10.1146/annurev-biochem-013118-110903>
- Lapuente-Brun, E., Moreno-Loshuertos, R., Acín-Pérez, R., Latorre-Pellicer, A., Colás, C., Balsa, E., . . . Enríquez, J. A. (2013). Supercomplex assembly determines electron flux in the mitochondrial electron transport chain. *Science*, *340*(6140), 1567-1570. <https://doi.org/10.1126/science.1230381>
- Larburu, N., Montellese, C., O'Donohue, M. F., Kutay, U., Gleizes, P. E., & Plisson-Chastang, C. (2016). Structure of a human pre-40S particle points to a role for RACK1 in the final steps of 18S rRNA processing. *Nucleic Acids Res*, *44*(17), 8465-8478. <https://doi.org/10.1093/nar/gkw714>
- Laurberg, M., Asahara, H., Korostelev, A., Zhu, J., Trakhanov, S., & Noller, H. F. (2008). Structural basis for translation termination on the 70S ribosome. *Nature*, *454*(7206), 852-857. <https://doi.org/10.1038/nature07115>
- Lavdovskaia, E., Denks, K., Nadler, F., Steube, E., Linden, A., Urlaub, H., . . . Richter-Dennerlein, R. (2020). Dual function of GTPBP6 in biogenesis and recycling of human mitochondrial ribosomes. *Nucleic Acids Res*, *48*(22), 12929-12942. <https://doi.org/10.1093/nar/gkaa1132>
- Lavdovskaia, E., Kolander, E., Steube, E., Mai, M. M., Urlaub, H., & Richter-Dennerlein, R. (2018). The human Obg protein GTPBP10 is involved in mitoribosomal biogenesis. *Nucleic Acids Res*, *46*(16), 8471-8482. <https://doi.org/10.1093/nar/gky701>
- Lazarou, M., Smith, S. M., Thorburn, D. R., Ryan, M. T., & McKenzie, M. (2009). Assembly of nuclear DNA-encoded subunits into mitochondrial complex IV, and their preferential integration into supercomplex forms in patient mitochondria. *FEBS J*, *276*(22), 6701-6713. <https://doi.org/10.1111/j.1742-4658.2009.07384.x>
- Lee, C. C., Timms, K. M., Trotman, C. N., & Tate, W. P. (1987). Isolation of a rat mitochondrial release factor. Accommodation of the changed genetic code for termination. *J Biol Chem*, *262*(8), 3548-3552.
- Lee, M., Matsunaga, N., Akabane, S., Yasuda, I., Ueda, T., & Takeuchi-Tomita, N. (2021). Reconstitution of mammalian mitochondrial translation system capable of correct initiation and long polypeptide synthesis from leaderless mRNA. *Nucleic Acids Res*, *49*(1), 371-382. <https://doi.org/10.1093/nar/gkaa1165>
- Lenaz, G., Tioli, G., Falasca, A. I., & Genova, M. L. (2016). Complex I function in mitochondrial supercomplexes. *Biochim Biophys Acta*, *1857*(7), 991-1000. <https://doi.org/10.1016/j.bbabi.2016.01.013>

- Lenicke, C., & Cochemé, H. M. (2021). Redox metabolism: ROS as specific molecular regulators of cell signaling and function. *Mol Cell*, *81*(18), 3691-3707. <https://doi.org/10.1016/j.molcel.2021.08.018>
- Letts, J. A., Fiedorczuk, K., & Sazanov, L. A. (2016). The architecture of respiratory supercomplexes. *Nature*, *537*(7622), 644-648. <https://doi.org/10.1038/nature19774>
- Letts, J. A., & Sazanov, L. A. (2017). Clarifying the supercomplex: the higher-order organization of the mitochondrial electron transport chain. *Nat Struct Mol Biol*, *24*(10), 800-808. <https://doi.org/10.1038/nsmb.3460>
- Levy, S., Allerston, C. K., Liveanu, V., Habib, M. R., Gileadi, O., & Schuster, G. (2016). Identification of LACTB2, a metallo- $\beta$ -lactamase protein, as a human mitochondrial endoribonuclease. *Nucleic Acids Res*, *44*(4), 1813-1832. <https://doi.org/10.1093/nar/gkw050>
- Lill, R. (2009). Function and biogenesis of iron-sulphur proteins. *Nature*, *460*(7257), 831-838. <https://doi.org/10.1038/nature08301>
- Lind, C., Sund, J., & Aqvist, J. (2013). Codon-reading specificities of mitochondrial release factors and translation termination at non-standard stop codons. *Nat Commun*, *4*, 2940. <https://doi.org/10.1038/ncomms3940>
- Lobo-Jarne, T., Pérez-Pérez, R., Fontanesi, F., Timón-Gómez, A., Wittig, I., Peñas, A., . . . Ugalde, C. (2020). Multiple pathways coordinate assembly of human mitochondrial complex IV and stabilization of respiratory supercomplexes. *EMBO J*, *39*(14), e103912. <https://doi.org/10.15252/embj.2019103912>
- Lobo-Jarne, T., & Ugalde, C. (2018). Respiratory chain supercomplexes: Structures, function and biogenesis. *Semin Cell Dev Biol*, *76*, 179-190. <https://doi.org/10.1016/j.semcdb.2017.07.021>
- Lorenzi, I., Oeljeklaus, S., Aich, A., Ronsör, C., Callegari, S., Dudek, J., . . . Rehling, P. (2018). The mitochondrial TMEM177 associates with COX20 during COX2 biogenesis. *Biochim Biophys Acta Mol Cell Res*, *1865*(2), 323-333. <https://doi.org/10.1016/j.bbamcr.2017.11.010>
- Lytvynenko, I., Paternoga, H., Thrun, A., Balke, A., Müller, T. A., Chiang, C. H., . . . Joazeiro, C. A. P. (2019). Alanine Tails Signal Proteolysis in Bacterial Ribosome-Associated Quality Control. *Cell*, *178*(1), 76-90.e22. <https://doi.org/10.1016/j.cell.2019.05.002>
- Maiti, P., Antonicka, H., Gingras, A. C., Shoubridge, E. A., & Barrientos, A. (2020). Human GTPBP5 (MTG2) fuels mitoribosome large subunit maturation by facilitating 16S rRNA methylation. *Nucleic Acids Res*, *48*(14), 7924-7943. <https://doi.org/10.1093/nar/gkaa592>
- Maiti, P., Lavdovskaia, E., Barrientos, A., & Richter-Dennerlein, R. (2021). Role of GTPases in Driving Mitoribosome Assembly. *Trends Cell Biol*, *31*(4), 284-297. <https://doi.org/10.1016/j.tcb.2020.12.008>
- Maranzana, E., Barbero, G., Falasca, A. I., Lenaz, G., & Genova, M. L. (2013). Mitochondrial respiratory supercomplex association limits production of reactive oxygen species from complex I. *Antioxid Redox Signal*, *19*(13), 1469-1480. <https://doi.org/10.1089/ars.2012.4845>
- Martijn, J., Vosseberg, J., Guy, L., Offre, P., & Ettema, T. J. G. (2018). Deep mitochondrial origin outside the sampled alphaproteobacteria. *Nature*, *557*(7703), 101-105. <https://doi.org/10.1038/s41586-018-0059-5>
- Meinecke, M., Wagner, R., Kovermann, P., Guiard, B., Mick, D. U., Hutu, D. P., . . . Rehling, P. (2006). Tim50 maintains the permeability barrier of the mitochondrial inner membrane. *Science*, *312*(5779), 1523-1526. <https://doi.org/10.1126/science.1127628>

- Mesecke, N., Terziyska, N., Kozany, C., Baumann, F., Neupert, W., Hell, K., & Herrmann, J. M. (2005). A disulfide relay system in the intermembrane space of mitochondria that mediates protein import. *Cell*, *121*(7), 1059-1069. <https://doi.org/10.1016/j.cell.2005.04.011>
- Michel, H., Behr, J., Harrenga, A., & Kannt, A. (1998). Cytochrome c oxidase: structure and spectroscopy. *Annu Rev Biophys Biomol Struct*, *27*, 329-356. <https://doi.org/10.1146/annurev.biophys.27.1.329>
- Mick, D. U., Dennerlein, S., Wiese, H., Reinhold, R., Pacheu-Grau, D., Lorenzi, I., . . . Rehling, P. (2012). MITRAC links mitochondrial protein translocation to respiratory-chain assembly and translational regulation. *Cell*, *151*(7), 1528-1541. <https://doi.org/10.1016/j.cell.2012.11.053>
- Milenkovic, D., Blaza, J. N., Larsson, N. G., & Hirst, J. (2017). The Enigma of the Respiratory Chain Supercomplex. *Cell Metab*, *25*(4), 765-776. <https://doi.org/10.1016/j.cmet.2017.03.009>
- Miranda, M., Bonekamp, N. A., & Kühl, I. (2022). Starting the engine of the powerhouse: mitochondrial transcription and beyond. *Biol Chem*, *403*(8-9), 779-805. <https://doi.org/10.1515/hsz-2021-0416>
- Mitchell, P. (1961). Coupling of phosphorylation to electron and hydrogen transfer by a chemi-osmotic type of mechanism. *Nature*, *191*, 144-148. <https://doi.org/10.1038/191144a0>
- Mokranjac, D., & Neupert, W. (2015). Cell biology: Architecture of a protein entry gate. *Nature*, *528*(7581), 201-202. <https://doi.org/10.1038/nature16318>
- Mora, L., Heurgué-Hamard, V., Champ, S., Ehrenberg, M., Kisselev, L. L., & Buckingham, R. H. (2003). The essential role of the invariant GGQ motif in the function and stability in vivo of bacterial release factors RF1 and RF2. *Mol Microbiol*, *47*(1), 267-275. <https://doi.org/10.1046/j.1365-2958.2003.03301.x>
- Moreno-Lastres, D., Fontanesi, F., García-Consuegra, I., Martín, M. A., Arenas, J., Barrientos, A., & Ugalde, C. (2012). Mitochondrial complex I plays an essential role in human respirasome assembly. *Cell Metab*, *15*(3), 324-335. <https://doi.org/10.1016/j.cmet.2012.01.015>
- Morgenstern, M., Peikert, C. D., Lübbert, P., Suppanz, I., Klemm, C., Alka, O., . . . Warscheid, B. (2021). Quantitative high-confidence human mitochondrial proteome and its dynamics in cellular context. *Cell Metab*, *33*(12), 2464-2483.e2418. <https://doi.org/10.1016/j.cmet.2021.11.001>
- Mourier, A., Matic, S., Ruzzenente, B., Larsson, N. G., & Milenkovic, D. (2014). The respiratory chain supercomplex organization is independent of COX7a2l isoforms. *Cell Metab*, *20*(6), 1069-1075. <https://doi.org/10.1016/j.cmet.2014.11.005>
- Murphy, M. P. (2009). How mitochondria produce reactive oxygen species. *Biochem J*, *417*(1), 1-13. <https://doi.org/10.1042/BJ20081386>
- Müller, C., Crowe-McAuliffe, C., & Wilson, D. N. (2021). Ribosome Rescue Pathways in Bacteria. *Front Microbiol*, *12*, 652980. <https://doi.org/10.3389/fmicb.2021.652980>
- Nadler, F., Lavdovskaia, E., Krempler, A., Cruz-Zaragoza, L. D., Dennerlein, S., & Richter-Dennerlein, R. (2022a). Human mtRF1 terminates COX1 translation and its ablation induces mitochondrial ribosome-associated quality control. *Nat Commun*, *13*(1), 6406. <https://doi.org/10.1038/s41467-022-34088-w>
- Nadler, F., Lavdovskaia, E., & Richter-Dennerlein, R. (2022b). Maintaining mitochondrial ribosome function: The role of ribosome rescue and recycling factors. *RNA Biol*, *19*(1), 117-131. <https://doi.org/10.1080/15476286.2021.2015561>



- Neubauer, C., Gillet, R., Kelley, A. C., & Ramakrishnan, V. (2012). Decoding in the absence of a codon by tmRNA and SmpB in the ribosome. *Science*, *335*(6074), 1366-1369. <https://doi.org/10.1126/science.1217039>
- Neupert, W. (2015). A perspective on transport of proteins into mitochondria: a myriad of open questions. *J Mol Biol*, *427*(6 Pt A), 1135-1158. <https://doi.org/10.1016/j.jmb.2015.02.001>
- Neupert, W., & Herrmann, J. M. (2007). Translocation of proteins into mitochondria. *Annu Rev Biochem*, *76*, 723-749. <https://doi.org/10.1146/annurev.biochem.76.052705.163409>
- Nicholls, T. J., Spåhr, H., Jiang, S., Siira, S. J., Koolmeister, C., Sharma, S., . . . Gustafsson, C. M. (2019). Dinucleotide Degradation by REXO2 Maintains Promoter Specificity in Mammalian Mitochondria. *Mol Cell*, *76*(5), 784-796.e786. <https://doi.org/10.1016/j.molcel.2019.09.010>
- Nozaki, Y., Matsunaga, N., Ishizawa, T., Ueda, T., & Takeuchi, N. (2008). HMRFL1 is a human mitochondrial translation release factor involved in the decoding of the termination codons UAA and UAG. *Genes Cells*, *13*(5), 429-438. <https://doi.org/10.1111/j.1365-2443.2008.01181.x>
- Nunnari, J., & Suomalainen, A. (2012). Mitochondria: in sickness and in health. *Cell*, *148*(6), 1145-1159. <https://doi.org/10.1016/j.cell.2012.02.035>
- Nürnberg-Goloub, E., & Tampé, R. (2019). Ribosome recycling in mRNA translation, quality control, and homeostasis. *Biol Chem*, *401*(1), 47-61. <https://doi.org/10.1515/hsz-2019-0279>
- Ohkubo, A., Van Haute, L., Rudler, D. L., Stentenbach, M., Steiner, F. A., Rackham, O., . . . Martinou, J. C. (2021). The FASTK family proteins fine-tune mitochondrial RNA processing. *PLoS Genet*, *17*(11), e1009873. <https://doi.org/10.1371/journal.pgen.1009873>
- Ojala, D., Montoya, J., & Attardi, G. (1981). tRNA punctuation model of RNA processing in human mitochondria. *Nature*, *290*(5806), 470-474. <https://doi.org/10.1038/290470a0>
- Ostergaard, E., Weraarpachai, W., Ravn, K., Born, A. P., Jønson, L., Duno, M., . . . Vissing, J. (2015). Mutations in COA3 cause isolated complex IV deficiency associated with neuropathy, exercise intolerance, obesity, and short stature. *J Med Genet*, *52*(3), 203-207. <https://doi.org/10.1136/jmedgenet-2014-102914>
- Peng, B. Z., Bock, L. V., Belardinelli, R., Peske, F., Grubmüller, H., & Rodnina, M. V. (2019). Active role of elongation factor G in maintaining the mRNA reading frame during translation. *Sci Adv*, *5*(12), eaax8030. <https://doi.org/10.1126/sciadv.aax8030>
- Perrone, E., Cavole, T. R., Oliveira, M. G., Virmond, L. D. A., Silva, M. F. B., Soares, M. F. F., . . . Micheletti, C. (2020). Leigh syndrome in a patient with a novel C12orf65 pathogenic variant: case report and literature review. *Genet Mol Biol*, *43*(2), e20180271. <https://doi.org/10.1590/1678-4685-GMB-2018-0271>
- Peske, F., Kuhlenkoetter, S., Rodnina, M. V., & Wintermeyer, W. (2014). Timing of GTP binding and hydrolysis by translation termination factor RF3. *Nucleic Acids Res*, *42*(3), 1812-1820. <https://doi.org/10.1093/nar/gkt1095>
- Peske, F., Rodnina, M. V., & Wintermeyer, W. (2005). Sequence of steps in ribosome recycling as defined by kinetic analysis. *Mol Cell*, *18*(4), 403-412. <https://doi.org/10.1016/j.molcel.2005.04.009>
- Petrov, A. S., Wood, E. C., Bernier, C. R., Norris, A. M., Brown, A., & Amunts, A. (2018). Structural Patching Fosters Divergence of Mitochondrial Ribosomes. *Mol Biol Evol*. <https://doi.org/10.1093/molbev/msy221>

- Petry, S., Brodersen, D. E., Murphy, F. V., Dunham, C. M., Selmer, M., Tarry, M. J., . . . Ramakrishnan, V. (2005). Crystal structures of the ribosome in complex with release factors RF1 and RF2 bound to a cognate stop codon. *Cell*, *123*(7), 1255-1266. <https://doi.org/10.1016/j.cell.2005.09.039>
- Pfanner, N., Warscheid, B., & Wiedemann, N. (2019). Mitochondrial proteins: from biogenesis to functional networks. *Nat Rev Mol Cell Biol*, *20*(5), 267-284. <https://doi.org/10.1038/s41580-018-0092-0>
- Pfeffer, S., Woellhaf, M. W., Herrmann, J. M., & Förster, F. (2015). Organization of the mitochondrial translation machinery studied in situ by cryoelectron tomography. *Nat Commun*, *6*, 6019. <https://doi.org/10.1038/ncomms7019>
- Pfeiffer, K., Gohil, V., Stuart, R. A., Hunte, C., Brandt, U., Greenberg, M. L., & Schagger, H. (2003). Cardiolipin stabilizes respiratory chain supercomplexes. *J Biol Chem*, *278*(52), 52873-52880. <https://doi.org/10.1074/jbc.M308366200>
- Protasoni, M., Pérez-Pérez, R., Lobo-Jarne, T., Harbour, M. E., Ding, S., Peñas, A., . . . Fernández-Vizarra, E. (2020). Respiratory supercomplexes act as a platform for complex III-mediated maturation of human mitochondrial complexes I and IV. *EMBO J*, *39*(3), e102817. <https://doi.org/10.15252/embj.2019102817>
- Pérez-Pérez, R., Lobo-Jarne, T., Milenkovic, D., Mourier, A., Bratic, A., García-Bartolomé, A., . . . Ugalde, C. (2016). COX7A2L Is a Mitochondrial Complex III Binding Protein that Stabilizes the III2+IV Supercomplex without Affecting Respirasome Formation. *Cell Rep*, *16*(9), 2387-2398. <https://doi.org/10.1016/j.celrep.2016.07.081>
- Quirós, P. M., Langer, T., & López-Otín, C. (2015). New roles for mitochondrial proteases in health, ageing and disease. *Nat Rev Mol Cell Biol*, *16*(6), 345-359. <https://doi.org/10.1038/nrm3984>
- Quirós, P. M., Mottis, A., & Auwerx, J. (2016). Mitonuclear communication in homeostasis and stress. *Nat Rev Mol Cell Biol*, *17*(4), 213-226. <https://doi.org/10.1038/nrm.2016.23>
- Rackham, O., Busch, J. D., Matic, S., Siira, S. J., Kuznetsova, I., Atanassov, I., . . . Filipovska, A. (2016). Hierarchical RNA Processing Is Required for Mitochondrial Ribosome Assembly. *Cell Rep*, *16*(7), 1874-1890. <https://doi.org/10.1016/j.celrep.2016.07.031>
- Rackham, O., & Filipovska, A. (2022). Organization and expression of the mammalian mitochondrial genome. *Nat Rev Genet*. <https://doi.org/10.1038/s41576-022-00480-x>
- Ramrath, D. J., Yamamoto, H., Rother, K., Wittek, D., Pech, M., Mielke, T., . . . Spahn, C. M. (2012). The complex of tmRNA-SmpB and EF-G on translocating ribosomes. *Nature*, *485*(7399), 526-529. <https://doi.org/10.1038/nature11006>
- Rawat, U. B., Zavialov, A. V., Sengupta, J., Valle, M., Grassucci, R. A., Linde, J., . . . Frank, J. (2003). A cryo-electron microscopic study of ribosome-bound termination factor RF2. *Nature*, *421*(6918), 87-90. <https://doi.org/10.1038/nature01224>
- Razew, M., Warkocki, Z., Taube, M., Kolondra, A., Czarnocki-Cieciura, M., Nowak, E., . . . Nowotny, M. (2018). Structural analysis of mtEXO mitochondrial RNA degradosome reveals tight coupling of nuclease and helicase components. *Nat Commun*, *9*(1), 97. <https://doi.org/10.1038/s41467-017-02570-5>
- Richman, T. R., Spähr, H., Ermer, J. A., Davies, S. M., Viola, H. M., Bates, K. A., . . . Filipovska, A. (2016). Loss of the RNA-binding protein TACO1 causes late-onset mitochondrial dysfunction in mice. *Nat Commun*, *7*, 11884. <https://doi.org/10.1038/ncomms11884>
- Richter, R., Rorbach, J., Pajak, A., Smith, P. M., Wessels, H. J., Huynen, M. A., . . . Chrzanowska-Lightowlers, Z. M. (2010). A functional peptidyl-tRNA hydrolase, ICT1, has been recruited into the human mitochondrial ribosome. *EMBO J*, *29*(6), 1116-1125. <https://doi.org/10.1038/emboj.2010.14>

- Richter, U., Lahtinen, T., Marttinen, P., Myöhänen, M., Greco, D., Cannino, G., . . . Battersby, B. J. (2013). A mitochondrial ribosomal and RNA decay pathway blocks cell proliferation. *Curr Biol*, *23*(6), 535-541. <https://doi.org/10.1016/j.cub.2013.02.019>
- Richter, U., Lahtinen, T., Marttinen, P., Suomi, F., & Battersby, B. J. (2015). Quality control of mitochondrial protein synthesis is required for membrane integrity and cell fitness. *J Cell Biol*, *211*(2), 373-389. <https://doi.org/10.1083/jcb.201504062>
- Richter-Dennerlein, R., Dennerlein, S., & Rehling, P. (2015). Integrating mitochondrial translation into the cellular context. *Nat Rev Mol Cell Biol*, *16*(10), 586-592. <https://doi.org/10.1038/nrm4051>
- Richter-Dennerlein, R., Oeljeklaus, S., Lorenzi, I., Ronsör, C., Bareth, B., Schendzielorz, A. B., . . . Dennerlein, S. (2016). Mitochondrial Protein Synthesis Adapts to Influx of Nuclear-Encoded Protein. *Cell*, *167*(2), 471-483.e410. <https://doi.org/10.1016/j.cell.2016.09.003>
- Rodnina, M. V. (2018). Translation in Prokaryotes. *Cold Spring Harb Perspect Biol*, *10*(9). <https://doi.org/10.1101/cshperspect.a032664>
- Rodnina, M. V., Fischer, N., Maracci, C., & Stark, H. (2017). Ribosome dynamics during decoding. *Philos Trans R Soc Lond B Biol Sci*, *372*(1716). <https://doi.org/10.1098/rstb.2016.0182>
- Rodnina, M. V., Peske, F., Peng, B. Z., Belardinelli, R., & Wintermeyer, W. (2019). Converting GTP hydrolysis into motion: versatile translational elongation factor G. *Biol Chem*, *401*(1), 131-142. <https://doi.org/10.1515/hsz-2019-0313>
- Roger, A. J., Muñoz-Gómez, S. A., & Kamikawa, R. (2017). The Origin and Diversification of Mitochondria. *Curr Biol*, *27*(21), R1177-R1192. <https://doi.org/10.1016/j.cub.2017.09.015>
- Rorbach, J., Gammage, P. A., & Minczuk, M. (2012). C7orf30 is necessary for biogenesis of the large subunit of the mitochondrial ribosome. *Nucleic Acids Res*, *40*(9), 4097-4109. <https://doi.org/10.1093/nar/gkr1282>
- Rorbach, J., Richter, R., Wessels, H. J., Wydro, M., Pekalski, M., Farhoud, M., . . . Chrzanowska-Lightowlers, Z. M. (2008). The human mitochondrial ribosome recycling factor is essential for cell viability. *Nucleic Acids Res*, *36*(18), 5787-5799. <https://doi.org/10.1093/nar/gkn576>
- Rudler, D. L., Hughes, L. A., Perks, K. L., Richman, T. R., Kuznetsova, I., Ermer, J. A., . . . Filipovska, A. (2019). Fidelity of translation initiation is required for coordinated respiratory complex assembly. *Sci Adv*, *5*(12), eaay2118. <https://doi.org/10.1126/sciadv.aay2118>
- Russell, J. B., & Cook, G. M. (1995). Energetics of bacterial growth: balance of anabolic and catabolic reactions. *Microbiol Rev*, *59*(1), 48-62. <https://doi.org/10.1128/mr.59.1.48-62.1995>
- Rutter, J., Winge, D. R., & Schiffman, J. D. (2010). Succinate dehydrogenase - Assembly, regulation and role in human disease. *Mitochondrion*, *10*(4), 393-401. <https://doi.org/10.1016/j.mito.2010.03.001>
- Sagan, L. (1967). On the origin of mitosing cells. *J Theor Biol*, *14*(3), 255-274. [https://doi.org/10.1016/0022-5193\(67\)90079-3](https://doi.org/10.1016/0022-5193(67)90079-3)
- Samatova, E., Daberge, J., Liutkute, M., & Rodnina, M. V. (2020). Translational Control by Ribosome Pausing in Bacteria: How a Non-uniform Pace of Translation Affects Protein Production and Folding. *Front Microbiol*, *11*, 619430. <https://doi.org/10.3389/fmicb.2020.619430>

- Sanchez, M. I., Mercer, T. R., Davies, S. M., Shearwood, A. M., Nygård, K. K., Richman, T. R., . . . Filipovska, A. (2011). RNA processing in human mitochondria. *Cell Cycle*, *10*(17), 2904-2916. <https://doi.org/10.4161/cc.10.17.17060>
- Saraste, M. (1999). Oxidative phosphorylation at the fin de siècle. *Science*, *283*(5407), 1488-1493. <https://doi.org/10.1126/science.283.5407.1488>
- Sasarman, F., Brunel-Guitton, C., Antonicka, H., Wai, T., Shoubbridge, E. A., & Consortium, L. (2010). LRPPRC and SLIRP interact in a ribonucleoprotein complex that regulates posttranscriptional gene expression in mitochondria. *Mol Biol Cell*, *21*(8), 1315-1323. <https://doi.org/10.1091/mbc.e10-01-0047>
- Schapira, A. H. (2012). Mitochondrial diseases. *Lancet*, *379*(9828), 1825-1834. [https://doi.org/10.1016/S0140-6736\(11\)61305-6](https://doi.org/10.1016/S0140-6736(11)61305-6)
- Schindelin, J., Arganda-Carreras, I., Frise, E., Kaynig, V., Longair, M., Pietzsch, T., . . . Cardona, A. (2012). Fiji: an open-source platform for biological-image analysis. *Nat Methods*, *9*(7), 676-682. <https://doi.org/10.1038/nmeth.2019>
- Schwartzbach, C. J., & Spremulli, L. L. (1989). Bovine mitochondrial protein synthesis elongation factors. Identification and initial characterization of an elongation factor Tu-elongation factor Ts complex. *J Biol Chem*, *264*(32), 19125-19131.
- Schäfer, E., Seelert, H., Reifschneider, N. H., Krause, F., Dencher, N. A., & Vonck, J. (2006). Architecture of active mammalian respiratory chain supercomplexes. *J Biol Chem*, *281*(22), 15370-15375. <https://doi.org/10.1074/jbc.M513525200>
- Schägger, H., & Pfeiffer, K. (2000). Supercomplexes in the respiratory chains of yeast and mammalian mitochondria. *EMBO J*, *19*(8), 1777-1783. <https://doi.org/10.1093/emboj/19.8.1777>
- Scolnick, E., Tompkins, R., Caskey, T., & Nirenberg, M. (1968). Release factors differing in specificity for terminator codons. *Proc Natl Acad Sci U S A*, *61*(2), 768-774. <https://doi.org/10.1073/pnas.61.2.768>
- Sharma, M. R., Koc, E. C., Datta, P. P., Booth, T. M., Spremulli, L. L., & Agrawal, R. K. (2003). Structure of the mammalian mitochondrial ribosome reveals an expanded functional role for its component proteins. *Cell*, *115*(1), 97-108. [https://doi.org/10.1016/s0092-8674\(03\)00762-1](https://doi.org/10.1016/s0092-8674(03)00762-1)
- Shi, X., & Joseph, S. (2016). Mechanism of Translation Termination: RF1 Dissociation Follows Dissociation of RF3 from the Ribosome. *Biochemistry*, *55*(45), 6344-6354. <https://doi.org/10.1021/acs.biochem.6b00921>
- Shimazaki, H., Takiyama, Y., Ishiura, H., Sakai, C., Matsushima, Y., Hatakeyama, H., . . . (JASPAC), J. S. P. R. C. (2012). A homozygous mutation of C12orf65 causes spastic paraplegia with optic atrophy and neuropathy (SPG55). *J Med Genet*, *49*(12), 777-784. <https://doi.org/10.1136/jmedgenet-2012-101212>
- Shimizu, Y. (2012). ArfA recruits RF2 into stalled ribosomes. *J Mol Biol*, *423*(4), 624-631. <https://doi.org/10.1016/j.jmb.2012.08.007>
- Shoemaker, C. J., & Green, R. (2012). Translation drives mRNA quality control. *Nat Struct Mol Biol*, *19*(6), 594-601. <https://doi.org/10.1038/nsmb.2301>
- Sies, H., & Jones, D. P. (2020). Reactive oxygen species (ROS) as pleiotropic physiological signalling agents. *Nat Rev Mol Cell Biol*, *21*(7), 363-383. <https://doi.org/10.1038/s41580-020-0230-3>
- Signes, A., & Fernandez-Vizarra, E. (2018). Assembly of mammalian oxidative phosphorylation complexes I-V and supercomplexes. *Essays Biochem*, *62*(3), 255-270. <https://doi.org/10.1042/EBC20170098>

- Siira, S. J., Spåhr, H., Shearwood, A. J., Ruzzenente, B., Larsson, N. G., Rackham, O., & Filipovska, A. (2017). LRPPRC-mediated folding of the mitochondrial transcriptome. *Nat Commun*, *8*(1), 1532. <https://doi.org/10.1038/s41467-017-01221-z>
- Soleimanpour-Lichaei, H. R., Kühl, I., Gaisne, M., Passos, J. F., Wydro, M., Rorbach, J., . . . Chrzanowska-Lightowlers, Z. (2007). mtRF1a is a human mitochondrial translation release factor decoding the major termination codons UAA and UAG. *Mol Cell*, *27*(5), 745-757. <https://doi.org/10.1016/j.molcel.2007.06.031>
- Sousa, J. S., Mills, D. J., Vonck, J., & Kühlbrandt, W. (2016). Functional asymmetry and electron flow in the bovine respirasome. *Elife*, *5*. <https://doi.org/10.7554/eLife.21290>
- Spiegel, R., Mandel, H., Saada, A., Lerer, I., Burger, A., Shaag, A., . . . Meiner, V. (2014). Delineation of C12orf65-related phenotypes: a genotype-phenotype relationship. *Eur J Hum Genet*, *22*(8), 1019-1025. <https://doi.org/10.1038/ejhg.2013.284>
- Spinelli, J. B., & Haigis, M. C. (2018). The multifaceted contributions of mitochondria to cellular metabolism. *Nat Cell Biol*, *20*(7), 745-754. <https://doi.org/10.1038/s41556-018-0124-1>
- Stenton, S. L., & Prokisch, H. (2020). Genetics of mitochondrial diseases: Identifying mutations to help diagnosis. *EBioMedicine*, *56*, 102784. <https://doi.org/10.1016/j.ebiom.2020.102784>
- Stiller, S. B., Höpker, J., Oeljeklaus, S., Schütze, C., Schrempp, S. G., Vent-Schmidt, J., . . . Wiedemann, N. (2016). Mitochondrial OXA Translocase Plays a Major Role in Biogenesis of Inner-Membrane Proteins. *Cell Metab*, *23*(5), 901-908. <https://doi.org/10.1016/j.cmet.2016.04.005>
- Stroud, D. A., Maher, M. J., Lindau, C., Vögtle, F. N., Frazier, A. E., Surgenor, E., . . . Ryan, M. T. (2015). COA6 is a mitochondrial complex IV assembly factor critical for biogenesis of mtDNA-encoded COX2. *Hum Mol Genet*, *24*(19), 5404-5415. <https://doi.org/10.1093/hmg/ddv265>
- Stroud, D. A., Surgenor, E. E., Formosa, L. E., Reljic, B., Frazier, A. E., Dibley, M. G., . . . Ryan, M. T. (2016). Accessory subunits are integral for assembly and function of human mitochondrial complex I. *Nature*, *538*(7623), 123-126. <https://doi.org/10.1038/nature19754>
- Sund, J., Andér, M., & Aqvist, J. (2010). Principles of stop-codon reading on the ribosome. *Nature*, *465*(7300), 947-950. <https://doi.org/10.1038/nature09082>
- Svidritskiy, E., & Korostelev, A. A. (2018). Conformational Control of Translation Termination on the 70S Ribosome. *Structure*, *26*(6), 821-828.e823. <https://doi.org/10.1016/j.str.2018.04.001>
- Takeuchi, N., & Ueda, T. (2003). Down-regulation of the mitochondrial translation system during terminal differentiation of HL-60 cells by 12-O-tetradecanoyl-1-phorbol-13-acetate: comparison with the cytoplasmic translation system. *J Biol Chem*, *278*(46), 45318-45324. <https://doi.org/10.1074/jbc.M307620200>
- Tan, B. G., Mutti, C. D., Shi, Y., Xie, X., Zhu, X., Silva-Pinheiro, P., . . . Gustafsson, C. M. (2022). The human mitochondrial genome contains a second light strand promoter. *Mol Cell*. <https://doi.org/10.1016/j.molcel.2022.08.011>
- Tang, J. X., Thompson, K., Taylor, R. W., & Oláhová, M. (2020). Mitochondrial OXPHOS Biogenesis: Co-Regulation of Protein Synthesis, Import, and Assembly Pathways. *Int J Mol Sci*, *21*(11). <https://doi.org/10.3390/ijms21113820>
- Temperley, R., Richter, R., Dennerlein, S., Lightowlers, R. N., & Chrzanowska-Lightowlers, Z. M. (2010a). Hungry codons promote frameshifting in human mitochondrial ribosomes. *Science*, *327*(5963), 301. <https://doi.org/10.1126/science.1180674>

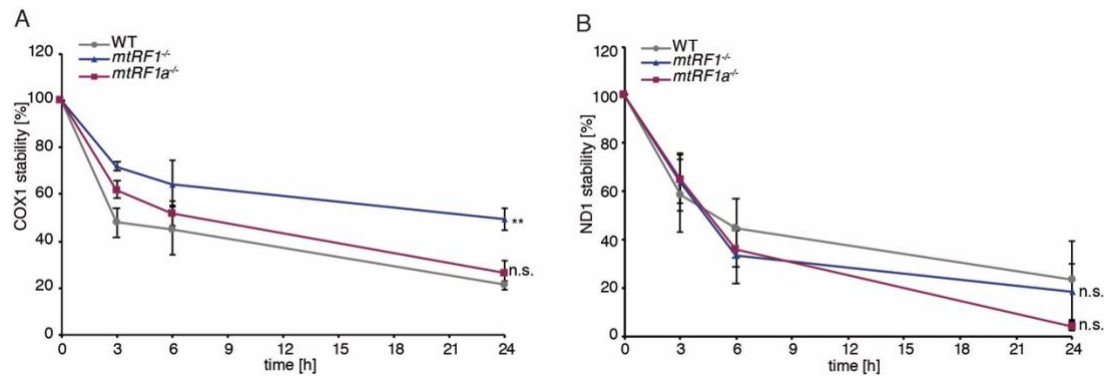
- Temperley, R. J., Wydro, M., Lightowers, R. N., & Chrzanowska-Lightowers, Z. M. (2010b). Human mitochondrial mRNAs--like members of all families, similar but different. *Biochim Biophys Acta*, *1797*(6-7), 1081-1085. <https://doi.org/10.1016/j.bbabi.2010.02.036>
- Thompson, K., Mai, N., Oláhová, M., Scialó, F., Formosa, L. E., Stroud, D. A., . . . Taylor, R. W. (2018). mutations cause mitochondrial encephalopathy and a combined oxidative phosphorylation defect. *EMBO Mol Med*, *10*(11). <https://doi.org/10.15252/emmm.201809060>
- Trumpower, B. L. (1990). The protonmotive Q cycle. Energy transduction by coupling of proton translocation to electron transfer by the cytochrome bc1 complex. *J Biol Chem*, *265*(20), 11409-11412.
- Tsuboi, M., Morita, H., Nozaki, Y., Akama, K., Ueda, T., Ito, K., . . . Takeuchi, N. (2009). EF-G2mt is an exclusive recycling factor in mammalian mitochondrial protein synthesis. *Mol Cell*, *35*(4), 502-510. <https://doi.org/10.1016/j.molcel.2009.06.028>
- Tsukihara, T., Aoyama, H., Yamashita, E., Tomizaki, T., Yamaguchi, H., Shinzawa-Itoh, K., . . . Yoshikawa, S. (1996). The whole structure of the 13-subunit oxidized cytochrome c oxidase at 2.8 Å. *Science*, *272*(5265), 1136-1144. <https://doi.org/10.1126/science.272.5265.1136>
- van Belzen, N., Diesveld, M. P., van der Made, A. C., Nozawa, Y., Dinjens, W. N., Vlietstra, R., . . . Bosman, F. T. (1995). Identification of mRNAs that show modulated expression during colon carcinoma cell differentiation. *Eur J Biochem*, *234*(3), 843-848. [https://doi.org/10.1111/j.1432-1033.1995.843\\_a.x](https://doi.org/10.1111/j.1432-1033.1995.843_a.x)
- van der Sluis, E. O., Bauerschmitt, H., Becker, T., Mielke, T., Frauenfeld, J., Berninghausen, O., . . . Beckmann, R. (2015). Parallel Structural Evolution of Mitochondrial Ribosomes and OXPHOS Complexes. *Genome Biol Evol*, *7*(5), 1235-1251. <https://doi.org/10.1093/gbe/evv061>
- Vidoni, S., Harbour, M. E., Guerrero-Castillo, S., Signes, A., Ding, S., Fearnley, I. M., . . . Zeviani, M. (2017). MR-1S Interacts with PET100 and PET117 in Module-Based Assembly of Human Cytochrome c Oxidase. *Cell Rep*, *18*(7), 1727-1738. <https://doi.org/10.1016/j.celrep.2017.01.044>
- Vinothkumar, K. R., Zhu, J., & Hirst, J. (2014). Architecture of mammalian respiratory complex I. *Nature*, *515*(7525), 80-84. <https://doi.org/10.1038/nature13686>
- Voorhees, R. M., Schmeing, T. M., Kelley, A. C., & Ramakrishnan, V. (2010). The mechanism for activation of GTP hydrolysis on the ribosome. *Science*, *330*(6005), 835-838. <https://doi.org/10.1126/science.1194460>
- Voorhees, R. M., Weixlbaumer, A., Loakes, D., Kelley, A. C., & Ramakrishnan, V. (2009). Insights into substrate stabilization from snapshots of the peptidyl transferase center of the intact 70S ribosome. *Nat Struct Mol Biol*, *16*(5), 528-533. <https://doi.org/10.1038/nsmb.1577>
- Wang, C., Richter-Dennerlein, R., Pacheu-Grau, D., Liu, F., Zhu, Y., Dennerlein, S., & Rehling, P. (2020). MITRAC15/COA1 promotes mitochondrial translation in a ND2 ribosome-nascent chain complex. *EMBO Rep*, *21*(1), e48833. <https://doi.org/10.15252/embr.201948833>
- Wang, D. D., Guo, X. E., Modrek, A. S., Chen, C. F., Chen, P. L., & Lee, W. H. (2014). Helicase SUV3, polynucleotide phosphorylase, and mitochondrial polyadenylation polymerase form a transient complex to modulate mitochondrial mRNA polyadenylated tail lengths in response to energetic changes. *J Biol Chem*, *289*(24), 16727-16735. <https://doi.org/10.1074/jbc.M113.536540>

- Wang, D. D., Shu, Z., Lieser, S. A., Chen, P. L., & Lee, W. H. (2009). Human mitochondrial SUV3 and polynucleotide phosphorylase form a 330-kDa heteropentamer to cooperatively degrade double-stranded RNA with a 3'-to-5' directionality. *J Biol Chem*, *284*(31), 20812-20821. <https://doi.org/10.1074/jbc.M109.009605>
- Waypa, G. B., Smith, K. A., & Schumacker, P. T. (2016). O<sub>2</sub> sensing, mitochondria and ROS signaling: The fog is lifting. *Mol Aspects Med*, *47-48*, 76-89. <https://doi.org/10.1016/j.mam.2016.01.002>
- Weixlbaumer, A., Jin, H., Neubauer, C., Voorhees, R. M., Petry, S., Kelley, A. C., & Ramakrishnan, V. (2008). Insights into translational termination from the structure of RF2 bound to the ribosome. *Science*, *322*(5903), 953-956. <https://doi.org/10.1126/science.1164840>
- Weraarpachai, W., Antonicka, H., Sasarman, F., Seeger, J., Schrank, B., Kolesar, J. E., . . . Shoubridge, E. A. (2009). Mutation in TACO1, encoding a translational activator of COX I, results in cytochrome c oxidase deficiency and late-onset Leigh syndrome. *Nat Genet*, *41*(7), 833-837. <https://doi.org/10.1038/ng.390>
- Weraarpachai, W., Sasarman, F., Nishimura, T., Antonicka, H., Auré, K., Rötig, A., . . . Shoubridge, E. A. (2012). Mutations in C12orf62, a factor that couples COX I synthesis with cytochrome c oxidase assembly, cause fatal neonatal lactic acidosis. *Am J Hum Genet*, *90*(1), 142-151. <https://doi.org/10.1016/j.ajhg.2011.11.027>
- Wesolowska, M., Gorman, G. S., Alston, C. L., Pajak, A., Pyle, A., He, L., . . . Chrzanowska-Lightowlers, Z. M. (2015). Adult Onset Leigh Syndrome in the Intensive Care Setting: A Novel Presentation of a C12orf65 Related Mitochondrial Disease. *J Neuromuscul Dis*, *2*(4), 409-419. <https://doi.org/10.3233/JND-150121>
- Westermann, B. (2010). Mitochondrial fusion and fission in cell life and death. *Nat Rev Mol Cell Biol*, *11*(12), 872-884. <https://doi.org/10.1038/nrm3013>
- Wiedemann, N., Kozjak, V., Chacinska, A., Schönfisch, B., Rospert, S., Ryan, M. T., . . . Meisinger, C. (2003). Machinery for protein sorting and assembly in the mitochondrial outer membrane. *Nature*, *424*(6948), 565-571. <https://doi.org/10.1038/nature01753>
- Wiedemann, N., & Pfanner, N. (2017). Mitochondrial Machineries for Protein Import and Assembly. *Annu Rev Biochem*, *86*, 685-714. <https://doi.org/10.1146/annurev-biochem-060815-014352>
- Wikström, M., Krab, K., & Sharma, V. (2018). Oxygen Activation and Energy Conservation by Cytochrome c Oxidase. *Chem Rev*, *118*(5), 2469-2490. <https://doi.org/10.1021/acs.chemrev.7b00664>
- Woriat, V. L., Bullard, J. M., Ma, L., Yokogawa, T., & Spremulli, L. L. (1997). Mechanistic studies of the translational elongation cycle in mammalian mitochondria. *Biochim Biophys Acta*, *1352*(1), 91-101. [https://doi.org/10.1016/s0167-4781\(97\)00002-x](https://doi.org/10.1016/s0167-4781(97)00002-x)
- Wu, M., Gu, J., Guo, R., Huang, Y., & Yang, M. (2016). Structure of Mammalian Respiratory Supercomplex I. *Cell*, *167*(6), 1598-1609.e1510. <https://doi.org/10.1016/j.cell.2016.11.012>
- Yamamoto, Y., Sunohara, T., Jojima, K., Inada, T., & Aiba, H. (2003). SsrA-mediated translation plays a role in mRNA quality control by facilitating degradation of truncated mRNAs. *RNA*, *9*(4), 408-418. <https://doi.org/10.1261/rna.2174803>
- Yankovskaya, V., Horsefield, R., Törnroth, S., Luna-Chavez, C., Miyoshi, H., Léger, C., . . . Iwata, S. (2003). Architecture of succinate dehydrogenase and reactive oxygen species generation. *Science*, *299*(5607), 700-704. <https://doi.org/10.1126/science.1079605>
- Yassin, A. S., Haque, M. E., Datta, P. P., Elmore, K., Banavali, N. K., Spremulli, L. L., & Agrawal, R. K. (2011). Insertion domain within mammalian mitochondrial translation initiation

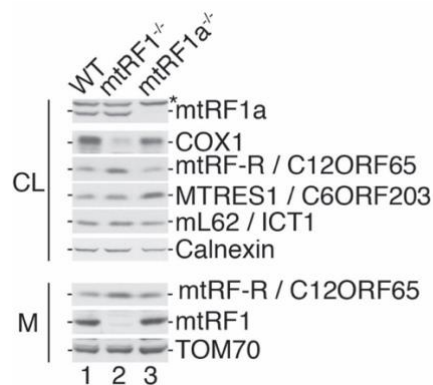
- factor 2 serves the role of eubacterial initiation factor 1. *Proc Natl Acad Sci U S A*, *108*(10), 3918-3923. <https://doi.org/10.1073/pnas.1017425108>
- Young, D. J., Edgar, C. D., Murphy, J., Fredebohm, J., Poole, E. S., & Tate, W. P. (2010). Bioinformatic, structural, and functional analyses support release factor-like MTRF1 as a protein able to decode nonstandard stop codons beginning with adenine in vertebrate mitochondria. *RNA*, *16*(6), 1146-1155. <https://doi.org/10.1261/rna.1970310>
- Youngman, E. M., McDonald, M. E., & Green, R. (2008). Peptide release on the ribosome: mechanism and implications for translational control. *Annu Rev Microbiol*, *62*, 353-373. <https://doi.org/10.1146/annurev.micro.61.080706.093323>
- Zavialov, A. V., Buckingham, R. H., & Ehrenberg, M. (2001). A posttermination ribosomal complex is the guanine nucleotide exchange factor for peptide release factor RF3. *Cell*, *107*(1), 115-124. [https://doi.org/10.1016/s0092-8674\(01\)00508-6](https://doi.org/10.1016/s0092-8674(01)00508-6)
- Zeng, F., Chen, Y., Remis, J., Shekhar, M., Phillips, J. C., Tajkhorshid, E., & Jin, H. (2017). Structural basis of co-translational quality control by ArfA and RF2 bound to ribosome. *Nature*, *541*(7638), 554-557. <https://doi.org/10.1038/nature21053>
- Zhang, M., Mileykovskaya, E., & Dowhan, W. (2002). Gluing the respiratory chain together. Cardiolipin is required for supercomplex formation in the inner mitochondrial membrane. *J Biol Chem*, *277*(46), 43553-43556. <https://doi.org/10.1074/jbc.C200551200>
- Zhang, Y., Mandava, C. S., Cao, W., Li, X., Zhang, D., Li, N., . . . Gao, N. (2015). HflX is a ribosome-splitting factor rescuing stalled ribosomes under stress conditions. *Nat Struct Mol Biol*, *22*(11), 906-913. <https://doi.org/10.1038/nsmb.3103>
- Zhang, Y., & Spremulli, L. L. (1998). Identification and cloning of human mitochondrial translational release factor 1 and the ribosome recycling factor. *Biochim Biophys Acta*, *1443*(1-2), 245-250. [https://doi.org/10.1016/s0167-4781\(98\)00223-1](https://doi.org/10.1016/s0167-4781(98)00223-1)
- Zhou, A., Rohou, A., Schep, D. G., Bason, J. V., Montgomery, M. G., Walker, J. E., . . . Rubinstein, J. L. (2015). Structure and conformational states of the bovine mitochondrial ATP synthase by cryo-EM. *Elife*, *4*, e10180. <https://doi.org/10.7554/eLife.10180>
- Zhu, J., Vinothkumar, K. R., & Hirst, J. (2016). Structure of mammalian respiratory complex I. *Nature*, *536*(7616), 354-358. <https://doi.org/10.1038/nature19095>
- Zong, S., Wu, M., Gu, J., Liu, T., Guo, R., & Yang, M. (2018). Structure of the intact 14-subunit human cytochrome c oxidase. *Cell Res*, *28*(10), 1026-1034. <https://doi.org/10.1038/s41422-018-0071-1>



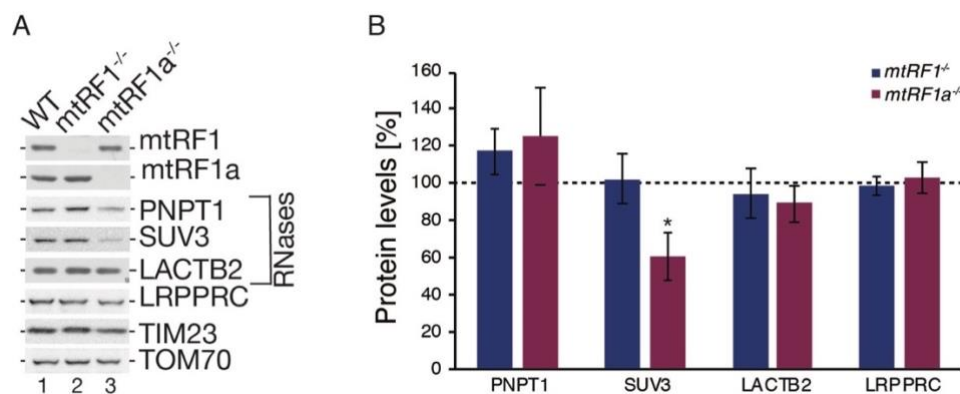
## Appendix



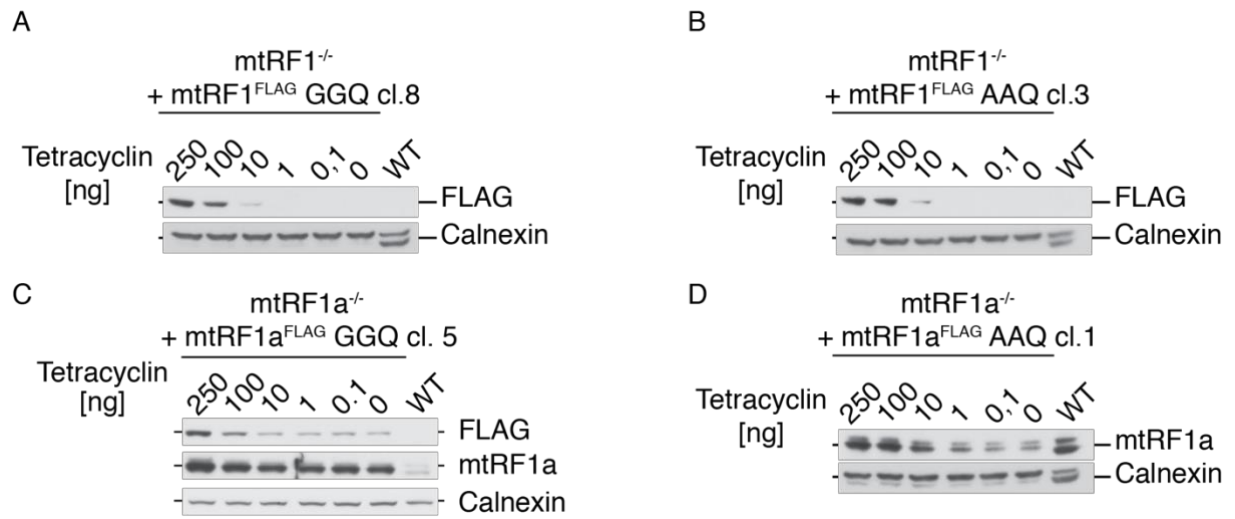
**Appendix Figure XIV: Stability of newly synthesized COX1 and ND1.** Graphs indicate the protein turnover of newly synthesized (A) COX1 and (B) ND1 quantified from the pulse chase experiment shown in Supplementary Figure 3. Statistical analysis was performed as two-sample one-tailed Student's t-test and significance was defined as  $p \leq 0.01$  \*\* and  $p > 0.05$  as not significant (n.s.).



**Appendix Figure XV: Steady state levels of mitochondrial release factors in mtRF1<sup>-/-</sup>.** Expansion of Figure 5a to show protein levels of mitochondrial release factors mtRF1, ICT1 and C12ORF65 as well as MTRES1 in mtRF1a-ablated cells.



**Appendix Figure XVI: Steady state levels of factors involved in RNA processing.** (A) Steady state protein levels of LRPPRC, the RNase LACTB2 and the subunits of the mitochondrial degradosome PNPase (PNPT1) and SUV3. (B) Quantification of (A). Statistical analysis was performed as two-sample one-tailed Student's t-test and significance was defined as  $p \leq 0.05$  \*.



**Appendix Figure XVII: Titration of tetracycline-inducible FLAG cell lines.** Titration of tetracycline-inducible FLAG-tagged rescue (GGQ) and mutant (AAQ) cell lines of *mtRF1*<sup>-/-</sup> and *mtRF1a*<sup>-/-</sup>.



## Acknowledgement

Scientific work is never the effort of a single person. It takes a village to make this thesis possible. Therefore, I would like to take this opportunity to thank everyone who supported and accompanied me during the last years.

First and foremost, I would like to thank Dr. Ricarda Richter-Dennerlein for giving me the chance to work on this exciting project, for supporting me with her advice, numerous smart ideas and fruitful scientific discussions to achieve the best possible results. Thank you for reminding me to always balance perfectionism and efficiency – ‘maybe just one more nice blot’ was probably one of my most-said sentences. And thank you for showing me that apparently, mitochondria are “my thing” and that it is worthwhile to be persistent.

Next, I would like to thank Prof. Dr. Holger Stark and Dr. Sarah Adio for being part of my thesis advisory committee, for sharing their knowledge regarding ribosomes and release factors and for our constant exchange which was always very helpful. And together with them, I would like to thank Prof. Dr. Markus Bohnsack, Prof. Dr. Ralph Kehlenbach and Dr. Alex Faesen for being members of my thesis examination board. Especially I would like to thank Markus for stepping in as 2<sup>nd</sup> referee last minute – I highly appreciate this.

I am thankful for being part of the GGNB program “Biomolecules: Structure – Function – Dynamics” of the Georg-August University of Göttingen. Although Covid unfortunately changed it, it was always fun to be with like-minded people – inside and outside of the scientific environment. The graduate school provided me with the opportunity to attend an international conference to present my research. I would also like to thank the SFB860 “Integrative Structural Biology and Dynamic Macromolecular Assemblies” for funding this project and giving me the opportunity to participate in scientific meetings and retreats. I will always remember the amounts of snow and the fun skiing sessions afterwards at Kleinwalsertal.

I owe many thanks to all current and former members of AG RRD for making daily lab business even more enjoyable. Thank you: Marleen and Angi for ‘*researching*’ which sour candy might be the best (result: *Haribo Sauerbrenner*) and filling my incubation times with much needed distractions; Elena and Venkat for your support during challenging times; and Emely for initially introducing me to all lab-related secrets. A big thank you goes out to all members of the Department of Cellular Biochemistry for being part of this exciting ride of doing a PhD, for never hesitating to share your knowledge and probably most importantly for our lunches which have been a great motivation to time experiments accordingly. There was never a dull moment with you guys! I like to thank Angela for advising me with seahorse measurements and Sabine for showing me all of her Blue Native magic tricks. I highly appreciated your help. Especially, I would like to thank our secretary Eva, who constantly helped with bureaucratic and organizational issues and for always having an open ear, as well as Carmen and Annette, who support all of us

with much more than just autoclaving buffers – because everyone knows how many scientists it would take to properly run a dish washer.

But most of all I have to thank Bettina and Sabine – I honestly do not know what I would have done without, particularly during the past 1 ½ years. You both have hearts of gold and you always put a smile on my face, especially when I did not feel like it. You guys are real friends!

A special thanks goes to Rica, Marleen and Franziska Oliveri for critically proofreading my thesis. I know that the full-stop key exists on my keyboard – I just have to be reminded from time to time that it is worth using it. Sorry for causing knots in your brain!

I would like to thank my family and friends from the bottom of my heart. Thank you for always standing by my side, for being my advocates and most importantly for your never-ending support. Life is so much more fun with all of you! I am truly thankful for my former fellow students – the ‘HuBis’ and ‘Mathe-Pros’ – as well as previous lab mates and supervisors who not only shaped me as a scientist but became dear friends. Sophie, Kathrin and Isabel – thank you for reminding me that there is a world outside the lab, I value our friendship so deeply. The same holds true for my ‘Reisegruppe Melsungen Mädels’: Lisa, Tamara, Annik, Denise, Franzi, Melissa, Johanna and Alisa, I am forever grateful for our friendship since we were kids and I know that we will always be ‘Nordhessinnen’ at heart, no matter where and at what point in life we are in this world. Especially I have to thank Lisa, Marcel, Tami and Martin for always, always being there, to listen to all my problems and concerns, even when I could not bear myself anymore and for always cheering me up. You truly deserve an award!

And, most importantly, I thank my parents for their unconditional love. Mama, I am nothing without you and I could not write this thesis without your support. Papa, I miss you so much and hope you would have been proud of me.